Parametric Design of Multi-Echelon Last-Mile Delivery Systems Using Emerging Technologies

Bahar D Viniche

A Thesis Submitted to the Faculty of Graduate Studies

In Partial Fulfillment of the Requirements for the Degree of

Doctor of Philosophy

Graduate Program in Civil Engineering

York University

Toronto, Ontario, Canada

May 2025

Abstract

The growing demand for fast and cost-effective last-mile delivery has prompted logistics operators to explore emerging delivery technologies such as autonomous vehicles (AVs) and drones. This dissertation investigates the design and strategic planning of multi-echelon last-mile delivery systems using emerging delivery technologies. Through three complementary studies, we explore the integration of AVs and drones into traditional truck-based delivery networks using analytical models and parametric design frameworks.

The first study examines recipient-dependent routing policies in AV-enabled deliveries, where recipients participate by using their AVs for parcel pickup. We introduce and analyze three delivery policies- AV pickup, Hybrid pickup, and Crowdsourced delivery— and derive upper and lower bounds on their total system costs. These policies are compared against the traditional truck delivery model, with results showing that recipient-dependent strategies become increasingly dominant as the number of deliveries grows.

The second study extends this concept to the delivery of perishable goods, where delivery time is critical. Using parametric design, we introduce length-constrained (time-sensitive) routing models and compare AV, Hybrid, and crowdsourcing policies to traditional truck delivery. Our findings show that AV integration offers significant advantages in reducing delivery failure for perishable goods, particularly under increasing hand-off costs and high delivery density.

The third study focuses on tactical fleet planning and routing in drone-assisted last-mile delivery. We model a mixed fleet of trucks and drones, considering drone range, truck and drone capacities, multi-launching, and vehicle synchronization. Using continuous approximation, we derive closed-form solutions for fleet composition and routing strategies under varying operational scenarios. The analysis yields policy spaces that guide optimal system design based on drone and truck operational parameters, such as vehicle speeds and capacity limits.

This dissertation, through its integrated studies, offers a unified framework for the strategic design and operational evaluation of multi-echelon last-mile delivery systems using emerging delivery technologies. The models developed provide managerial insights for logistics planners, policymakers, and researchers seeking scalable and efficient delivery solutions.

Acknowledgment

PhD is an incredible journey, made all the more remarkable when accompanied by the right fellow travelers and mentors.

I am grateful for the support of my supervisor, Dr. Mehdi Nourinejad, and my advisors, Dr. Opher Baron and Dr. Oded Berman. Their commitment to academic excellence has shaped my path, and I feel privileged to have learned from them and worked alongside them. They have shown me how meaningful and beautiful every step of a PhD journey can be, and I am forever grateful for the opportunity to witness such a rich perspective on the academic path.

I would also like to express my sincere gratitude to my supervisory committee members, Dr. Peter Park and Dr. Kevin Gingerich, for their invaluable guidance and support throughout my academic endeavors.

Lastly, I extend my heartfelt thanks to my colleagues at York University and the Rotman School of Management for enriching my academic experience and contributing to a collaborative and stimulating environment.

Dedication

There is an old video of me on my 10th birthday. Someone asks, "What do you want to be when you grow up?" and without missing a beat, I say, "Go abroad and become a scientist."

Well, I'm almost there! I dedicate this work to the one and only family who made that dream possible: Afi, Hadi, Raha, Ala :) You are all rooted in the world of art and literature, yet when it came to my path through science, you cheered me on like seasoned pros. Thank you for believing in me every step of the way, even when I doubted myself. I couldn't have asked for a better crew in this play called life.

And to Bahador, my best friend, my partner, and the love of my life. From the first lecture halls of our undergrad days to the late nights of dissertation writing, you have been by my side. You have witnessed every chapter of this journey, from sweet victories to stressed-out exams and life-changing decisions. Your love, patience, and unwavering faith in me have been my anchor through it all. I am, and always will be, forever grateful.

Finally, to all my wonderful friends in Toronto and around the world: Whether near or far, your steady encouragement and love lit the way forward.

Table of Contents

List of Figures

List of Tables

Chapter One Introduction

This chapter introduces the growing significance of last-mile delivery in modern logistics and the critical role emerging technologies play in enhancing its efficiency. As consumer expectations for faster and more reliable delivery continue to rise, the final leg of the supply chain faces increasing pressure to adapt, often constrained by challenges such as traffic congestion, limited parking availability, and high delivery costs. This research examines how integrating emerging delivery technologies and autonomous delivery mediums—such as drones and autonomous vehicles—into existing logistics systems can help meet these challenges. The chapter outlines the background, problem statement, research scope, and objectives, setting the foundation for a comprehensive study on the design and analysis of multi-echelon last-mile delivery systems that incorporate emerging technologies.

Section A: Background

The final stage of the supply chain, known as last-mile delivery, is the process of transporting goods from distribution centers to their ultimate destination. This final leg accounts for the 28% of the total delivery cost (Hochfelder 2017), primarily due to challenges such as traffic congestion, limited parking, and the high expenses of reaching remote locations, which often require lengthy detours (Goodman 2005, Dolan 2022). The goal of last-mile delivery is to ensure prompt service at the least possible cost, a goal increasingly pursued by integrating innovative delivery technologies. Recent advancements in automation and robotics, including drones and Automated Vehicles, have significantly transformed urban logistics operations with the potential to enhance service reliability and relieve urban traffic congestion. (He, Liu, and Shen 2022). The global last-mile delivery market is expected to reach $470 billion (similar to the GDP of Belgium), and automation is key to achieving efficient and sustainable growth in this sector. Automation will be key to achieving efficient and sustainable growth in this sector, and autonomous transportation mediums are expected to significantly impact last-mile delivery, potentially handling up to 80% of all shipments within the forthcoming decade (McKinsey 2019). Currently, Europe, China, and the United States are at the forefront of this increasing trend (He 2021). With the US and China leading the way in this sector, many retailers have already taken the initiative to include Autonomous Vehicles (AVs) in their fleets, including Starship Technologies and Nuro.

In the US, Walmart and Kroger have partnered with Nuro to use AVs to deliver groceries in Scottsdale and Houston. China is conducting trial runs in logistic parks, private communities, university campuses, and open public roads in major cities like Beijing and Shenzhen. Neolix has also begun mass production of delivery AVs to serve tech giants such as Huawei (Li et al. 2020a). Feasibility studies on drone-enabled deliveries were initiated by Amazon Prime Air, which performed the first-ever drone-enabled package delivery in 2016 (Wells and Stevens 2016), and the first public delivery in the USA in 2017 adhering to the federal regulations (Rubin 2017). Other examples include DHL's parcelcopter project (Discover 2022) and Google's Project Wing (Kanellos 2014). Amazon claims that 85% of their products are less than 5lb (McEntegart 2013), which is within the current drone average payload capacity. Delivery drones are expected to carry a higher ratio of products as they advance in-flight power and payload capacity. The drone delivery market alone is projected to surpass $7 billion globally by 2027, reflecting its growing role as a scalable solution within modern logistics systems. Drone delivery also has several applications in other sectors, such as applications of drone delivery in the medical sector, which have been implemented through feasibility studies, including the collaboration of UPS and Zipline for blood deliveries (Tilley 2016), Zipline medicine delivery in North Carolina (Koetsier 2022), Matternet logistic network for medical samples delivery(Alley 2019), and the joint project of UPS and CyPhy for delivering medical supplies (Carey 2016).

As logistics firms continue exploring innovative strategies for improving last-mile delivery in urban and rural areas, combining emerging technologies with traditional delivery fleets presents a promising direction. While autonomous delivery mediums offer significant advantages,

Figure One.1: Last-mile delivery systems with emerging technologies. Traditional truck-based delivery routes are shown with thick black lines. AV routes are shown with purple dotted lines and drone flight paths shown as dashed blue lines.

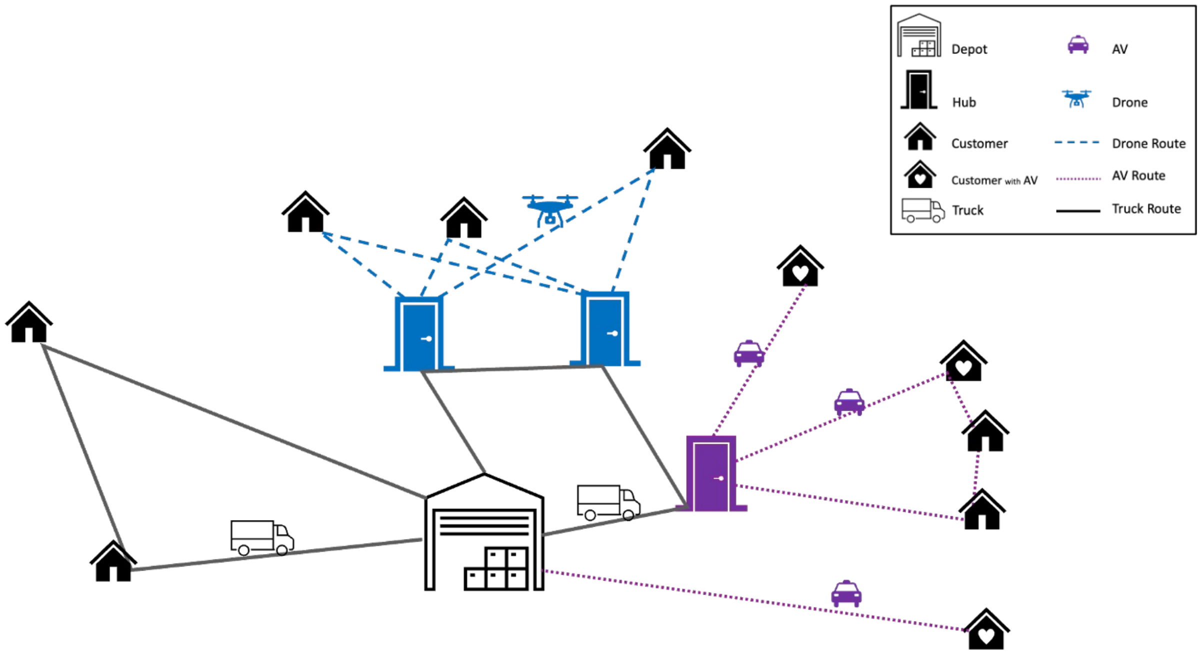

they also come with operational limitations that can be mitigated through integration with conventional trucks. Schematic representation of last-mile delivery systems with and without emerging technologies in shown in Figure One.1. Traditional truck-based delivery routes are shown, where trucks depart from a central depot and follow a TSP tour to directly serve recipients. With the integration of emerging delivery technologies such as AVs and drones, alternative strategies emerge. These include recipient AVs traveling directly to the depot for self-pickup; multi-echelon delivery systems, where trucks transport parcels to intermediate hubs and the second leg is completed either by recipient AVs or through crowdsourced AV deliveries, in which recipients use their AVs to deliver to nearby neighbors. Drone-assisted delivery is also depicted, where drones are launched from hubs to deliver parcels directly to recipient locations. This schematic highlights the structure of multi-echelon last-mile delivery systems enabled by emerging technologies. This research investigates the design of multi-echelon last-mile delivery systems, considering hybrid fleets of trucks and autonomous mediums. We focus on two specific configurations involving autonomous vehicles and drones, which are detailed in Section 1.2 Problem Statement.

Section B: Problem Statement

Using emerging technologies such as drones and autonomous vehicles in logistics operations requires planning at the tactical level and delivery management at the operational level. In this study, we focus on two-echelon truck-augmented delivery systems.

This research focuses on the strategic planning of truck-augmented last-mile delivery systems. There are three main streams of this research as follows:

- Recipient-Dependent Last-Mile Delivery Routing With Autonomous Vehicle Applications.
- Parametric Design of Time-Sensitive Routing With Recipient-Dependent Contributions
- Tactical Fleet Planning for Drone-Based Delivery Systems.

Operational-level routing strategies support finding the optimal sequence of recipient visits, hand-off locations from one delivery medium to the other, assignment of orders to trucks, and other route-related properties. Such decisions often require detailed information about the location of recipients and the route's characteristics, including time-window restrictions, package size, and so on. The prominent methodology for operational-level decisions relies heavily on integer programming formulations that can capture the inherent constraints (Murray and Chu 2015), (Murray and Raj 2020), (Poikonen and Golden 2020). In contrast, strategic planning addresses high-level decisions such as the optimal fleet composition or facility location. It requires less detailed data and aims to compare the growth order of cost (or revenue) with respect to the size of recipients. A gap in the literature at the strategic level of planning is the absence of key operational-level conditions, which are often neglected because they complicate the analysis process.

B.1 Parametric Design

Parametric design is a modeling approach grounded in algorithmic thinking, where mathematical rules and logical dependencies are employed to generate and manipulate complex system configurations. Originally developed in architecture and urban planning, parametric modeling enables designers to explicitly define a set of parameters and rules that govern the relationships between design variables and outcomes. Unlike conventional static modeling methods, parametric design allows for dynamic model adjustments, facilitating rapid evaluation of alternative scenarios and system configurations. Figure One.2 illustrates a classical example of parametric design in architecture, where geometric forms are generated and refined through adjustable parameters.

In the context of last-mile delivery, parametric design supports the development of flexible optimization models that capture the complex interdependencies among variables such as routing strategies, fleet compositions, hub locations, and recipient assignments. By systematically manipulating these input parameters, it becomes possible to evaluate how changes in operational conditions—such as vehicle speed, drone range, or customer density—affect overall system performance and cost efficiency.

Figure One.2: Examples of Parametric Design modeling in architecture (Koumari 2022, Avetisyan 2022, Sharan Architecture 2024).

A key advantage of parametric design in logistics modeling lies in its scalability and adaptability. It facilitates rapid exploration of ”what-if” scenarios, which is particularly valuable in dynamic logistics environments where systems must frequently adjust to shifts in demand, urban infrastructure, or technological capabilities. This flexibility also enables detailed sensitivity analyses, helping to identify the operational parameters that most significantly influence system performance and cost-effectiveness. In addition, parametric design fosters transparency and traceability in the decision-making process. By clearly articulating the relationships between model inputs and outputs, it supports the development of analytically tractable solutions and enables deeper insights into the structural and operational trade-offs inherent in multi-echelon last-mile delivery systems.

To capture the complexities of strategic planning in multi-echelon last-mile delivery, this research proposes a parametric design framework that integrates routing parameters (e.g., vehicle speeds and drone range limitations), facility location-allocation decisions (e.g., the number and spatial distribution of hubs), and fleet composition characteristics (e.g., number of trucks and drones, vehicle capacities, and coordination constraints). This structured and flexible framework enables closed-form analytical derivations and provides a systematic basis for comparing the cost and performance of alternative delivery policies involving emerging technologies.

B.2 Recipient-dependent Last-Mile Delivery Routing With Autonomous Vehicle Applications

Recent technological advancements in the automation industry have enabled recipient participation in last-mile delivery. A notable technology in this context is autonomous vehicles, which can transport and pick up goods without human drivers. AVs offer the opportunity to avoid visiting retail stores in person. AV owners can instead send their AVs to collect items ordered online, thereby promoting a form of self-pickup for customers. Self-pickup with AVs is compatible with existing drive-through pickup stations at Walmart and Loblaws, initially designed for human-operated vehicles, demonstrating adaptability to AVs. AVs are also compatible with curb-side pickup remedies, which have seen a significant increase in adoption for various applications, such as grocery and retail goods collection. This trend reflects a broader shift towards more contactless and efficient delivery methods. For instance, many grocery stores and restaurants have expanded their curbside pickup services to facilitate a contactless shopping experience, allowing customers to receive orders without leaving their vehicles. AV pickups would also alleviate the discomfort of recipients who previously had to remain onsite (at home) during delivery time windows dictated by carriers. AVs introduce more flexibility, allowing recipients to choose their pickup time more flexibly to reduce the likelihood of missed deliveries. Delivery outside of the imposed time window affects recipient loyalty, retailer reputation, and delivery cost. Voxware reports from a survey of 500 recipients that 69% of respondents are less likely to choose the same retailer if an item is not received within two days of the promised delivery date (Kela, 2016).

AVs will also promote the sharing economy in the last mile. AV-equipped recipients can leverage peer-to-peer (P2P) sharing and lend their cars to make deliveries for neighbors within a vicinity. General Motors is promoting P2P sharing as it plans to launch a rental program, allowing GM vehicle owners to post their AVs to rent through the automaker's car-sharing platform, thus generating revenue for the company's vehicle owners (Washington Post 2018). AV sharing is more convenient and effective than existing ridesharing and crowd-shipping services because AVs do not need human drivers (with work shifts) and can be shared more seamlessly. This allows mobility service operators to increase the supply of vehicles and improve the level of service provided to recipients (Fagnant and Kockelman 2015). Existing logistics firms are currently exploiting the benefits of crowdsourcing. Amazon Flex and Roadie are crowdsourcing firms that recruit on-demand drivers to make deliveries (Economist, 2019). Roadie generates 80% of its revenue from deliveries for Walmart, Macy's, and Home Depot. AVs could advance current crowdsourcing platforms as they are more flexible and generate revenue for owners.

Our research focuses on emerging delivery policies that depend on recipient participation. We consider three operational policies in which recipients (i) pick up from the central depot, i.e., directly send their AVs to a retailer's location (AV policy), (ii) pick up from a hub located by the logistics firm close to them, i.e., send their AVs to designated hubs selected by the retailer (Hybrid policy), or (iii) pick up from a hub and make deliveries to other nearby recipients as well, i.e., lend their AVs to complete deliveries for themselves and their neighbors (Crowdsourcing policy). AVs would enable such policies by reducing their cost, as the opportunity cost of the driver is no longer present. While these recipient-dependent policies can have applications other than AVs, we use AV-related terminology to explain them and discuss their future impacts.

Recipients incur discomfort when partaking in the delivery process, primarily because it requires them to actively spend their time or use their vehicles to collect parcels. Logistics firms can alleviate this burden by providing financial compensation or allowing recipients to visit designated pickup stations instead of a farther away depot. Pickup stations are dispersed in an area and operated by the logistics firm. For example, Amazon uses Whole Foods store locations as potential pickup locations for its e-commerce recipients. All major Chinese e-retailers also offer pickup locations in many major cities where universities and subway stations are common pickup locations.

At the operational level, the quest to find the optimal set of remote pickup locations is a multi-echelon routing problem. In our context, this problem is a variant of the vehicle routing problem with trucks that travel between a depot and the pickup stations and AVs that travel between the pickup stations and recipient homes (Perboli, Tadei, and Vigo 2011). The vehicle routing problem takes precise parameters and provides detailed recipient visit schedules for each vehicle. This level of detail is helpful for day-to-day operational-level decisions. However, in strategic-level decisions, the objective is to have a holistic comparison of various policies without complete or accurate data on operating conditions, such as the exact location of recipients each day.

We study strategic-level decisions and analyze alternative recipient-dependent delivery policies to gain insights into the parameters of the system that affect its performance and make different policies preferable. Our analysis stems from the literature on vehicle routing approximations that assume the recipients are: (i) dispersed on a surface with a given spatial distribution (Newell and Daganzo 1986a,c), (ii) served by vehicles, or (iii) located on a stylized geometrical shape (e.g., the arc of a circle) (Archetti, Savelsbergh, and Speranza 2006). Such approximations often yield closed-form derivations of the length of tours required to visit a set of recipients (Bertsimas and Van Ryzin 1991). Our approximations are similar in nature to the worst-case scenario routing analysis in Archetti, Savelsbergh, and Speranza (2006).

B.3 Parametric Design of Time-Sensitive Routing With Recipient-Dependent Contributions

Recent advances in AV technologies have enabled new forms of recipient participation in last-mile logistics. A particularly promising direction involves the delivery of perishable goods. The last-mile delivery of perishable goods presents a unique set of challenges due to the inherent time sensitivity of these items. Perishable goods, such as fresh food, pharmaceuticals, or medical supplies, often require rapid and reliable delivery within strict time constraints to preserve their integrity. Traditional delivery systems that rely solely on trucks face significant inefficiencies in this context, particularly due to urban congestion and failed delivery attempts.

These inefficiencies not only increase operational costs but also raise the risk of spoilage and customer dissatisfaction (Gustavsson et al. 2011, Hsu, Hung, and Li 2007, Lagin et al. 2022).

Recipient-dependent delivery (RDD) strategies have emerged as a promising alternative for improving the success rate and responsiveness of last-mile deliveries. These strategies shift a portion of the delivery burden to recipients, who retrieve their packages from depots, hubs, or designated collection points. RDD can further benefit from emerging autonomous technologies, particularly Autonomous Vehicles, which enable recipients to participate in deliveries with minimal effort or coordination. AVs can be dispatched to collect parcels independently, aligning with existing curbside or drive-through pickup infrastructure used by major retailers such as Walmart and Target (Bagloee et al. 2016).

Building on our earlier investigation of AV-enabled recipient-dependent deliveries, this study focuses on the application of RDD in the context of perishable goods, where delivery performance is governed by delivery time. We investigate how the design of last-mile delivery systems can be adapted to account for these time constraints by bounding vehicle tour lengths, a key consideration for goods that degrade rapidly in transit. We propose a parametric design framework for modeling and comparing different delivery policies, including traditional truck delivery, AV-based self-pickup, hybrid delivery system with retailer-located hubs, and AV-enabled crowdsourced deliveries.

For strategic analyses of this delivery system, we adopt stylized models to explore the effect of routing constraints on delivery system performance. These models build upon previous studies in vehicle routing approximations (Newell and Daganzo 1986a, Carlsson and Song 2018) and integrate design variables inspired by network design theory. We develop stylized models assuming recipients are uniformly distributed along a known geometry, where we first consider a one-dimensional ring structure for the service region and later extend the analysis to a two-dimensional circular surface. These models allow for closed-form approximations using the continuous approximation framework, which is especially suited for strategic-level decisions with limited operational data. By framing the problem around tour length rather than truck capacity, we capture the urgency of perishable deliveries and the trade-offs that emerge in time-sensitive logistics environments. This framework offers a foundation for analyzing and designing AV-assisted last-mile delivery strategies that are robust to perishability constraints and adaptable to future logistics infrastructures.

This research contributes to the literature on AV-enabled last-mile logistics by providing an analytical comparison of recipient-dependent delivery models under time-sensitive constraints. The parametric design framework enables flexibility in exploring how varying operational parameters, such as hand-off costs, AV operating costs, and delivery density, influence routing strategy performance. The insights derived from this analysis offer practical guidance for fleet operators and policymakers on the design of scalable, cost-effective, and timely last-mile systems for perishable goods. These models are validated through numerical experiments using a Walmart delivery case study in Toronto, showing consistency between theoretical insights and practical performance. This work lays the foundation for further exploration of time-sensitive RDD strategies within emerging smart city environments.

B.4 Tactical Fleet Planning for Drone-Based Delivery Systems

Logistic operators can benefit from adding drones to their fleets for delivery to congested urban or remote sub-urban areas, thus shifting part of the last-mile traffic from roads to air where drones can fly at higher speeds and on more flexible routes. The cost of adding drones to a fleet can be substantially lower than the expansion of the existing fleet by adding more vehicles. Nevertheless, drones have operational constraints, including their payload and battery capacity, which limits their flight's maximum time and distance, known as flight endurance and flight range, respectively. A mixed fleet of trucks and drones can provide the necessary flexibility and speed to provide an optimal last-mile delivery strategy while overcoming the operational constraints of delivery using only truck-exclusive fleets.

A gap in the literature at the strategical level of planning is the absence of key operational-level conditions, which are often neglected due to complicating the analysis process. Five of such conditions are: multi-truck multi-drone delivery, the drone range limitation, Truck limited capacity, drone multi-launching (launching more than one drone at a time), and flight coordination. For example, Carlsson and Song (2018) consider a coordinated single-truck single-drone system without multi-launching, and Perera et al. (2020) consider a drone-exclusive system with unlimited flight range. Multi-launching is an operational condition whereby more than one drone can be launched from a single location, and each headed toward its designated recipient. Multi-launching further complicates the flight coordination process, requiring a truck to be present at a promised retrieval hub prior to the arrival of the first drone and idle until the arrival of the last drone.

In this research, we seek to find the optimal fleet composition for multi-truck multi-drone parcel delivery to a set of recipients by proposing a parametric design and providing strategic analyses. In our problem, multiple drones can be assigned to each truck, and the synchronization between truck movement and drone flight is taken into account both in terms of minimizing the delivery time and considering the operational limits of the truck and its assigned drones, including their speed. The optimized routing strategy and fleet composition are introduced based on drone operational constraints, including their payload capacity, flight range, and limited capacity of trucks. We also introduce the concept of multi-launching of drones by each truck, i.e., each truck can launch more than one drone at each launch hub in addition to the concept of drone re-launching, which stands for the drone's ability to get back to the truck after finalizing a delivery to resupply itself and relaunch to the next delivery as far as it does not violate drone range.

Section C: Literature Overview

C.1 Last-Mile Delivery with emerging Technologies

The integration of autonomous vehicles (AVs) and drones in last-mile delivery systems has been a significant area of research over the past few decades. These emerging delivery technologies promise to address the challenges of urban congestion, limited parking, and the increasing demand for faster delivery times. Early studies focused on optimizing vehicle routing for trucks, AVs, and drones using integer programming (IP) formulations. These models aimed to optimize the routes, fleet compositions, and scheduling decisions to improve efficiency and reduce costs, setting the foundation for further advancements in this field.

C.1.1 Autonomous Vehicles in Last-Mile Delivery

The application of autonomous vehicles (AVs) in last-mile delivery has attracted considerable attention in recent years, driven by the potential for cost reduction and operational efficiency. Early works in this area focused on developing optimization models to manage the deployment and routing of AVs alongside traditional truck fleets.

AVs are rapidly reshaping the transportation landscape with the potential to enhance mobility and logistics. The three C's of AVs, namely *Connectivity*, *Comfort*, and *Collaborative consumption*, underline their transformative potential Baron, Berman, and Nourinejad (2020). Several studies have addressed various aspects of AVs. For instance, Bansal and Kockelman (2017) assesses consumer willingness to adopt this emerging technology, Mersky and Samaras (2016) discusses AVs' potential to improve fuel economy and promote environmental sustainability, Mahmassani (2016) evaluates AVs' potential impact on traffic flow and congestion management, de Oliveira (2017) provides an in-depth analysis of the traffic patterns induced by AVs, Mirzaeian, Cho, and Scheller-Wolf (2020) uses queueing theory to understand and optimize AV traffic flow, Harper et al. (2016) estimates the potential increase in traffic due to widespread AV adoption, Nourinejad and Roorda (2018) explores the potential issues and solutions related to AVs and urban parking, Fagnant and Kockelman (2014) investigates the feasibility of shared AV fleets, and Chen et al. (2016) proposes methods for optimizing shared AV operations to increase efficiency and minimize costs.

However, the intersection of AVs with last-mile deliveries and logistics services remains relatively unexplored and forms the basis of this study's investigation.

C.1.2 Drone-Assisted Last-Mile Delivery

Drones have a wide range of applications in sectors such as logistics, disaster management, and healthcare. A survey by Otto et al. (2018) highlighted the potential of drone delivery across industries such as healthcare, agriculture, and disaster response. D'Andrea (2014) discussed the economic benefits of drone delivery in these sectors based on cost-per-mile analysis. Chung, Sah, and Lee (2020) surveys the civil application of drone delivery in different sectors, among them are transportation and logistics, with a focus on optimization approaches in the Drone and Truck

Coordinated Operations. Finally, Poikonen and Campbell (2021) reviewed the routing problem of drone delivery in logistics, emphasizing the future of drone-enabled deliveries given their lower operational cost and accessibility to remote areas. They identified the gap of inadequate consideration of operational constraints, including flight range, battery capacity, speed, and payload limitations. They further suggested that the synchronization of drone trajectories and truck paths poses the most significant challenge in multi-truck multi-drone systems. We thus consider this synchronization in our model.

We next review research focused on coordinated truck and drone delivery systems. Pioneering research in truck and drone delivery systems focused on single-truck, single-drone operations. Murray and Chu (2015) addressed the multi-echelon delivery as the *Flying Sidekick Traveling Salesman Problem* (FSTSP), which was a novel variant of the classic Vehicle Routing Problem (VRP). A mixed-integer linear program was used, but due to the complexity of the problem, they later proposed a heuristic solution for larger instances (Murray and Raj 2020). Several studies further tackled FSTSP and its complex variants. Agatz, Bouman, and Schmidt (2018) and Jeong, Song, and Lee (2019) both contributed integer program solutions, with the latter improving the algorithm complexity of FSTSP by considering the limited flight range of drones and its dependency on carrying payloads. Furthermore, Bouman, Agatz, and Schmidt (2018) used dynamic programming to obtain the exact optimal solution of the traveling salesman problem with a single drone to minimize tour costs in a setting where all recipients are serviced by either the truck or drone.

In extending the problem scope, a body of literature studied multiple-drone multiple-truck scenarios. Sacramento, Pisinger, and Ropke (2019) examined multiple trucks and one drone per truck, while others considered trucks with multiple drones with the carrying capability of one parcel (Wang, Poikonen, and Golden 2017) or multiple parcels (Wang and Sheu 2019). In addition, Kitjacharoenchai et al. (2019) modelled a multi-drone multi-truck problem where drones can transit between trucks (launch from one truck and return to another), adding an extra dimension to the logistical problem. However, critical operational limitations of drone-enabled deliveries are missing in these studies, including the limited battery capacity of drones, which leads to range or endurance constraints. We focus on the multi-truck multi-drone operation while considering the operational characteristics and limitations of the truck-and-drone delivery system, including but not limited to their limited payload capacity and drone battery limitation, which leads to flight range constraints in addition to scheduling constraints of trucks and drones.

C.2 Vehicle Routing Problems

The vehicle routing problem seeks to find the optimal set of routes for a fleet of vehicles that visit a set of recipients only once. The conventional formulation is a combinatorial optimization problem that is *NP*-hard (Laporte 1992) and commonly solved by integer programming. This approach is data hungry (because it requires the exact location of recipients and their delivery loads) and less suitable for strategic-level decisions where data is limited, and the level of accuracy in terms of finding exact routes is less important. A plausible alternative is to approximate the vehicle routing problem, typically using one of the following three approaches.

The first approach is *continuum approximation* that shifts from the conventional integer programming formulation to a continuous space by assuming that recipients are spread out on an Euclidean surface with a density distribution. Ansari et al. (2018) provides a comprehensive review of continuous approximation (CA) techniques and their application in addressing various challenges within the transportation domain. Carlsson and Song (2018) uses the continuous approximation method to approximate the cost of a two-echelon vehicle routing problem with trucks and drones that serve a set of recipients distributed on a surface. The drones are dispatched from the trucks at designated launch points to visit their assigned recipients and return to the truck at a retrieval point. The model approximates the total delivery time w.r.t. the density of recipients. Agatz et al. (2011) studies the home delivery problem of e-retailers who commonly suffer from narrow delivery times. To lessen this burden on the recipients, a set of time slots are assigned to each zip code and the delivery routes are generated using the approximation method of Daganzo (2005). Carlsson et al. (2016) studies the household scheduling problem as a variant of the generalized travelling salesman problem. Each household member performs errands in the course of a day (e.g., going to the bank and grocery shopping afterward) and must choose a location for performing each task. They derive the approximate length of the household trips using continuum approximations that generalize the derivations of Beardwood, Halton, and Hammersley (1959) and Redmond and Yukich (1994) for the travelling salesman problem with a large number of recipients. For a review of continuum approximation models, we suggest Langevin, Mbaraga, and Campbell (1996) and Ansari et al. (2018).

The second approach treats vehicles as servers of a queue system. Bertsimas and Van Ryzin (1991) study the dynamic and stochastic vehicle routing problem with the objective of minimizing the waiting time of recipients for service. They assume recipients arrive according to a Poisson process and are independent and uniformly distributed in an Euclidean service region. The model shows that the waiting time grows faster than the waiting time in conventional queues under heavy traffic, and the stability condition does not depend on the system geometry, which validates the use of the approximation for an otherwise complex vehicle routing model. Other examples of using queue models for service routing can be found in Bellos, Ferguson, and Toktay (2017), Psaraftis (1995), and Bertsimas and Simchi-Levi (1996).

The third approach assumes recipients are located on a geometric shape (e.g., a circle). Archetti, Savelsbergh, and Speranza (2006) studies the worse-case of the split vehicle routing problem (where recipients can be visited more than once) originally presented by Dror and Trudeau (1989, 1990), and use an approximation to derive closed-form performance measures. In their analysis, recipients are located on the arc of a circle. Another similar approach is to use space-filling curves that are continuous mappings from a lower-dimensional to a higher-dimensional space (Sagan 2012). As an example, the Sierpinski curve is formed by repeatedly copying and shrinking a simple pattern (Bartholdi III 1995). Bartholdi III and Platzman (1988) use space-filling curves to develop novel heuristics for routing and partitioning combinatorial problems. This approach follows the setting where recipients are located on a circle similar to Archetti, Savelsbergh, and Speranza (2006).

C.2.1 Integer Programming Methodology

A widely adopted approach to solving delivery-routing problems, including sidekick-routing variants, is integer programming (IP). IP-based approaches typically require detailed data, such as the exact locations and delivery loads of recipients. Mathew, Smith, and Waslander (2015) and Peng et al. (2019) focused on the delivery strategy where trucks carry and launch drones with parcels but do not make the final hand-off to recipients, whereas Poikonen and Golden (2020) modeled one truck and k drones, solving a k-multi-visit drone routing problem. Kang and Lee (2021) presented a mixed-integer programming formulation considering a fleet with one truck and multiple drones, all capable of delivery. They proposed a heterogeneous routing problem with multiple drones classified based on speed and battery limits, yet simplistically required drones to return to their launch point, leading to excess truck waiting times and extended total delivery time. Unlike the aforementioned studies where drones deliver packages (alone or parallel to the trucks), Dayarian, Savelsbergh, and Clarke (2020) considered a case where drones resupply trucks and proposed a vehicle routing problem with drone resupply. From a distribution network perspective, Baloch and Gzara (2020) studied the economic desirability of drone delivery compared to traditional delivery services and analyzed the effect of government regulations and customer behavior in addition to the technological constraints on drone adoption. However, they do not consider the hybrid truck-and-drone delivery scenarios. Roberti and Ruthmair (2021) proposed a dynamic programming recursion-based branch-and-price approach to solve traveling salesman problems with drone (TSP-D) variants. Their method outperformed prior approaches by solving instances with up to 39 customers to optimality. Their results demonstrated that even a single drone could substantially reduce delivery time with consideration of synchronization between drone flight and the truck movement. Tiniç et al. (2023) introduced the traveling salesman problem with multiple drones (TSP-mD), modeling truck and drone synchronization by incorporating individual waiting times into the objective function. Their proposed branch-and-cut algorithms outperform standard methods when allowing flexible launch and retrieval locations. Morandi, Leus, and Yaman (2024) extended the orienteering problem (OP) to incorporate multiple drones cooperating with a truck to maximize the total collected prize under a time constraint. Their model considered drones with limited battery endurance and developed a mixed-integer linear programming formulation and a tailored branch-and-cut algorithm that solves instances with up to 50 nodes. One of the prominent limitations of using IP to address the side-kick routing problems lies in its non-polynomial order of complexity. In addition, solving these models often requires a high level of detail, such as the exact location of recipients, delivery time windows, and recipient-specific constraints like drone acceptability.

This complex structure and reliance on detailed input data often prevent identifying key insights needed for strategic decision-making.

C.2.2 Continuous Approximation

Continuum approximation (CA) transforms the traditional integer programming formulation into a continuous space, assuming that recipients are dispersed on an Euclidean surface with known density distributions. The CA methodology replaces detailed data, such as recipient locations, with concise summaries using a continuous density function over time and space (Daganzo 2005). This approach offers simplified yet plausible analysis, often allowing the derivation of closed-form analytical solutions. Langevin, Mbaraga, and Campbell (1996) and Ansari et al. (2018) provided comprehensive overviews of CA applications in logistics and freight transportation, respectively. CA has been applied to various logistics and routing problems. It has been used to analyze the costs of two-echelon vehicle routing problems involving trucks and drones (Carlsson and Song 2018), where an unmanned aerial vehicle (UAV) provides service to customers while making return trips to a moving truck that contains packages. Their work analytically showed that efficiency improvements are proportional to the square root of the UAV-to-truck speed ratio. Additionally, CA has been applied to the home delivery problem of e-retailers who commonly suffer from narrow delivery times slots (Agatz et al. 2011), showing that while these slots improve customer convenience, they can increase delivery costs.Another application is in the household scheduling problems, which is a variant of the generalized traveling salesman problem (TSP) (Carlsson et al. 2016), where CA-based models reveal that centralized delivery services require large-scale adoption before achieving significant efficiency gains over independent customer travel.

The CA paradigm has also been extended to autonomous vehicles in transit, where it aids in fleet dispatching and service optimization. Studies have applied CA to optimize modular autonomous vehicles in transit corridors (Chen, Li, and Qu 2022), to design semi-on-demand hybrid transit routes with shared autonomous vehicles (Ng et al. 2024), and to determine the optimal integration of shared autonomous vehicles with public transit (Levin et al. 2019). While these studies highlight CA's effectiveness in autonomous mobility-on-demand, their focus on public transit operations differs from our emphasis on last-mile delivery.

Another related line of research applies CA to last-mile delivery robots, which shares some similarities with our work but differ in the fundamental aspect of recipient participation and neglects the time-sensitive delivery of perishable goods. CA has been used to optimize two-echelon truck-and-robot systems and provide insights on air and ground delivery robot applications in different cities (Lemardelé et al. 2021) and evaluate hybrid drone-truck and ground robot models (Figliozzi 2020, Jennings and Figliozzi 2019). These studies provide valuable insights into autonomous last-mile logistics but focus on company-owned robots, whereas our research explores the role of recipients in the delivery process and the unique challenges posed by perishable goods.

The Continuous Approximation (CA) methodology replaces detailed data, such as recipient locations, with concise summaries using a continuous density function over time and space (Daganzo 2005). This approach offers simplified yet plausible analysis, often allowing the derivation of closed-form analytical solutions. Carlsson and Song (2018) adopted CA modelling techniques to overcome the mentioned computational challenges while still utilizing a single drone and truck. Whereas, Campbell, Sweeney, and Zhang (2017) used CA considering multiple drones per truck and provided strategic-level insights on the economical advantages of drone delivery and the critical role of synchronization. Li et al. (2020b) studied a delivery setting where recipients are uniformly distributed on a circular service region with a centrally located depot. They applied continuous approximation methods to minimize total delivery costs and optimize service sub-region partitioning. Their model also incorporated package deliveries by truck, aiming to optimize the package delivery ratio between truck and drone while accounting for constraints such as limited truck capacity. Meanwhile, Perera et al. (2020) modelled a drone delivery system where recipients are uniformly distributed on the circumference of a circle and evaluated the impact of drone technologies on logistics systems parameters and efficiency gains over traditional truck logistics. Their findings highlight that, as drone technologies mature and become more cost-effective, decentralized delivery systems become more profitable and can offer more delivery options (e.g., same-day or one-hour delivery guarantees) and greater profit. An existing gap in the literature on such strategic models is the lack of consideration of operational limitations such as drone payload capacity and flight range. We address these gaps while considering the operational characteristics and limitations of drone delivery. Although a mixed fleet of trucks and drones adds complexity to this problem due to the necessary synchronization between truck paths and drone trajectories, a mixed fleet is more practical, as it offers greater flexibility and economic advantage.

C.3 Last-Mile Delivery of Perishable Goods

Researchers have addressed specific challenges associated with managing perishability in supply chains to extend the discussion on VRPs for perishable deliveries. In this section, we are focusing on the delivery of perishable goods, and readers are referred to (Karaesmen, Scheller-Wolf, and Deniz 2011) and (Baron 2010) for a more in-depth read on perishable inventory management.

Hwang (1999) developed a distribution model aimed at optimizing food supply in famine relief, emphasizing inventory allocation and minimizing human suffering rather than travel distance or time. In contrast, Tarantilis, Kiranoudis, and Vassiliadis (2004) proposed a threshold-accepting algorithm to address the fresh milk distribution problem, treating it as a heterogeneous fixed fleet vehicle routing problem, although they did not consider perishability explicitly. Further contributions include models that incorporate perishability and time windows. Chen, Hsueh, and Chang (2009) introduced a non-linear model for the VRP with time windows (VRPTW) for perishable food, focusing on maximizing supplier profit while considering both production and routing under stochastic demand. Osvald and Stirn (2008) extended the VRPTW by accounting for time-dependent travel times and perishability, presenting a heuristic algorithm for the distribution of fresh vegetables. Hsu, Hung, and Li (2007) considered the randomness in perishable food delivery with a stochastic VRPTW model that optimized routes, loads, and dispatch times. For further reviews on the role of perishability in VRP, Amorim and Almada-Lobo (2014) and Utama et al. (2020) provide detailed insights.

Few studies address the role of emerging technologies in perishable goods delivery. Zhao and Lee (2023) explores the potential of connected and autonomous vehicles (CAVs) in supply chain systems, discussing how higher CAV adoption rates can reduce travel time, particularly for long-distance deliveries of perishable products. Haji et al. (2020) conducted a comprehensive review of the role of technology in improving perishable food supply chains, with an emphasis on automated systems and sensors that monitor product quality. Gharehgozli et al. (2017) highlighted technological advances in agricultural production and food preparation while noting the limited focus on logistics. Although technological advancements are beginning to influence logistics for perishable goods, the role of autonomous vehicles in this domain remains unexplored.

C.4 Crowdsourcing in Last-Mile Delivery

Due to mounting economic pressures in the last decade, consumers are more inclined to share goods and services, and the propensity to own is slowly fading. One prominent example of the sharing economy is mobility services (Hu 2019). Crowdsourced delivery (crowd-shipping) is a mobility service where recipients acquire the role of drivers and make deliveries from retailer locations to other recipients; they become ad-hoc delivery drivers. Qi et al. (2018) present approximation models to assess the impacts of crowdsourcing in the last mile delivery. Their analysis of realistic settings shows that crowdsourcing is not as scalable as the conventional truck-only system in terms of operating cost. Liu, He, and Shen (2018) study driver routing behaviour in crowdsourcing services to assess the on-time performance of last-mile delivery. Using continuum approximations, they integrate travel time predictors with order assignment optimization and show the importance of learning behavioural features from operational data. Other examples of crowdsourcing can be found in (Dayarian and Savelsbergh 2017, Behrend and Meisel 2018, Mak 2018, Macrina et al. 2020).

Crowdsourcing initiatives are also becoming more ubiquitous in practice. ShipperBee is a crowd-sourced distributor that owns pickup and delivery lockers throughout the City of Toronto (shipperbee.com). According to ShipperBee's crowdsourcing business model, ad hoc drivers choose an item to deliver and open a designated pickup station with an assigned lock code. This analysis explicitly considers the advantages of locating pickup stations to reduce the delivery load on ad-hoc drivers in crowdsourcing systems.

Section D: Study Scope and Research Objectives

This research focuses on designing multi-echelon last-mile delivery systems, particularly two-echelon deliveries, using a hybrid fleet of trucks and autonomous mediums. Last-mile delivery is the process of delivering packages from distribution centers to a customer's location. In the proposed system, trucks carry the packages for the first part of the delivery and stop at predefined stops (hubs), where the first echelon ends. At these hubs, packages are handed off to the second delivery medium. This research considers two autonomous mediums for the final part of the delivery: i) AVs and ii) Drones.

In ”Recipient-dependent Last-Mile Delivery Routing With Autonomous Vehicle Applications,” we explore the role of recipient-dependent deliveries, where recipients use their AVs to participate in deliveries. In ”Parametric Design of Time-Sensitive Routing With Recipient-Dependent Contributions,” we extend recipient-dependent delivery using AVs to the case of perishable deliveries, where the time goods spend in transit becomes a critical constraint. In ”Tactical Fleet Planning for Drone-Based Delivery Systems,” we focus on the case where trucks leave the depot with both packages and drones, and drones are responsible for the final delivery to customers. This analysis highlights several managerial insights on the efficacy of multi-echelon last-mile delivery systems with autonomous mediums.

The main objective of this study is to explore how emerging technologies—specifically autonomous vehicles and drones—can improve last-mile delivery systems. This is achieved through the following research objectives:

- To analyze the operational role and performance impact of emerging delivery technologies in last-mile delivery systems, focusing on their potential to address key logistical challenges such as delivery speed and cost.
- To develop strategic-level parametric models that capture the design complexities of the delivery systems involving emerging technologies, incorporating constraints related to fleet composition, routing, vehicle coordination, and facility location.
- To evaluate the evolution of traditional last-mile delivery paradigms by benchmarking

technology-enabled delivery policies against conventional truck-based models, identifying dominance regions, cost-efficiency thresholds, and scalability conditions through analytical comparisons and numerical validation.

To achieve this, the research develops mathematical models that capture the complex relationships and trade-offs inherent in hybrid delivery systems composed of both traditional and autonomous mediums. These models are designed to reflect key operational characteristics such as delivery costs, time sensitivity, fleet composition, and routing constraints. One of the core modeling principles used is parametric design, which provides a flexible framework for exploring how system outcomes change with variations in structural and operational parameters. The models aim to offer analytical results that are generalizable and supported by practical case studies, with the goal of deriving meaningful managerial insights that can assist researchers, logistics planners, and policymakers in making informed decisions about the adoption and integration of emerging delivery technologies.

Section E: Dissertation Outline

This dissertation is organized into three main chapters, each representing a distinct yet interconnected contribution to the design and optimization of multi-echelon last-mile delivery systems using emerging technologies. Following the introduction, Chapter 2 examines recipient-dependent delivery models facilitated by autonomous vehicles, analyzing a set of routing policies in which recipients participate in the delivery process through direct pickup, hub-based collection, or crowdsourced delivery. Chapter 3 builds on this framework by addressing the time-sensitive delivery of perishable goods, introducing length-constrained routing strategies that reflect the urgency of such deliveries, and comparing their performance to capacity-constrained models. Chapter 4 focuses on drone-assisted last-mile delivery, presenting a tactical fleet planning model that incorporates key operational constraints, such as drone range, truck capacity, and vehicle synchronization, using a continuous approximation approach. Each chapter begins with a research summary, followed by an introduction that details the research question and outlines the motivation and relevance of the study and reviews related literature specific to the research. This is followed by detailed sections on methodology and analysis, presentation of results, and validation through a case study. Each chapter concludes with a summary of key insights and directions for future research. The final part of the dissertation includes appendices corresponding to each chapter, which provide supplementary material, extended formulations, and additional numerical analysis supporting the core contributions.

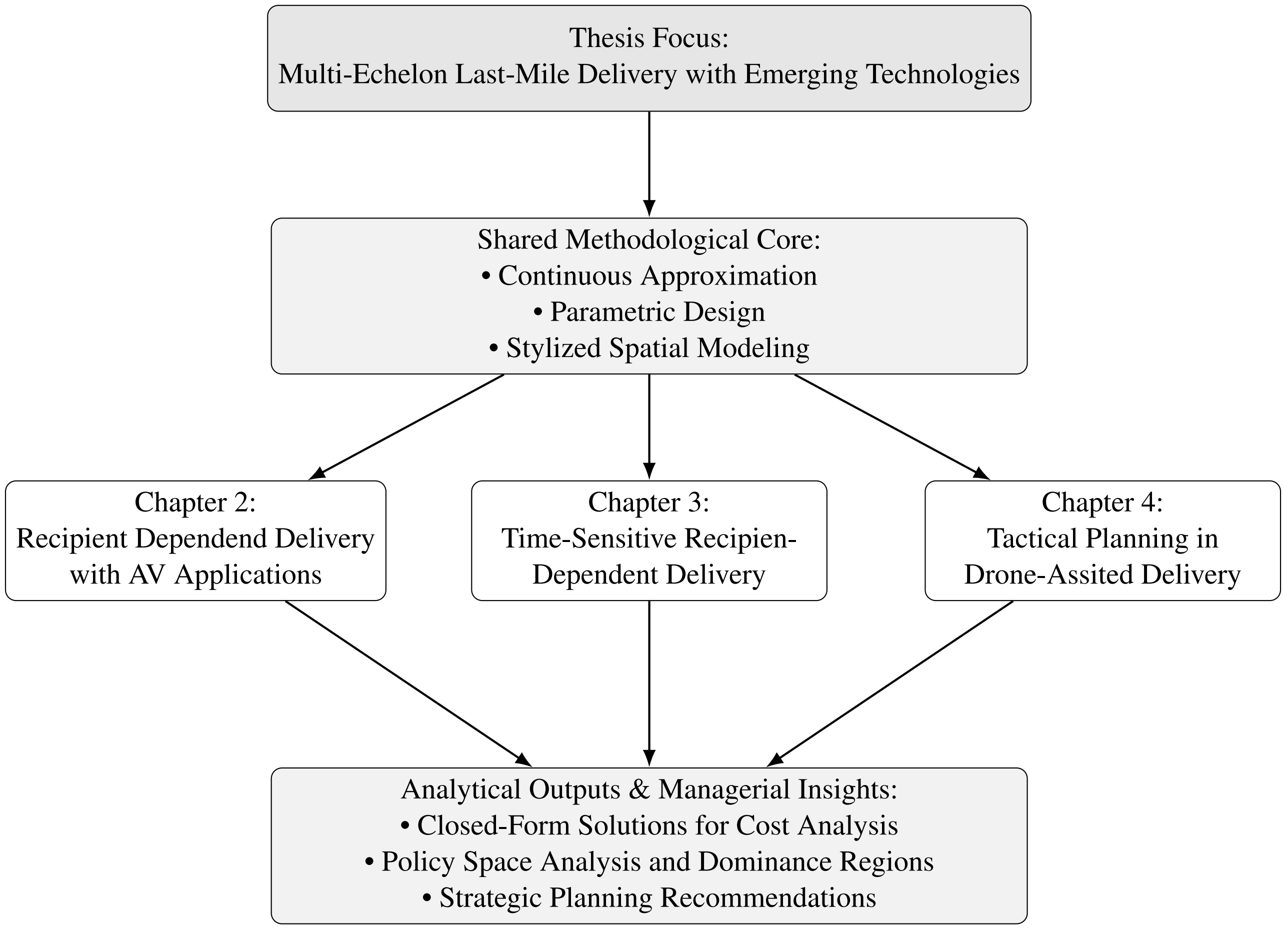

Figure One.3: Integration roadmap of the thesis chapters and their shared methodological core.

Chapter Two Recipient-Dependent Last-Mile Delivery Routing With Autonomous Vehicle Applications

Research Summary

Last-mile delivery contributes to a drastic 28% of the total cost of shipping. Recent technological advancements enable recipients to participate in these deliveries, relieving the cost of this final leg of the supply chain. We present models of recipient-dependent routing policies in last-mile logistics. The policies are not limited to but are motivated by the future applications of autonomous vehicles in smart cities and their role in enabling recipient-dependent deliveries as they relinquish the need for drivers. The policies are based on scenarios where recipients use their AVs to pick up from (i) a central depot, (ii) a hub located by the logistics firm close to them (Hybrid), and (iii) a hub and deliver to other nearby recipients (Crowdsourcing). We present upper and lower bounds on the total cost of each policy, compare these policies with the status quo truck delivery, and investigate the potential cost savings. The analysis shows a robust dominance space pattern against key operational parameters. In particular, (i) status quo truck routing is the currently preferred delivery policy, (ii) the Hybrid and Crowdsourcing policies are a combination of AV and status quo Truck policies in terms of dominance space, and (iii) recipient-dependent routing policies dominate the status quo Truck policy as the number of recipients increases. We validate the insights from the stylized model with a case study of Walmart in Toronto. (D Viniche et al. 2023a)

Section A: Introduction

Last-mile delivery is the movement of goods from distribution centers to final destinations, often residences. Last-mile delivery aims to make speedy deliveries to recipients at minimum cost. This final leg of the supply chain makes up a drastic 28% of the total cost of delivery (Hochfelder 2017). An emerging approach to alleviating the load of the last mile has been to request recipients to partake in the delivery by making a self-pickup from a designated location, either a depot or a hub operated by the logistics firm. There are several examples of such recipient-dependent deliveries in practice. Superstores such as Walmart and Loblaws currently provide self-pickup stations where staff load vehicles with items previously ordered online. Recent technological advancements in the automation industry have facilitated recipient participation in last-mile delivery. A notable technology in this context is autonomous vehicles (AVs), which can transport and pick up goods without human drivers.

The global last-mile delivery market is expected to reach $470 billion (similar to the GDP of Belgium), and automation and electrical vehicles (EVs) will be keys to achieving efficient and sustainable growth in this sector (McKinsey 2019). Currently, Europe, China, and the United States are at the forefront of this increasing trend (He 2021). With the US and China leading the way in this sector, many retailers have already taken the initiative to include AVs in their fleets, including Starship Technologies and Nuro. In the US, Walmart and Kroger have partnered with Nuro to use AVs to deliver groceries in Scottsdale and Houston. China is conducting trial runs in logistic parks, private communities, university campuses, and open public roads in major cities like Beijing and Shenzhen. Moreover, Neolix has begun mass production of delivery AVs to serve tech giants such as Huawei.

AVs offer the opportunity to avoid visiting retail stores in person. AV owners can instead send their AVs to collect items ordered online, thereby promoting a form of self-pickup for customers. Self-pickup with AVs is compatible with existing drive-through pickup stations at Walmart and Loblaws, initially designed for human-operated vehicles, demonstrating adaptability to AVs. AVs are also compatible with curb-side pickup remedies, which have seen a significant increase in adoption for various applications, such as grocery and retail goods collection. This trend reflects a broader shift towards more contactless and efficient delivery methods. For instance, many grocery stores and restaurants have expanded their curbside pickup services to facilitate a contactless shopping experience, allowing customers to receive orders without leaving their vehicles. AV pickups would also alleviate the discomfort of recipients who previously had to remain onsite (at home) during delivery time windows dictated by carriers. AVs introduce more flexibility, allowing recipients to choose their pickup time more flexibly to reduce the likelihood of missed deliveries. Delivery outside of the imposed time window affects recipient loyalty, retailer reputation, and delivery cost. Voxware reports from a survey of 500 recipients that 69% of respondents are less likely to choose the same retailer if an item is not received within two days of the promised delivery date (Kela, 2016).

AVs will also promote the sharing economy in the last mile. AV-equipped recipients can leverage peer-to-peer (P2P) sharing and lend their cars to make deliveries for neighbors within a vicinity. General Motors is promoting P2P sharing as it plans to launch a rental program, allowing GM vehicle owners to post their AVs to rent through the automaker's car-sharing platform, thus generating revenue for the company's vehicle owners (Washington Post 2018). AV sharing is more convenient and effective than existing ridesharing and crowd-shipping services because AVs do not need human drivers (with work shifts) and can be shared more seamlessly. This allows mobility service operators to increase the supply of vehicles and improve the level of service provided to recipients (Fagnant and Kockelman 2015). Existing logistics firms are currently exploiting the benefits of crowdsourcing. Amazon Flex and Roadie are crowdsourcing firms that recruit on-demand drivers to make deliveries (Economist, 2019). Roadie generates 80% of its revenue from deliveries for Walmart, Macy's, and Home Depot. AVs could advance current crowdsourcing platforms as they are more flexible and generate revenue for owners.

Our research focuses on emerging delivery policies that depend on recipient participation. We consider three operational policies in which recipients (i) pick up from the central depot, i.e., directly send their AVs to a retailer's location (AV policy), (ii) pick up from a hub located by the logistics firm close to them, i.e., send their AVs to designated hubs selected by the retailer (Hybrid policy), or (iii) pick up from a hub and make deliveries to other nearby recipients as well, i.e., lend their AVs to complete deliveries for themselves and their neighbors (Crowdsourcing policy). AVs would enable such policies by reducing the cost, as the opportunity cost of the driver is no longer present. While these recipient-dependent policies are relevant even without AVs, we use AV-related terminology to explain them and discuss their future impacts. We model these three policies and derive upper and lower bounds on the total cost of each policy. We compare these policies with the status quo Truck policy, where retailers use a fleet of trucks for deliveries (Truck policy).

Recipients incur discomfort when partaking in the delivery process, primarily because it requires them to actively spend their time or use their vehicles to collect parcels. Logistics firms can alleviate this burden by providing financial compensation or allowing recipients to visit designated pickup stations instead of a depot that is farther away. Pickup stations are dispersed in an area and operated by the logistics firm. For example, Amazon uses Whole Foods store locations as potential pickup locations for its e-commerce recipients. All major Chinese e-retailers also offer pickup locations in many major cities where universities and subway stations are common pickup locations.

At the operational level, the quest to find the optimal set of remote pickup locations is a multi-echelon routing problem. In our context, this problem is a variant of the vehicle routing problem with trucks that travel between a depot and the pickup stations and AVs that travel between the pickup stations and recipient homes (Perboli, Tadei, and Vigo 2011). The vehicle routing problem takes precise parameters and provides detailed recipient visit schedules for each vehicle. This level of detail is helpful for day-to-day operational-level decisions. However, in strategic-level decisions, the objective is to have a holistic comparison of various policies without complete or accurate data on operating conditions, such as the exact location of recipients each day.

We study strategic-level decisions and analyze alternative recipient-dependent delivery policies to gain insights into the parameters of the system that affect its performance and make different policies preferable. Our analysis stems from the literature on vehicle routing approximations that assume the recipients are: (i) dispersed on a surface with a given spatial distribution (Newell and Daganzo 1986a,c), (ii) served by vehicles, or (iii) located on a stylized geometrical shape (e.g., the arc of a circle) (Archetti, Savelsbergh, and Speranza 2006). Such approximations often yield closed-form derivations of the length of tours required to visit a set of recipients (Bertsimas and Van Ryzin 1991). Our approximations are similar in nature to the worst-case scenario routing analysis in Archetti, Savelsbergh, and Speranza (2006).

We develop two stylized models: the ring and disk models. The ring model assumes a one-dimensional distribution where the depot is located in the center of a ring, with a radius of one, and n recipients, each with unit demand, are located on the circumference of the ring with equal spacing. The disk model assumes a two-dimensional distribution with the same location of the depot in the center of the unit radius disk, with the recipients dispersed on the surface of the disk rather than only on the circumference of the ring. We consider a linear cost of travelling for trucks and AVs per unit distance traveled and a hand-off cost relative to the number of locations where shipment ownership changes (e.g., from a truck to a recipient). We use stylized models as abstractions of reality to identify the dominant policy with the lowest total system cost under various operating conditions. For routing on a disk, we derive analytical expressions for the upper and lower bounds of the costs of the different policies and compare these costs with each other. We derive the asymptotic properties for the upper and lower bounds of each policy when the number of recipients tends to infinity, to compare these bounds. Moreover, we derive the asymptotic properties for both ring and disk routing strategies to provide an approximation of policy costs, and we compare the asymptotic costs of the two strategies and show their similarity up to a constant factor.

This analysis allows us to highlight several managerial insights on the efficacy of different recipient-dependent last-mile delivery policies. We characterize the dominant policy and its dependence on the relative cost of AVs to trucks and the hand-off cost; see Figures Two.8, Two.9 and their discussion. We demonstrate that the status quo Truck policy is still the preferred delivery method because of the high cost of AVs (see Insight 1). We also show that the Hybrid and Crowdsourcing policies are sandwiched between the AV and Truck policies (see Insight 2 and Figures Two.8 and Two.9). Although AVs are not currently owned at scale, they will become more prominent with time due to improvements in mass production and technology (e.g., Lidar detection). Transitioning to full fleet automation is gradual and may require a phase where

Hybrid and Crowdsourcing policies dominate. Crowdsourcing delivery policies predominantly offered for food delivery services can evolve as AVs replace manned delivery vehicles, i.e., reduce the per-mile cost of this delivery method. As more recipients enter the system, the cost of the Truck policy becomes larger than the cost of other policies (see Insight 3 and Figures Two.8 and Two.9), and when the number of recipients asymptotically tends to infinity, the Truck policy is dominated by one of the other three policies (see Insights 4 and 5, and Figures Two.8b). We also show that varying the hand-off cost perturbs the dominance space boundaries, but the overall pattern of the dominance space remains the same (see Insight 6).

We validate the findings and managerial insights from the stylized model with numerical experiments from a case study of a Walmart branch in Toronto and recipients who are dispersed around this branch according to population densities. We observe that the dominant policies and the main insights from the stylized model are aligned with those from the case study. Extensive analysis of several parameters, including the hand-off cost, shows that although the dominance space boundaries are perturbed, the overall pattern of the dominance space remains the same.

The remainder of this paper is organized as follows. In Section B, we review the related literature. In Section C, we present the four policies and derive the optimal cost of each policy for routing on a ring. In Section 4, we present an extension to our model: routing on a disk. In Section E, we compare the policies to determine which one is dominant and when, and in Section F, we present a case study. In Section G, we provide conclusions. All proofs are in Appendix A in the e-companion.

Section B: Related works

We review relevant literature on vehicle routing approximation models, crowdsourcing deliveries, and future applications and existing uses of AVs in Sections B.1, B.2, and B.3, respectively.

B.1 Vehicle routing approximations

The vehicle routing problem seeks to find the optimal set of routes for a fleet of vehicles that visit a set of recipients only once. The conventional formulation is a combinatorial optimization problem that is *NP*-hard (Laporte 1992) and commonly solved by integer programming. This approach is data hungry (because it requires the exact location of recipients and their delivery loads) and less suitable for strategic-level decisions where data is limited, and the level of accuracy in terms of finding exact routes is less important. A plausible alternative is to approximate the vehicle routing problem, typically using one of the following three approaches.

The first approach is *continuum approximation* that shifts from the conventional integer programming formulation to a continuous space by assuming that recipients are spread out on an Euclidean surface with a density distribution. Ansari et al. (2018) provides a comprehensive review of continuous approximation (CA) techniques and their application in addressing various challenges within the transportation domain. Carlsson and Song (2018) uses the continuous approximation method to approximate the cost of a two-echelon vehicle routing problem with trucks and drones that serve a set of recipients distributed on a surface. The drones are dispatched from the trucks at designated launch points to visit their assigned recipients and return to the truck at a retrieval point. The model approximates the total delivery time w.r.t. the density of recipients. Agatz et al. (2011) studies the home delivery problem of e-retailers who commonly suffer from narrow delivery times. To lessen this burden on the recipients, a set of time slots are assigned to each zip code and the delivery routes are generated using the approximation method of Daganzo (2005). Carlsson et al. (2016) studies the household scheduling problem as a variant of the generalized travelling salesman problem. Each household member performs errands in the course of a day (e.g., going to the bank and grocery shopping afterward) and must choose a location for performing each task. They derive the approximate length of the household trips using continuum approximations that generalize the derivations of Beardwood, Halton, and Hammersley (1959) and Redmond and Yukich (1994) for the travelling salesman problem with a large number of recipients. For a review of continuum approximation models, we suggest Langevin, Mbaraga, and Campbell (1996) and Ansari et al. (2018).

The second approach treats vehicles as servers of a queue system. Bertsimas and Van Ryzin (1991) study the dynamic and stochastic vehicle routing problem with the objective of minimizing the waiting time of recipients for service. They assume recipients arrive according to a Poisson process and are independent and uniformly distributed in an Euclidean service region.

The model shows that the waiting time grows faster than the waiting time in conventional queues under heavy traffic, and the stability condition does not depend on the system geometry, which validates the use of the approximation for an otherwise complex vehicle routing model. Other examples of using queue models for service routing can be found in Bellos, Ferguson, and Toktay (2017), Psaraftis (1995), and Bertsimas and Simchi-Levi (1996).

The third approach assumes recipients are located on a geometric shape (e.g., a circle). Archetti, Savelsbergh, and Speranza (2006) studies the worse-case of the split vehicle routing problem (where recipients can be visited more than once) originally presented by Dror and Trudeau (1989, 1990), and use an approximation to derive closed-form performance measures. In their analysis, recipients are located on the arc of a circle. Another similar approach is to use space-filling curves that are continuous mappings from a lower-dimensional to a higher-dimensional space (Sagan 2012). As an example, the Sierpinski curve is formed by repeatedly copying and shrinking a simple pattern (Bartholdi III 1995). Bartholdi III and Platzman (1988) use space-filling curves to develop novel heuristics for routing and partitioning combinatorial problems. This approach follows the setting where recipients are located on a circle similar to Archetti, Savelsbergh, and Speranza (2006).

B.2 Crowdsourcing delivery

Due to mounting economic pressures in the last decade, consumers are more inclined to share goods and services, and the propensity to own is slowly fading. One prominent example of the sharing economy is mobility services (Hu 2019). Crowdsourced delivery (crowd-shipping) is a mobility service where recipients acquire the role of drivers and make deliveries from retailer locations to other recipients; they become ad-hoc delivery drivers. Qi et al. (2018) present approximation models to assess the impacts of crowdsourcing in the last mile delivery. Their analysis of realistic settings shows that crowdsourcing is not as scalable as the conventional truck-only system in terms of operating cost. Liu, He, and Shen (2018) study driver routing behaviour in crowdsourcing services to assess the on-time performance of last-mile delivery. Using continuum approximations, they integrate travel time predictors with order assignment optimization and show the importance of learning behavioural features from operational data.

Other examples of crowdsourcing can be found in (Dayarian and Savelsbergh 2017, Behrend and Meisel 2018, Mak 2018, Macrina et al. 2020).

Crowdsourcing initiatives are also becoming more ubiquitous in practice. ShipperBee is a crowd-sourced distributor that owns pickup and delivery lockers throughout the City of Toronto (shipperbee.com). According to ShipperBee's crowdsourcing business model, ad hoc drivers choose an item to deliver and open a designated pickup station with an assigned lock code. This analysis explicitly considers the advantages of locating pickup stations to reduce the delivery load on ad-hoc drivers in crowdsourcing systems.

B.3 Autonomous vehicles

AVs can radically alter mobility patterns and improve the performance of transportation systems. They have many advantages over regular vehicles, including their ability to communicate with each other and the infrastructure, which makes traffic smoother with less abrupt acceleration and braking. Their driverless capability also allows for new travel behaviour and consumption patterns. For example, household activity schedules may vary as some parents no longer need to drive their children to school and can use an AV as a chauffeur (Fagnant and Kockelman 2014, Xu, Mahmassani, and Chen 2019a,b). Baron, Berman, and Nourinejad (2020) introduce the properties of AVs and assess their impacts in terms of three C's: *Connectivity* with other AVs on the road and the transportation infrastructure, the *Comfort* of not driving and instead engaging in productive activities whilst in the car, and *Collaborative consumption* which allows travellers to share AVs together. Exploring the three C's, Baron, Berman, and Nourinejad (2020) show that AVs may negatively impact social welfare in cities that are not yet prepared with the proper infrastructure needs.

The literature on AVs is diverse and focuses on topics such as willingness-to-pay for AVs (Bansal and Kockelman 2017), fuel economy (Mersky and Samaras 2016), traffic flow (Mahmassani 2016, de Oliveira 2017, Mirzaeian, Cho, and Scheller-Wolf 2020), induced traffic (Harper et al. 2016), AV parking (Nourinejad and Roorda 2018), and the use of AVs as a shared fleet between a group of recipients (Fagnant and Kockelman 2014, Chen et al. 2016). Although many features of AVs are currently being investigated, their impacts on logistics services are less explored. In this paper, we consider that recipients have access to AVs and can use them for last-mile deliveries.

Section C: Routing on a Ring

Consider a depot located at the center of a circle with a radius normalized to 1. A total of n recipients are located on the circle's boundary. We consider two alternative recipient distributions, a 1-dimensional and a 2-dimensional one. Here, we explain our policies for the 1-dimensional model. Under this model, the n recipients are located on the circumference of the circle (a ring) with density $\delta = n/2\pi$. The expected distance between every two adjacent recipients is $\Delta = 2\pi/n$. The analysis of the 2-dimensional model, where recipients are located on the surface of the circle, is presented in section 4. We assume all recipients are willing to make a self-pickup if they are reimbursed for their discomfort, e.g., via a discount on the shipping fee.

The operator serves recipients from the depot using one of the four policies depicted in Figure Two.1. In the *Truck* policy, a fleet of trucks leaves the depot, visits a set of recipients, and returns to the depot. In the *Autonomous Vehicle* policy, each recipient sends their unoccupied AV to the depot and back. The operator reimburses these recipients in proportion to the distance traveled. An extension is considering the tendency of AV owners to participate in the last-mile delivery if the reimbursement is larger than their opportunity cost, which requires remodelling the problem as a two-sided market with ad-hoc earning sensitive AV owners and is beyond the scope of our study. The *Hybrid* policy combines the first two policies, where the operator dispatches its trucks to designated hubs (pickup stations) and AVs visit the hubs. Finally, the operator crowdsources deliveries to designated AVs in the *Crowdsourcing* policy. The operator first dispatches its trucks to designated hubs; designated AVs are responsible for delivering to a set of recipients by driving to their closest hub, making deliveries to the set of recipients, and returning to their original owners.

Let the subscript $j = \{q, v\}$ denote the truck and AV modes of transportation, respectively, and let the superscript $i = \{t, a, h, w\}$ denote the Truck, AV, Hybrid, and Crowdsourcing policies, respectively. The operator incurs a travel cost for trucks and AVs in each policy. The travel cost per unit distance of trucks and AVs is c_q and c_v, respectively, where c_v is the opportunity cost of AV owners per unit distance traveled. The cost, c_v, also incorporates any payments made by the logistics firm to the AV owners for their inconvenience. The total distance of mode j in policy i is d^i_j. Thus, the travel cost of policy i is $c_q d^i_q + c_v d^i_v$. We assume a fixed truck acquisition cost is prorated in the variable cost per unit distance of a truck (c_q).

The operator also incurs a hand-off cost to support the infrastructure needed to allow items to change ownership. It is equivalent to a setup cost, e.g., trucks need to find parking when making a delivery to a recipient, or AV-enabled deliveries require a platform that tracks the location of AVs to prepare and load the requested items at the time of the vehicle's arrival. This hand-off cost is proportional to the number of stops where the ownership changes from one party to another.

Let s^i and c^i_s be the number and marginal cost of hand-offs in policy i. The total hand-off cost of policy i is $c^i_s s^i$. We denote the total cost of policy i as z^i, expressed as

$$z^i = c_q d^i_q + c_v d^i_v + c^i_s s^i. \tag{Two.1}$$

C.1 Truck policy

Consider the Truck policy of Figure Two.1a, which has f^t truck routes of the same length (each covered by one truck), visiting x^t recipients, such that $f^t = \lceil n/x^t \rceil$. We assume that $n \gg x^t$, and

Figure Two.1: Four distribution policies. The thick black and thin gray lines represent truck and AV routes, respectively.

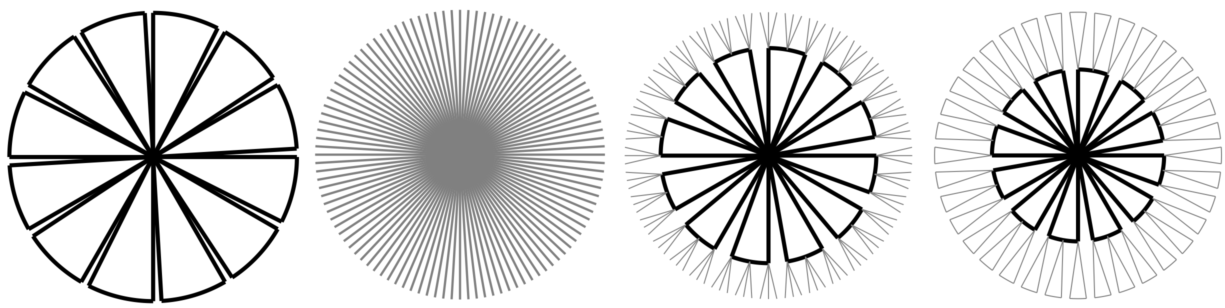

(a) Truck (b) Autonomous Vehicle (c) Hybrid (d) Crowdsourcing thus approximate f^t as

$$f^t = \frac{n}{x^t}. \tag{Two.2}$$

The length of each truck route l^t is

$$\begin{aligned} l^t &= 2 + (x^t - 1)\Delta \\ &\approx 2 + x^t \Delta, \end{aligned} \tag{Two.3}$$

where $\Delta = 2\pi/n$ is negligible in the approximation when n is large. The two terms in (Two.3) represent the length of inbound and outbound trips (each with length 1) and the sum of traveled arcs on the ring to visit the recipients, respectively. The total truck distance is $d_q^t = f^t l^t$ obtained from (Two.2) and (Two.3). We relax all approximations in the case study of Section F.

Each truck has a capacity of visiting K recipients. Thus, in this policy, the number of recipients per truck route is equal to the truck's capacity:

$$x^t = K. \tag{Two.4}$$

The hand-off in the Truck policy represents the inconvenience of finding a parking spot near the recipient's location and finding the recipient's door on foot. There are n hand-offs in the Truck policy because the trucks stop at every recipient's location.

Given (1) and our discussion in this section, the total cost of the Truck policy is $z^t = c_q f^t l^t + c_s^t n$. We derive the Truck policy cost, z^t, in the following proposition.

PROPOSITION C.1.1. The Truck policy cost under the approximated tour length and size is

$$z^t = 2c_q(\pi + \frac{n}{K}) + c_s^t n \tag{Two.5}$$

C.2 Autonomous Vehicle policy

In the Autonomous Vehicle (AV) policy, the AVs perform the deliveries, as shown in Figure Two.1b. The total AV travel length is $d_v^a = 2n$, where 2 accounts for each recipient's inbound and outbound trips. In the AV policy, the hand-off is the cost of establishing an automation center at the depot that connects to arriving AVs and loads them with the requested items. There is only one stop at the center of the circle where the operator loads the items onto the AVs, i.e., $s^a = 1$. Hence, the hand-off cost is c_s^a. The total AV policy cost, z^v, is

$$z^v = 2c_v n + c_s^a. \tag{Two.6}$$

C.3 Hybrid policy

In the Hybrid policy, each truck travels a radius of r from the depot, stops at x^h hubs on the ring (each at a distance r away from the depot and equally spaced), and then returns to the depot. Recipients send their AVs to pick up their orders from these hubs. There are m recipients that use their AVs to visit the same closest hub, e.g., $m = 3$ in Figure Two.1c. The number of recipients per hub, m, times the number of hubs per truck, x^h, is obviously bounded by the truck capacity, i.e., $mx^h \leq K$. Figure Two.2 shows two special cases of the Hybrid policy where $m = 1$ and $m = K$. The number of hand-offs in this policy is equal to the number of hubs as it stands for where the ownership changes. Since m recipients send their AVs to each hub, the total number of hubs and, consequently, the number of hand-offs is n/m. For example, where $m = 1$, there are $s^h = n$ hand-offs because each recipient has a designated hub, and for $m = K$, there are $s^h = n/K$ hand-offs as each truck route has a single hub. The n/m hubs are equally spaced from each other, located at a distance r from the depot, and their distance from each other is $\Delta^h = 2rm\pi/n$.

We note that both r and m are decision variables chosen to minimize the operator's cost. Note that when $r = 1$, the travel cost of the Hybrid policy is identical to the Truck policy, but the Hybrid policy has fewer hand-offs. Similarly, when $r = 0$, the travel cost of the Hybrid policy is identical to the AV policy, but the Hybrid policy has more hand-offs.

There are f^h truck routes that have the same length, and each visits an average of mx^h

Figure Two.2: Boundary condition cases of the Hybrid policy. Thick black lines represent truck routes, and thin gray lines represent AV routes. Panel a) $m = 1$; Panel b) $m = K$.

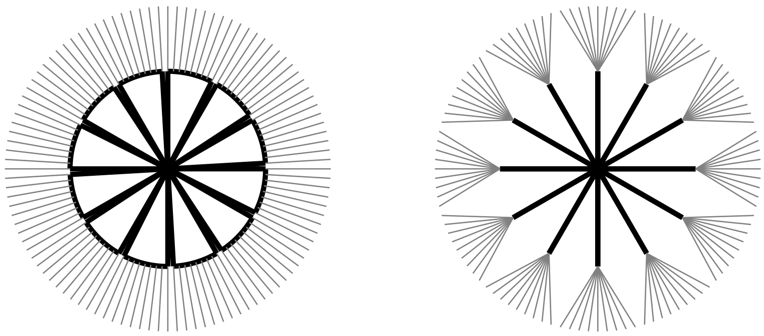

(a) (b)

recipients such that $f^h = \lceil n/mx^h \rceil$. When $n/m \gg x^h$, we approximate f^h as

$$f^h = \frac{n}{mx^h}. \tag{Two.7}$$

The length of each route is l^h, given by

$$\begin{aligned} l^h &= 2r + (x^h - 1)\Delta^h \\ &\approx 2r + x^h \Delta^h, \end{aligned} \tag{Two.8}$$

where similar to (Two.3), Δ^h is negligible when n is large. We relax the approximation in $(Two.8)$ in the case study of Section F. The number of hubs per route is bounded by the truck capacity:

$$x^h = \frac{K}{m}, \tag{Two.9}$$

We use (Two.9) to derive the number of truck routes (Two.7) and the length of each route (Two.8).

The number of hand-offs in the Hybrid policy is the number of hubs, which is $s^h = n/m$, and the hand-off cost is $c_s^h n/m$. The truck cost is $c_q d_q^h$ where $d_q^h = f^h l^h$ and the AV cost is $c_v d_v^h$.

We approximate the AV distance d_v^h given in Lemma A.1 of Appendix A in e-companion as:

$$d_v^h \approx 2n(1-r) + \frac{m^2\pi^2 r}{3(1-r)}. \tag{Two.10}$$

As a special case of (Two.10), when $r = 0$, the AV distance is $d_v^h \approx 2n$, which indicates that the recipients send their individual AVs to the depot as in the AV policy.

We minimize the cost of the Hybrid policy, z^h, at the optimal truck travel radius r_h^* and the optimal number of recipients per hub m^*. We derive r_h^* and m_h^* in the following proposition.

PROPOSITION C.3.1. The cost of the Hybrid policy, z^h, is

$$z^h \approx c_s^h \frac{n}{m} + c_v(2n(1-r) + \frac{m^2\pi^2 r}{3(1-r)}) + 2c_q(\frac{nr}{k} + r\pi) \tag{Two.11}$$

For any given number of recipients per hub, m, the Hybrid policy cost, z^h, is minimized at the following optimal radius

$\mathrm{r}_h^* = 1 - m\pi\sqrt{\frac{c_v K}{6(c_v Kn - c_q n - c_q K\pi)}}\mathrm{if}\ \frac{6(n+K\pi)}{6Kn - Km^2\pi^2} \leq \frac{c_v}{c_q},$

0 if $\frac{6(n+K\pi)}{6Kn - Km^2\pi^2} > \frac{c_v}{c_q},$

and for any given truck radius, r, the optimal number of recipients per hub is $\mathrm{m}_h^* = 1\mathrm{if}$

$\frac{3n(1-r)}{2\pi^2 r} \leq \frac{c_v}{c_s^h},$

$\sqrt[3]{\frac{3c_s^h n(1-r)}{2c_v\pi^2 r}}\mathrm{if}\ \frac{3n(1-r)}{2K^3\pi^2 r} \leq \frac{c_v}{c_s^h} < \frac{3c_s^h n(1-r)}{2\pi^2 r},$

K if $\frac{3n(1-r)}{2K^3\pi^2 r} > \frac{c_v}{c_s^h}.$

According to Proposition C.3.1, the optimal radius is related to the vehicle travel cost ratio c_v/c_q, whereas the number of recipients per hub depends on the ratio of the AV cost to the hand-off cost, c_v/c_s^h. Proposition C.3.1 presents a system of two equations with two unknowns. While these are easy to solve numerically, in general, there are no closed-form solutions for r_h^* and m_h^*. The lack of a closed-form expression also reduces the tractability of the Hessian matrix required to establish the optimality of the solutions. Nevertheless, in a detailed numerical experiment, the Hessian matrix showed convexity w.r.t. both r and m. In Section E.2, we numerically solve this system of equations to find r_h^* and m_h^*, and in Section E.3, we derive an asymptotic cost, z^h, in closed-form.

According to (C.3.1), r_h^* decreases linearly with m. Similarly, from $\partial m_h^*/\partial r$ in (C.3.1), m_h^* decreases with r_h^*. As a consequence, the operator experiences a trade-off in locating the hub closer to recipients but serving fewer recipients per hub and vice versa. Moreover, from $\partial r_h^*/\partial n$ in (C.3.1), when $K > c_q/c_v$ then r increases with the number of recipients n. That is the operator benefits from economies of scale of serving more recipients per truck and is willing to increase r_h^* to locate the hubs closer to recipients. Furthermore, as the cost ratio, c_v/c_q, increases, the operator locates the hubs closer to recipients to limit the large total AV distance.

C.4 Crowdsourcing policy

In the Crowdsourcing policy, each truck travels a radius r from the depot, stops at x^w hubs, and returns to the depot. Recipients lend their AVs to the operator to perform the deliveries. Each AV leaves the recipient's location, drives to the nearest hub, and returns to the ring to serve $m-1$ other recipients until it reaches its own location, as shown in Figure Two.1d. Thus, each AV serves m recipients, including its owner. For simplicity, we assume that AVs have a large enough capacity to serve these m recipients. It is evident that m is smaller than the truck capacity K.

The generic routing of the Crowdsourcing policy is presented in Figure Two.3, where for illustration purposes, $m = K$ (i.e., AVs have the same capacity as trucks) and $r \in (0,1)$. We present two boundary conditions of the Crowdsourcing policy in Figure Two.3 where $m = K$ and $r = \{0,1\}$. When $r = 1$, Figure Two.3b shows that the operator locates the hubs on the ring and AVs travel only on select arcs of the ring. In the other boundary condition, Figure Two.3c shows that when $r = 0$, the tours are traveled exclusively by recipient AVs. Here, the travel cost of the Crowdsourcing policy differs from the AV policy as AVs travel less to the depot.

The design of the Crowdsourcing policy routes is as follows. There are f^w truck routes that each visit x^w hubs. The length of each route is l^w. Similar to (Two.7) and (Two.8), we have

$$f^w \approx n/mx^w \quad and \quad l^w \approx 2r + x^w \Delta^w. \qquad \text{(Two.12)}$$

Figure Two.3: Boundary conditions of the Crowdsourcing policy. Thick black lines represent truck routes, and thin gray lines represent AV routes. In all panels, we set $m = K$. Panel a) $0 < r < 1$; Panel b) $r = 1$; Panel c) $r = 0$.

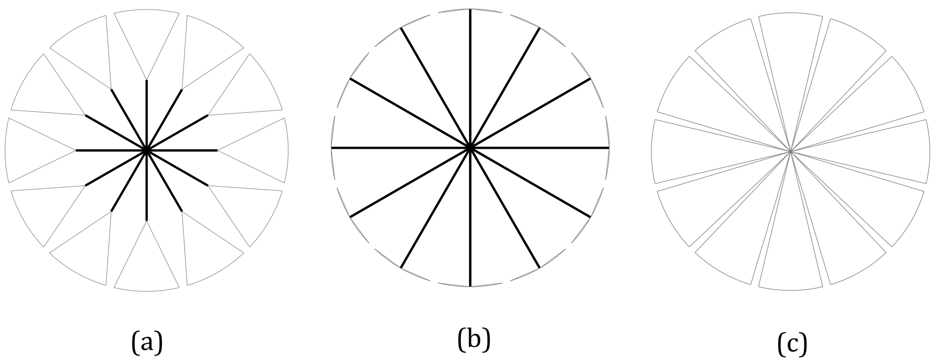

The hand-off cost for the Crowdsourcing policy is equal to the number of hubs (hand-off to AVs), in addition to the number of recipients (hand-off to recipients). Note that there would be no hand-off cost at the AV owner's location (similar to the AV policy), but we ignore this difference for simplicity. Thus, there are $s^w = n/m + n$ hand-offs.

The operator minimizes the sum of costs, z^w, according to (Two.1). The hand-off cost is $c_s^w(n/m+n)$, the truck cost is $c_q f^w l^w$, and the AV cost is $c_v d_v^w$. We approximate the AV distance d_v^w given in Lemma A.2 of Appendix A in e-companion as:

$$d_v^w \approx 2\pi + \frac{2n(1-r)}{m} + \frac{r\pi^2 m}{n(1-r)}, \tag{Two.13}$$

where the first term is the approximate distance traveled on the ring (the exact distance is $2\pi - n/m\Delta$), and the second and third terms are the line-haul distances. When $r = 0$, the AV distance is $d_v^w \approx 2\pi + 2n/m$ according to (Two.13), indicating that each of the n/m AVs has a line-haul distance of 2 and travels a distance of $2\pi m/n$ on the arcs of the ring to visit recipients.

We minimize the cost of the Crowdsourcing policy, z^w, at the optimal truck travel radius, r_w^*, and the optimal number of recipients per hub, m_w^*. The components of the Crowdsourcing policy cost, z^w, have been discussed in (Two.12) and (Two.13), and we use assumptions similar to the Hybrid Policy. We derive z^w, r_w^* and m_w^* in the following proposition.

PROPOSITION C.4.1. The Crowdsourcing policy cost, z^w, is

$$z^w \approx c_s^w(n+\frac{n}{m})+c_v(2\pi+\frac{2n(1-r)}{m}+\frac{r\pi^2 m}{n(1-r)})+2c_q(\frac{nr}{k}+r\pi) \qquad \text{(Two.14)}$$

For any given number of recipients per hub, m, the Hybrid policy cost, z^w, is minimized at the following optimal radius

$r_w^* = 1-m\pi\sqrt{\frac{c_vK}{2n(c_vKn-c_qmn-c_qKm\pi)}}$ if $\frac{2mn(n+K\pi)}{2Kn^2-Km^2\pi^2} \leq \frac{c_v}{c_q}$,

0 if $\frac{2mn(n+K\pi)}{2Kn^2-Km^2\pi^2} > \frac{c_v}{c_q}$, and for any given truck radius, r, the optimal number of recipients per hub is

$m_w^* = 1$ if $\frac{n^2(1-r)}{\pi^2 r-2n^2(1-r)^2} \leq \frac{c_v}{c_s^w}$,

$\frac{n}{\pi}\sqrt{\frac{c_s^w(1-r)+2c_v(1-r)^2}{rc_v}}$ if $\frac{n^2(1-r)}{K^2\pi^2 r-2n^2(1-r)^2} \leq \frac{c_v}{c_s^w} < \frac{n^2(1-r)}{\pi^2 r-2n^2(1-r)^2}$,

K if $\frac{c_v}{c_s^w} < \frac{n^2(1-r)}{K^2\pi^2 r-2n^2(1-r)^2}$.

Proposition C.4.1 also presents a system of two equations with two unknowns. In Section E.2, we numerically solve this system of equations to find r_w^* and m_w^* and in Section E.3, we derive an asymptotic cost, z^w, in closed-form.

According to (C.4.1), r_w^* decreases with m if $n > \frac{c_qKm\pi}{c_vK-c_qm}$ and according to (C.4.1), m_w^* decreases with r_w^*. Consequently, similar to the Hybrid policy, the operator experiences a trade-off in locating the hub closer to recipients but serving fewer recipients per hub and vice versa. Our numerical analysis shows that this system of equations is numerically convex.

Section D: Routing on a disk

In this section, we extend the previous model by assuming recipients are dispersed on the surface of a disk rather than only on the circumference of a ring. This setting is practical and requires minor modifications to each policy's routing strategy. We introduce additional bounds on the performance of each policy and compare the ring and circular routing results.

Following the previous notation convention, we use $j = \{q, v\}$ to denote the truck and AV modes of transportation, and $i = \{t, a, h, w\}$ to denote the Truck, AV, Hybrid, and Crowdsourcing policies, respectively. We consider that the depot is located at the center of a unit disk, and recipients are uniformly dispersed on the surface of the disk. The recipient density on the disk is δ so that there are $n = \pi\delta$ recipients in total. For the Truck, Hybrid, and Crowdsourcing policies, we propose the following routing heuristics for the truck routes. The heuristic divides the circular service area into C concentric rings, with equal distance, τ, between them and these rings are traversed by the trucks. The rings radii, R_i for $i = 1 \ldots C$, increase incrementally by τ, which is a decision variable of the heuristic, yielding the following radii:

$$R_1 = \tau/2 \,, \quad R_2 = 3\tau/2 \,, \quad R_i = (i - \frac{1}{2})\tau. \tag{Two.15}$$

We derive upper and lower bounds for each policy, considering that each truck services a specific neighborhood defined by its ring. Furthermore, we show that for each policy, the costs obtained under the lower and upper bounds have the same asymptotic properties (sandwich policy). Figure Two.4 illustrates an example of routing on a disk, where the circular surface is divided into a number of rings. These rings, shown by black lines, are traversed by trucks, and the AV distances are shown by thin yellow lines. Trucks may not always travel along the shortest paths within neighborhoods due to the higher density of obstacles like buildings. We considered this by using Euclidean travel distances (L2 norm) and Manhattan distances (L1 norm) in different scenarios. We explain the bounds within the descriptions of each policy. Additionally, the AV distances follow a specific routing strategy in the Hybrid and Crowdsourcing policies, which is consistent with the concept of short travels on local roads within each recipient's neighborhood. These strategies are depicted for a subset of recipients in Figure Two.4 and will be detailed in subsequent sections.

D.1 Truck policy on a disk

We first define the Truck policy heuristic, inspired by the Beardwood-Halton-Hammersley (BHH) Theorem and extended in studies such as Beardwood, Halton, and Hammersley (1959) to approximate the vehicle routing problem. As mentioned in the previous section, the circular service area is divided into concentric rings and each recipient is allocated to the ring nearest to them; therefore, the number of recipients on ring i can be obtained from the probability that a random recipient is closer to ring i than to any other ring. The number of recipients on ring i, derived in Appendix A in e-companion, is

$$n_i = (2i-1)\tau^2\pi\delta. \tag{Two.16}$$

Figure Two.4: Routing heuristics on a disk. Thick black and thin yellow lines represent truck and AV routes. Black squares represent hubs in panels (c) and (d). In panels (a), (c), and (d), the disk is divided into concentric rings. Dots represent recipients, and each color colour represent recipients assigned to each ring.

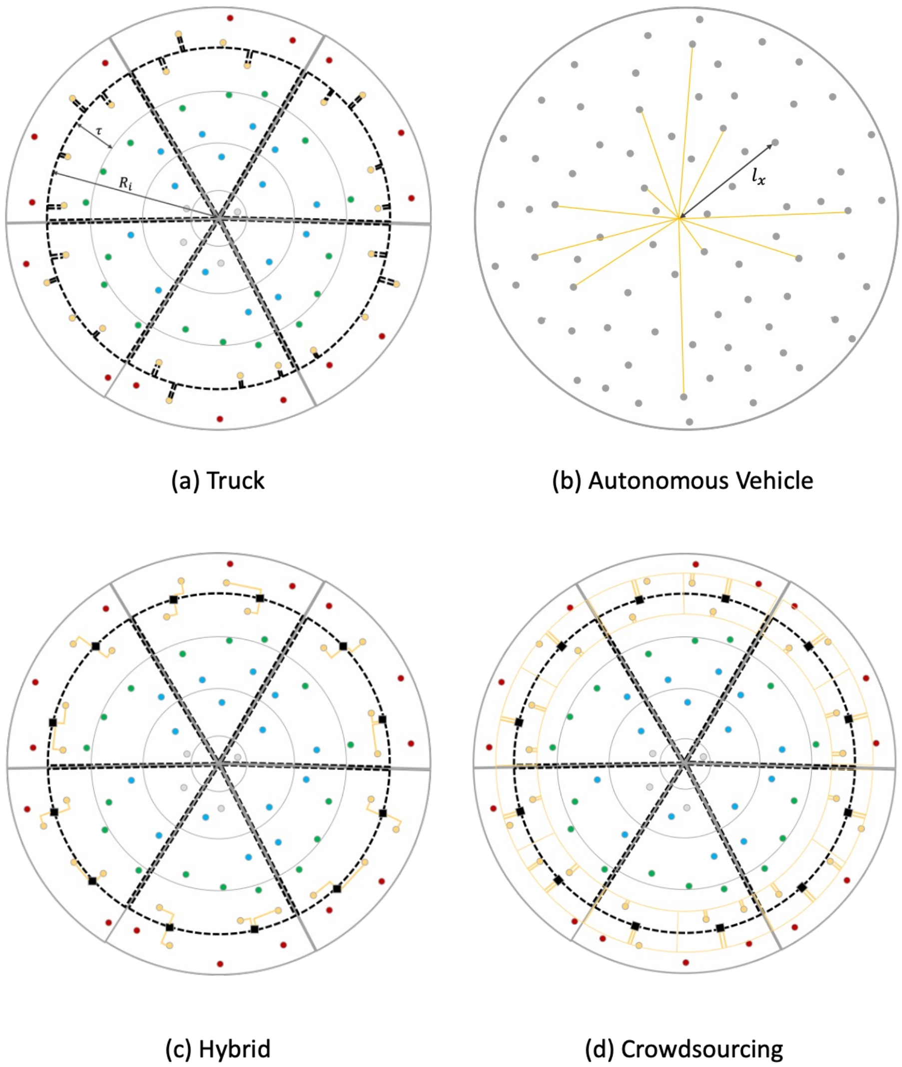

(a) Truck

(b) Autonomous Vehicle

(c) Hybrid

(d) Crowdsourcing

The number of truck routes on ring i is f_i^t, each having a distance of l_i^t. Recall that in the single ring case, the total cost of the Truck policy with n recipients is $z^t = c_q f^t l^t + c_s^t n$ (derived at the end of 3.1) where f^t and l^t were the number of truck routes and the average length of each truck route on the single ring, respectively. We expand this expression for the case of multiple rings by adding the index i for each ring such that

$$z^t(\tau) = c_q \sum_{i=1}^{C} f_i^t l_i^t + c_s^t \delta\pi, \tag{Two.17}$$

where f_i^t is the number of routes on ring i and l_i^t is the average length of each such route. We next obtain an upper bound and a lower bound for each truck tour length.

An Upper Bound: We derive the upper bound by assuming each truck departs from the depot, drives to a ring, and then travels an arc on the ring. While moving on the arc, the truck travels to and from each recipient, following the shortest distance between the arc and the recipient, as shown in Figures Two.4a and Two.5a. As mentioned earlier, each recipient is visited by the truck on the nearest ring.

We assume all routes are bounded by the truck capacity, and each truck route holds K recipients. Given the number of recipients assigned to each ring, derived in (Two.16) , the number of routes in each ring i is $f_i^t = n_i/K$. Thus, from (Two.16), the number of routes on ring i is

$$f_i^t = (2i-1)\tau^2\pi\delta/K. \tag{Two.18}$$

The average length of each route on ring i consists of three terms (i) the sum of inbound and outbound distances between the depot and the ring, (ii) the distance traveled on the ring by each truck, which is dictated by the truck capacity and the average distance on the ring between two consecutively visited recipients, and (iii) an average detour for each of the K recipients on each route. Since the rings are separated in a radius by τ and recipients are uniformly dispersed, the maximum and minimum detours would be $\tau/2$ and zero, respectively; thus, the average detour under the uniform distribution is $\tau/4$, which would be doubled since there are inbound and outbound detours for each recipient. Thus, the average length of each detour is $2(\tau/4) = \tau/2$

and the average route length on ring i is

$$l_i^t = 2R_i + \frac{2\pi R_i K}{n_i^t} + \frac{K\tau}{2}. \tag{Two.19}$$

PROPOSITION D.1.1. Given that R_i, n_i^t, f_i^t, and l_i^t are all characterized by τ, we can re-write (Two.17) as $z_u^t(\tau) \approx c_q(\frac{4\delta\pi}{3K} + \frac{\pi}{\tau} + \frac{\delta\pi\tau}{2K}) + c_s^t\delta\pi$, which from the first and second order conditions is minimized at $\tau^* = \sqrt{\frac{2}{\delta}}$, giving the following approximation for the optimal cost of the Truck policy

$$z_u^{t\,*} \approx c_q\pi(\frac{4\delta}{3K} + \sqrt{2\delta}) + c_s^t\delta\pi. \tag{Two.20}$$

A Lower Bound: We derive the lower-bound by assuming that each truck initiates its route from the depot, travels to a specific ring, and then visits the assigned recipients by traveling the shortest path. Figure Two.5b shows the lower bound on the truck route in each service area. Each truck route has two parts: (i) the sum of inbound and outbound travel distances between the depot and the ring, and (ii) the distance travelled within each truck's service area to deliver to K recipients. This solution is a lower bound, as the shortest path may not always be feasible, e.g., when there are buildings in the way. We prove the lower bound using *Lemma A.3* and *Theorem 1* in the Appendix, which is inspired by the *Lemma 2* in Carlsson et al. (2016). We extend the unit square derivation to a rectangular derivation, providing a more accurate representation of the truck service area.

Under the Truck policy, the service area takes an approximately rectangular shape with the

Figure Two.5: Travel distances in lower and upper bounds in the Truck policy. The dashed arcs specify the service area of one truck, and the thick black lines show truck route. The yellow circles represent recipients in this service area.

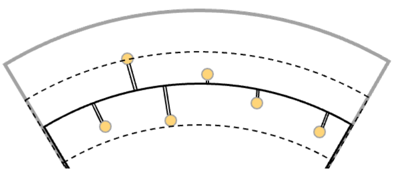

(a) Upper bound.

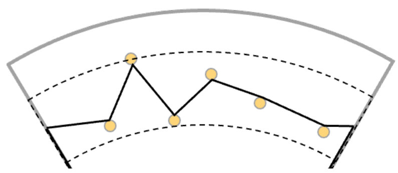

(b) Lower bound.

length of $\frac{2\pi R_i K}{n_i^t} = \frac{K}{\tau\delta}$ and width of τ, and the number of recipients in each service area is the truck's capacity K. Thus, using *Theorem 1*, the average length of truck route on ring i is:

$$l_i^t = 2R_i + \alpha\sqrt{K\frac{K}{\tau\delta}\tau} = 2R_i + \alpha K\sqrt{\frac{1}{\delta}}. \tag{Two.21}$$

PROPOSITION D.1.2. Using (Two.21), a lower bound on the total cost of the Truck policy as

$$z_l^t(\tau) \approx c_q(\frac{4\delta\pi}{3K} + \alpha\pi\sqrt{\delta}) + c_s^t\delta\pi. \tag{Two.22}$$

We now derive the cost per recipient in asymptotic condition for large δ:

$$\lim_{\delta\to\infty}\frac{z_l^t}{\pi\delta} = \lim_{\delta\to\infty} c_q\frac{4}{3K} + c_q\frac{\alpha}{\sqrt{\delta}} + c_s^t. \tag{Two.23}$$

In the classic TSP and its extensions to the vehicle routing problem, with recipients uniformly distributed on a surface, the cost per recipient is proportional to $1/\sqrt{\delta}$ for large δ (Daganzo 2005). This is validated in our work through (Two.20) and (Two.23).

We now compare the total costs of upper and lower bounds in the Truck policy, presented in (Two.20) and (Two.23), respectively.

$$\lim_{\delta\to\infty}\frac{z_l^t}{\pi\delta} = \lim_{\delta\to\infty}\frac{z_u^t}{\pi\delta} = \frac{4c_q}{3K} + c_s^t. \tag{Two.24}$$

Thus, the total costs of the upper and lower bounds in the Truck policy exhibit the same asymptotic properties, which will be used later in the comparative analysis.

D.2 AV policy on a disk

In the AV policy, the AVs travel directly to and back from the depot. There are no upper and lower bounds for this policy as we are able to derive the exact travel distances. The total AV distance is obtained from integration over the surface of the disk

$$d_v^a = \delta\int_0^1 (2l)2\pi l\,\mathrm{d}l = 4/3\delta\pi, \tag{Two.25}$$

whereby based on the density of recipients, $2\pi l\,\mathrm{d}l$ recipients impose a travel of distance of $2l$ for AV travel to and from the depot. Each AV has a single stop at the depot, i.e., $s^a = 1$; hence, the hand-off cost is c_s^a, and the total AV policy cost is

$$z^v = 4/3\pi\delta c_v + c_s^a. \tag{Two.26}$$

D.3 Hybrid policy on a disk

In the Hybrid policy, each truck departs from the depot, travels to a designated service area, visits a series of hubs, and returns to the depot. Recipients, in turn, use their AVs to travel to a hub for package pickup. We use the proposed heuristic of dividing the circular area into concentric rings. In this routing strategy, the number of truck routes on ring i is f_i^h, each with a length of l_i^h. The total AV distance in the Hybrid policy is d_v^h, where the notation is similar to that of the routing on a single ring (Section 3.3). There are s^h hand-offs, corresponding to the number of hubs, which are the transition points where delivery shifts from trucks to AVs. Therefore, the cost of the Hybrid policy is

$$z^h(\tau, m) = c_q \sum_{i=1}^{C} f_i^h l_i^h + c_v d_v^h + c_s^h s^h. \tag{Two.27}$$

Each truck departs from the depot, travels to a ring, and stops at a number of evenly spaced hubs on the ring. Therefore, the length of each truck route consists of (i) the inbound and outbound travel distances between the depot and the ring and (ii) the cumulative distance traveled by the truck as it visits the hubs located on that ring, as shown in Figures Two.4c and Two.6. Given that there are n_i recipients assigned to ring i, and each hub is tasked with serving m recipients, the total number of hubs on ring i is n_i/m. Since the number of hand-offs in the Hybrid policy directly corresponds to the number of hubs, the total number of hand-offs in this policy is obtained by aggregating the number of hubs across all rings, $s^h = \sum_{i=1}^{C} \frac{n_i^h}{m} = \frac{n}{m}$.

With n_i recipient on ring i and K recipients per truck, we have f_i^h routes on each ring such that $f_i^h = \lceil \frac{n_i}{K} \rceil$. When $n_i \gg K$, we approximate f_i^h as

$$f_i^h \approx \frac{n_i}{K} \tag{Two.28}$$

We establish lower and upper bounds for the travel distances of trucks and AVs with the following rationale. For AV routes, we consider that travelling along the shortest paths within neighborhoods may not always be possible due to the higher density of buildings and other obstacles. We addressed this in our analysis, where we set the lower bound, assuming that AVs travel in neighbourhoods following a Euclidean travel distance, while the upper bound is based on Manhattan distances.

An Upper Bound: We propose an upper bound where the circular area is divided into a number of concentric rings, and truck routes are as follows: each truck departs from the depot, travels to a specific ring, traverses an arc of this ring while it stops at a series of evenly spaced hubs on the ring, and returns to the depot. This routing strategy is illustrated for the entire fleet in Figure Two.4c and for an individual truck in Figure Two.6a.

The distance between consecutive hubs on Ring i, using (Two.16), is:

$$\Delta_i^h = \frac{2R_i m\pi}{n_i} = \frac{(2i-1)\tau m\pi}{\pi\delta\tau^2(2i-1)} = \frac{m}{\delta\tau}. \tag{Two.29}$$

Figure Two.6: Lower and upper bounds in the Hybrid policy. The thick black lines show truck route, and the black squares represent hubs. The gray lines show AV routes, and the yellow disk represents recipients in this service area. This figure is for one truck and the dashed arcs specify the service area of one truck.

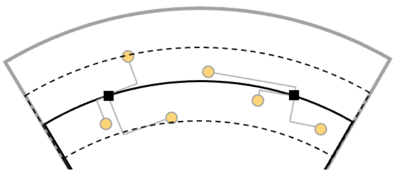

(a) Upper bound.

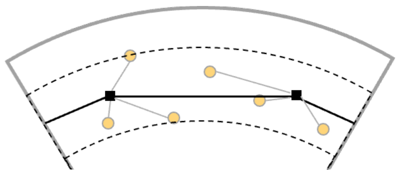

(b) Lower bound.

The length of each route is

$$l_i^h \approx 2R_i + \frac{2\pi R_i K}{n_i}. \tag{Two.30}$$

In deriving the upper bound for the traveling distances of AVs, we assume that AVs follow a Manhattan distance and travel in the ring and radial directions to and from each hub, as illustrated in Figure Two.4c and Figure Two.6a. This approach is consistent with the concept of short travels on local roads within each recipient's neighborhood. The AV distance in the Hybrid policy is dictated by the number of recipients and the sum of the expected ring and radial distances per recipient:

$$d_v^h = \sum_{i=1}^{C} 2n_i\left(\frac{\tau}{4} + \frac{\Delta_i^h}{4}\right) \approx \frac{\delta\pi\tau^2 + m\pi}{2\tau}. \tag{Two.31}$$

PROPOSITION D.3.1. The cost of the Hybrid policy, $z_u^h(\tau, m) \approx c_q(\frac{\pi}{\tau} + \frac{4\pi\delta}{3K}) + c_v\frac{\delta\pi\tau^2+m\pi}{2\tau} + c_s^h\frac{n}{m}$, is minimized at $\tau^* = \sqrt{\frac{2c_q+c_v m}{c_v\delta}}$ from the first and second order conditions, giving the following approximation for the optimal cost of the Hybrid policy:

$$z_u^h(m)^* \approx \frac{4\pi\delta c_q}{3K} + \pi\sqrt{c_v\delta}\sqrt{2c_q + c_v m} + c_s^h\frac{\delta\pi}{m}. \tag{Two.32}$$

Proposition D.3.1 validates the $1/\sqrt{\delta}$ scale in the literature when $\delta \to \infty$ in $z^h(m)/\delta$ given the expression of $z^h(m)$ in (Two.32).

A Lower Bound: We use a lower bound heuristic where each truck travels from the depot to a ring, traverses the ring to visit x^h hubs along the ring and then returns to the depot. The distance traveled by truck, particularly along an arc of the ring, is approximated using (Two.30), where the truck follows a predetermined arc during its route. For the AV travel distance, a lower bound is determined by considering the direct routes from the hub to the recipient locations and back. This differs from the AV distances in upper bound (Two.31) in terms of considering Euclidean travel distances of direct routes instead of ring-radial (Manhattan) distances, as shown in Figure Two.6b.

$$d_v^h = \sum_{i=1}^{C} 2n_i \sqrt{(\frac{\tau}{4})^2 + (\frac{\Delta_i^h}{4})^2} = \frac{\pi}{2\tau}\sqrt{\delta^2\tau^4 + m^2} \tag{Two.33}$$

PROPOSITION D.3.2. Using (Two.33) and (Two.30), a lower bound on the total cost of the Hybrid policy is:

$$z_l^h(\tau, m) \approx c_q(\frac{4\pi\delta}{3K} + \frac{\pi}{\tau}) + c_v(\frac{\pi}{2\tau}\sqrt{\delta^2\tau^4 + m^2}) + c_s^h\frac{\delta\pi}{m}, \tag{Two.34}$$

which is minimized at $\tau^* \approx \sqrt{\frac{2c_q}{c_v\delta}}$ from the first and second order conditions, and gives:

$$z_l^h(m)^* \approx c_q(\frac{4\pi\delta}{3K} + \pi\sqrt{\frac{c_v\delta}{2c_q}}) + c_v(\frac{\pi\delta}{2}\sqrt{\frac{2c_q}{c_v\delta}}) + c_s^h\frac{\delta\pi}{m}. \tag{Two.35}$$

We now derive the cost per recipient in asymptotic conditions, which again validates the $1/\sqrt{\delta}$ scale in the literature:

$$\lim_{\delta\to\infty}\frac{z_l^{h*}}{\pi\delta} = \lim_{\delta\to\infty}\frac{4c_q}{3K} + \sqrt{\frac{c_vc_q}{2\delta}} + \sqrt{\frac{c_vc_q}{2\delta}} + \frac{c_s^h}{m}. \tag{Two.36}$$

Comparing the upper and lower bound in the asymptotic condition gives:

$$\lim_{\delta\to\infty}\frac{z_l^{h*}}{\pi\delta} = \lim_{\delta\to\infty}\frac{z_u^{h*}}{\pi\delta} = \frac{4c_q}{3K} + \frac{c_s^h}{m}, \tag{Two.37}$$

which shows the same result for the asymptotic properties of the upper and lower bounds costs in the Hybrid policy.

D.4 Crowdsourcing policy on a disk

In the Crowdsourcing policy, the truck routing is similar to that of the Hybrid policy, with inbound/outbound travels between the depot and the ring and visiting hubs in each truck service area. Each truck travels radius R_i to ring i, stops at x^w hubs, and returns back to the depot.

Figure Two.7: Lower and upper bounds in the Crowdsourcing policy. The thick black lines show truck routes, and the black squares represent hubs. The gray lines show AV routes and the yellow circle represents recipients. This figure is for one truck and two AVs that are crowdsourcing to their neighbors. Each dashed area represent the service area of one Av.

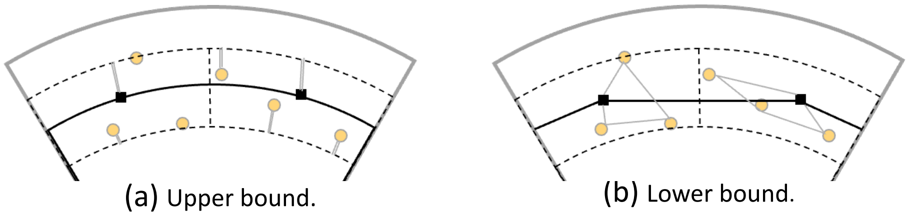

Similar to (Two.30), the length of each route is:

$$l_i^w \approx 2R_i + x^w \Delta_i^w, \tag{Two.38}$$

where Δ_i^w is the distance between consecutive hubs. The number of routes per each ring, similar to (Two.28), is obtained as $f_i^w \approx \frac{n_i}{mx^w}$, where $x^w = \dfrac{K}{m}$. Thus,

$$f_i^w \approx \frac{n_i}{K}. \tag{Two.39}$$

As shown in Figure Two.4d and Figure Two.7, for a group of m recipients closest to each hub in the Crowdsourcing policy, one AV travels to that hub and later delivers to other $m-1$ recipients in its neighborhood. The hand-off cost of the Crowdsourcing policy is equal to the number of hubs (hand-off to AVs) in addition to the number of recipients (hand-off to the recipients):

$$s^w = n + \sum_{i=1}^{C} \frac{n_i}{m} = n(1 + \frac{1}{m}). \tag{Two.40}$$

An Upper Bound: We propose an upper bound for the Crowdsourcing policy in which trucks traverse the rings and stop at hubs on the rings that are equally distant, and AVs take over the second part of the delivery from these hubs to the recipient's location. The truck routing is similar to that of the upper-bound solution in the Hybrid policy. For the AV routing, one AV in each hub travels to the hub and delivers to the m recipients closest to that hub, including the location of the AV owner itself. The upper bound on AV tour length in the Crowdsourcing policy accounts for the AV navigating the perimeter of the area assigned to each hub, in addition to covering radial local distances to each recipient's location, shown in Figure Two.7a and Figure .3. Consequently, the average travel distance for each AV is $2\frac{\tau}{2}+2(\tau+\Delta_i^w)+m\frac{\tau}{4}$ where the first term approximates the inbound and outbound AV travel distances, the second term represents the perimeter of the designated area, and the third term accounts for perpendicular detours to recipients. Given $f_i^w x^w$ hubs on ring i, the total AV distance is calculated in Appendix A in e-companion as:

$$d_v^w = \sum_{i=1}^{C} f_i^w x^w d_{v\,i}^w \approx \frac{2\pi}{\tau} + \frac{\tau\delta\pi(12+m)}{4m}. \tag{Two.41}$$

PROPOSITION D.4.1. The operator's cost $z_u^w(\tau,m) \approx c_q(\frac{\pi}{\tau}+\frac{4\pi\delta}{3K}-\frac{\pi\delta\tau^2}{3K})+c_v(\frac{2\pi}{\tau}+\frac{\tau\delta\pi(12+m)}{4m})+c_s^w(n(1+\frac{1}{m}))$ is minimized at $\tau^* = \sqrt{\frac{2m(c_q+2c_v)}{c_v\delta(12+m)}}$, giving the following approximation for the optimal cost of the Crowdsourcing policy:

$$z_u^w(m)^* \approx c_q\frac{4\delta\pi}{3K} + \frac{\sqrt{m(c_q+2c_v)}\sqrt{c_v\delta\pi(12+m)}}{m} + c_s^w\frac{\delta\pi(m+1)}{m}. \tag{Two.42}$$

Similar to Proposition D.3.1, Proposition D.4.1 also validates the $1/\sqrt{\delta}$ scale when $\delta \to \infty$ in $z^w(\tau,m)/\delta$ given the expression of $z^w(\tau,m)$ in (Two.42).

A Lower Bound: We establish a lower bound for the Crowdsourcing routing problem by assuming that in each hub neighbourhood, the AV responsible for crowdsourcing travels from the AV owner location to the hub, starts its TSP tour from the hub and visits the recipients in that neighborhood by traveling the shortest path. We prove this lower bound through *Lemma A.3* and *Theorem 1* in the appendix. This provides the TSP tour length of each crowdsourcing AV, which is responsible for visiting m recipients who are distributed within an approximately rectangular area with a length of $\Delta_i^w = \frac{m}{\delta\tau}$ and width of τ, as shown in Figure Two.7b, which gives the TSP tour length of $\alpha_2\sqrt{m\Delta_i^w\tau}$. We also account for the travel distance of the crowdsourcing AV from its location to the hub (to start the TSP tour), which has an average of $2\sqrt{(\frac{\tau}{4})^2+(\frac{\Delta_i^h}{4})^2}$, similar to derivation in the lower bound of the Hybrid policy. Thus, the average travel distance of each

AV is:

$$d^w_{v\ i} = 2\sqrt{(\frac{\tau}{4})^2 + (\frac{\Delta^h_i}{4})^2} + \alpha_2\sqrt{\frac{m^2}{\delta}}. \tag{Two.43}$$

Given $f^w_i x^w$ hubs on ring i, where $f^w_i \approx \frac{n_i}{mx^w}$, the lower bound on the total AV distance is:

$$d^w_v = \sum_{i=1}^{C} f^w_i x^w d^w_{v\ i} \approx \sum_{i=1}^{C} \frac{n_i}{mx^w} x^w (2\sqrt{(\frac{\tau}{4})^2 + (\frac{\Delta^h_i}{4})^2} + \alpha_2\sqrt{\frac{m^2}{\delta}}) \approx \frac{\pi\delta\tau}{2m} + \alpha_2\pi\sqrt{\delta}. \tag{Two.44}$$

For trucks, we use a routing strategy similar to the Hybrid policy; each truck travels from the depot to a ring, visits x^w evenly spaced hubs on each ring, and returns to the depot at the center.

PROPOSITION D.4.2. Using (Two.44), a lower bound on the total cost of the Crowdsourcing policy is:

$$z^w_l(\tau, m) \approx c_q(\frac{\pi}{\tau} + \frac{4\pi\delta}{3K}) + c_v(\frac{\pi\delta\tau}{2m} + \alpha_2\pi\sqrt{\delta}) + c^w_s(\pi\delta(1 + \frac{1}{m})), \tag{Two.45}$$

which is minimized at $\tau^* = \sqrt{\frac{2c_q m}{c_v\delta}}$ and gives the optimal cost as:

$$z^w_l(m)^* \approx c_q(\frac{4\pi\delta}{3K} + \pi\sqrt{\frac{c_v\delta}{2c_q m}}) + c_v(\pi\delta\sqrt{\frac{c_q}{2mc_v\delta}} + \alpha_2\pi\sqrt{\delta}) + \frac{c^w_s\pi\delta(m+1)}{m}. \tag{Two.46}$$

Obtaining the cost per recipient in asymptotic condition, we have:

$$\lim_{\delta\to\infty} \frac{z^{w*}_l}{\pi\delta} = \lim_{\delta\to\infty} \frac{4c_q}{3K} + \sqrt{\frac{c_q c_v}{2m\delta}} + \sqrt{\frac{c_v c_q}{2m\delta}} + \frac{c_v\alpha_2}{\sqrt{\delta}} + \frac{c^w_s(m+1)}{m}. \tag{Two.47}$$

which validates the $1/\sqrt{\delta}$ scale when $\delta \to \infty$ in $z^w(\tau, m)/\delta$.

Comparing the asymptotic properties of the lower and upper bound costs of the Crowdsourcing policy, we have:

$$\lim_{\delta\to\infty} \frac{z^{w*}_l}{\pi\delta} = \lim_{\delta\to\infty} \frac{z^{w*}_u}{\pi\delta} = \frac{4c_q}{3K} + \frac{c^w_s(m+1)}{m}. \tag{Two.48}$$

Thus, for the Crowdsourcing policy, the lower and upper bounds show similar results in the asymptotic conditions.

Section E: Comparative analysis

In this section, we derive the asymptotic properties for both ring and disk routing strategies when the number of recipients tends to infinity. We show that both strategies yield the same structure for the optimal cost function. Given the agreement on the cost structure, we thereafter focus on the ring model to derive a dominance space, identifying which policy has the lowest cost for different marginal cost realizations. We lastly investigate the role of hand-off costs on the policy costs, obtain insights from the special cases of zero and ordered hand-off costs, and investigate the effect of unequal hand-off costs.

E.1 Asymptotic properties and comparison of the ring and the disk models

We compare the policies when $n \to \infty$ and consider the cost per recipient defined as z^i/n for policy i. We assume the hand-off costs are equal and denoted by c_s but later relax this assumption in Section E.3. The asymptotic cost per recipient of policy i in the ring model is

$$z^i_{\infty,r} = \lim_{n\to\infty} \frac{z^i}{n}. \tag{Two.49}$$

Similarly, as $n = \pi\delta$, the asymptotic cost per recipient in the disk model can be expressed with the recipient density δ using (Two.49) as

$$z^i_{\infty,c} = \lim_{\delta\to\infty} \frac{z^i}{\pi\delta}. \tag{Two.50}$$

We have shown in the previous section that for routing on a disk, the lower and upper bound costs in each policy give the same asymptotic properties.

For the ring model, we express the asymptotic cost of each policy in the following proposition.

PROPOSITION E.1.1. For the ring routing, as $n \to \infty$, the asymptotic cost of each policy i is:

$$z^t_{\infty,r} = \frac{2c_q}{K} + c^t_s \tag{Two.51}$$

$$z^a_{\infty,r} = 2c_v \tag{Two.52}$$

$$z^h_{\infty,r} = \begin{cases} \dfrac{2c_q}{K} + \dfrac{c^h_s}{K} & c_q \leq Kc_v \\ 2c_v + \dfrac{c^h_s}{K} & c_q > Kc_v \end{cases} \tag{Two.53}$$

$$z^w_{\infty,r} = \begin{cases} \dfrac{2c_q}{K} + \dfrac{c^w_s(K+1)}{K} & c_q \leq c_v \\ \dfrac{2c_v}{K} + \dfrac{c^w_s(K+1)}{K} & c_q > c_v \end{cases} \tag{Two.54}$$

The following proposition derives the asymptotic costs for routing on a disk.

PROPOSITION E.1.2. For routing on a disk, as $\delta \to \infty$, the asymptotic cost of each of the four policies, for both upper and lower bound derivations, is given by

$$z^t_{\infty,c} = \frac{4c_q}{3K} + c^t_s \tag{Two.55}$$

$$z^a_{\infty,c} = \frac{4c_v}{3} \tag{Two.56}$$

$$z^h_{\infty,c} = \frac{4c_q}{3K} + \frac{c^h_s}{K} \tag{Two.57}$$

$$z^w_{\infty,c} = \frac{4c_q}{3K} + \frac{c^w_s(K+1)}{K} \tag{Two.58}$$

From Propositions E.1.1 and E.1.2, it is evident that for both the ring and disk routing, the asymptotic cost of each policy per recipient has the same scale w.r.t. the truck capacity, and marginal travel and hand-off costs. For the Hybrid and Crowdsourcing policies, the marginal costs of circular routing, i.e., (Two.57)-(Two.58), are consistent in scale (in terms of truck capacity and marginal costs) with their ring routing counterparts, i.e., (Two.53)-(Two.54), when $c_q \leq c_v$. This outcome is representative of the inability of the disk routing model and other similar continuum approximation methods of vehicle routing to capture cases where the second

Figure Two.8: Dominance space under asymptotic conditions with $c_q = 1 - c_v$.

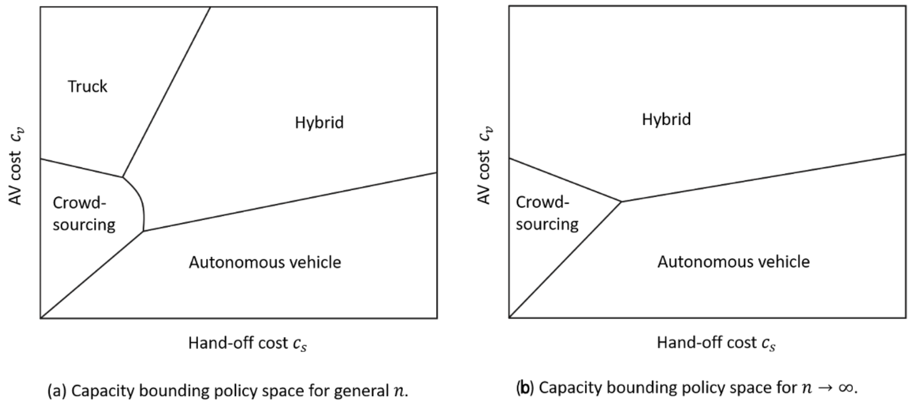

mode of a two-echelon system, AVs in this paper, also contribute to the long-haul segments of the route. These models only capture the local segments of the second transportation mode.

E.2 Dominant policies in generic settings

Given the discussion following Propositions E.1.1 and E.1.2, and the agreement on the cost structure of ring and disk routing strategies, we analyze the ring model for deriving a dominance space shown in Figure Two.8. Hereafter, we use the following definition to compare the policies.

Policy i dominates policy j if it has a lower cost, i.e., $z^i < z^j$. The dominant policy is one that dominates all other policies.

The mathematical expressions of the dominant policy boundaries are not all derivable in closed-form due to the computational complexity. We discuss these boundary expressions in the asymptotic analysis of the next section. The insights from the dominance space in Figures Two.8 and Two.9 are as follows:

Insight 1 (dominance space patterns): The AV policy is dominant when the marginal AV cost, c_v, is low, and the Truck policy is dominant when the marginal AV cost, c_v, is high.

Insight 2 (sandwiched policies): Crowdsourcing and Hybrid policies are sandwiched between Truck and AV policies. Between Hybrid and Crowdsourcing policies, the latter is dominant when the hand-off cost is small because the Crowdsourcing policy has more hand-offs than the Hybrid policy.

We now present numerical experiments to show the evolution of the dominance space with respect to the number of recipients n. For each n, we numerically solve the system of equations in Propositions $C.3.1$ and C.4.1 to compute the radius and number of users per hub that can be used to derive the cost of the Hybrid and Crowdsourcing policies.

Insight 3 (Impact of recipients): Figure Two.9 shows increasing the number of recipients shrinks the dominance space of Truck, AV, and Crowdsourcing policies but grows the space of the Hybrid policy.

Based on Proposition E.1.1, we depict the asymptotic dominance space for the asymptotic case in Figure Two.8b, and the following insights are evident from the dominance space.

Insight 4 (asymptotic dominated Truck policy): The Hybrid policy dominates the Truck policy when $n \to \infty$. Thus, the availability of recipient-dependent deliveries (in either AV, Hybrid, or Crowdsourcing policies) eliminates the conventional method of distribution using only trucks. Moreover, given that the Truck policy is never dominant and the AV policy's hand-off cost does not appear in the asymptotic costs; only the hand-off cost of the Hybrid and Crowdsourcing policies determine the dominant policy.

Insight 5 (asymptotic dominant policies): When $c_q \leq c_v$, either the Hybrid or AV policies dominate the others. Moreover, the Hybrid policy dominates the AV policy if $(2c_q + c_s)/2c_v < K$, which happens when the capacity is large, making only the hand-off cost of the Hybrid policy detrimental in the final cost of delivery.

E.3 Analysis of hand-off costs

In general settings, the hand-off costs of the four policies are not equal. Nevertheless, the asymptotic analysis above suggests that the form of the dominant space is robust with respect to these costs. We consider three scenarios with different hand-off costs to investigate this robustness further. Specifically, in Section E.3.1, we consider the case with no hand-off costs. In Section E.3.2, we consider cases with low, medium, or high hand-off costs. Finally, in Section E.3.3, we consider three special cases of hand-offs related to the cost of automation and distribution.

Figure Two.9: Dominant policy at different n. The truck capacity is $K = 10$. The letters t,a,h,w represent the Truck, AV, Hybrid, and Crowdsourcing policies, respectively.

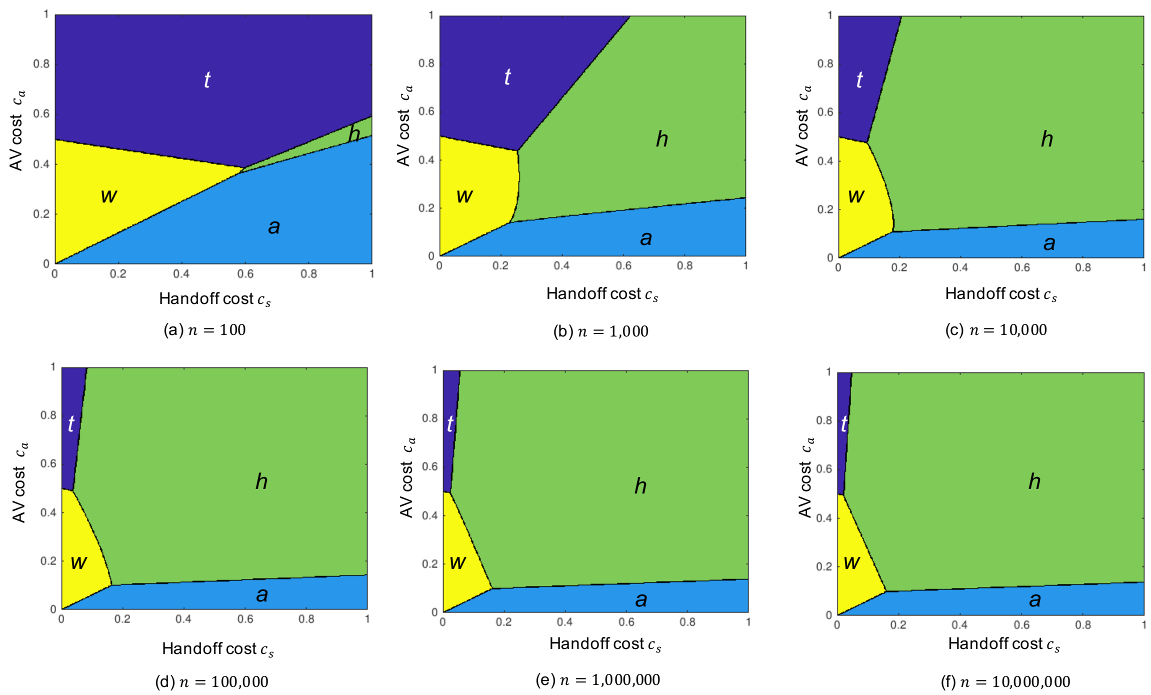

E.3.1 No hand-off costs

Consider a special case where hand-offs are inexpensive, i.e., $c_s = 0$. Then, the Crowdsourcing policy dominates the Hybrid policy because for each pair (r,m), the truck costs are the same, but the AV cost of Crowdsourcing is lower than the cost of the Hybrid policy due to the geometry of the routes; In the Hybrid policy, each of the m recipients has to access the hub individually, whereas in the Crowdsourcing policy, only one recipient accesses the hub and the remaining travel is completed on an arc of the ring.

We now compare the Truck and AV policies. According to (Two.5) and (Two.6) and under $c_s = 0$, the AV policy dominates the Truck policy if the cost ratio c_v/c_q is less than a threshold such that

$$z^v \leq z^t \Leftrightarrow \frac{c_v}{c_q} \leq \frac{\pi K + n}{nK} \tag{Two.59}$$

As K decreases, the Truck policy is dominated because each route covers fewer recipients and consequently, the number of routes increases. Moreover, according to (Two.59), when $n \geq c_q K\pi/(c_v K - c_q)$, the Truck policy is dominant because each truck benefits from economies of scale by serving many recipients for a single inbound and outbound trip. In contrast, the AV policy serves only one recipient for each inbound and outbound trip.

E.3.2 Low, medium, or high hand-off costs

Consider cases where the hand-off cost is low ($c_s = 0.1$), medium ($c_s = 0.5$), or large ($c_s = 0.9$). We also vary the AV cost, c_v, in the same increments as those of the hand-off cost and present the cost breakdown of the four policies in Figure Two.10 for $n = 1,000$.

According to Figure Two.10, the hand-off cost, c_s, has a small effect on the AV policy because it has only one hand-off (compare panels a-c). Moreover, when the hand-off cost is small (panel a), the difference in policy costs is large, which is attributed to the distinctive transportation costs. Moreover, Figure Two.10 also demonstrates that the AV cost decreases the Truck policy and increases the AV policy costs as expected. However, the impact of c_v on the Hybrid and Crowdsourcing policies is more intricate as the cost of Crowdsourcing in all three panels (and the cost of the Hybrid policy in panel a) first increases and then decreases with c_v. According to these trends, the initial increase in cost occurs because of a larger c_v, and the latter decrease in cost occurs because the operator reduces its usage of AVs in its optimal routing compositions. Figure Two.10 also presents the cost percentage of AV routes in the Hybrid and Crowdsourcing policies. In all cases but one (panel a, $c_v = 0.5$), the AV cost percentage of

Figure Two.10: Policy costs. In Panels a, b, and c, the hand-off costs are 0.1, 0.5, and 0.9, respectively. The AV cost percentage of the total cost is shown on top of the Hybrid and Crowdsourcing bars.

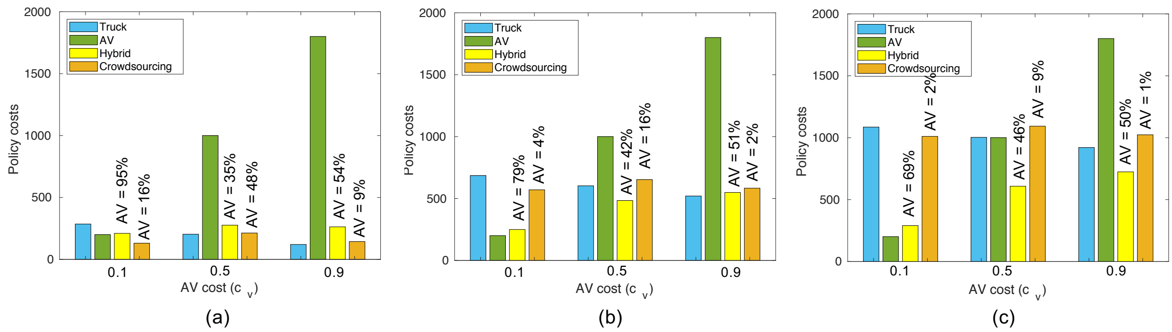

the Hybrid policy is larger than Crowdsourcing because of the larger number of in-bound and out-bound trips in the Hybrid policy where each recipient individually sends an AV to a hub, whereas there is only one inbound and outbound trip per hub in the Crowdsourcing policy.

E.3.3 Different hand-off costs

We now consider three scenarios for the relative hand-of costs of the different policies. The first scenario assumes the hand-off cost is predominantly related to the automation technology required by AV, Hybrid, and Crowdsourcing policies. For example, the vehicles in the AV policy first enter a pickup facility, then communicate their orders with a central system and proceed to receive their orders (the entire process can be automated using robotics that load the AVs with their requested items). In this scenario, we assume the hand-off cost of the Truck policy is half the hand-off cost of the other policies, i.e., the dominance space is presented in Figure Two.11a, which can be compared to the original one presented in Figure Two.9b. As expected, the Truck policy space is much larger in this scenario. However, the boundaries of the AV policy remain somewhat intact because this policy shares boundaries with the Hybrid and Crowdsourcing policies, which both include AV automation as well.

The second scenario assumes the hand-off cost is predominantly related to the construction and maintenance of the pickup facility for the AV policy. We assume that the hand-off cost for the AV policy is twice the hand-off cost of the other policies, as the other policies do not

Figure Two.11: Dominant policy for the different hand-off scenarios when $n = 1{,}000$ and $K = 10$. The letters t,a,h,w represent the truck, AV, Hybrid, and Crowdsourcing policies, respectively. Panels a, b, and c correspond with the three scenarios.

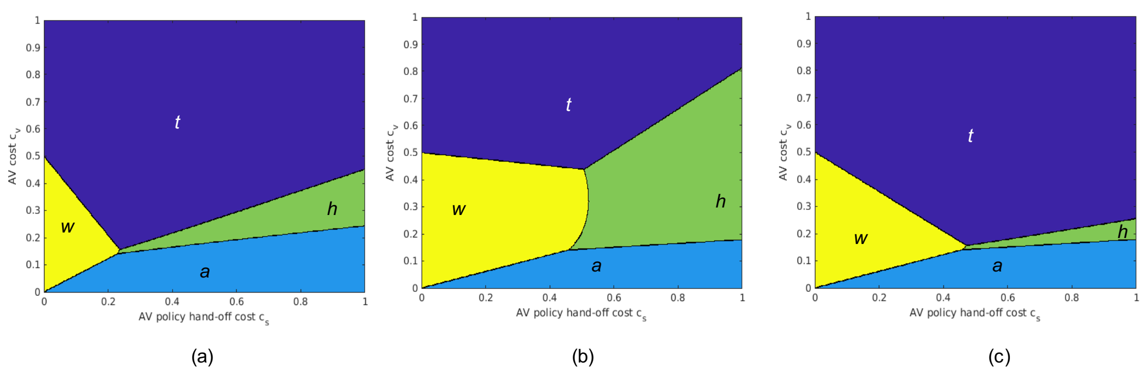

experience this large facility cost. The dominance space is presented in Figure Two.11b. As expected, the dominant space for the Hybrid and Crowdsourcing policies increases in this scenario as these policies dominate the AV policy in more cases.

The third scenario assumes the hand-off cost is predominantly related to the facility cost in the AV policy and the automation technologies in the Hybrid and Crowdsourcing policies. We assume the Truck policy hand-off cost is a quarter of the AV hand-off cost, and the hand-off costs of the Crowdsourcing and Hybrid policies are half the AV hand-off cost, i.e., the dominance space is presented in Figure Two.11c. As expected and similar to Figure Two.11a, the Truck policy space is much larger in this scenario, and the boundaries of the AV policy remain somewhat intact. However, the Crowdsourcing policy is better (dominated) over a larger range in this scenario. We summarize this analysis in the following insight.

Insight 6 (robustness to hand-off costs): In the case of policy-specific hand-offs, although the dominance space boundaries are perturbed, the overall pattern of the dominance space remains the same. Moreover, the large dominance space of the Truck policy supports its applicability in today's logistics operations.

Section F: Case study

In this section, we present a case study to assess the validity of the analytical results derived from the stylized model. We choose Walmart as the retailer in our analysis. Walmart serves roughly 2.4 million recipients who shop daily in-store and online. The website "Walmart.ca" is visited more than 900,000 times on a daily basis, which complicates the last-mile delivery of shopping items from the superstore to recipients homes.

There are currently 20 Walmart superstores in the Greater Toronto Area. We choose the single superstore with the largest geographical catchment area shown in Figure Two.12. We assume a fixed number of recipients geographically dispersed on the map. The location of the recipients is proportional to the population density shown as a heat-map in Figure Two.12, i.e., land parcels with larger populations are more likely to produce recipients. We calculate the distance between the recipients and the depot and the distance between the recipients using the

Euclidean metric.

We derive the cost of each policy using heuristic models that provide sub-optimal solutions. We keep the heuristics simple as we only intend to approximate the policy costs.

For the Truck policy, we solve a vehicle routing problem (VRP) using a Simulated Annealing algorithm (Osman 1993). This method is known to perform well in finding local optimum solutions for large-scale discrete optimization problems. The inputs to the VRP include the recipient and depot locations, the capacity of the trucks and the allowable tour length. Each recipient generates one unit of delivery load. Hence, the number of recipients in each route should be smaller than the truck capacity. The output is the set and sequence of recipients visited in each tour. In the simulated annealing algorithm, we set the initial temperature to 100, the damping rate to 0.98, the maximum internal iterations to 100, and the maximum external iterations to 2,000.

In the AV policy, we simply connect each recipient directly to the depot and sum the inbound and outbound costs of visiting recipients.

In the Hybrid policy, we begin by allocating recipients to clusters using the k-means algorithm (Hartigan and Wong 1979). The recipients in each cluster are served via a single hub. We locate the hubs at the centroid of each cluster. We then solve a VRP using the simulated

Figure Two.12: Walmart superstore in the Greater Toronto Area with the largest geographical catchment area. The shades of purple represent the population of the land parcels. [source: censusmapper.ca]

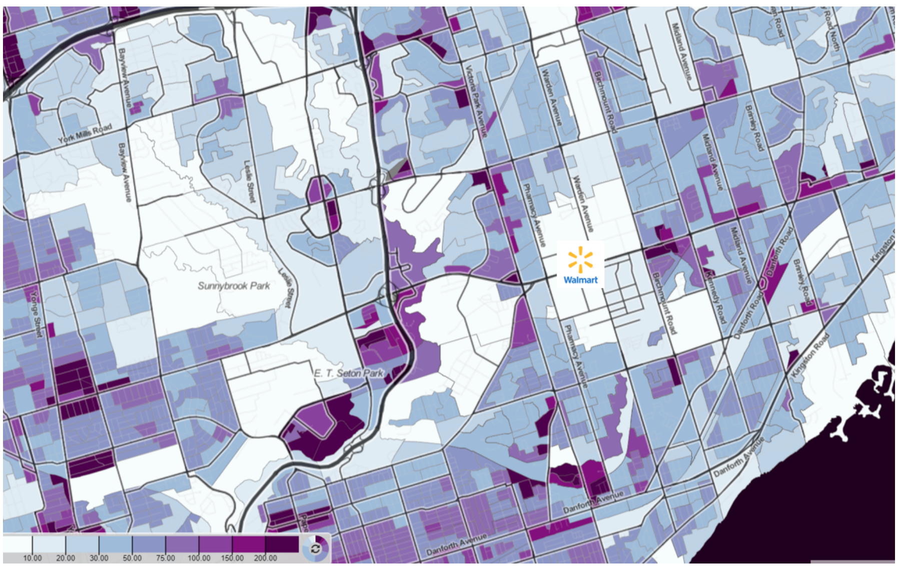

annealing algorithm, where the destinations are the hubs. The pickup load at every hub is the sum of the number of recipients assigned to that hub, as each recipient has a unit load of delivery.

In the Crowdsourcing policy, we also use the k-means algorithm to allocate the recipients to clusters. For each cluster, we solve a Traveling Salesman Problem (TSP) to find a near-optimal solution for visiting all recipients (of each cluster) in one tour. We then find the recipient in each tour that is closest to the depot and locate the hub there. We then solve a VRP using the simulated annealing algorithm, where the destinations are the hubs.

For $n = 100$ recipients and $K = 10$, Figure Two.13 depicts the solution of the four policies. We vary the marginal AV and truck cost within the range of 0 to 1 dollars per km and assume $c_v = 1 - c_q$. We also vary the hand-off cost from 0 to 10 dollars per hand-off. The policy space for $n = 100$ and $n = 1{,}000$ are presented in Figures Two.14. It is evident that Figure Two.14a closely resembles Figure Two.8, thus showing that the case study displays the same dominance space patterns as the analytical model. We observe that Insight 1 holds in the case study with regard to the marginal AV cost. Insight 2 holds as well because the Hybrid and Crowdsourcing policies are sandwiched by the truck and AV policies.

The policy space for $n = 1{,}000$ in Figure Two.14b also closely resembles Figure Two.8c-d of the analytical model. Moreover, it is evident that the space of the Truck and Crowdsourcing policies shrink when increasing n from 100 to 1,000, thus validating the asymptotic properties of the analytical model as discussed in Insight 3. The case study also validates Insight 4, given that the Truck policy is almost entirely dominated when n is large. The linear pattern introduced in Insight 5 cannot be strictly validated. Although we observe the equivalent pattern

Figure Two.13: Four distribution policies. The Black and gray lines represent truck and autonomous vehicle routes, respectively.

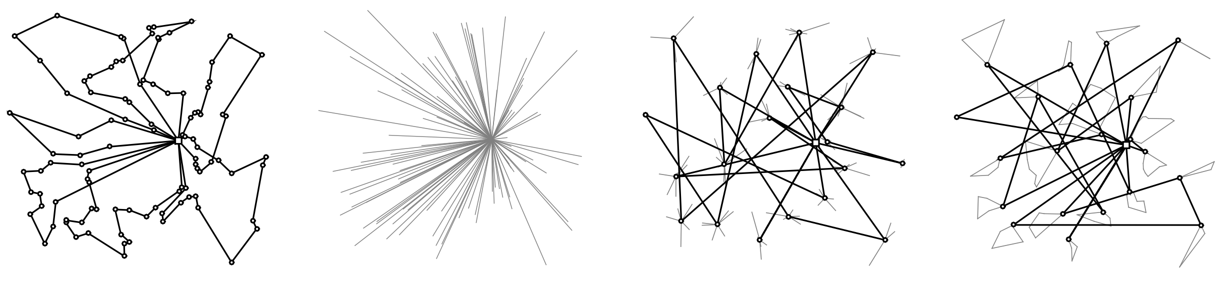

(a) Truck (b) Autonomous Vehicle (c) Hybrid (d) Crowdsourcing

Figure Two.14: Dominant policy for at different n. The letters t,a,h,w represent the truck, AV, Hybrid, and Crowdsourcing policies, respectively.

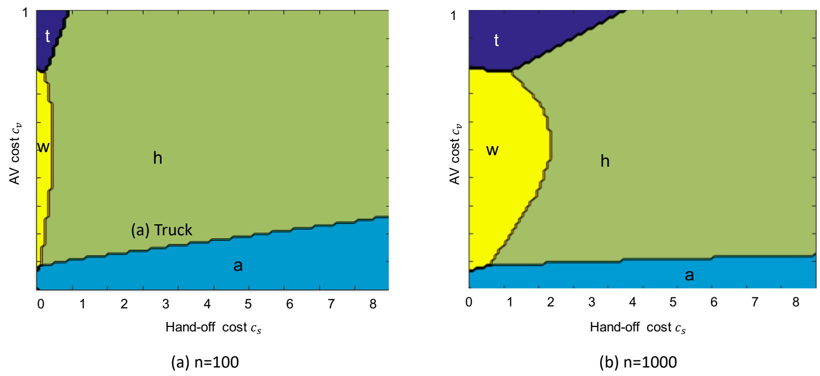

for Crowdsourcing policy here, it has nonlinear behaviour. Our extensive numerical experiments with different hand-off costs also show similar patterns in the dominance space, thus validating Insight 6.

Section G: Conclusions

Recipient participation in last-mile logistics can lead to new patterns of delivery. The ultimate goal of analyzing these new delivery patterns is to reduce the cost of last-mile logistics while compensating recipients for taking a role in the process. Recipient participation has also become more viable due to recent advancements in technology. The emergence of AVs has the potential to alter delivery patterns further. The ability of AVs to drive without humans reduces their opportunity cost (i.e., the cost of driver time) and thus creates new opportunities for using them to do household errands such as picking up online shopping. AVs can also support a Crowdsourcing delivery policy, i.e., they could be outsourced to make deliveries for neighboring recipients to generate revenue for their owners.

This paper studies the role of incorporating recipients in last-mile logistics. We consider four policies: status quo Truck delivery, AV pickup, Hybrid combination of trucks and AVs, and Crowdsourcing. We present two stylized models for routing on a ring and on a disk, derive upper and lower bounds for routing in each policy, and show the consistency between the asymptotic properties of the costs based upon both bounds. We then derive the optimal cost of the policies and compare them using a dominance space that is sensitive to driving and hand-off costs.

Under general settings, increasing the hand-off cost (related to the number of locations where ownership changes) makes the AV and Hybrid policies more dominant, and increasing the truck cost makes the AV and Crowdsourcing policies more dominant. When the number of deliveries tends to be infinite, the status quo Truck policy is dominated by other policies.

Using a detailed case study for a grocery delivery service in Toronto, we further demonstrate that the insights from our stylized models also remain valid for these practical settings. The insights of this paper can assist in strategic-level decisions related to incorporating AVs in last-mile logistics. Our analysis focuses mainly on comparing the costs of the four policies. Some policies require a model detailed assessment if implemented for day-to-day operations. The Crowdsourcing policy is, by nature, a two-sided market where the number of drivers is sensitive to the wage offered by the platform, and the number of recipients is sensitive to the charged delivery cost. Future research may also consider the environmental benefits of AVs as they can drive in platoons with fewer abrupt acceleration and breaking. Service providers may be more inclined to incorporate AVs as they become aware of these environmental advantages.

Chapter Three Parametric Design of Time-Sensitive Routing with Recipient-Dependent Contributions

Research Summary

Last-mile delivery complexities intensify for perishable goods, which must maintain quality, mainly when transported on non-refrigerated vehicles. If recipients are unavailable, delivery failure may prolong the delivery of perishable goods, thus jeopardizing their integrity. This study proposes recipient-dependent last-mile delivery solutions for perishable goods with time-sensitive delivery routes where the recipients contribute to the process. We explore applications of Autonomous Vehicles (AVs) in recipient-dependent deliveries of perishable goods and compare traditional truck delivery with a proposed AV pickup policy and other multi-echelon routing policies. We propose a parametric design of the policies, characterizing each policy by a set of variables inspired by the network design literature. In this study, routes are regarded as length-constrained, which is essential for the time-sensitive delivery of perishable goods. We compare the optimal cost of policies in length-bounding (time-sensitive) with capacity-bounding routes. Increasing hand-off costs also lead to the dominance of AV and hybrid policies over traditional truck delivery. We validate the proposed managerial insights through a case study of a Walmart location delivery service in Toronto, proving the applicability of the models. This research contributes to the strategic integration of AVs in the last-mile delivery of perishable goods. (D Viniche et al. 2024)

Section A: Introduction

Transporting packages from distribution centers to final destinations, commonly known as last-mile delivery, is the final leg of the supply chain, comprising about 28% of total shipment costs (Goodman 2005, Ranieri et al. 2018). The growing demand for fast and responsive delivery relies on the efficiency of the last mile, influencing customer satisfaction and loyalty (Jacobs et al. 2019). In the already competitive and laser-thin profit sector of last-mile logistics, delivering perishable goods, such as food and medical supplies, further complicates operations due to strict delivery regulations that maintain product integrity (Hsu, Hung, and Li 2007, Nguyen et al. 2013, Nguyen, Dessouky, and Toriello 2014, Lagin et al. 2022). Lengthy deliveries increase the risk of spoilage or quality degradation of perishable goods, ultimately leading to direct product loss, affecting customer trust, and causing future losses (Gustavsson et al. 2011, A. Rijpkema, Rossi, and GAJ van der Vorst 2014). Globally, 14% of food production is lost within the supply chain, amounting to a substantial 931 million tonnes of food (FAO, UN 2023, UN 2024). Another complexity in the last mile logistics is the challenge of failed deliveries, a problem not exclusive to but notably intensified for perishable goods. First-time delivery attempts have an average 20% chance of failure in urban areas, such as Chicago city (Stanley Lim 2023). However, the time-sensitive nature of perishable goods often does not allow for multiple delivery attempts, which can degrade the quality of the perishable order. One way of reducing failed deliveries is to rely on recipients to partake in the delivery process so they have more flexibility in pickup time, leading to a higher chance of successful delivery.

Many logistics firms are adopting recipient-dependent delivery (RDD) strategies, shifting a portion of the delivery responsibility to the recipients. RDD relies on receivers to collect their items from either hubs or other specified locations, such as local collection stores or secure lockers strategically placed in accessible areas. RDD strategies can also benefit from emerging technologies, such as autonomous vehicles (AVs), which can enhance accessibility to goods and services (Bagloee et al. 2016). In such a setting, recipients can dispatch an AV to pick up their packages, eliminating the need for physical store visits. This delivery strategy is compatible with pickup infrastructure at major grocery retailers, such as the drive-through pickup stations at Target and Walmart. This study proposes RDD-enabling last-mile logistics solutions for perishable items, considering differing delivery policies inspired by integration with AVs.

AVs can streamline delivery by reducing human involvement, enhancing crowdsourcing, and supporting the sharing economy. AV-equipped recipients can pick up packages and distribute them in their neighborhoods, creating a shared delivery network that cuts costs and delivery times. General Motors (GM) supports peer-to-peer sharing, allowing owners to rent AVs for delivery, generating income (Washington Post 2018). Crowdsourcing AVs also reduces the need for multiple pick-up stations. In cases of recipient unavailability, AVs use secure kiosks or lockers, offering real-time notifications for timely deliveries.

This paper addresses the research question of designing last-mile delivery strategies for the time-sensitive delivery of perishable goods with the participation of the AV-owned recipient. We base the analysis on the established framework of Continuum approximation for the cost analyzed of two-echelon last-mile delivery system (Carlsson and Song 2018) and vehicle routing approximations with a given spatial distribution of the recipients (Newell and Daganzo 1986a,c). To analyze the impact of length-bounding constraints, we adopt a two-stage modeling approach. We first develop an analytical framework assuming a uniform spatial distribution of recipients, leveraging the symmetry of the circular structure to provide analytical tractability. The circular models are widely used in the operations management literature, particularly when demand is assumed to be uniformly distributed, as they allow for the formulation of total cost functions using continuous approximation methods. Moreover, many major cities, such as Beijing and Indianapolis, have a circular or ring structure with business hubs near the center and residential areas expanding outward, making the circular approximation both mathematically convenient and empirically relevant. We later extend this analysis to a two-dimensional service area, allowing for a more generalized comparison between length-bounding and capacity-bounding constraints in real-world delivery networks.

The emerging RDD policies facilitated by AVs are explored in Chapter Two, where they focus on scenarios where recipients own and use AVs to participate in last-mile delivery. Their model primarily considers capacity constraints in routing strategies but does not account for the time-sensitive nature of perishable goods. This study expands Chapter Two by introducing recipient-dependent AV-enabled delivery of perishable goods. We contribute to the literature on AV-facilitated RDD, focusing on time-sensitive perishable deliveries. This study addresses time-sensitive delivery by incorporating a delivery tour length constraint to limit the goods spent in transit. Furthermore, we compare the cases when delivery tours are constrained by either the truck's capacity (capacity-bounding case) or tour length (length-bounding case). The proposed optimization model in this study is not limited to truck-AV applications; it is adaptable to the routing characteristics of any two-echelon last-mile delivery system. While AVs are used as an example of emerging technologies that enhance last-mile delivery efficiency, this framework can be applied more broadly to recipient-dependent strategies. For instance, Amazon's two-echelon delivery system typically uses large line-haul trucks for shipments from distribution centers to local hubs, followed by smaller delivery vans or regional carriers for last-mile distribution to customers' locations. Nevertheless, this work contributes to the ongoing discussion on AV integration in last-mile logistics, providing valuable insights for shaping future policies and practices in AV-assisted delivery systems.

Including length-bounded travel tours in the model adds valuable insights for fleet management decisions, in addition to addressing the time sensitivity in the delivery process. This addition improves fleet management strategies and emphasizes the importance of delivery timing. We identify similarities between length-bounding and capacity-bounding scenarios, particularly when the number of deliveries grows, demonstrating the model's robustness under these constraints. For instance, with a large number of recipients in both cases, the status quo truck policy is dominated by other policies, indicating its reduced effectiveness. Furthermore, under varying marginal AV costs, we observe comparable levels of cost-effectiveness between AV and truck policies (single-echelon policies) in both length- and capacity-bounding cases. However, key differences emerge in two-echelon truck-AV delivery scenarios. The asymptotic analysis shows that the two-echelon optimal costs are affected by customer-to-hub allocations only in the case of time-sensitive deliveries, where truck routes are constrained by tour lengths. Moreover, in the time-sensitive delivery of perishable goods, the hybrid policy becomes more cost-effective and gains dominance across broader conditions in the length-bounding case. These findings highlight the potential of AV-equipped RDD strategies to enhance the efficiency, cost-effectiveness, and scalability of last-mile logistics for perishable goods, especially within smart city frameworks. This study provides valuable insights for logistics companies, policymakers, and transportation planners regarding the benefits of these strategies for perishable goods delivery.

The organization of the paper is as follows: In Section 2, we review the literature relevant to this research. Section 3 briefly introduces the modelling policies for using autonomous vehicles in recipient-participated last-mile delivery. Section 4 details the modelling strategy, which employs a ring-structure service area, and compares the policies in this stylized setting. Section 5 presents the results of the comparative analysis of the length-bounding case with the capacity-bounding case and their asymptotic costs. In Section 6, we extend the one-dimensional distribution of recipients to a two-dimensional distribution model and compare the analytics results and asymptotic cases of these two modelling approaches. In Section 7, we conduct a case study on Walmart delivery to validate the analytical framework and findings. Section 8 presents the conclusion of this study, providing insights and potential implications for the future.

Section B: Related works

We review the literature on three areas: approximation models for vehicle routing, the concept of crowdsourcing deliveries, and the use and potential of autonomous vehicles (AVs) in logistics.

B.1 Approximation Models for Vehicle Routing Problem

Vehicle routing problems (VRPs) aim to determine the optimal set of routes for a fleet of vehicles to serve a set of customers. VRP is a *NP*-hard combinatorial optimization problem; that is, conventionally addressed via integer programming methods which can provide optimal routing details such as the assignment of customers to individual vehicles and the sequence of customer visits for each vehicle (Laporte 1992). However, the constraints of traditional vehicle routing formulations often limit their value in scenarios with limited data, a large number of recipients, or for strategic-level decisions where precision is not the foremost concern. In such situations, approximation strategies offer a suitable alternative. The two prominent methods to approximate VRP are continuum approximation and geometric approximation.

Continuum approximation (CA) transforms the traditional integer programming formulation into a continuous space, assuming that recipients are dispersed on an Euclidean surface with known density distributions. The CA methodology replaces detailed data, such as recipient locations, with concise summaries using a continuous density function over time and space (Daganzo 2005). This approach offers simplified yet plausible analysis, often allowing the derivation of closed-form analytical solutions. Langevin, Mbaraga, and Campbell (1996) and Ansari et al. (2018) provided comprehensive overviews of CA applications in logistics and freight transportation, respectively. CA has been applied to various logistics and routing problems. It has been used to analyze the costs of two-echelon vehicle routing problems involving trucks and drones (Carlsson and Song 2018), where an unmanned aerial vehicle (UAV) provides service to customers while making return trips to a moving truck that contains packages. Their work analytically showed that efficiency improvements are proportional to the square root of the UAV-to-truck speed ratio. Additionally, CA has been applied to the home delivery problem of e-retailers who commonly suffer from narrow delivery times slots (Agatz et al. 2011), showing that while these slots improve customer convenience, they can increase delivery costs.Another application is in the household scheduling problems, which is a variant of the generalized traveling salesman problem (TSP) (Carlsson et al. 2016), where CA-based models reveal that centralized delivery services require large-scale adoption before achieving significant efficiency gains over independent customer travel.

The CA paradigm has also been extended to autonomous vehicles in transit, where it aids in fleet dispatching and service optimization. Studies have applied CA to optimize modular autonomous vehicles in transit corridors (Chen, Li, and Qu 2022), to design semi-on-demand hybrid transit routes with shared autonomous vehicles (Ng et al. 2024), and to determine the optimal integration of shared autonomous vehicles with public transit (Levin et al. 2019). While these studies highlight CA's effectiveness in autonomous mobility-on-demand, their focus on public transit operations differs from our emphasis on last-mile delivery.

Another related line of research applies CA to last-mile delivery robots, which shares some similarities with our work but differ in the fundamental aspect of recipient participation and neglects the time-sensitive delivery of perishable goods. CA has been used to optimize two-echelon truck-and-robot systems and provide insights on air and ground delivery robot applications in different cities (Lemardelé et al. 2021) and evaluate hybrid drone-truck and ground robot models (Figliozzi 2020, Jennings and Figliozzi 2019). These studies provide valuable insights into autonomous last-mile logistics but focus on company-owned robots, whereas our research explores the role of recipients in the delivery process and the unique challenges posed by perishable goods.

Geometric approximations assume the distribution of recipients follows a particular geometric shape or area, such as the arc of a circle. This approach has been used to study the split vehicle routing problem and develop novel heuristics for routing and partitioning combinatorial problems, which provide strategic-level insights. The application of space-filling curves, which are continuous mappings from a lower-dimensional to a higher-dimensional space, is also part of this approach (Archetti, Savelsbergh, and Speranza 2006, Bartholdi III 1995, Bartholdi III and Platzman 1988).

In this study, we adopt the CA paradigm to analyze recipient-dependent delivery with time-sensitive perishable goods, leveraging it to approximate vehicle routing costs and compare the optimal last-mile delivery policies. In addition, for analytical tractability, we introduce a circular geometric approximation, considering two stylized models where recipients are distributed on (i) a ring and (ii) a circular surface. This assumption enables closed-form solutions for our optimization model and provides valuable managerial insights. By combining CA with this geometric simplification, we ensure that our model remains both computationally efficient and practically relevant for last-mile delivery analysis.

B.2 VRP of Perishable Goods

Researchers have addressed specific challenges associated with managing perishability in supply chains to extend the discussion on VRPs for perishable deliveries. In this section, we are focusing on the delivery of perishable goods, and readers are referred to (Karaesmen, Scheller-Wolf, and Deniz 2011) and (Baron 2010) for a more in-depth read on perishable inventory management.

Hwang (1999) developed a distribution model aimed at optimizing food supply in famine relief, emphasizing inventory allocation and minimizing human suffering rather than travel distance or time. In contrast, Tarantilis, Kiranoudis, and Vassiliadis (2004) proposed a threshold-accepting algorithm to address the fresh milk distribution problem, treating it as a heterogeneous fixed fleet vehicle routing problem, although they did not consider perishability explicitly. Further contributions include models that incorporate perishability and time windows. Chen, Hsueh, and Chang (2009) introduced a non-linear model for the VRP with time windows (VRPTW) for perishable food, focusing on maximizing supplier profit while considering both production and routing under stochastic demand. Osvald and Stirn (2008) extended the VRPTW by accounting for time-dependent travel times and perishability, presenting a heuristic algorithm for the distribution of fresh vegetables. Hsu, Hung, and Li (2007) considered the randomness in perishable food delivery with a stochastic VRPTW model that optimized routes, loads, and dispatch times. For further reviews on the role of perishability in VRP, Amorim and Almada-Lobo (2014) and Utama et al. (2020) provide detailed insights.

Few studies address the role of emerging technologies in perishable goods delivery. Zhao and Lee (2023) explores the potential of connected and autonomous vehicles (CAVs) in supply chain systems, discussing how higher CAV adoption rates can reduce travel time, particularly for long-distance deliveries of perishable products. Haji et al. (2020) conducted a comprehensive review of the role of technology in improving perishable food supply chains, with an emphasis on automated systems and sensors that monitor product quality. Gharehgozli et al. (2017) highlighted technological advances in agricultural production and food preparation while noting the limited focus on logistics. Although technological advancements are beginning to influence logistics for perishable goods, the role of autonomous vehicles in this domain remains unexplored.

B.3 Crowdsourced deliveries with pickup locations

Crowdsourced delivery (or crowd-shipping) has become an increasingly viable solution in the field of mobility services as a part of the sharing economy (Hu 2019). In the sharing economy, recipients transition from only receivers to active delivery drivers. The scalability and logistical implications of crowdsourcing have been examined by Arslan et al. (2019), Qi et al. (2018), Dayarian and Savelsbergh (2017), Behrend and Meisel (2018), Macrina et al. (2020), and its real-world application is already visible in various crowdsourcing initiatives. For example, ShipperBee, a company in Toronto, Canada, uses pickup and delivery lockers throughout the city. Their business model allows ad-hoc drivers to select an item for delivery, which they retrieve from a specific locker using an assigned code. This model highlights the benefits of designated pickup stations, which can significantly reduce the delivery load on drivers in crowdsourcing systems.

We extend this line of research by proposing two-echelon last-mile delivery models in which RDD using AVs can be either individual participation or crowdsourcing models.

B.4 Applications of Autonomous Vehicles

AVs are rapidly reshaping the transportation landscape with the potential to enhance mobility and logistics. The three C's of AVs, namely *Connectivity*, *Comfort*, and *Collaborative consumption*, underline their transformative potential Baron, Berman, and Nourinejad (2020). Several studies have addressed various aspects of AVs. For instance, Bansal and Kockelman (2017) assesses consumer willingness to adopt this emerging technology, Mersky and Samaras (2016) discusses AVs' potential to improve fuel economy and promote environmental sustainability, Mahmassani (2016) evaluates AVs' potential impact on traffic flow and congestion management, de Oliveira (2017) provides an in-depth analysis of the traffic patterns induced by AVs, Mirzaeian, Cho, and Scheller-Wolf (2020) uses queueing theory to understand and optimize AV traffic flow, Harper et al. (2016) estimates the potential increase in traffic due to widespread AV adoption, Nourinejad and Roorda (2018) explores the potential issues and solutions related to AVs and urban parking, Fagnant and Kockelman (2014) investigates the feasibility of shared AV fleets, and Chen et al. (2016) proposes methods for optimizing shared AV operations to increase efficiency and minimize costs.

However, the intersection of AVs with last-mile deliveries and logistics services remains relatively unexplored and forms the basis of this study's investigation. Chapter Two presents models for routing policies in recipient-dependent last-mile logistics using AVs. Motivated by potential applications of AVs in smart cities, these policies are compared to traditional truck delivery, revealing potential cost savings and superiority in scalability as the number of recipients increases. They consider two-echelon delivery strategies involving trucks and AVs, where trucks have a limited capacity on the number of recipients each truck can serve, which dictates the truck routes. We further enhance their model by considering that truck routes can be either truck's capacity or tour length, and we compare the results of different policies in both cases.

Section C: The policies

Focusing on the RDD of perishable goods, we propose three policies based on the application of AVs and compare their performance with conventional truck-based deliveries (Truck Policy). We adopt the definitions of "AV policy", "Hybrid Policy", and "Crowdsourcing Policy" and explore these policies for the case of perishable goods delivery with constrained tour lengths. Due to the time-sensitive nature of perishable goods, we impose a tour length constraint on truck routes for both the single-echelon (truck-only) and two-echelon (hybrid and crowdsourcing) policies. In the hybrid policy, each AV handles only a single delivery per trip, and in the crowdsourcing policy, each AV is responsible for fewer deliveries than trucks, which hold a higher number of deliveries across more dispersed locations. As a result, AVs are expected to cover significantly shorter distances. Thus, tour length constraints are not applied to AV travel routes. Details on AV travel distances are provided in the appendix. Finally, we compare the results of the proposed length-bounding case for the delivery of perishable goods and the capacity-bounding alternative to provide further insights.

Truck Policy: In the status quo Truck Policy, a fleet of trucks departs from the depot, visits a set of recipients to make deliveries, and returns to the depot. This traditional approach relies on trucks as the only means of delivery. This policy is consistent with the current literature on the vehicle routing Problem (VRP).

AV Policy: In the AV Policy, the assumption is that recipients own AVs, and they send their unoccupied AVs to the depot to pick up a package and return to the recipient location. In this policy, the recipients will receive a reimbursement for their contribution, such as a discounted shipping fee.

Hybrid Policy: The Hybrid Policy is a combination of the Truck and AV policies such that the operator dispatches its trucks to designated hubs, which act as pickup stations for AVs, and recipients use AVs to visit these hubs. AVs are loaded with the package of each recipient at this hub and return to their recipient's location afterward. This is a two-echelon delivery setting that facilitates efficient and coordinated deliveries.

Crowdsourcing Policy: Crowdsourcing policy is the other two-echelon delivery setting. The operator dispatches trucks to designated hubs, and then from recipients closest to that hub, one recipient crowdsources the AV for delivery. The AV is responsible for delivery to a set of locations in its neighbourhood and then returning to its original owner's location.

The transportation modes are denoted with the subscript $j = \{u, v\}$ representing the truck and AV modes of transportation, respectively, and the policies are denied with the superscript $i = \{t, a, h, w\}$ for the truck, AV, hybrid, and crowdsourcing policies, respectively. The delivery cost of each policy consists of travel costs and hand-off costs. The travel cost for each policy is derived from the cumulative travel costs of each mode (i.e., truck and AV), with the cost of each mode being proportional to its respective travel distance. The cost per unit of travel distance for trucks and AVs are denoted as s_{u} and s_{v}, respectively. The total distance travelled by mode j under policy i is represented as d^i_j. Consequently, the travel cost under policy i can be expressed as $s_{\mathrm{u}} d^{\mathrm{i}}_{\mathrm{u}} + s_{\mathrm{v}} d^{\mathrm{i}}_{\mathrm{v}}$. The per unit distance travel cost for AVs includes any compensation given to AV owners from the delivery firm for their involvement in the delivery process. Additionally, a fixed acquisition cost for trucks is considered in the variable cost per unit distance of a truck.

The operator also incurs a hand-off cost, which reflects the operational complexities involved in supporting and maintaining the infrastructure that facilitates the change of item ownership. This cost also stands for delays associated with transferring goods ownership at transfer points, such as locating parking spaces at recipient locations in the Truck policy or preparing and loading packages onto AVs at depots or hubs in AV-based policies. This hand-off cost is directly proportional to the number of stops where the ownership changes from one party to another. For instance, in the truck policy, there are n hand-offs as the trucks make a stop at each recipient's location. In contrast, in the AV policy, there's just one hand-off since there's a single transfer location at the center of the circle. The number of hand-offs and the marginal cost of these hand-offs under policy i are denoted as f and $s^{\mathrm{i}}_{\mathrm{f}}$, respectively; thus, the total hand-off cost of policy i is $s_{\mathrm{f}}^{\mathrm{i}} f$. Therefore, the total cost of policy i, represented by C^{i}, can be determined by the following equation:

$$C^{\mathrm{i}} = s_{\mathrm{u}} d_u^{\mathrm{i}} + s_{\mathrm{v}} d_{\mathrm{v}}^{\mathrm{i}} + s_{\mathrm{f}}^{\mathrm{i}} f^{\mathrm{i}}. \tag{Three.1}$$

The policies offer distinct strategies for optimizing the last-mile, emphasizing recipient participation and the integration of AVs. Each policy has unique advantages and potential trade-offs in last-mile delivery of perishable goods, which are analytically assessed in this research.

Section D: Ring-Structured Model

The model considers a delivery operation with a single depot located at the center of a circle. Recipients are uniformly distributed along the circumference of the circle. The total number of recipients is denoted by n, and the circle radius is normalized to 1 for simplicity. This uniform distribution results in a recipient density of $\rho = n/2\pi$, and the expected distance between any two consecutive recipients is $\delta = 2\pi/n$.

D.1 Truck Policy

In the truck policy, the service area is equally divided among truck routes of identical delivery lengths. Each truck route is covered by a single truck, serving m^{t} recipients, such that the number of truck routes is $\gamma^t = \lceil n/m^{\mathrm{t}} \rceil$. Here, we assume $n \gg m^{\mathrm{t}}$, and estimate the number of routes as $\gamma^t \approx \frac{n}{m^{\mathrm{t}}}$. Figures Three.1 and Three.2 are structured based on the presence of truck routes. Figure Three.1 presents the one-echelon policies, detailing the truck and AV policies, and Figure Three.2 focuses on the truck-based policies, including truck, hybrid, and crowdsourcing policies. The truck policy appears in both figures for a clearer comparison.

The length of each truck route consists of the inbound and outbound trips to the ring's circumference and the arc-shaped distances travelled on the ring to visit the recipients. Note that the ring radius is normalized to one. Thus, it follows that $l^{\mathrm{t}} = 2 + (m^{\mathrm{t}} - 1)\delta$ where $\delta = 2\pi/n$ is the distance between two consecutive recipients. Assuming a large number of recipients, we

Figure Three.1: Ring-Structured Service Area with radius normalized to 1. (a) Truck Policy. The Circular service area is divided into γ^t truck routes (here $\gamma^t = 10$ and $m^{\mathrm{t}} = 6$). The thick black line shows a truck route. (b) AV Policy. Dashed gray lines show AV routes.

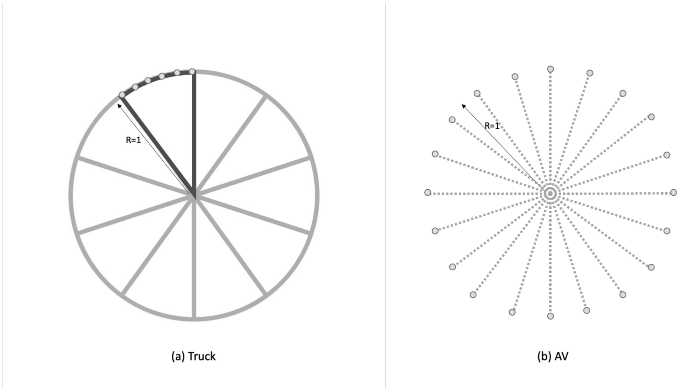

approximate the length of the truck route as:

$$l^{\mathrm{t}} \approx 2 + m^{\mathrm{t}}\delta, \qquad \text{(Three.2)}$$

Considering that truck routes can be either capacity bounding or length bounding, the number of recipients per truck route, m^{t}, is approximately (up to integrality)

$$m^{\mathrm{t}} = \min\{K, \frac{(T-2)n}{2\pi}\}, \qquad \text{(Three.3)}$$

where the two terms present constraints on the trucks capacity and their route length, respectively. We consider cases where at least one of the constraints in (3) is active: the length-bounding case when $l^{\mathrm{t}} = T$ and (Three.2) gives $m^{\mathrm{t}} = (T-2)n/2\pi$, and the capacity bounding case when $m^{\mathrm{t}} = K$. The feasibility of the problem requires $T \geq 2$ (sum of inbound and outbound trips) for the feasibility of the problem so that each truck can travel from the depot to the ring's circumference and visit at least one recipient.

The total truck travel distance is $d_u^t = \gamma^t l^{\mathrm{t}}$, where the length of each truck route is

$$l^{\mathrm{t}} = \begin{cases} 2 + \dfrac{2\pi K}{n} & \text{if } K \leq \dfrac{n(T-2)}{2\pi} \\ T & \text{if } K > \dfrac{n(T-2)}{2\pi} \end{cases} \qquad \text{(Three.4)}$$

In the truck policy, a hand-off refers to the challenge of locating a parking spot close to the recipient's location and reaching their doorstep on foot. As trucks halt at each recipient's location, the truck policy involves $f^{\mathrm{t}} = n$ hand-offs.

Considering (1), it follows that the total cost of the truck policy is

$$C^{\mathrm{t}} = s_{\mathrm{u}}\gamma^{t} l^{\mathrm{t}} + s_{\mathrm{f}}^{t} n. \qquad \text{(Three.5)}$$

D.2 Autonomous Vehicle Policy

In the Autonomous Vehicle (AV) policy, AVs are responsible for making the deliveries to the recipients, and their total travel length is $d_{\mathrm{v}}^{a} = 2n$. This follows as each AV travels from the depot at the center to the circumference of the ring, visits one recipient, and returns to the depot, as shown in Figure Three.1b. The hand-off in the AV policy corresponds to the expense of setting up an automation center at the depot with the cost of s_{f}^{a} to connect to vehicles and load the AVs with ordered items. There is one such hand-off that happens at the depot, thus $f^{\mathrm{a}} = 1$. This leads to a hand-off cost of s_{f}^{a} for this policy. Therefore, the total cost under the AV policy, expressed as C^{a}, is as follows:

$$C^{\mathrm{a}} = 2 s_{\mathrm{v}} n + s_{\mathrm{f}}^{a}. \qquad \text{(Three.6)}$$

Note that capacity-bounding and length-bounding strategies are for truck routing and do not affect the AV policy.

D.3 Hybrid Policy

The hybrid policy involves a multi-echelon delivery setting where both trucks and AVs contribute to the process. As shown in Figure Three.2b, the truck routing in this policy is similar to the pizza-slice pattern in the truck policy, and these truck routes are constrained by tour length. However, there is a key distinction between hybrid and truck policy: in the hybrid policy, instead of traveling directly to the recipients located at the circumference of the ring, each truck travels a distance $r < 1$ from the depot and traverses an inner ring with the radius r, stopping at m^{h} hubs

Figure Three.2: Truck, Hybrid, and Crowdsourcing policies. The black pizza slices indicate one truck route, and the dashed gray lines indicate AV routes. The gray circles show recipients and gray triangles show hubs. a)Truck policy with $m^{\mathrm{t}} = 6$. b and c) Hybrid and Crowdsourcing policies with $m^{\mathrm{h}} = m^{\mathrm{w}} = 2$ and $x = 3$.

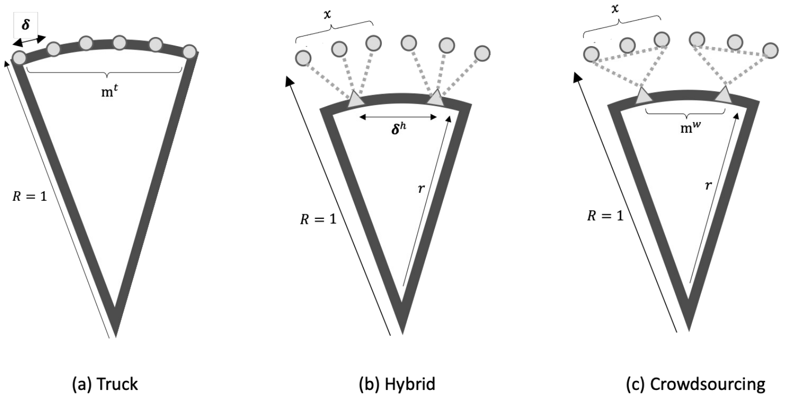

on this route. AVs visit these hubs to pick up the packages instead of traveling all the way to the depot and save time. Once the truck stops at all designated hubs, it finalizes its delivery route by returning to the depot.

Each AV owner dispatches their AV to collect packages from a hub, subsequently delivering them to the owner's location. Recipients select the nearest hub for their AVs to retrieve the packages, and each hub experiences visits from x AVs.

In this policy, the number of hand-off points corresponds to the number of hubs at which ownership of the packages changes. Given that x recipients send their AVs to each hub, the total number of hubs amounts to $f^{\mathrm{h}} = n/x$. For example, when $x = 1$, the number of hand-offs equals n since each recipient is paired with a distinct hub. Conversely, when $x = K$ in the capacity-bounding case, there are $f^{\mathrm{h}} = n/K$ hand-offs in total, as every truck's route incorporates a single hub. Overall, in the hybrid policy, the number of hubs can be expressed as $f^{\mathrm{h}} = n/x$, and their distance from each other is $\delta^{\mathrm{h}} = 2rx\pi/n$. Since AVs in the hybrid policy return directly to their owners without requiring additional labor or facility costs, there is no additional hand-off cost at the recipient's (owner) location.

The travel distances and costs observed in the special scenarios of the hybrid policy where $r = 1$ and $r = 0$ match those of the truck and AV policies, respectively. This can be observed by comparing Figures Three.1 and Three.2. Yet, regarding hand-offs, the hybrid policy demonstrates more hand-offs than the AV policy when $r = 0$ and fewer hand-offs than the truck policy when $r = 1$.

There are γ^{h} truck routes with the same length l^{h}, each visiting an average n/x hubs such that $\gamma^{\mathrm{h}} = \lceil n/xm^{\mathrm{h}} \rceil$. When $n/x \gg m^{\mathrm{h}}$, we approximate the number of truck routes as $\gamma^{\mathrm{h}} = \frac{n}{xm^{\mathrm{h}}}$. The length of each route is approximated similar to (Three.2):

$$l^{\mathrm{h}} \approx 2r + m^{\mathrm{h}}\delta^{h}. \tag{Three.7}$$

Truck routes can be length-bounding or capacity-bounding in the hybrid policy. Thus, the number of hubs per route is obtained as follows:

$$m^{\mathrm{h}} = \min\{\frac{K}{x}, \frac{(T-2r)n}{2rx\pi}\}, \tag{Three.8}$$

where the first term stands for the capacity-bounding case and the second term for the length-bounding case. Similar to (Three.3), m^{h} is an integer, but (Three.8) provides a reasonable approximation when n is large. Thus, total truck travel distance $d_{\mathrm{u}}^{\mathrm{h}} = \gamma^{\mathrm{h}} l^{\mathrm{h}}$ for the length-bounding case is:

$$d_{\mathrm{u}}^{\mathrm{h}} = \frac{2\pi rT}{T-2r}. \tag{Three.9}$$

The AV travel distance $d_{\mathrm{v}}^{\mathrm{h}}$ is approximated using a Taylor expansion of error order two:

$$d_{\mathrm{v}}^{\mathrm{h}} \approx 2n(1-r) + \frac{x^2\pi^2 r}{3(1-r)}. \tag{Three.10}$$

As a special case of (Three.10), when $r = 0$, the hybrid policy and AV policy are the same, where $d_{\mathrm{v}}^{\mathrm{h}} \approx 2n$ and means that recipients send their AVs to the depot.

Using (Three.9) and (Three.10), and with the cost parameters s_{u}, s_{v}, and s_{f}, the total cost of the hybrid policy is as follows:

$$C^{\mathrm{h}} \approx s_{\mathrm{u}}\frac{2\pi rT}{T-2r} + s_{\mathrm{v}}(2n(1-r) + \frac{x^2\pi^2 r}{3(1-r)}) + s_{\mathrm{f}}^{\mathrm{h}}\frac{n}{x}. \tag{Three.11}$$

D.4 Crowdsourcing Policy

In the crowdsourcing policy, the truck routing follows a similar pattern to the hybrid policy wherein each truck travels a radius r from the depot, traverses a ring route, stops at m^{w} hubs, and then returns to the depot. Moreover, there are again x closest recipients allocated to each hub. However, as shown in Figure Three.2c, the routing for AVs differs from the previously mentioned policies in the crowdsourcing policy. Under the crowdsourcing policy, recipients use their AVs to perform the deliveries to their $x-1$ neighbours. In this policy, each AV serves all x recipients allocated to its hub, including its owner. After serving all its recipients, the AV reaches its owner's location. The recipient on the edge of the AV routes is responsible for the crowdsourcing, i.e., the first recipient on the row for recipients assigned to each hub, as shown in Figure Three.2c. For simplicity, assume that the AVs have sufficient capacity to accommodate the demands of these x recipients.

The design of the crowdsourcing policy routing is as follows. There are γ^{w} truck routes, each visiting m^{w} hubs where the length of each route is l^{w}. Similar to the hybrid policy, $\gamma^{\mathrm{w}} \approx n/xm^{\mathrm{w}}$ and $l^{\mathrm{w}} \approx 2r + m^{\mathrm{w}}\delta^{\mathrm{w}}$. The hand-off cost under the crowdsourcing policy equals the number of hubs (which corresponds to hand-offs to AVs) plus the number of recipients (which stands for hand-offs to recipients). Thus, there are $f^{\mathrm{w}} = n + n/x$ hand-offs. The cost associated with truck travel is represented as $s_{\mathrm{u}}\gamma^{\mathrm{w}} l^{\mathrm{w}}$, while the AV travel cost is $s_{\mathrm{v}} d_{\mathrm{v}}^{\mathrm{w}}$.

We use an approximation for the AV distance $d_{\mathrm{v}}^{\mathrm{w}}$ as follows:

$$d_{\mathrm{v}}^{\mathrm{w}} \approx 2\pi + \frac{2n(1-r)}{x} + \frac{r\pi^2 x}{n(1-r)}, \tag{Three.12}$$

The first term is the approximate distance travelled on the ring, and the second and third terms are the line-haul distances.

Finally, the total cost of the crowdsourcing policy is:

$$C^{\mathrm{w}} \approx s_{\mathrm{u}}\gamma^{\mathrm{w}} l^{\mathrm{w}} + s_{\mathrm{v}}\left(2\pi + \frac{2n(1-r)}{x} + \frac{r\pi^2 x}{n(1-r)}\right) + s_{\mathrm{f}}^{\mathrm{h}}\left(n + \frac{n}{x}\right). \tag{Three.13}$$

Section E: Comparative Analysis

In this section, we assess the optimal design of routes in the four introduced policies, compare the length bounding case with the capacity bounding case, and analyze the asymptotic conditions for all policies in the length bounding case. In Section 5.1, we derive the optimal design parameters for each policy, except for the AV policy with cost is presented in (Three.6).

We use this optimal policy design to derive a dominance space in Section 5.2. Policy i dominates policy j if it exhibits a lower cost, denoted by $C^{\mathrm{i}} < C^{\mathrm{j}}$. Ultimately, the dominant policy is the one that outperforms all other policies in terms of cost-effectiveness. The dominance space plot, shown in Figure Three.3, identifies which policy has the lowest cost out of the four policies. We also compare the dominance space for the capacity and length-bounding cases. The results reveal the following consistencies for capacity and length bounding cases (Insight 1): Both cases have similar dominance patterns, the hybrid and crowdsourcing policies are sandwiched between the truck and AV policies, and increasing the number of recipients diminishes the area where the truck policy is dominant. Moreover, in Section 5.3, we derive closed-form expressions for the policy costs when $n \to \infty$ and under these asymptotic conditions, we show that the truck policy is dominated in both length and capacity bounding cases (Insight 2).

There are also some differences between the capacity and length-bounding dominance space analysis: Unlike the capacity-bounding case, in the length-bounding case, the crowdsourcing policy is dominated by other policies in the asymptotic conditions (Insights 3), and in the length-bounding case, the asymptotic cost of hybrid and crowdsourcing policies also depends on the number of customers allocated to each hub, in addition to their dependency to the hand-off cost (Insight 4).

E.1 Optimal policy design

In this section, we use the approximated cost of the hybrid and crowdsourcing policies in (Three.11) and (Three.13), respectively, to derive their optimal radius. We relax all approximations in the numerical analysis in the case study of Section G.

E.1.1 Truck Policy Optimal Design

For the truck policy cost, C^{t}, in the length-bounding, using (Three.5), the following proposition holds:

PROPOSITION E.1.1. The truck policy cost in the length-bounding case under the assumption (i), i.e., the approximated tour length and size, is

$$C^{\mathrm{t}} \approx \frac{2\pi T s_{\mathrm{u}}}{T-2} + s_{\mathrm{f}}^{\mathrm{t}} n. \tag{Three.14}$$

E.1.2 Hybrid Policy Optimal Design

To minimize the overall operational costs in the hybrid policy, we compute the hybrid policy cost C^{h} as per (Three.11). We minimize the associated cost by identifying the optimal truck travel radius r_h^* and the optimal number of recipients per hub x_h^*. In the following proposition, we derive the optimal cost and the optimal values of r_h^* and x_h^* for the hybrid policy in the length-bounding case.

PROPOSITION E.1.2. The hybrid policy cost in the length-bounding, where $l^{\mathrm{h}} = T$, is

$$C^{\mathrm{h}} \approx 2s_{\mathrm{v}}n + s_{\mathrm{f}}\frac{n}{x} + (2s_{\mathrm{u}}\pi + \frac{s_{\mathrm{v}}x^2\pi^2}{3} - 2s_{\mathrm{v}}n)r + (\frac{s_{\mathrm{v}}x^2\pi^2}{3} + \frac{4s_{\mathrm{u}}\pi}{T})r^2. \tag{Three.15}$$

The optimal radius for any given x is approximated as

$$r_{\mathrm{h}}^* \approx \begin{cases} 1 & \text{if } \dfrac{2\pi(4+T)}{(2n-x^2\pi^2)T} \leq \dfrac{s_{\mathrm{v}}}{s_{\mathrm{u}}}, \\ \dfrac{(6s_{\mathrm{v}}n - 6s_{\mathrm{u}}\pi - s_{\mathrm{v}}x^2\pi^2)T}{24s_{\mathrm{u}}\pi + 2s_{\mathrm{v}}x^2\pi^2 T} & \text{if } \dfrac{6\pi}{6n-x^2\pi^2} \leq \dfrac{s_{\mathrm{v}}}{s_{\mathrm{u}}} < \dfrac{2\pi(4+T)}{(2n-x^2\pi^2)T}, \\ 0 & \text{if } \dfrac{6\pi}{6n-x^2\pi^2} > \dfrac{s_{\mathrm{v}}}{s_{\mathrm{u}}}. \end{cases} \tag{Three.16}$$

For any given r, the optimal number of recipients per hub is

$$x_h^* = \begin{cases} 1 & \text{if } \dfrac{3n(1-r)}{2\pi^2 r} \leq \dfrac{s_\mathrm{v}}{s_\mathrm{f}^h}, \\ \sqrt[3]{\dfrac{3s_\mathrm{f}^h n(1-r)}{2s_\mathrm{v}\pi^2 r}} & \text{if } \dfrac{s_\mathrm{v}}{s_\mathrm{f}^h} < \dfrac{3s_\mathrm{f}^h n(1-r)}{2\pi^2 r}. \end{cases} \tag{Three.17}$$

According to Proposition E.1.2, the optimal radius in the length-bounding case is correlated with the vehicle's travel cost ratio ($s_\mathrm{v}/s_\mathrm{u}$). Additionaly, from $\partial r_\mathrm{h}^*/\partial m$ in (Three.16), it follows that r_h^* decreases with x only if $n > \frac{s_\mathrm{u}\pi(T-2)}{s_\mathrm{v}T}$. These insights are similar to those of the capacity-bounding case. However, in the length-bounding case, if $n < \frac{s_\mathrm{u}\pi(T-2)}{s_\mathrm{v}T}$ then r_h^* increases with x to keep the total truck distance bellow the tour limit T.

In Proposition E.1.2, a system of two equations and two unknowns is proposed where finding closed-form solutions for the unknowns, r_h^* and x_h^*, is challenging due to the complex coupling between the equations, which reduces the system's traceability. However, in the numerical experiment presented in Section G, we find r_h^* and x_h^*, and the Hessian matrix showed convexity w.r.t. both r and m. Moreover, in Section E.3, we derive an asymptotic cost when $n \to \infty$ and get closed-form solutions for the optimal cost of each policy.

E.1.3 Crowdsourcing Policy Optimal Design

We minimize the cost of the crowdsourcing policy C^w, according to (Three.13) at the optimal truck travel radius r_w^* and the optimal number of recipients per hub x_h^* for the length-bounding case. The optimal truck travel radius, r_w^*, for the capacity-bounding case and the optimal number of recipients per hub, x_w^*, are detailed in the appendix.

PROPOSITION E.1.3. The crowdsourcing policy cost in the length-bounding case is

$$C^\mathrm{w} = s_\mathrm{v}\left(2\pi + \frac{2n}{x}\right) + s_\mathrm{f}\frac{n(x+1)}{x} + (s_\mathrm{v}(\frac{\pi^2 x}{n} - \frac{2n}{x}) + 2\pi s_\mathrm{u})r + (\frac{2\pi^2 s_\mathrm{v} x}{n} + \frac{8\pi s_\mathrm{u}}{T})\frac{r^2}{2}. \tag{Three.18}$$

The optimal radius is approximated as

$$r_{\mathrm{w}}^{*} \approx \begin{cases} 1 & \text{if } \dfrac{2xn\pi(4+T)}{(2n^2-3x^2\pi^2)T} \leq \dfrac{s_{\mathrm{v}}}{s_{\mathrm{u}}}, \\ \dfrac{2s_{\mathrm{v}}n^2T - 2s_{\mathrm{u}}xn\pi T - s_{\mathrm{v}}x^2\pi^2 T}{2m\pi(4s_{\mathrm{u}}n + s_{\mathrm{v}}x\pi T)} & \text{if } \dfrac{2xn\pi}{2n^2-x^2\pi^2} \leq \dfrac{s_{\mathrm{v}}}{s_{\mathrm{u}}} < \dfrac{2xn\pi(4+T)}{(2n^2-3x^2\pi^2)T}, \\ 0 & \text{if } \dfrac{2xn\pi}{2n^2-x^2\pi^2} > \dfrac{s_{\mathrm{v}}}{s_{\mathrm{u}}}. \end{cases} \tag{Three.19}$$

The optimal number of recipients per hub for any given r is

$$x_{w}^{*} = \begin{cases} 1 & \text{if } \dfrac{n^2(1-r)}{\pi^2 r - 2n^2(1-r)^2} \leq \dfrac{s_{\mathrm{v}}}{s_{\mathrm{f}}^{w}}, \\ \dfrac{n}{\pi}\sqrt{\dfrac{s_{\mathrm{f}}^{w}(1-r) + 2s_{\mathrm{v}}(1-r)^2}{rs_{\mathrm{v}}}} & \text{if } \dfrac{s_{\mathrm{v}}}{s_{\mathrm{f}}^{w}} < \dfrac{n^2(1-r)}{\pi^2 r - 2n^2(1-r)^2}. \end{cases} \tag{Three.20}$$

In the length bounding case, from $\partial r_{\mathrm{w}}^{*}/\partial x$ in (Three.19), r_{w}^{*} decreases with x only if $n > \frac{s_{\mathrm{u}}\pi x\sqrt{T(4+s_{\mathrm{v}}^2 T/s_{\mathrm{u}}^2)-8} - s_{\mathrm{v}}x\pi T}{4s_{\mathrm{u}}}$, showing a similar pattern to the capacity bounding case.

E.2 Comparative Analysis for Length-bounding and Capacity-bounding Cases

We employ the concept of policy dominance to compare the total cost of the four introduced policies. We compare the general dominance space for the capacity-bounding case in Figure Three.3a with the analysis of the dominance space in the length-bounding case, shown in Figure Three.3b. Due to the computational complexity, the mathematical expressions of dominant policy boundaries are not all derivable in closed form. We discuss these boundary expressions in the asymptotic analysis of the next section. The findings from the dominance space analysis, shown in Figure Three.3, are as follows:

Insight 1: The results show robustness across both length-bounding and capacity-bounding cases. The analysis of dominance policies notably reveals that the dominant policy space in both cases has a similar pattern, where the AV policy dominates other policies when the marginal AV cost, s_{v}, is low, while the truck policy dominates other policies when the marginal AV

Figure Three.3: Dominance space under asymptotic conditions. Panels (b) and (d) belong to the length-bounding case, while panels (a) and (c) from Chapter Two belong to the capacity-bounding case.

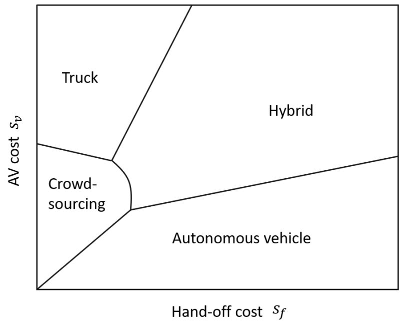

(a) Capacity bounding policy space for general n.

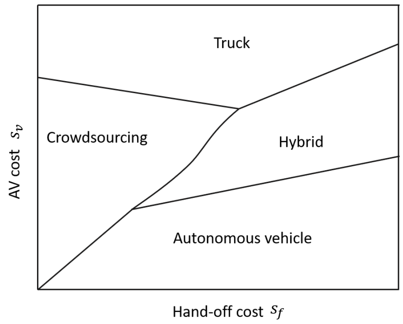

(b) Length bounding policy space for general n.

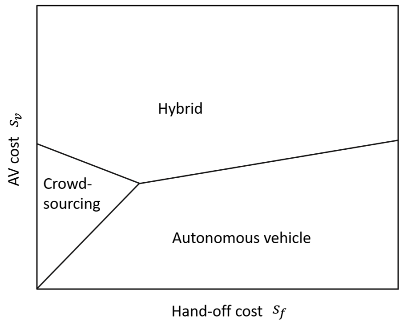

(c) Capacity bounding policy space for $n \to \infty$.

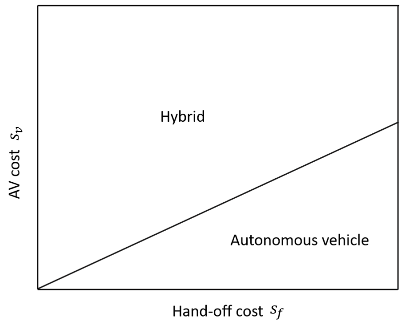

(d) Length bounding policy space for $n \to \infty$.

cost is high. We also observe the sandwiched policies in both cases where crowdsourcing and hybrid policies are sandwiched between the truck and AV policies. Moreover, the hand-off cost significantly impacts these sandwiched policies, where the hybrid policy dominates the crowdsourcing policy in higher hand-off costs due to the smaller number of hand-offs in the hybrid policy.

Moreover, in both cases, increasing the number of recipients expands the dominance space of the hybrid policy and reduces the dominance space of the truck, AV, and crowdsourcing policies. Figure Three.4 shows how increasing the number of recipients grows the policy space of the hybrid policy but shrinks the dominance space of the AV, truck, and crowdsourcing policies to the point that the crowdsourcing policy is non-existent at the largest n. We further analyze the effect of the number of recipients in the next section, where we analyze the asymptotic case.

Figure Three.4: Dominant policy for the length bounding case at different n. The tour length limit is $T = 2.2$, and the truck capacity is $K = 5$. The letters t, a,h,w represent the truck, AV, hybrid, and crowdsourcing policies, respectively.

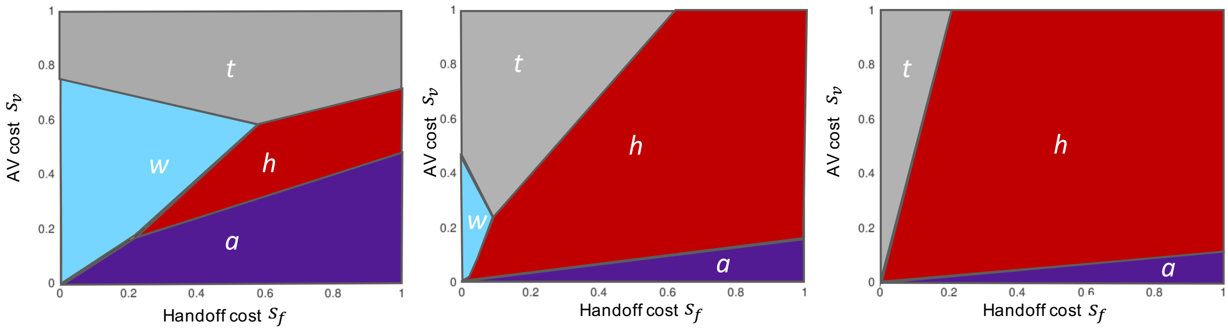

(a) $n = 100$ (b) $n = 1{,}000$ (c) $n = 10{,}000$

E.3 Asymptotic Analysis

We next compare the cost of the different policies when $n \to \infty$ and consider the cost per recipient defined as C^{i}/n for policy i. The asymptotic cost per recipient of policy is denoted i by $C^{i}_{\infty} = \lim_{n\to\infty} \frac{C^{\mathrm{i}}}{n}$. The following proposition presents the asymptotic cost of each policy in the length-bounding case.

PROPOSITION E.3.1. In the length bounding case, as $n \to \infty$, the asymptotic cost of policies are:

$$C^{\mathrm{t}}_{\infty} = s_{\mathrm{f}}, \qquad C^{\mathrm{a}}_{\infty} = 2s_{\mathrm{v}}, \qquad C^{\mathrm{h}}_{\infty} = \frac{s_{\mathrm{f}}}{x}, \qquad C^{\mathrm{w}}_{\infty} = s_{\mathrm{f}}\left(\frac{x+1}{x}\right). \tag{Three.21}$$

Based on Proposition E.3.1, we depict the asymptotic dominance space for the length-bounding case in Figure Three.3d. The following insights are derived from the dominance space analysis. This analysis assumes that hand-off costs are equal across different policies.

Insight 2 (Asymptotic dominated truck policy): In the length-bounding case, the hybrid policy dominates the truck policy. This follows from a direct comparison of the asymptotic costs of truck and hybrid policies presented in (Three.21) as the number of recipients per hub $x \geq 1$. Thus, introducing recipient participation in time-sensitive delivery of perishable goods—whether through the exclusive use of autonomous vehicles, hybrid systems, or crowdsourcing models— eliminates the conventional method of distribution using only trucks. Additionally, considering that the truck policy never holds dominance and the AV policy's hand-off cost is not a factor in the asymptotic costs, the dominant policy is determined solely by the hand-off costs associated with the hybrid and crowdsourcing policies.

Insight 3 (Asymptotic dominant policies): In the length bounding case, the crowdsourcing policy is dominated by the truck and AV policies due to the need for a significant number of hand-offs in the crowdsourcing policy. Here, the asymptotic cost of crowdsourcing, $s_{\mathrm{f}} + s_{\mathrm{f}}/x$, equals the sum of the asymptotic costs of the truck policy, s_{f}, and hybrid policy, s_{f}/x. Additionally, as per (Three.21), the hybrid policy dominates the AV policy when $s_{\mathrm{f}} < 2s_{\mathrm{v}}x$. This occurs when the number of recipients assigned to each truck route is large, enabling the hybrid policy to benefit from the economies of scale in the truck portions of the routes.

Comparing this result with the capacity bounding case, the main difference in crowdsourcing policy dominating other policies over a broader range of parameters under the former. Nevertheless, in both cases, the dominant patterns are similar.

Insight 4 (Hub allocation in multi-echelon policies): The number of recipients per hub does not influence the asymptotic cost per recipient in single-echelon policies (AV and Truck). However, as indicated in (Three.21), the number of recipients allocated to each hub impacts the asymptotic costs per recipient in two-echelon policies (hybrid and crowdsourcing). Since truck routes have a fixed maximum tour length, the cost per recipient in the hybrid policy decreases as the number of recipients per hub increases. As the number of recipients approaches infinity, with the tour length at its maximum, the cost per recipient can approach zero asymptotically. On the other hand, in crowdsourcing policy, the asymptotic cost for a large number of recipients is comparable to that of the truck policy, provided that crowdsourcing AVs have sufficient capacity to carry a high volume of packages. This similarity can also be observed by comparing panels a and c in Figure Three.2, which show the similarity between truck routes in the truck policy and AV routes in the crowdsourcing policy if the number of recipients on those routes is the same.

Section F: Routing on a Circle

In this section, w expand the model for two-dimensional routing when recipients are distributed on the face of a surface. We are inspired by the routing policies on a circle introduced in Chapter Two, where, different from our work, truck routes were bounded by truck capacity. In the two-dimensional routing, the service area is a circular surface, with the radius normalized to one and the depot at the center. They propose the following heuristic for the routing on this circular surface is as follows: The circular service is divided into C concentric rings, which are equally distanced, and these delivery rings are for truck routing in truck, hybrid, and crowdsourcing policies, as shown in Figure Three.5. There is an additional decision variable τ as the distance between every two consecutive rings to find the optimal number of delivery rings for the given circular surface; thus, the radii of rings are:

$$R_1 = \tau/2\,, \quad R_2 = 3\tau/2\,, \quad R_i = (i - \frac{1}{2})\tau\,, \quad R_C = 1. \tag{Three.22}$$

In this circular surface, n recipients are distributed with the density of ρ, so the number of recipients can be calculated as $n = \pi\rho$. In this section, we adapt this heuristic for routing on a circle to modify the four previously introduced policies for the length-bounding case, extending the routing from a one-dimensional ring to a two-dimensional circular surface. As we focus on truck routes constrained by tour lengths for the time-sensitive delivery of perishable goods, the AV routes in two-echelon policies remain intact. Therefore, we use their derivation in the upper bound of the hybrid and crowdsourcing policies on a circle from Chapter Two. For completeness, we have included these derivations in the appendix.

F.1 Truck Policy for Routing on a Circle

In truck policy, trucks travel to each ring and make small perpendicular detours from the ring to visit each recipient assigned to that ring, as shown in Figure Three.5a. In this policy, each recipient will be served from the ring closest to them. Since recipients are distributed uniformly, the number of recipients assigned to each ring is:

$$n_i = (2i-1)\tau^2\pi\rho. \tag{Three.23}$$

The routing choices for truck routes consider that trucks may not always follow the shortest paths within neighborhoods due to real-world constraints such as buildings, restricted roads, and traffic regulations. Thus, trucks follow longer but more feasible paths along highways or ring roads rather than navigating through dense local neighborhoods. The length of each truck route consists of the inbound and outbound travel distances to and from each ring, the portion of the ring traversed by each truck, and the sum of detours from the ring to the recipient's locations for m^{t} recipients assigned to each truck. Figure Three.5a shows one truck route, in truck policy, in detail. We analyze the case of length bounding truck routes in (Three.4), leading to the following relationship between the routing parameters and length constraint:

$$l_i^{\mathrm{t}} = 2R_i + \frac{2\pi R_i m^{\mathrm{t}}}{n_i^t} + \frac{m^{\mathrm{t}}\tau}{2} = T. \tag{Three.24}$$

Thus, the number of recipients assigned to each truck in this policy is

$$m^{\mathrm{t}} = \frac{T-2R_i}{\frac{2\pi R_i}{n_i^t} + \frac{\tau}{2}}. \tag{Three.25}$$

Figure Three.5: Truck routing in Truck, Hybrid, and Crowdsourcing policies, in routing on a circle. Policies are shown for a single truck route. The black dots are recipients, and the gray triangles are hubs. The thick black lines show truck routes, and the dashed gray lines show AV routes.

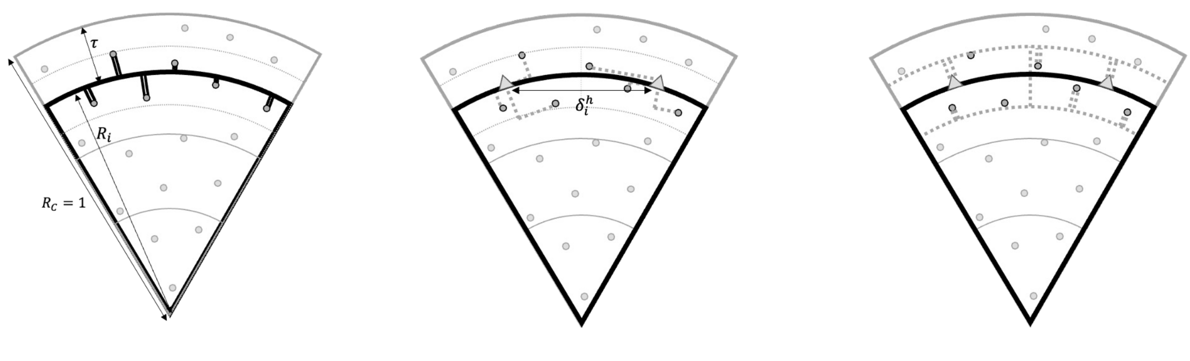

(a) Truck (b) Hybrid (c) Crowdsourcing

Based on the number of recipients on each ring in (Three.23), and the number of recipients on each truck route in (Three.25), the number of truck routes is

$$\gamma_i^{\mathrm{t}} = \frac{n_i}{m^{\mathrm{t}}} = n_i \frac{\frac{2\pi R_i}{n_i^t} + \frac{\tau}{2}}{T - 2R_i} = \frac{2\pi R_i + \frac{n_i^t \tau}{2}}{T - 2R_i}. \tag{Three.26}$$

Finally, the total cost of the truck policy on the circular surface is

$$C^{\mathrm{t}} = s_{\mathrm{u}} \sum_{i=1}^{C} \gamma_i^{\mathrm{t}} l_i^{\mathrm{t}} + s_{\mathrm{f}}^t \rho\pi. \tag{Three.27}$$

We approximate the cost in (Three.27) assuming $\sum_{i=1}^{C} \gamma_i^{\mathrm{t}} l_i^{\mathrm{t}} \approx \int_{i=0}^{C} \gamma_i^{\mathrm{t}} l_i^{\mathrm{t}}$. We also use the approximation of $T + \tau \approx T$ as τ is relatively small compared to T; see details in the appendix.

PROPOSITION F.1.1. Given that l_i^{t} and γ_i^{t} are characterized by τ, the approximated cost is C^{t} minimized at $\tau^* = \sqrt{\frac{2}{\rho}}$, giving the following approximation for the optimal cost of the truck policy on a circle

$$C^{\mathrm{t}*} \approx \frac{\sqrt{2} T s_{\mathrm{u}} (2 - T \log[\frac{T-2}{T}]) + s_{\mathrm{f}} \pi\rho \sqrt{\frac{1}{\rho}}}{\sqrt{\frac{1}{\rho}}} = \sqrt{2\rho} T s_{\mathrm{u}} (2 - T \log[\frac{T-2}{T}]) + s_{\mathrm{f}} \pi\rho. \tag{Three.28}$$

F.2 AV Policy for Routing on a Circle

The AV policy here has a similar setting to the AV policy in routing on a ring where AVs were sent directly from each recipient's location to the depot and back, shown in Figure Three.6. The only difference is that recipients are distributed on the surface, so the total AV travel distance is:

$$d_v^a = \rho \int_0^1 (2l) 2\pi l \, \mathrm{d}l = \frac{4}{3} \rho\pi, \tag{Three.29}$$

where we take integral over the surface of the circle.

There is one single hand-off location at the center of the circle, where AVs are loaded with the packages. Thus, the total cost of the AV policy for routing on a circle is:

$$C^{\mathrm{a}} = \frac{4}{3} \pi\rho s_{\mathrm{v}} + s_{\mathrm{f}}^a. \tag{Three.30}$$

Figure Three.6: AV policy in the circular service area. Dashed gray lines show AV routes.

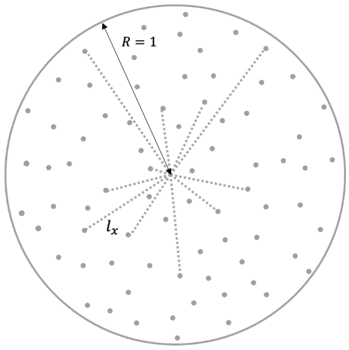

F.3 Hybrid Policy for Routing on a Circle

For the hybrid policy, the truck routing heuristic introduced in the truck policy is applied, where trucks travel to a ring to serve the recipients closest to that ring. However, in this policy, trucks stop at a number of hubs on the ring, and recipients send their AVs to those hubs to pick up their items, as shown in Figure Three.5b. There are n_i customers assigned to each ring, and x customers visit each hub on the ring. Thus, the distance between each two consecutive hubs is:

$$\delta_i^h = \frac{2\pi R_i x}{n_i} = \frac{\pi(2i-1)\tau x}{\pi\rho\tau^2(2i-1)} = \frac{x}{\rho\tau}. \tag{Three.31}$$

Similar to the truck policy, each truck travels from the depot to ring i with radius R_i, traverses the ring, and goes back to the depot. while on the ring, the truck visits m^{h} hubs distanced δ_i^h from each other. Thus, the truck travel distance in the hybrid policy is obtained as follows, bounded by the tour length constraint,

$$l_i^{\mathrm{h}} \approx 2R_i + m^{\mathrm{h}}\delta_i^h = T. \tag{Three.32}$$

The next step is calculating the number of hubs on each truck route:

$$m^{\mathrm{h}} = \frac{T-2R_i}{\delta_i^h} = \frac{(T-2R_i)\rho\tau}{x} \tag{Three.33}$$

The number of length-bounded truck routes in the hybrid policy can be calculated from the ratio of the total number of recipients assigned to each ring and the number of recipients served in each route:

$$\gamma_i^{\mathrm{h}} = \frac{n_i}{m^{\mathrm{h}} x} = \frac{n_i x}{(T - 2R_i)\rho\tau x}. \tag{Three.34}$$

We use the following approximation of the AV travel distance in the hybrid policy; see the appendix for details.

$$d_{\mathrm{v}}^{h} \approx \frac{\tau\pi}{2}(\rho\tau^2 + x)\frac{1}{\tau^2} = \frac{\tau^2\rho\pi + x\pi}{2\tau}. \tag{Three.35}$$

Finally, the cost of the hybrid policy on the circular surface is

$$C^{\mathrm{h}} = s_{\mathrm{u}} \sum_{i=1}^{C} \gamma_i^{\mathrm{h}} l_i^{\mathrm{h}} + s_{\mathrm{v}} d_{\mathrm{v}}^{h} + s_{\mathrm{f}}^{h} s^{h}. \tag{Three.36}$$

We approximate the cost in (Three.36) by assuming $\sum_{i=1}^{C} \gamma_i^{\mathrm{h}} \approx \int_{i=1}^{C} \gamma_i^{\mathrm{h}}$ and approximating the number of rings as $C \approx 1/\tau$; see details in the appendix.

PROPOSITION F.3.1. Using (Three.32), (Three.34), and (Three.35), which are all characterized by τ, the approximated cost C^{h}, is minimized at $\tau^* = \sqrt{\frac{\pi(s_{\mathrm{u}} T^2 \log[\frac{T}{T-2}] + s_{\mathrm{v}} x)}{4 s_{\mathrm{u}} T + \pi s_{\mathrm{v}} \rho}}$, giving the following approximation for the optimal cost of the hybrid policy in routing on a circle

$$\begin{aligned} C^{\mathrm{h}*} \approx \frac{\pi T s_{\mathrm{u}} x \sqrt{\frac{T^2 s_{\mathrm{u}} \log[\frac{T}{T-2}] + s_{\mathrm{v}} x}{T s_{\mathrm{u}} + s_{\mathrm{v}} \rho}}}{2} + 2 T s_{\mathrm{u}} x \sqrt{\frac{T^2 s_{\mathrm{u}} \log[\frac{T}{T-2}] + s_{\mathrm{v}} x}{T s_{\mathrm{u}} + s_{\mathrm{v}} \rho}} \\ -2 T s_{\mathrm{u}} x + \pi s_{\mathrm{v}} x \rho \sqrt{\frac{T^2 s_{\mathrm{u}} \log[\frac{T}{T-2}] + s_{\mathrm{v}} x}{T s_{\mathrm{u}} + s_{\mathrm{v}} \rho}} + \frac{s_{\mathrm{f}}^{h} \rho\pi}{x} \end{aligned} \tag{Three.37}$$

F.4 Crowdsourcing Policy for Routing on a Circle

In the crowdsourcing policy, trucks travel from the depot toward a ring and stop at certain hub locations on the ring, similar to the hybrid policy. Thus, the truck travel distance on each route and the number of truck routes in this policy can be obtained using (Three.32) and (Three.34) in the hybrid policy, respectively.

In this policy, we use AVs for crowdsourcing and consider the m^{w} recipients who visit each hub as one neighbourhood. We use the following approximation of AV travel distance, which is detailed in the appendix.

$$d_{\mathrm{v}}^{w} \approx \frac{\tau\rho\pi(12+x)}{4x} + \frac{2\pi}{\tau}. \tag{Three.38}$$

The number of hand-offs in crowdsourcing policy equals the number of hubs in which hand-offs happen from trucks to AVs, plus the number of recipients, which stands for the recipient's location where AVs are delivering to other recipients $s^{w} = n + \sum_{i=1}^{C} \frac{n_i}{x} = n(1+\frac{1}{x})$.

Finally, the total cost of the crowdsourcing policy is

$$C^{\mathrm{w}} = s_{\mathrm{u}} d_{u}^{w} + s_{\mathrm{v}} d_{v}^{w} + s_{\mathrm{f}}^{w} s^{w}. \tag{Three.39}$$

We approximate the cost in (Three.39) by assuming $\sum_{i=1}^{C} \gamma_i^{\mathrm{h}} \approx \int_{i=1}^{C} \gamma_i^{\mathrm{h}}$ and approximating the number of rings as $C \approx 1/\tau$; see details in the appendix.

PROPOSITION F.4.1. Using (Three.32), (Three.34) and (Three.38), all characterized by τ, the approximate cost C^{w} is minimized at $\tau^* = \sqrt{2}\sqrt{\frac{x\pi\left(4s_{\mathrm{v}}+s_{\mathrm{u}}T^2\log(\frac{T}{T-2})\right)}{s_{\mathrm{v}}\rho\pi(12+x)+8s_{\mathrm{u}}Tx}}$, giving the following approximation for the optimal cost of the crowdsourcing policy in routing on a circle

$$C^{\mathrm{w}*} = \sqrt{2}\sqrt{\frac{x\pi\left(4s_{\mathrm{v}}+s_{\mathrm{u}}T^2\log[\frac{T}{T-2}]\right)}{s_{\mathrm{v}}\rho\pi(12+x)+8s_{\mathrm{u}}Tx}}\left(2s_{\mathrm{u}}T + \frac{s_{\mathrm{v}}\rho\pi(12+x)}{4x}\right) - \tag{Three.40}$$

$$\sqrt{2}\sqrt{\frac{s_{\mathrm{v}}\rho\pi(12+x)+8s_{\mathrm{u}}Tx}{x\pi(4s_{\mathrm{v}}+s_{\mathrm{u}}T^2\log[\frac{T}{T-2}])}}\left(\frac{s_{\mathrm{u}}T^2\pi}{2\tau}\log[\frac{T}{T-2}] + \frac{2s_{\mathrm{v}}\pi}{\tau}\right) - 2s_{\mathrm{u}}T + s_{\mathrm{f}}^{w}\rho\pi(1+\frac{1}{x})$$

F.5 Asymptotic Case for Routing on a Circle

Given the complex cost functions of the policies in routing on a circle and the optimal costs obtained in the previous section, in this section, the goal is to calculate the asymptotic costs of the policies and compare the routing on a circle with the routing on a ring when $n \to \infty$. For routing on a circle, as $n = \pi\delta$, the cost per recipient in policy i is defined as $C^{\mathrm{i}}/\rho\pi$ and the asymptotic cost per recipient of policy i is $C^i_\infty = \lim_{n\to\infty} \frac{C^{\mathrm{i}}}{\pi\rho}$. The following proposition presents the asymptotic cost of each policy in the length-bounding case for routing on a circle.

PROPOSITION F.5.1. For routing on a circle in the length bounding case, as $n \to \infty$, the asymptotic cost of policies are:

$$C^{\mathrm{t}}_\infty = s_{\mathrm{f}}, \qquad C^{\mathrm{a}}_\infty = \frac{4}{3}s_{\mathrm{v}}, \qquad C^{\mathrm{h}}_\infty = \frac{s_{\mathrm{f}}}{x}, \qquad C^{\mathrm{w}}_\infty = \frac{s_{\mathrm{f}}(x+1)}{x}. \tag{Three.41}$$

Insight 5 (Robustness of asymptotic costs): The asymptotic results obtained from the two-dimensional circular routing model in (Three.41) are consistent with those from the one-dimensional ring routing model in (Three.21), differing only by a constant factor in the AV policy. This reinforces the robustness of the models across different routing strategies. Moreover, this consistency implies that *Insight 1-4* discussed there also hold for the more realistic routing on a circle case.

Section G: Case study

This case study is designed to validate the analytical results of the previous sections by incorporating real-world constraints of the last-mile delivery of perishable goods. We propose a heuristic model that accounts for routing limitations, where truck-based policies (truck, hybrid, and crowdsourcing) are constrained by a maximum travel length (T), ensuring the feasibility of perishable goods delivery. Recipient locations are proportional to population density, ensuring that routing decisions reflect real-world demand distributions. The models also integrate variable travel costs for AVs and trucks, as well as variable hand-off costs, allowing insights to remain applicable across different economic conditions. Moreover, we compare the results of this case study for the length-bounding case with the numerical results of the capacity-bounding case.

A Walmart Superstore location is chosen due to Walmart's large customer base, including about 2.4 million daily in-store and online shoppers and over 900,000 visits to its website. The focus is on the Greater Toronto Area, with 18 Walmart superstores currently operating. Among these, the location chosen for detailed analysis is the superstore with the most extensive geographical catchment area, as depicted in Figure Three.7. We consider that recipients are dispersed on the map with their location proportional to the population density, obtained from the heat map in Figure Three.7, i.e., there are more potential customers in the areas with larger populations.

Figure Three.7: Walmart superstore in the Greater Toronto Area with the largest geographical catchment area. The darker shades of brown indicate the higher population density of the land parcels. [source: ArcGIS.com]

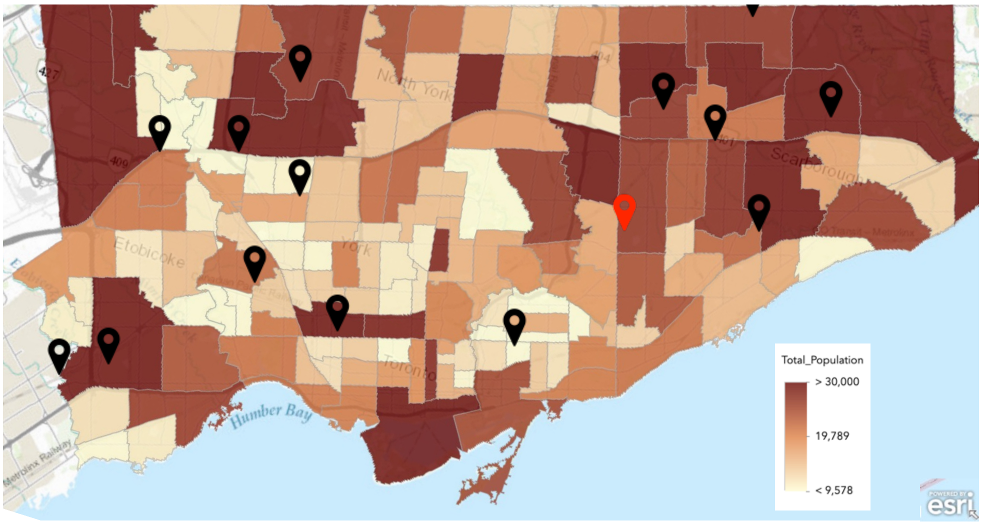

We here consider that truck movement can be either length bounding (the length of each truck tour has to be shorter than T) or capacity bounding (trucks have a capacity of K). To compare the length and capacity bounding cases, we derive the cost of each policy using heuristic models that provide sub-optimal solutions.

We are interested in comparing the validation of the length-bounding and capacity-bounding cases using this case study. Thus, we briefly discuss the heuristic model used for the four policies. In the truck policy, a VRP is addressed using the Simulated Annealing algorithm (Osman 1993), an effective method for finding local optimum solutions for large-scale discrete optimization problems. This requires the location data of recipients and the depot, truck capacity, and the allowable tour length. We encourage readers to refer to Kinderlehrer and Stampacchia (1980) and Blum and Roli (2003) for more in depth readings on such heuristics. The output is the set and sequence of recipients visited in a tour by one truck. The parameter of the simulated annealing algorithm is presented in Table 1. For the AV policy, each recipient's AV is directly sent to the depot, and the cost of the visit equals the length of inbound and outbound trips. In two-echelon policies (hybrid and crowdsourcing policies), we first allocate recipients to clusters using the k-means algorithm (Hartigan and Wong 1979), where recipients in each cluster are served from one hub. The location and number of recipients are proportional to the population density from Figure Three.7. This ensures that areas with higher population densities contain a greater concentration of recipients. The k-means clustering algorithm is then applied to group these recipients based on their spatial distribution. As a result, the formed clusters reflect the population density pattern. In the hybrid policy, the hubs are positioned at the centroid of each cluster, which are formed using the k-means algorithm applied to recipient locations that follow the population density distribution. After clustering, we then solve a VRP using the simulated annealing algorithm, where the destinations are the hubs. The pickup load at every hub is the sum of the number of recipients assigned to that hub. In the crowdsourcing policy, we solve a TSP for each cluster to find a near-optimal solution for visiting all the cluster's recipients in one tour. Here, we find the recipient in each tour closest to the central depot and locate the hub in that recipient's location. Similar to the hybrid policy, we next solve a VRP using the simulated annealing algorithm, where the destinations are the hubs. For all policies, we consider that each recipient generates a single unit of delivery load.

Table Three.1: Simulated Annealing Algorithm Parameter.

Parameter	Value
Initial Temperature	100
Damping Rate	0.98
Maximum Internal Iterations	100
Maximum External Iterations	2,000

We impose the length bounding cases by setting the maximum truck tour length $T = 30km$ in addition to the capacity constraint of setting the truck's maximum capacity at $K = 10$ and analyze this case study with 100 recipients. Figure Three.8 shows the results of the described heuristic models for the four policies and the comparison between length and capacity bounding cases presented in the top and bottom rows, respectively. The AV policy does not incorporate truck routes and their constraints, so it remains unchanged across both cases. Nonetheless, noticeable differences can be seen when comparing the truck routing in truck, hybrid, and crowdsourcing policies. In the truck policy, the number of required trucks increases in the length-bounding case compared to the capacity-bounding case. Furthermore, the clustering of recipients in truck routes varies across the truck, hybrid, and crowdsourcing policies. That is, as the truck tours differ, different recipients are clustered together. In the multi-echelon policies (hybrid and crowdsourcing), clustering and assignment of recipients to hubs also vary within each truck route. In the length-bounding case, the total travel distances for truck and AV modes in each policy are as follows: total truck travel distance of 281.28 km in the truck policy; total AV travel distance of 757.38 km in the AV policy; total truck travel distance of 275.37 km and total AV travel distance of 124.11 km in the hybrid policy; and total truck travel distance of 211.77 km and total AV travel distance of 145.68 km in the crowdsourcing policy.

Figure Three.8: Four policies with the black and gray lines representing truck and autonomous vehicle routes. The top panels from Chapter Chapter Two represent capacity-bounding cases, while the bottom panels represent length-bounding cases.

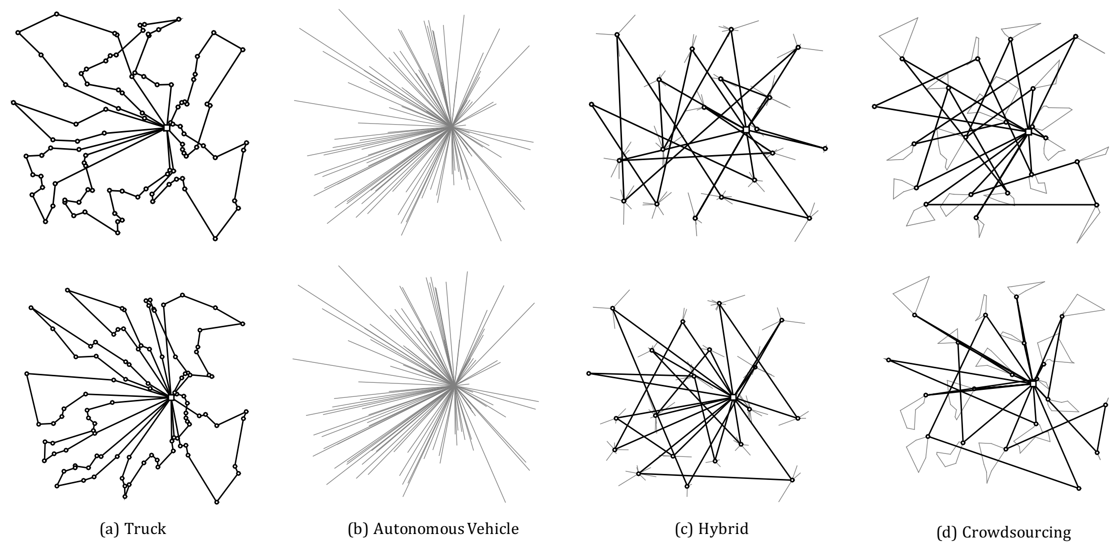

We vary the marginal AV and truck travelling costs within a range of 0 to 1 dollar per km, assuming $s_{\mathrm{v}} = 1 - s_{\mathrm{u}}$. We also vary the hand-off cost from 0 to 10 dollars per hand-off. The policy spaces for $n = 100$ and $n = 1,000$ are represented in Figures Three.9 and Three.10, respectively, to evaluate the delivery cost of a higher number of recipients. In both figures, panels (a) correspond to the capacity-bounding case, which we compare with the length-bounding case in panels (b). Notably, Figure Three.9 exhibits a similar pattern to Figure Three.3, indicating that the case study displays the same dominance space patterns as the analytical model. Key observations include: i) The hybrid and crowdsourcing policies consistently fall between the truck and AV policies in both capacity-bounded and length-bounded scenarios (the so-called "sandwiched" effect). ii) We observe that Insight 1 holds in the case study, given that capacity and length bounding cases have similar dominance patterns.

The policy space for a large number of recipients ($n = 1,000$), in Figure Three.10, closely resembles Figure Three.3c-d from the analytical model validating the asymptotic analysis. It is shown here that the policy space of the truck and crowdsourcing policies shrink as n increases from 100 to 1,000. This observation supports Insight 2, confirming that the truck policy is predominantly outperformed once n is significantly large. Finally, the comparison between the asymptotic cost of length and capacity bounding cases further validates Insight 3, as the crowdsourcing policy space has a smaller share in the length bounding case compared to the capacity bounding case. Beyond validating individual insights, these findings illustrate how the theoretical model serves as a benchmark for real-world policy decisions. Despite the stylized assumptions of the theoretical model, the case study preserves the key dominance relationships, reinforcing the model's practical applicability. This consistency suggests that decision-makers can use the analytical framework to approximate cost-effective policies in diverse operational settings, even when exact optimality is unattainable.

Figure Three.9: Dominant policy for $n = 100$. Letters $\{t, a, h, w\}$ represent truck, AV, hybrid, and crowdsourcing policies, respectively. (a) Capacity-bounding case Chapter Two. (b) Length-bounding case.

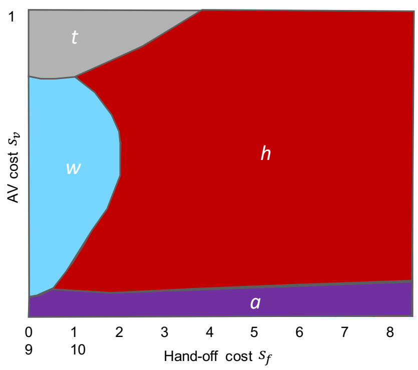

(a) Capacity-bounding

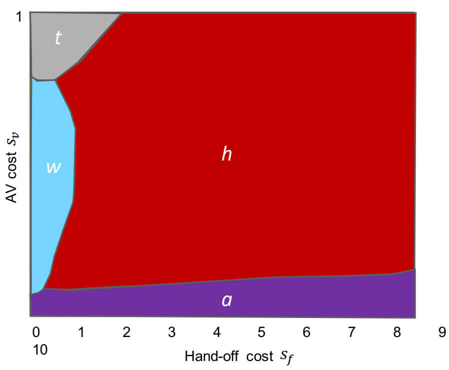

(b) Length-bounding

Figure Three.10: Dominant policy for $n = 1{,}000$. The letters $\{t, a, h, w\}$ represent the truck, AV, hybrid, and crowdsourcing policies, respectively. (a) Capacity-bounding case from Chapter Two. (b) Length-bounding case.

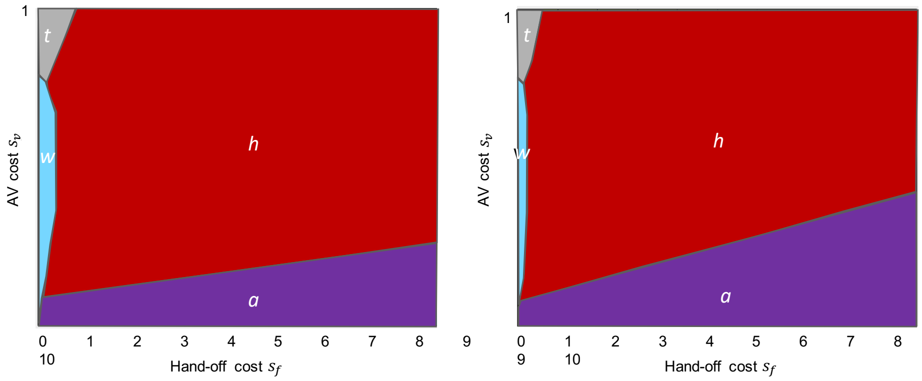

(a) Capacity-bounding

(b) Length-bounding

Section H: Conclusions

The complexity of last-mile logistics is particularly challenging when delivering perishable goods, as it becomes difficult to maintain product quality. In response, to address part of these challenges, we study recipient-dependent last-mile logistics in the time-sensitive delivery of perishable goods, which offers the advantage of higher delivery success rates. This research provides new insights into RDD by focusing on the application of AVs and their role in RDD. This is a relatively unexplored area that demands more attention, given the rapid advancements in AV technology. To focus on the RDD of perishable goods and explore AV-enabled policies, we used the stylized model for routing policies and significantly expanded the literature by comparing aspects of length-bounding routes for time-sensitive deliveries and capacity-bounding truck routes, a key point missing in the existing literature.

One of the primary contributions of this study is comparing different policies under length-bounding and capacity-bounding cases. We found similarities between cases, such as the similar dominance patterns of the AV and truck policies under different marginal AV costs. Furthermore, we observed that when the number of deliveries tends to infinity, the status quo truck policy is dominated by other policies in both cases. We also presented unique patterns in the time-sensitive delivery case, such as the dependency of the asymptotic cost to the hub allocation in two-echelon policies. Additionally, we note the expansion of the hybrid policy's dominance space with the increase in the number of recipients under the length-bounding case.

As we push forward, the impact of this research extends to practical applications, particularly in shaping policies for AV integration in last-mile logistics. While the analysis was mainly centered on comparing costs, it is essential to understand that practical implementation requires a more detailed assessment incorporating various factors such as wage rates, delivery charges, and environmental impact. This study presents significant insights into new opportunities and challenges associated with AVs in last-mile logistics and paves the way for future research. More comprehensive models are needed that factor in the dynamics of two-sided markets, environmental benefits, and the sensitivity of driver and recipient numbers to cost changes. The ultimate goal remains to develop an optimal, efficient, and sustainable model for last-mile logistics that brings maximum benefits to all parties involved.

Chapter Four Tactical Routing and Fleet Planning in Drone-Assisted Last-Mile Delivery

Abstract

Problem definition: Last-mile delivery is the most time-sensitive and expensive leg of the logistic process, requiring innovative solutions to optimize delivery in urban and suburban locations. Drones bring substantial value to this sector by avoiding congested routes and following aerial pathways at higher speeds. Strategically, the decision to incorporate drones into the existing fleet requires a balanced assessment of the benefits of reduced delivery time against operational constraints and acquisition expenses. We formulate a problem of optimal routing and fleet composition in drone-assisted delivery, providing a comprehensive assessment of drone characterization and operational constraints on delivery performance. We consider a drone-assisted delivery setting whereby trucks travel to designated hubs from which drones are launched and retrieved. ***Methodology:*** We adopted the continuous approximation (CA) paradigm, using a continuous distribution of recipients to minimize total delivery time and fleet configuration. We use CA to approximate expected delivery distances in stylized settings and analyze the effect of operational constraints, including drone range, truck and drone capacity, and their synchronization, on delivery performance. We use parametric design to capture the complexities of strategic planning to optimize routing strategies, hub location-allocation, and fleet composition, and we obtain the closed-form expressions for the routing strategy decision variables and optimal fleet composition. ***Managerial implications:*** This research bridges the gap

between incorporating routing-based operational-level constraints, such as drone flight range, coordination of truck routes with drone trajectories, and the potential for launching multiple drones from a single hub. The study identifies policy regions based on the operational parameters of the delivery model, including the truck-to-drone speed ratio, flight range, and truck capacity. The policy spaces developed in this study analyze system efficiency under varying conditions and guide strategic decisions to optimize fleet composition and routing strategies based on technological advancements and operational parameters. (D Viniche et al. 2025)

Section A: Introduction

Last-mile delivery is the final leg of the supply chain involving the transportation of goods from distribution centers to their final destinations. The last mile constitutes about one-third of the average cost of shipping an item due to the complexities of traffic congestion, limited parking availability, and the high detour costs of reaching remote recipients (Dolan 2022). As warehouses and recipients are at the two ends of this leg, last-mile delivery directly influences the customer experience and the profitability of the delivery firm. Last-mile delivery firms aim to provide prompt and efficient service at the least feasible cost by incorporating innovative technologies, business models, and logistics strategies. Among the most promising advances in this space are autonomous transport mediums such as drones, which significantly improve last-mile delivery and can handle up to 80% of shipments in the next decade (McKinsey 2019). Due to their advantages in saving delivery time and cost, drone delivery services are expected to grow to $100 billion market by the end of the next decade (Liu and Sun 2022). Drones are small unmanned aerial vehicles (UAVs) that can be automated or remotely controlled. They offer faster deliveries than conventional vehicles by operating independently of road networks, yielding benefits in dense urban areas, where they can avoid traffic congestion, and remote suburban regions, where they can fly directly on shorter paths.

Any large-scale deployment of drones in the last mile requires proof-of-concept pilots to demonstrate feasibility and efficiency. Major industry leaders have already conducted feasibility studies and pilot programs to explore drone applications in last-mile logistics. Feasibility studies of drone-assisted deliveries were initiated by Amazon Prime Air, performing the first-ever drone-enabled package delivery in 2016 (Wells and Stevens 2016), and the first public delivery in the USA in 2017 (Rubin 2017). Amazon claims that 85% of its products are less than 5lb (McEntegart 2013), within the current drone average payload capacity. Walmart also offers the largest drone delivery program among US retailers, recently expanding its service to up to 1.8 million households throughout the Dallas-Fort Worth metroplex (Walmart 2024). The program provides customers with fast delivery options, with orders arriving in 10-30 minutes, further advancing the role of drone technology in retail logistics. As drone technology improves in-flight power and payload capacity, more products are expected to become eligible carriable items, thus expanding their reach to more customers. Drone delivery has also shown significant potential across other delivery sectors besides the last mile, such as healthcare supply delivery. For instance, Boutilier and Chan (2022) proposed a drone network design to deliver defibrillators in response to out-of-hospital cardiac arrests, demonstrating the potential of modest drone networks to reduce response times and increase survival rates. Feasibility studies have demonstrated the potential of drones through projects such as the UPS and Zipline collaborations for blood deliveries (Tilley 2016), Zipline's medicine delivery initiative in North Carolina (Koetsier 2022), Matternet's logistics network for transporting medical samples (Alley 2019), and the joint UPS and CyPhy project for delivering medical supplies (Carey 2016).

Logistic firms can benefit from integrating drones into their delivery fleets in congested downtown cores and remote suburban regions. In densely populated city centers, drones can bypass traffic congestion and reduce delivery times by taking aerial routes. In remote suburban areas, drones provide an environmentally friendly alternative by eliminating the need for large delivery vehicles to travel long distances to reach geographically isolated customers. Nonetheless, drones have operational constraints, including their battery capacity, which limits their flight's maximum airborne time and distance, known as flight endurance and range. A mixed fleet of trucks and drones can leverage the strengths of both modes of transportation and offer the necessary flexibility and efficiency of an optimal last-mile delivery strategy while effectively overcoming the operational constraints of truck-exclusive or drone-explosive fleets.

Integrating drones to last-mile operations requires planning at the tactical level and delivery management at the operational level. Operational-level routing decisions are day-to-day and related to finding the optimal sequence of visits, assigning orders to trucks, selecting drone launch/retrieval locations, and configuring route-related properties. Such decisions often require detailed information about the location of recipients and other properties like time-window restrictions, package size, and so on. The problem of operational-level decisions is classically posed as mixed integer-linear programs, which find the optimal visit sequence for each truck in the fleet and other drone-related decisions such as their launch and rendezvous points (Murray and Chu 2015, Murray and Raj 2020, Poikonen and Golden 2020). In contrast, strategic planning addresses high-level decisions like configuring the fleet composition and choosing facility locations. Strategic planning requires less detailed data and aims to compare the growth order of cost (or revenue) with respect to the size of recipients. Carlsson and Song (2018) proposed a strategic planning model with one truck and one drone and showed that the efficiency of adding a drone to a truck depends on the square root of the ratio of the truck and the drone speeds.

A gap in the literature at the strategical level of planning is the absence of key operational-level conditions, which complicate any analytical modeling of the problem. Five such complexities are the drone range limitation, limited capacity of drones and trucks, synchronization between truck and drone movements, and launching (or retrieving) multiple drones from (or at) a single launch point. For example, Carlsson and Song (2018) proposed a coordinated single-truck, single-drone delivery system where the drone picks up packages from the moving truck, delivers them, and returns to the vehicle. They use the Continuous Approximation (CA) paradigm to analyze the system and show that efficiency improvement depends on the square root of the truck-to-drone speed ratio. This finding is further validated through computational experiments. Perera et al. (2020) focuses on the decentralization problem of partitioning the market using a multi-drone delivery network with a drone-exclusive delivery system without limitation on the drone flight range. Li et al. (2020b) use CA to provide analytical insights for a multi-truck multi-drone joint delivery system without drone operational constraints.

This study seeks the optimal fleet composition for multi-truck multi-drone delivery to a set of recipients by proposing a parametric design and providing strategic analyses. To capture the complexities of strategic planning, we propose a parametric design framework that enables the formation of a flexible, rule-based routing strategy to optimize fleet configurations and delivery strategies through parameter manipulation. Initially derived from architecture and construction engineering, parametric design facilitates the management of complex design variables. The complex nature of the multi-drone, multi-truck fleet composition problem requires considering i) routing parameters, including vehicle speeds and drone range limitation; ii) facility location-allocation parameters, including the number of hubs, their distance from the central depot, and the allocation of recipients to those hubs; and iii) fleet composition parameters, i.e., number of trucks and drones in the fleet and their respective capacities. Parametric design allows for the integration of all these characteristics into the mathematical model, ensuring clear and explicit relationships between the various components. As a result, parametric design facilitates the analysis of how different parameter changes influence the decision variables. By capturing the complex interactions, this design approach facilitates the derivation of closed-form analytical results and provides valuable managerial insights.

This study proposes an optimal routing strategy and fleet composition policy based on drone operational constraints, including their payload capacity, flight range, and truck-load capacity. We consider a multi-truck multi-drone problem, where multiple drones can be assigned to each truck. Trucks travel from a depot, carrying drones and packages, while they stop at designated hubs on their path to launch and retrieve the drones. Drones are launched from those hubs, delivering the packages to recipients. We consider drone re-launching, where a drone is intercepted by a truck and relaunched to the next delivery point while staying within the drone range. We also consider the multi-launching of drones by each truck, where each truck can launch more than one drone at a single launch hub and retrieve them together at the next hub. The synchronization of truck and drone movements is considered for proper scheduling between the truck and its drones while minimizing the delivery time. Trucks need to be at the retrieval hub prior to the first drone, which we name the scheduling constraint. Furthermore, trucks need to wait at the retrieval point to retire the last drone before leaving that hub. Multi-launching further complicates the scheduling process, requiring a truck to be present at the designated retrieval hub before the arrival of the first drone and idle until the arrival of the last drone.

We focus on a stylized setting with a circular service area and a single depot at the center. This assumption leverages the symmetry of the circular structure and provides analytical tractability. The circular models are widely used in the operations management literature, particularly when demand is assumed to be uniformly distributed, as they allow for the formulation of total cost functions using continuous approximation methods. Many major cities, such as Beijing and Indianapolis, have a circular or ring structure with business hubs near the center and residential areas expanding outward, making the circular approximation both mathematically convenient and empirically relevant. We first consider the one-dimensional distribution of recipients along the circle's boundary, i.e., the circle's circumference. Later, we consider a two-dimensional distribution of recipients on the entire circular surface.

The models in this study identify three distinct policy regions based on the operational parameters of the delivery model, including the truck-to-drone speed ratio, flight range, and truck capacity. In the regions of the policy space, the following features become the limiting factor in deciding the optimal delivery time of the routes: drone range, truck capacity, and the synchronization of each truck's movement with its assigned drones. We derived the closed-form expression for the routing decision variables and the critical speed ratios that define the boundaries of policy regions. The policy space from this analysis illustrates that in low speed ratios, drones fly to their full range, necessary synchronization between truck and drone movement is limiting the delivery performance, and trucks carry partial load below their capacity. For medium speed ratios, drones are flying to their full range, the synchronization between truck and drone movements does not affect the total travel time, and trucks are full to their capacity. In high speed ratios, drones do not fly to their full range, the synchronization is bounding, and trucks are full to their capacity. Moreover, we show that, while amortized ownership costs of trucks and drones influence the critical speed ratios, the optimal fleet composition in each policy region depends solely on the routing strategies rather than vehicle ownership costs. Finally, we validate the total delivery cost for routing on the surface model by demonstrating consistency with the classical Traveling Salesman Problem (TSP) literature, confirming that for uniformly distributed recipients, the cost per recipient scales proportionally to the square roots of the number of recipients.

The remainder of this paper is structured as follows. In Section B, we provide an overview of the most related academic works. In Section C, we first formally introduce the mathematical model, provide the non-linear relationships between the components of the problem, and later introduce the routing problem in a stylized setting. In Section D, we analyze optimal routing for two different settings, followed by the fleet composition optimization problem in D.3. In Section E, we expand the one-dimensional stylized distribution with recipients on the boundary of a circle to a two-dimensional distribution model where recipients are distributed on a surface and how the consistency between the optimized route and fleet composition optimization in the two settings. Finally, the conclusions and directions for future research are provided in Section F. All the proofs are in the appendix.

Section B: Related works

Drones have a wide range of applications in sectors such as logistics, disaster management, and healthcare. A survey by Otto et al. (2018) highlighted the potential of drone delivery across industries such as healthcare, agriculture, and disaster response. D'Andrea (2014) discussed the economic benefits of drone delivery in these sectors based on cost-per-mile analysis. Chung, Sah, and Lee (2020) surveys the civil application of drone delivery in different sectors, among them are transportation and logistics, with a focus on optimization approaches in the Drone and Truck Coordinated Operations. Finally, Poikonen and Campbell (2021) reviewed the routing problem of drone delivery in logistics, emphasizing the future of drone-enabled deliveries given their lower operational cost and accessibility to remote areas. They identified the gap of inadequate consideration of operational constraints, including flight range, battery capacity, speed, and payload limitations. They further suggested that the synchronization of drone trajectories and truck paths poses the most significant challenge in multi-truck multi-drone systems. We thus consider this synchronization in our model.

We next review research focused on coordinated truck and drone delivery systems. Pioneering research in truck and drone delivery systems focused on single-truck, single-drone operations. Murray and Chu (2015) addressed the multi-echelon delivery as the *Flying Sidekick Traveling Salesman Problem* (FSTSP), which was a novel variant of the classic Vehicle Routing Problem (VRP). A mixed-integer linear program was used, but due to the complexity of the problem, they later proposed a heuristic solution for larger instances (Murray and Raj 2020). Several studies further tackled FSTSP and its complex variants. Agatz, Bouman, and Schmidt (2018) and Jeong, Song, and Lee (2019) both contributed integer program solutions, with the latter improving the algorithm complexity of FSTSP by considering the limited flight range of drones and its dependency on carrying payloads. Furthermore, Bouman, Agatz, and Schmidt (2018) used dynamic programming to obtain the exact optimal solution of the traveling salesman problem with a single drone to minimize tour costs in a setting where all recipients are serviced by either the truck or drone.

In extending the problem scope, a body of literature studied multiple-drone multiple-truck scenarios. Sacramento, Pisinger, and Ropke (2019) examined multiple trucks and one drone per truck, while others considered trucks with multiple drones with the carrying capability of one parcel (Wang, Poikonen, and Golden 2017) or multiple parcels (Wang and Sheu 2019). In addition, Kitjacharoenchai et al. (2019) modelled a multi-drone multi-truck problem where drones can transit between trucks (launch from one truck and return to another), adding an extra dimension to the logistical problem. However, critical operational limitations of drone-enabled deliveries are missing in these studies, including the limited battery capacity of drones, which leads to range or endurance constraints. We focus on the multi-truck multi-drone operation while considering the operational characteristics and limitations of the truck-and-drone delivery system, including but not limited to their limited payload capacity and drone battery limitation, which leads to flight range constraints in addition to scheduling constraints of trucks and drones.

A widely adopted approach to solving delivery-routing problems, including sidekick-routing variants, is integer programming (IP). IP-based approaches typically require detailed data, such as the exact locations and delivery loads of recipients. Mathew, Smith, and Waslander (2015) and Peng et al. (2019) focused on the delivery strategy where trucks carry and launch drones with parcels but do not make the final hand-off to recipients, whereas Poikonen and Golden (2020) modeled one truck and k drones, solving a k-multi-visit drone routing problem. Kang and Lee (2021) presented a mixed-integer programming formulation considering a fleet with one truck and multiple drones, all capable of delivery. They proposed a heterogeneous routing problem with multiple drones classified based on speed and battery limits, yet simplistically required drones to return to their launch point, leading to excess truck waiting times and extended total delivery time. Unlike the aforementioned studies where drones deliver packages (alone or parallel to the trucks), Dayarian, Savelsbergh, and Clarke (2020) considered a case where drones resupply trucks and proposed a vehicle routing problem with drone resupply. From a distribution network perspective, Baloch and Gzara (2020) studied the economic desirability of drone delivery compared to traditional delivery services and analyzed the effect of government regulations and customer behavior in addition to the technological constraints on drone adoption. However, they do not consider the hybrid truck-and-drone delivery scenarios. Roberti and Ruthmair (2021) proposed a dynamic programming recursion-based branch-and-price approach to solve traveling salesman problems with drone (TSP-D) variants. Their method outperformed prior approaches by solving instances with up to 39 customers to optimality. Their results demonstrated that even a single drone could substantially reduce delivery time with consideration of synchronization between drone flight and the truck movement. Tiniç et al. (2023) introduced the traveling salesman problem with multiple drones (TSP-mD), modeling truck and drone synchronization by incorporating individual waiting times into the objective function. Their proposed branch-and-cut algorithms outperform standard methods when allowing flexible launch and retrieval locations. Morandi, Leus, and Yaman (2024) extended the orienteering problem (OP) to incorporate multiple drones cooperating with a truck to maximize the total collected prize under a time constraint. Their model considered drones with limited battery endurance and developed a mixed-integer linear programming formulation and a tailored branch-and-cut algorithm that solves instances with up to 50 nodes. One of the prominent limitations of using IP to address the side-kick routing problems lies in its non-polynomial order of complexity. In addition, solving these models often requires a high level of detail, such as the exact location of recipients, delivery time windows, and recipient-specific constraints like drone acceptability. This complex structure and reliance on detailed input data often prevent identifying key insights needed for strategic decision-making. To address this, our model adopts an approximation of recipients' distribution rather than their exact location, allowing us to estimate the total travel distance in drone-assisted scenarios. At the strategic level, the available data is more aggregate, and the emphasis is on comparison policies in terms of their order of cost. This approach facilitates the derivation of managerial insights for strategic decision-making by leveraging approximations of the aggregated data to compare policies in terms of their order of cost.

The Continuous Approximation (CA) methodology replaces detailed data, such as recipient locations, with concise summaries using a continuous density function over time and space (Daganzo 2005). This approach offers simplified yet plausible analysis, often allowing the derivation of closed-form analytical solutions. Carlsson and Song (2018) adopted CA modelling techniques to overcome the mentioned computational challenges while still utilizing a single drone and truck. Whereas, Campbell, Sweeney, and Zhang (2017) used CA considering multiple drones per truck and provided strategic-level insights on the economical advantages of drone delivery and the critical role of synchronization. Li et al. (2020b) studied a delivery setting where recipients are uniformly distributed on a circular service region with a centrally located depot. They applied continuous approximation methods to minimize total delivery costs and optimize service sub-region partitioning. Their model also incorporated package deliveries by truck, aiming to optimize the package delivery ratio between truck and drone while accounting for constraints such as limited truck capacity. Meanwhile, Perera et al. (2020) modelled a drone delivery system where recipients are uniformly distributed on the circumference of a circle and evaluated the impact of drone technologies on logistics systems parameters and efficiency gains over traditional truck logistics. Their findings highlight that, as drone technologies mature and become more cost-effective, decentralized delivery systems become more profitable and can offer more delivery options (e.g., same-day or one-hour delivery guarantees) and greater profit. An existing gap in the literature on such strategic models is the lack of consideration of operational limitations such as drone payload capacity and flight range. We address these gaps while considering the operational characteristics and limitations of drone delivery. Although a mixed fleet of trucks and drones adds complexity to this problem due to the necessary synchronization between truck paths and drone trajectories, a mixed fleet is more practical, as it offers greater flexibility and economic advantage.

Section C: Delivery Routing and Allocation

Consider a distribution firm with a mixed fleet of trucks and drones. Trucks start their route from a depot and visit a set of hubs before returning to the depot. Drones are launched and/or retrieved on these hubs. The first and last hubs visited by each truck are exclusively used for launching and retrieving, respectively, and all other hubs are used for both. We consider a routing policy in which the final drop-off is made by drones; i.e., trucks do not visit the recipients. We consider the following operational restrictions for the truck and drone delivery model.

1. *Drone Range:* Drones have certain flight restrictions that shall not be violated during the course of delivery. The maximum distance each drone can fly is flight "range," which is restricted by the drone's limited battery capacity. Drones can be re-launched multiple times along the truck route as long as their entire flight distance does not exceed their range. Drones are fully charged at the beginning of the delivery, starting from the depot, and cannot recharge during operations.

2. *Truck-and-Drone Synchronizing:* Each drone is operated (launched and retrieved) by a single truck. Each truck can operate multiple drones. Truck paths and their drone trajectories must be coordinated such that launched drones do not arrive at their retrieval hub prior to the arrival of the truck, indicating that there is no drone hovering and a retrieving truck is to be present at the retrieval hub before the drone's arrival. Moreover, trucks cannot leave the rendezvous hub before retrieving all drones of the batch.

3. *Trucks Capacity:* Trucks have a limited capacity represented by the maximum number of recipients they can serve during a delivery day. We assume each recipient takes one unit of the truck's capacity, and each drone serves only one recipient per launch.

The objective is to find the optimal mixed fleet of trucks and drones that minimizes the fleet acquisition and routing (operating) costs. Let n_t and n_d be the number of trucks and drones, respectively, and F_t and F_d be their respective marginal amortized ownership costs. The routing cost of visiting a set of N recipients depends on the fleet composition (number of trucks and drones), and the routing strategy. Hence, we denote the routing cost as $T(n_t, n_d, \psi)$, where ψ represents the properties of a feasible routing strategy and recipient information, such as their locations. Feasible routing conditions must satisfy the drone range, truck-and-drone synchronization, and truck capacity constraints.

We seek to minimize the fleet acquisition and routing costs expressed as

$$C = \min_{n_t, n_d, \psi} T(n_t, n_d, \psi) + F_t n_t + F_d n_d. \tag{Four.1}$$

The conventional discrete formulation of (Four.1) suffers from the curse of dimensionality due to the combinatorial nature of the route structure in $T(n_t, n_d, \psi)$ for any given n_t and n_d, as discussed in the related works section. Therefore, we use a stylized setting of the problem for the routing strategy.

C.1 Routing Strategy

We consider a delivery strategy with a single depot from which N recipients are served. There are n_t trucks, each with capacity K in the fleet to serve these customers. We consider that the number of recipients per truck is equal to x_t, which has to satisfy the truck capacity constraint:

$$x_t \leq K. \tag{Four.2}$$

The required number of trucks is then $\lceil N/x_t \rceil$. The number of trucks in the fleet must be sufficient to meet the service needs of all customers, and therefore it must exceed the required number of trucks:

$$\lceil \frac{N}{x_t} \rceil \leq n_t. \tag{Four.3}$$

Each truck visits $m \geq 1$ hubs on its path to launch and/or retrieve the drones. We consider equal distanced hubs, with the inter-hub distance being δ. Each truck holds a batch of q drones simultaneously launched from each hub, except for the last hub; Therefore, each drone is launched at most $m-1$ times. Each batch of drones will be retrieved together at the subsequent hub along the truck path. Figure Four.1 presents three geometric realizations with various values for m and q. For example, in Figure Four.1a, a batch of $q = 3$ drones is launched one time, given that $m - 1 = 1$, whereas in Figure Four.1c, the same batch is launched twice, given that $m - 1 = 2$.

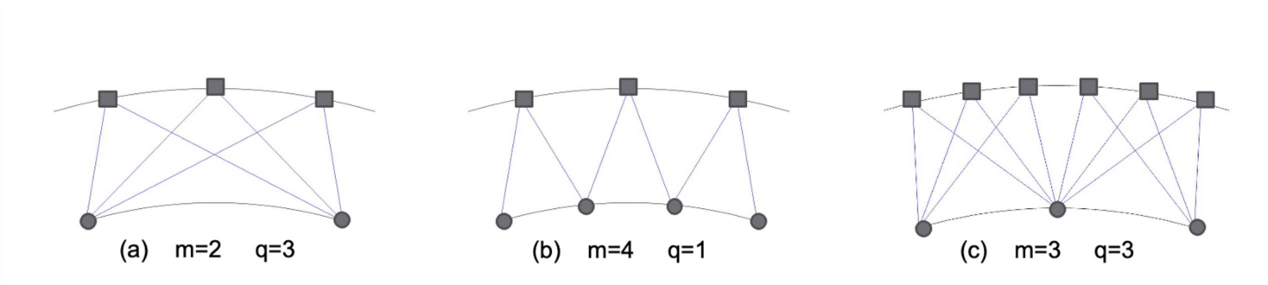

Figure Four.1: Examples with various values for m and q.

Drones on each truck can visit $q(m-1)$ recipients, which we term the truck's drone capacity. Thus, the number of recipients per truck must be less than or equal to the truck's drone capacity:

$$q(m-1) \geq x_t. \tag{Four.4}$$

We next describe the drone-imposed restrictions. The available number of drones in the fleet, n_d, must be greater than the required number of drones. Given $\lceil N/x_t \rceil$ trucks and q drones per truck, we have:

$$n_d \geq q\lceil \frac{N}{x_t} \rceil. \tag{Four.5}$$

The two constraints in (Four.4) and (Four.5) guarantee the sufficient number of drones in the fleet to serve N recipients in addition to satisfying the drone capacity per truck.

Each of the q drones launched by a truck from a given hub flies a unique trajectory between launch and retrieval hubs. We denote the maximum and minimum flight distances in these trajectories by $\underline{L}$ and $\overline{L}$, respectively. An upper bound to each drone's flight distance is when a drone flies a maximum distance of $\overline{L}$ between every two consecutive hubs, i.e., for $m-1$ relaunches. We ensure that drone flight range is not violated in the worst-case scenario, where a single drone travels the longest possible distance of $\overline{L}$ in each of its $(m-1)$ launches. Thus, for a flight range R, the range constraint is

$$(m-1)\overline{L} \leq R. \tag{Four.6}$$

To ensure trucks are at the retrieval point prior to all drones assigned to them, truck travel time between two consecutive hubs should be less than the shortest flight time of those drones, which we call the scheduling constraint. With the shortest travel time as the extreme case, we thus require the following:

$$\frac{\underline{L}}{s_d} \geq \frac{\delta}{s_t}, \tag{Four.7}$$

where s_t and s_d represent the average speeds of trucks and drones, respectively. $s_d \geq s_t$, reflecting that drones travel along aerial trajectories and are not constrained by traffic congestion or associated limitations. The assumed speeds also account for the detours that trucks must make due to the geometry of road networks, while drones can traverse direct distances with greater flexibility.

In addition to the scheduling constraint, trucks leave a hub only after retrieving all their q drones. This condition leads to a waiting time at each of the last $m-1$ hubs, accounting for the period between the truck's arrival and the receiving of the last drone of the batch, i.e., the drone that travels the longest distance. Given $m-1$ retrieval hubs per route, the total waiting time of each truck at all its visiting hubs is

$$(\frac{\overline{L}}{s_d}-\frac{\delta}{s_t})(m-1). \tag{Four.8}$$

The routing cost per truck consists of i) truck routing time and ii) truck waiting time at all hubs. Considering that each truck travels the distance of l_t, and using the truck waiting time given in (Four.8), the routing cost per truck, with a marginal cost of time that is normalized to 1, is

$$T(n_t,n_d)=\frac{l_t}{s_t}+(\frac{\overline{L}}{s_d}-\frac{\delta}{s_t})(m-1). \tag{Four.9}$$

We note that the routing cost and its associated constraints depend on the fleet composition, n_t and n_d, as well as on the routing strategy that can be characterized by the decision variable set $\psi=\{m,q,x_t\}$, which is dropped for brevity from $T(n_t,n_d,\psi)$ in (Four.9).

We seek to minimize the total cost of the presented delivery model. We discuss the optimal fleet composition, i.e., the optimal number of trucks n_t^* and drones n_d^* in the fleet, and the routing decision variables $\psi=\{m^*,q^*,x_t^*\}$ of the truck and drone delivery operations by optimizing a non-linear mathematical model with the objective function (Four.1), and the set of constraints (Four.2)-(Four.7).

The proposed mathematical model is non-linear due to constraints (Four.2), (Four.4), (Four.5), (Four.6), and (Four.7), which include products of decision variables and square-root terms. Given this non-linearity, direct analysis of the Karush–Kuhn–Tucker conditions leads to a large system of equations, with solutions sets that are not easily comparable (Wu 2007). We, therefore, propose a backward induction methodology, whereby we first consider a given fleet composition of n_t trucks and n_d drones and minimize the total routing cost $T(n_t,n_d)$ obtained from (Four.9). This approach requires that we bound the number of trucks such that $n_t \geq \frac{N}{K}$, otherwise, the trucks would not have enough capacity to serve all recipients.

We use the backward induction to solve the mathematical model for a given fleet composition, given the non-linearity of (Four.1)-(Four.7). To address the integrality of the number of trucks, $\lceil N/x_t \rceil$, we consider a continuous relaxation of this term and approximate the truck fleet size as N/x_t. This approximation becomes more accurate for $N \gg K$ as the deviation between the continuous and discrete decision variables is diminished. The relaxed mathematical model is

$$\begin{aligned} \min_{x_t,m,q} \quad & T(n_t,n_d) = \frac{l_t}{s_t} + (\frac{\overline{L}}{s_d} - \frac{\delta}{s_t})(m-1) \\ \text{s.t.} \quad & (m-1)\overline{L} \leq R, \\ & x_t \leq K \\ & x_t \leq q(m-1) \\ & \frac{\delta}{s_t} \leq \frac{\underline{L}}{s_d} \\ & \frac{N}{x_t} \leq n_t \\ & q\frac{N}{x_t} \leq n_d. \end{aligned} \tag{Four.10}$$

In the interest of deriving closed-form expressions and meaningful insights, we consider a stylized setting of the problem, which we refer to as “circular routing,” where demand is only on the circumference of the circle. Section D proposes a routing strategy for a given n_t and n_d, using the circular routing model. We obtain the closed-form solution of the optimal circular routing in Section D.1 and present a ring-radial routing model, which is a modification of circular routing in Section D.2. We then solve for the optimal fleet composition (optimal number of trucks and drones) in Section D.3, where we approximate (Four.1) and derive the optimal fleet composition and routing strategy. Finally, in Section E, we analyze the case where demand occurs over the entire circular surface.

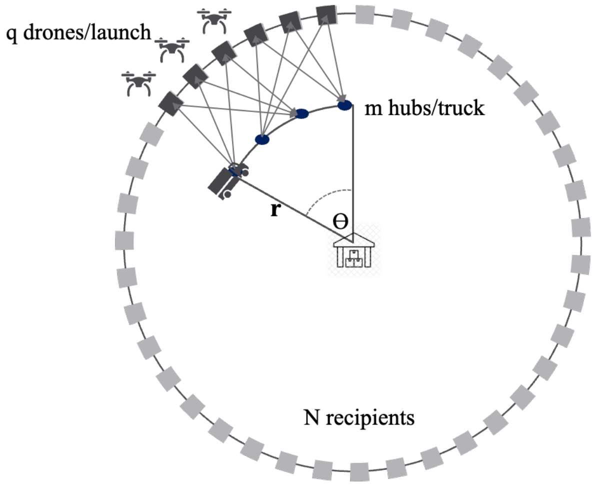

Figure Four.2: Circular routing model.

Section D: Circular Routing

Consider a depot located at the center of a circle with N recipients uniformly distributed on the circle's circumference, as shown in Figure Four.2. Trucks travel a distance r away from the depot, then traverse an arc of radius r , as shown in Figure Four.2. Thus, each truck travels the distance of $l_t = r + l_{arc}$, where the terms represent the outbound and arc lengths. Without loss of generality, we do not consider the truck's inbound trip from the final hub to the depot, as this segment does not affect the delivery time or the delay experienced by the recipients. We normalize the circle radius to 1. The arc length is inversely proportional to the number of trucks, and therefore, the length of each truck route is

$$l_t = r + \frac{2\pi r}{\lceil N/x_t \rceil}. \tag{Four.11}$$

Each truck visits m hubs that are equally spaced and located a distance r away from the depot, as shown in Figure Four.2. Given that the perimeter of the inner circle is $2\pi r$, the inter-hub distance, δ, is

$$\delta = \frac{2\pi r}{m\lceil N/x_t \rceil}. \tag{Four.12}$$

We calculate the maximum and minimum flight distances of the drones in each batch, accounting for the different flight trajectories among drones in each batch. We approximate the geometry of the flight trajectory by converting the two arcs of Figure Four.3a into two parallel lines as in Figure Four.3b. Using the Pythagorean Theorem, the maximum flight distance is

$$\overline{L} = (1-r) + \sqrt{(\delta)^2 + (1-r)^2}, \tag{Four.13}$$

and the minimum flight distance is

$$\underline{L} = 2\sqrt{(\delta/2)^2 + (1-r)^2}. \tag{Four.14}$$

We now use the derivation of the circular routing strategy in constraints (Four.3)-(Four.7), to obtain the closed-form solution for optimal routing cost per truck, presented in (Four.9).

D.1 Optimal Circular Routing

We solve the mathematical model presented in (Four.10) for a given fleet composition of trucks and drones using the proposed circular routing model. We leverage the circular routing derivations presented in (Four.11)-(Four.14) to obtain the closed-form expressions for the optimal routing decision variables $\psi_{\text{circle}} = \{m, q, r, x_t\}$, proved in the appendix, which leads to the following propositions.

Proposition 1 The optimal number of recipients per truck x_t^*, the optimal number of launches per hub q^*, and the optimal number of hubs m^* are derived in the appendix as

$$x_t^* = \frac{N}{n_t}, q^* = \frac{n_d}{n_t}, m^* = \frac{N}{n_d} + 1, \tag{Four.15}$$

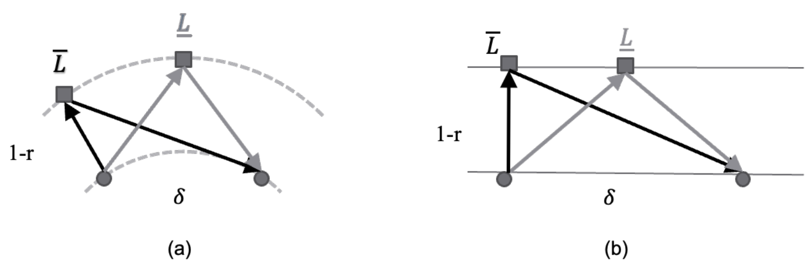

Figure Four.3: Minimum and maximum flight distance for drones are launched from one truck in a batch together (only the shortest and longest routes are shown).

Proposition 2 The optimal truck travel radius r^* is derived in the Appendix as

$$r^* = \begin{cases} \frac{-m^* NR\sqrt{4{x_t^*}^2\pi^2(R-2m^*+2)+R{m^*}^2N^2}+Rm^*N}{4{x_t^*}^2\pi^2(m^*-1)} & s_t/s_d \leq \tau \\ \frac{{m^*}^2N^2s_t^2-\pi m^* N s_t x_t^* \sqrt{s_d^2-s_t^2}}{{m^*}^2N^2s_t^2-\pi^2{x_t^*}^2(s_d^2-s_t^2)} & s_t/s_d > \tau, \end{cases} \tag{Four.16}$$

where τ is the critical speed ratio, derived in the Appendix as:

$$\tau = \frac{n_d\sqrt{4\pi^2r^2n_d^2+(1-r)^2N^2n_t^2}}{N\sqrt{4\pi^2r^2n_d^2+(1-r)^2N^2n_t^2}-(4\pi^2rn_d^2-(1-r)N^2n_t^2)}, \tag{Four.17}$$

which depends on the number of recipients and fleet composition.

We demonstrate the results of Propositions 1 and 2 in Figure Four.4. The main insights from Propositions 1 and 2 are:

Insight 1: Proposition 1 shows that recipients are equally divided amongst trucks; each truck holds n_d/n_t drones, where all drones are launched together (starting from the first hub visited by the truck), and each drone is launched N/n_d times.

Insight 2: When the truck-to-drone speed ratio is below the critical speed ratio, the drone's range becomes the primary factor affecting the optimal radius. In this case, since the drone speed is "sufficiently" higher than the truck speed, drones are favored more and use their full flight range for optimal operation. Therefore, the range constraint (Four.6) is binding. Moreover, the speed parameters do not affect the optimal radius here; thus, the scheduling constraint (Four.7) is not binding.

Insight 3: When the speed ratio is above the critical speed ratio, the speeds are the primary factor affecting the optimal radius., e.g., the optimal radius is independent of R. In this case, drones are favored less because their speed is not "sufficiently" higher than the speed of the trucks, and therefore, the full drone range is not depleted. In such cases, the range constraint is not binding, and the routing is governed by the coordination between trucks and drones as expressed in (Four.7).

Figure Four.4 depicts the optimal radius and the associated routing cost, where different colors represent different flight ranges $R = 0.5, 1, ..., 2.5$. The speed ratio ranges from zero to

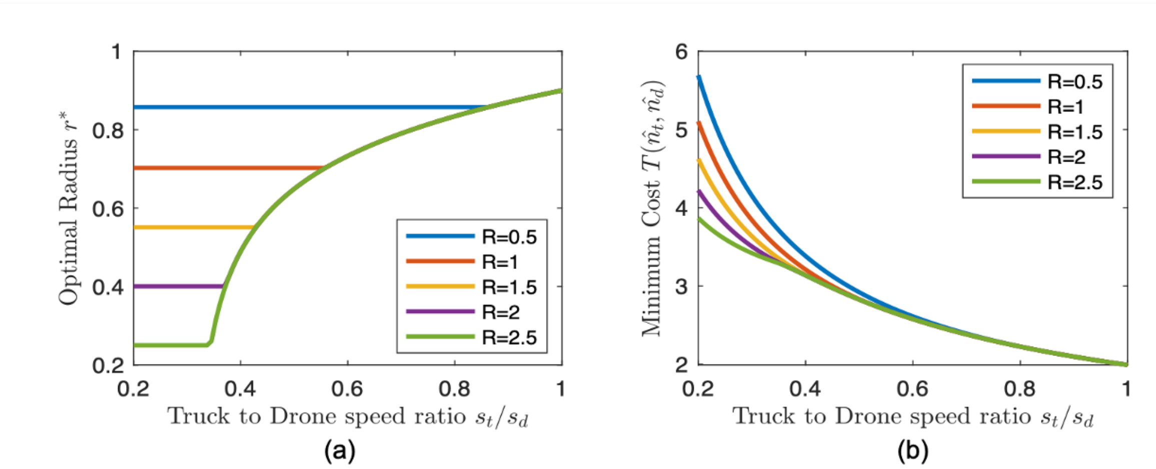

Figure Four.4: Optimal radius and Minimum Routing Cost based on speed Ratio s_t/s_d for Different Fligh Range R.

one, where we fix the drone speed and increase the truck speed from zero to s_d. When the speed ratio is below the critical speed ratio, Figure Four.4a shows that the optimal radius depends only on the range as the binding constraint in this region, consistent with *Insight 1*. On the other hand, when the speed ratio is above the critical point, the range does not affect the optimal radius, and all travel radii overlap, following the reasoning of *Insight 2*. In the extreme case when the truck speed is close to the drone speed, based on (Four.16), the optimal radius approaches one, and trucks get as close as possible to the recipients. This means that drones do not travel any distance because of the financial advantages of trucks when they can travel at the same speed.

As drone range increases, trucks can launch drones from greater distances toward the recipients, resulting in hubs being positioned closer to the depot. Consequently, the optimal radius starts from smaller values. As illustrated in Figure Four.4a, the critical speed ratio decreases as the range increases. Figure Four.4b shows that the routing cost consistently decreases with the speed ratio, both below and above the critical speed ratio, τ. However, as previously discussed, below the critical speed ratio, the routing cost is influenced by the drone range, with higher ranges resulting in lower costs. In contrast, above the critical speed ratio, the routing cost becomes solely dependent on the speed ratio and is no longer affected by the range. Consequently, as shown in Figure Four.4b, the routing costs for all ranges converge to a single curve of minimum cost beyond the critical speed.

The number of trucks and drones in the fleet affects the optimal routing decision variables.

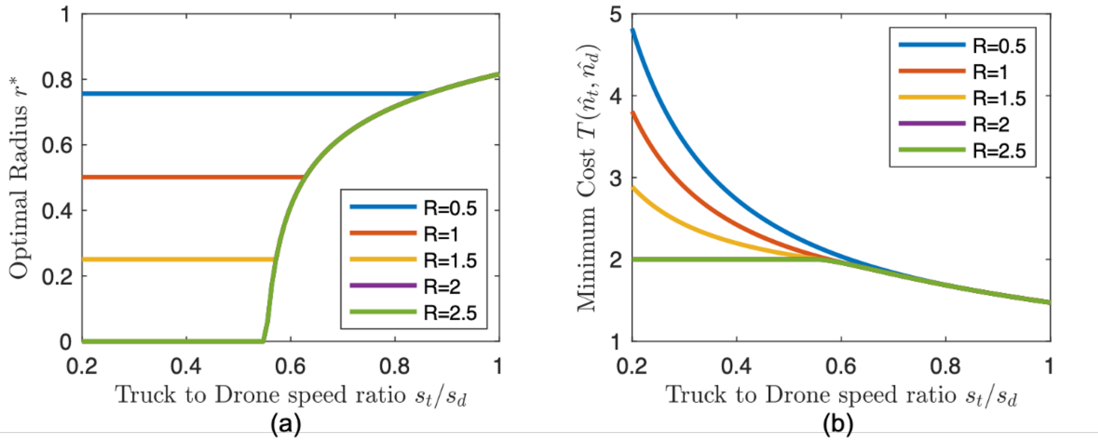

Figure Four.5: Effect of fleet composition on Optimal Radius and Minimum Routing Cost.

Figure Four.5 illustrates the effect of fleet composition on these decision variables by increasing the number of drones to match the number of recipients. Comparing Figure Four.5 with Figure Four.4, which depicts a scenario with a higher number of drones, we observe that for the same flight range, the optimal radius decreases as the number of drones increases. This is because a sufficient number of drones allows each recipient to be served by a single drone, eliminating the need for relaunching. In this case, each drone utilizes its full range for a single delivery, allowing trucks to travel shorter distances, which results in a lower optimal radius. In the extreme case depicted in Figure Four.5a, when $R = 2$ (double the normalized radius of the circle), the fleet has a sufficient number of drones to serve all recipients directly. Consequently, the optimal radius r^* is zero before the critical speed ratio, as drones can complete direct flights from the depot to each recipient and back. Since trucks do not leave the depot in this scenario, the minimum associated routing cost remains constant and independent of the speed ratio before the critical point, as shown in Figure Four.5b. Furthermore, increasing the flight range beyond this point (e.g., from $R = 2$ to $R = 2.5$) does not change the result, as the same optimal values are achieved for those ranges.

Despite having an interpretable solution, the circular routing model has some drawbacks. The closed-form derivation of the optimal routing cost $T(n_t, n_d)$ is not mathematically tractable due to complexities such as the co-dependence of the optimal radius and the critical speed ratio in (Four.16) and (Four.17). This caveat also complicates the derivation of the optimal fleet composition, which is a primary objective of this study. Therefore, we consider a slightly modified “ring-radial” routing strategy that exhibits similar patterns as circular routing and is tractable in deriving the optimal fleet composition.

D.2 Ring-Radial Setting

We present an alternative model of the circular routing problem that provides an upper bound on the objective function (Four.9). The ring-radial routing strategy allows drones and trucks to move in four directions: two radial directions towards and away from the depot, and two ring directions along an arc such that the distance of any point on the arc from the depot remains the same (i.e., along arcs of concentric rings with a radius smaller or equal to one). Figure Four.6 depicts examples of circular routing from Section D.1 and ring-radial routing.

The ring-radial setting is similar to circular routing in terms of constraints and objective function, except for the definitions of the maximum and minimum flight distances of the drones in each batch. As shown in Figure Four.6, truck movements are identical in both settings. However, the drones follow distinct flight patterns in the ring-radial configuration, where the minimum and maximum flight distances are equal and can be expressed as:

$$\underline{L} = \overline{L} = L = 2(1-r) + \delta. \tag{Four.18}$$

Again, we consider the optimization routing problem for a given number of trucks and drones and discuss the optimal decision variables in the following proposition.

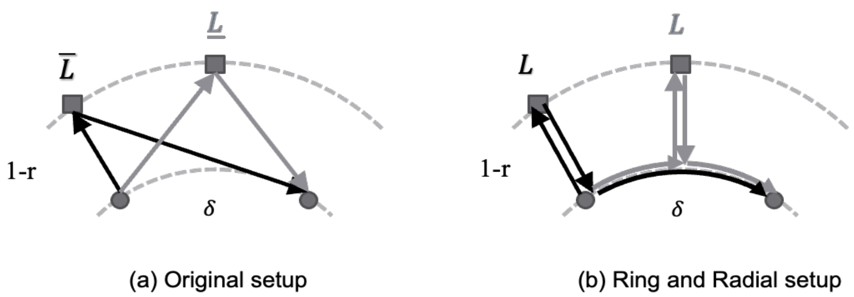

Figure Four.6: Ring Radial Routing Setting. Minimum and maximum flight distances for drones are launched from one truck in a batch together (only the shortest and longest routes are shown).

Proposition 3 The optimal decision variables of the ring-radial setting are identical to those in the circular routing setting, except for the optimal radius, as given by (Four.15) and detailed in the Appendix.

$$r^* = \begin{cases} \frac{2Nn_t - n_d n_t R}{2Nn_t - 2\pi n_d} & s_t/s_d \leq \tau \\ \frac{Nn_t s_t}{\pi n_d (s_d - s_t) + Nn_t s_t} & s_t/s_d > \tau, \end{cases} \tag{Four.19}$$

where the critical speed ratio is derived in the appendix as

$$\tau = \frac{Nn_t n_d + n_t n_d^2}{2N^2 n_t + 2Nn_t n_d - 2\pi N n_d}. \tag{Four.20}$$

The optimal radius for the ring-radial routing simplifies to a tractable expression that, similar to the circular routing case, depends on the truck-to-drone speed ratio, where τ is the critical speed ratio for the ring-radial setting, given in the Appendix.

Insight 4: The ring-radial routing setting exhibits similar trends to the circular routing model with respect to the dependency of the optimal radius and total cost on the critical speed ratio. When the truck-to-drone speed ratio is below the critical speed ratio, the optimal radius depends on the drone's range, while above the critical speed ratio, the optimal radius becomes independent of the range and is influenced solely by the speed ratio.

Insight 5: Different from the circular setting, in the ring-radial setting, the critical speed

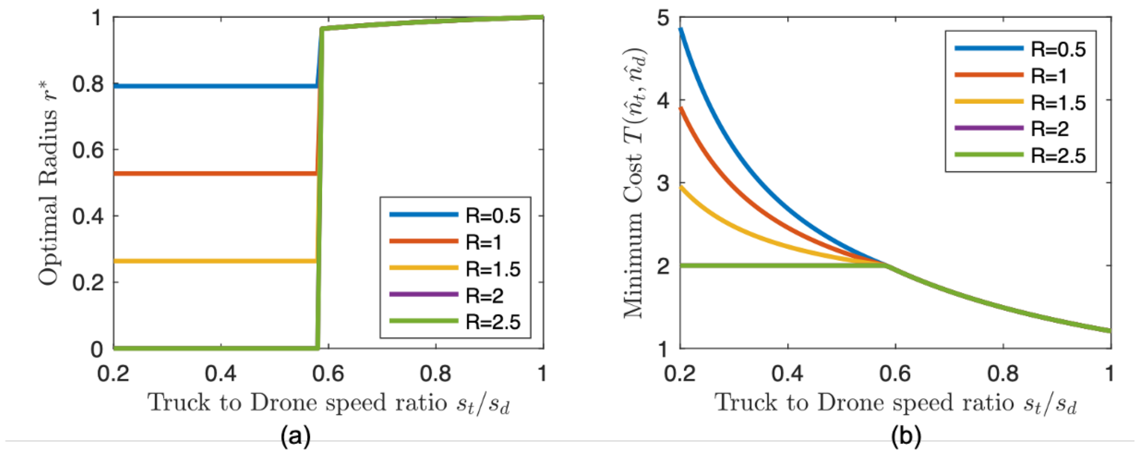

Figure Four.7: Optimal radius and Minimum Routing Cost in the Ring-Radial Setting.

ratio is independent of the drone's range. This independence simplifies the optimization problem by decoupling the critical speed ratio from the optimal radius, which makes it possible to express the optimal ring-radial routing cost in a more tractable form.

Figure Four.7 shows that optimal radius and routing cost in the ring-radial setting follow a similar trend to circular routing. The radius below the critical speed ratio depends on the drone's range, as shown by the different colors, as the range constraint is binding. However, once the speed ratio exceeds the critical value, the optimal radii for all ranges converge, and the radius is influenced solely by the speed ratio. The associated routing cost, shown in Figure Four.7b, also decreases with the speed ratio, as in the circular setting. The key distinction is that in the ring-radial model, the critical speed ratio is independent of the drone's range. This simplifies the optimization problem by decoupling the critical speed ratio from the optimal radius, which was a source of complexity in the circular routing model. The ring-radial setting retains the same binding constraints as circular routing: the range constraint is binding below the critical speed ratio, and the scheduling constraint governs routing decisions above it. The critical speed ratio in ring-radial routing is independent of the optimal radius, which provides a tractable framework for deriving the close-form optimal routing cost.

$$T^*(n_t, n_d) = \begin{cases} \frac{R}{s_d} + \frac{2Nn_t - n_d n_t R}{2s_t(Nn_t - \pi n_d)} & s_t/s_d \leq \tau \\ \frac{N(n_t+2\pi)}{n_d\pi(s_d - s_t) + n_t s_t N} & s_t/s_d > \tau. \end{cases} \tag{Four.21}$$

The critical speed ratio and optimal cost also depend on fleet composition, i.e., the number of trucks and drones in the fleet, and the number of recipients.

D.3 Fleet composition optimization

With the closed-form solutions of the optimal routing strategy for a given fleet composition, we now turn to the problem of determining the optimal fleet composition to minimize the total cost of the delivery operation. The total cost is influenced by both the routing strategy and the fleet composition. We derive the optimal fleet composition using the optimal routing results from

Propositions 1 and *3*,

$$C = n_t T^*(n_t, n_d) + F_t n_t + F_d n_d. \tag{Four.22}$$

We consider the entire fleet cost in contrast to (Four.9), where only one truck route was considered. Here, T^* is the minimized routing cost from the ring-radial setting. The routing constraints in (Four.2)-(Four.7) of Section C.1 hold for the fleet composition optimization problem as well.

Proposition 4 We find the optimal solution for minimizing (Four.22) where the closed-form expressions for the optimal number of hubs m^* and the number of launches per hub q^* are the same as for the optimal routing problem. The optimal number of recipients per truck x_t^* is related to both the number of trucks and the truck capacity.

$$x_t^* = \min\{K, \frac{N}{n_t^*}\},\ q^* = \frac{n_d^*}{n_t^*},\ m^* = \frac{N}{n_d^*} + 1, \tag{Four.23}$$

Proposition 5 The optimal fleet composition, i.e., the optimal number of trucks n_t^* and drones n_d^* in the fleet, are:

$$n_t^* = \begin{cases} \frac{2\pi r^* s_d}{R s_t} & s_t/s_d \leq \tau_1 \\ \frac{N}{K} & s_t/s_d \geq \tau_1 \end{cases}, \tag{Four.24}$$

and

$$n_d^* = \begin{cases} \frac{2Ns_d(1-r^*)}{R(s_d-s_t)} & s_t/s_d \leq \tau_1 \\ \frac{2N^2(1-r)}{NR-2\pi KR} & \tau_q \leq s_t/s_d \leq \tau_2 \\ \frac{N}{K} & s_t/s_d \geq \tau_2 \end{cases}, \tag{Four.25}$$

where

$$r^* = \begin{cases} \frac{n_t(2N-n_dR)}{2Nn_t-2\pi n_d} & s_t/s_d \leq \tau_2 \\ \frac{Nn_ts_t}{\pi n_d(s_d-s_t)+Nn_ts_t} & s_t/s_d > \tau_2 \end{cases}. \tag{Four.26}$$

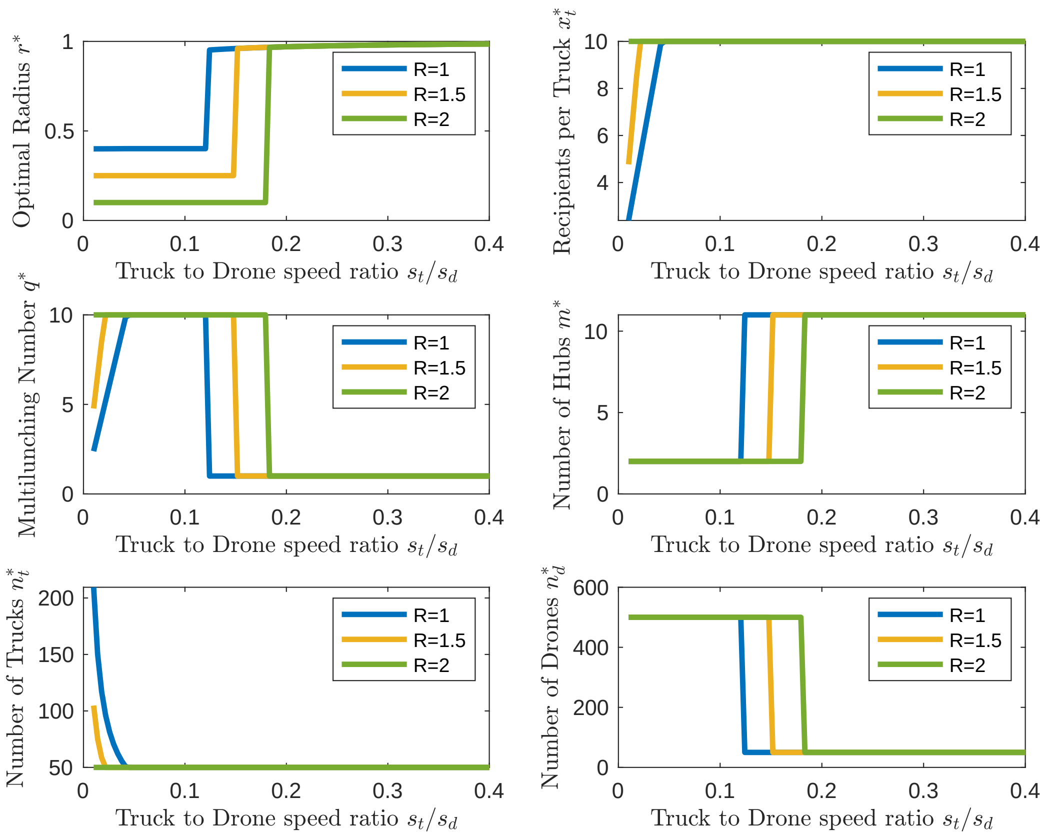

Figure Four.8: Fleet Composition Optimal Radius and Cost

We observe that the fleet optimization problem involves three critical speed ratios. Equations (Four.23) to (Four.25) detail how these critical speed ratios influence the routing solution. The two critical speed ratios identified in *Proposition 4* align with three key constraints: range, scheduling, and capacity. Figures Four.8 and Four.9 show the optimal decision variables for the fleet optimization problem across different flight ranges, based on the routing and fleet compositions derived in *Propositions 3* and *4*. The plots correspond to the two critical speed ratios and depict three distinct regions governed by the key constraints. Each region in Figures Four.9 is labeled according to the corresponding non-binding constraint within that region, as discussed below.

Excess Truck Capacity Region: When the truck-to-drone speed ratio is significantly lower than the drone speed, i.e., below the first critical speed ratio, the optimal routing strategy favors drones flying longer distances due to their ”sufficiently” high speeds relative to trucks. In this scenario, drones fly their maximum allowable distance, determined by their range, to

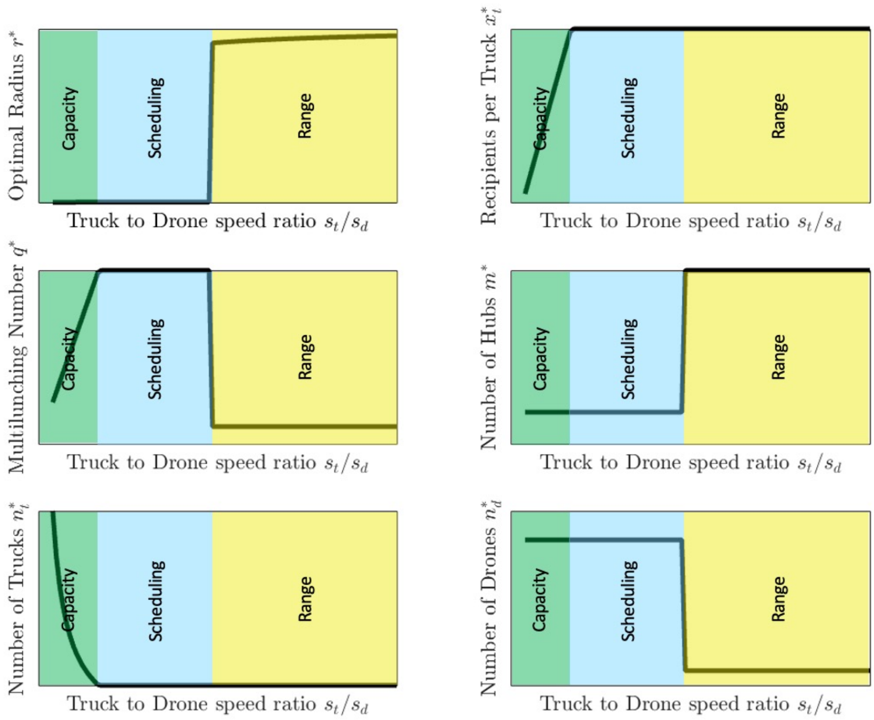

Figure Four.9: Optimal fleet composition regions formed based on key constraints. Each region is named after the constraint that is not binding in that region.

fully leverage their speed advantage; thus, the drone range constraint becomes binding. For this spectrum of speed ratios, the optimal radius r^* is relatively small, bounded by the drone range limitation, as shown in Figure Four.8a. In extreme cases where the drone range is large enough, the optimal radius can reduce to zero, meaning drones are launched directly from the central depot to customers and retrieved at the depot. Since trucks are slower and responsible for covering a shorter portion of the delivery route, they do not utilize their full capacity. Consequently, the share of recipients per truck x_t^* remains below the truck's capacity, as depicted in Figure Four.8b. As a result, the number of trucks n_t^* required in this scenario is relatively high, as shown in Figure Four.8e. In this region, multi-launching occurs, with $q^* > 1$, as illustrated in Figure Four.8c, meaning multiple drones are launched from each hub. The drones in each batch follow different trajectories with varying lengths, detailed in (Four.13)-(Four.6). Therefore, the scheduling constraint becomes binding to ensure synchronization between all drones and their associated truck movements. As the speed ratio increases within this spectrum while still remaining below the first critical point, the optimal radius increases to better leverage the higher speed (Figures Four.8a). Consequently, the number of recipients per truck x_t^* increases (Figure Four.8b), and the total number of trucks in the fleet n_t^* decreases (Figure Four.8e).

Scheduling Region: When the truck-to-drone speed ratio exceeds the first critical speed ratio, drones remain the preferred mode of delivery. As shown in Figure Four.8a, the optimal radius does not change, and the range constraint continues to be binding. The optimal radii for various range limitations are illustrated using different colors in Figure Four.8, indicating that the radius varies depending on the specific range limitation. To take advantage of the slightly higher truck speed, the optimal number of recipients per truck x_t^* increases and eventually reaches the truck's full capacity K, as depicted in Figure Four.8b. Thus, the capacity constraint is binding in this scenario. Since each truck now responds to higher demand by operating at full capacity, the optimal number of required trucks n_t^* decreases, while the optimal number of drones in the fleet n_d^* remains unchanged, as shown in Figures Four.8e and Four.8e, respectively. Moreover, the optimal number of drones launched in each batch increases to the truck's capacity, as shown in Figure Four.8c. Since the number of recipients per truck equals its capacity, each truck carries exactly one drone for each recipient. Therefore, relaunching is not required in this scenario. As shown in Figure Four.8d, each truck stops at exactly two hubs along its route: at the first hub, it launches all $q = K$ drones to deliver to $x_t = K$ recipients, and at the second hub, it retrieves all the drones before returning to the depot.

Excess Range scenario: When trucks are faster, and the speed ratio exceeds the last critical speed ratio, trucks become the preferred mode of delivery due to their higher speed, and the optimal travel radius increases, as shown in Figure Four.8a. In this scenario, drones no longer need to fly to their full range to complete deliveries; thus, the drone range constraint is no longer binding. Consequently, the optimal travel radius becomes independent of range limitations, and from this point onward, all range-based plots in Figure Four.8 converge into a single plot, represented by a single color. Unlike previous scenarios, where the optimal radius remained constant, here, an increase in truck speed directly impacts the delivery process, resulting in a continuous increase in the optimal radius as truck speed rises. Similar to the Scheduling Region, trucks operate at their full capacity to maximize the benefits of higher speeds, and the optimal number of recipients per truck x_t^* reaches the truck's capacity K, as depicted in Figure Four.8b.

Thus, the capacity constraint is binding in this scenario. In addition, as the speeds of trucks and drones become comparable, ensuring synchronization between their movements becomes more challenging, making the scheduling constraint binding. According to (Four.24) and (Four.25), the optimal number of trucks and drones in the fleet, n_t^* and n_d^* respectively, reach a fixed point in this scenario, as shown in Figures Four.8e and Four.8f. Each truck is equipped with exactly one drone, $q^* = 1$, as shown in Figure Four.8c. Furthermore, as the closed-form solutions in (Four.25) indicate, the optimal number of drones n_d^* becomes independent of the range limitation in this scenario. This convergence is illustrated in Figure Four.8f, where all previously distinct plots merge into a single unified plot. Therefore, each truck carrying one drone stops at multiple hubs along its route and relaunches the same drone at each hub to complete deliveries efficiently.

Insight 6: The marginal amortized ownership costs of trucks and drones affect the critical speed ratios, i.e., the speed ratios determining the three operational regions. However, these fixed costs do not affect the optimal fleet composition within each region.

D.4 Dominant Constraint Analysis

The policy analysis in Figure Four.10 illustrates the three introduced regions and their positioning based on the truck-to-drone speed ratio. The policy plot confirms the findings from the previous section, showing that, for a fixed truck capacity or drone range, increasing the truck-to-drone

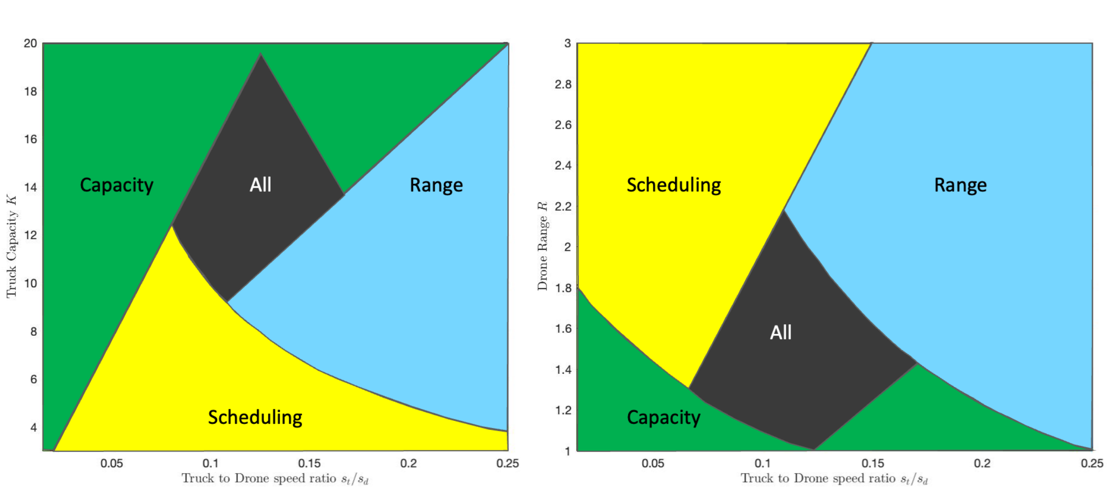

Figure Four.10: Fleet Composition Policy Plot. The green, blue, and yellow regions are named based on the constraint that is not binding in that region. All constraints are binding in the gray region.

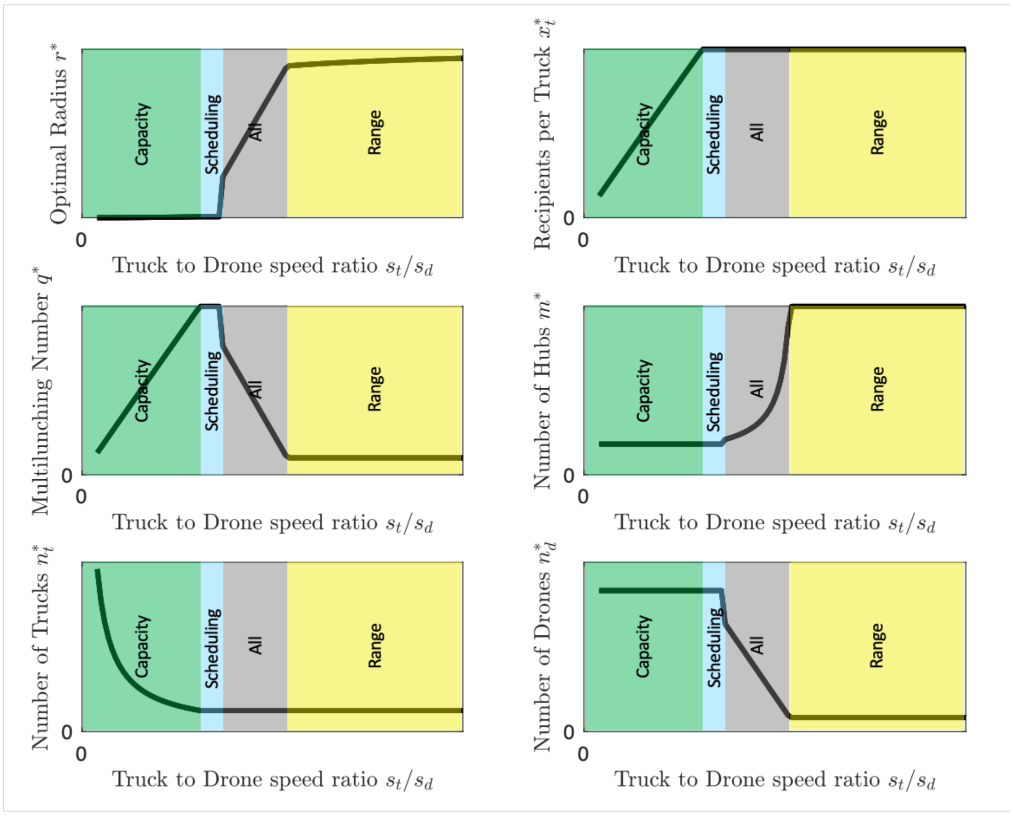

Figure Four.11: Fleet Composition - Low Flight Range

speed ratio transitions the system through these three distinct regions. Similar to Figure Four.9, which depicted these regions for a specific delivery scenario, the policy plot in Figure Four.10 extends this analysis to various delivery scenarios across different range and capacity limitations. As the speed ratio increases: I) The delivery operation first enters the *Excess Truck Capacity Region*, where the truck capacity constraint is not fully utilized. II) With increasing truck speed, it then transitions into the *Scheduling Region*, where synchronization between drones and trucks becomes critical. III) Finally, it reaches the *Excess Range Region*, where the drone range is no longer a limiting factor.

In addition to these primary regions, the policy plot reveals the existence of a fourth region under specific conditions. In this region, all three constraints—range, capacity, and scheduling—are simultaneously binding. For fixed range and capacity limitations, this region positions between the Scheduling Region and the Excess Range Region, as shown in Figures Four.10 and Four.11.

All binding scenario: In this region, the truck-to-drone speed ratio is higher than that of the Scheduling Region but still not sufficiently high to reach the Excess Range Region. Drones continue to use their full range and cover a larger portion of the delivery route, making the range constraint binding, as shown in Figure Four.11a. However, with increasing truck speed, unlike in the Capacity and Scheduling Regions, the optimal radius increases, and drones are launched closer to the recipients. Consequently, the optimal number of drones in each batch q^* decreases but is still more than one, shown in Figures Four.11c, indicating the occurrence of multi-launching. Moreover, the optimal number of hubs m^* increases from one, indicating that relaunching also occurs, as shown in Four.11d. The occurrence of both multi-launching and relaunching complicates the synchronization between trucks and drones, binding the scheduling constraint in this region. Similar to the Scheduling Region, trucks operate at full capacity, with the optimal number of recipients per truck $x_t^* = K$, as shown in Figure Four.11b, making the capacity constraint binding.

The *All Binding Scenario* does not always appear; in some cases, when the flight range is sufficiently large, and the range scenario begins at lower speed ratios, as the speed ratio increases further, the system transitions directly from the *Scheduling Region* to the *Excess Range Region*.

Section E: Routing on a surface

The circular routing model discussed in the previous section was a stylized representation designed to capture the trade-offs between the key operational constraints in drone routing. While effective for capturing these complex dynamics, it can be argued that, in practical applications, recipients are dispersed across a surface. To address this, we extend the circular model to a surface-based routing model, allowing for a more realistic analysis of delivery scenarios.

Consider a depot located at the center of a circular surface. Unlike the circular model, in this surface routing model, recipients are uniformly distributed across the entire face of the circular region with a density of ρ. We propose a routing heuristic for the surface-based distribution and compare its performance with the original circular routing model to evaluate the impact of distributions on operational efficiency and routing decisions.

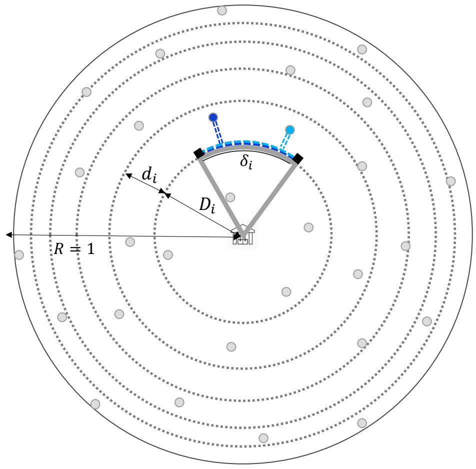

Figure Four.12: Routing on a circular surface

For routing on a surface model, we apply a heuristic that divides the circular surface into S concentric rings, each with radius D_i for $i = 1, 2, ..., S$. Recipients are assigned to the closest ring, as illustrated in Figure Four.12. This division simplifies the routing process by allowing the truck to focus on a specific ring, making the model comparable to the previous section. For each ring, a truck departs from the depot, travels to the designated ring, and follows an arc along the ring while launching and retrieving drones. Similar to the stylized setting discussed in Section C, drones are launched from hubs along the truck's route, deliver packages to recipients within their designated range, and are retrieved at hubs further along the truck's path. Here, we normalize the circle's radius (the outermost ring) to 1.

We define the distance between consecutive rings $i-1$ and i as d_i. Based on this definition, the radius of ring i, denote by D_i, is obtained as follows:

$$D_1 = d_0 \,, \quad D_2 = d_0 + d_1 \,, \quad D_i = \sum_{z=0}^{i-1} d_z. \tag{Four.27}$$

Each ring i is served by n_{ti} trucks. A truck departs from the depot, travels a distance D_i to the ring, and then traverses an arc while launching and retrieving drones to serve x_t recipients. Following the approach used in Section C.1, the return trip from the ring to the depot is excluded from the routing analysis, as it does not impact the delivery time. The details of truck travel distance for routing on a surface are derived in the Appendix.

We adopt the polar coordinate system introduced in Section D.2, using ring and radial routes for drone flight paths. The key distinction between the circular and surface distribution models is that, in the surface model, the maximum and minimum flight distances in the ring-radial setting differ due to the two-dimensional distribution of recipients. In the one-dimensional circular model, illustrated in Figure Four.6, all drones travel the same distance. In contrast, in the surface model, variations in recipient locations result in different flight distances, represented by two shades of blue in Figure Four.12. Each drone flight consists of two components: ring distance and radial distance. The ring distance is the fixed distance between two consecutive hubs, denoted by δ_i and depicted in Figure Four.12. This component remains consistent across all drone trajectories. However, the radial distance varies based on recipient locations within each ring, resulting in differing total flight distances. By applying the Extreme Value Distribution Theorem for uniformly distributed recipients, the minimum and maximum drone flight distances for ring i are:

$$\underline{L}_i = \delta_i + \frac{d_i}{N_i} \quad \& \quad \overline{L}_i = \delta_i + d_i(\frac{N_i - 1}{N_i}), \tag{Four.28}$$

where N_i is the number of recipients assigned to the ring, detailed in the Appendix.

The routing cost per truck on each ring follows the same structure as in equation (Four.9), accounting for both travel time and waiting time,

$$T_i(D_i, d_i) = \frac{l_i}{s_t} + (\frac{\overline{L}_i}{s_d} - \frac{\delta_i}{s_t})(m-1), \tag{Four.29}$$

where s_t and s_d represent the truck and drone speeds, respectively. This objective function is subject to the same set of constraints outlined for the one-dimensional stylized routing model in Section C.1.

The total routing cost on a circular surface is the sum of the routing costs across all rings, $\Sigma_{i=1}^{S} n_{ti} T_i(D_i, d_i)$, with the overall cost comprising both the routing cost and the fleet's amortized ownership costs:

$$C = \Sigma_{i=1}^{S} n_{ti} T_i(D_i, d_i) + n_t F_t + n_d F_d. \tag{Four.30}$$

We propose the following strategy for solving the circular surface model, leveraging insights from the one-dimensional model's results regarding the optimal number of drones per truck. Specifically, we adopt the insight that when the speed ratio exceeds the first critical point, the capacity constraint becomes binding, and the optimal number of drones dispatched in each batch equals the truck's capacity. This is discussed in detail in Section 4.3 and illustrated in Figures Four.8 and Four.9. Therefore, each truck is equipped with a single drone, making the number of drones in the fleet equal to the number of trucks (see (Four.25)). In the surface-based model, we assume trucks operate at full capacity, with each truck serving exactly K recipients, i.e., $x_t^* = K$. Given that the capacity constraint is binding in this scenario, the routing strategy aligns with the results derived for the ring-based model in Section 4.3.

Similar to the routing model in Section C.1, the range constraint ensures that a drone's total flight distance does not exceed its range limitation, R, even when operating at its maximum travel distance in each relaunching. In scenarios where the capacity constraint is binding, the number of drones equals the number of trucks, $n_d = n_t$ with each truck equipped with a single drone to serve K recipients. As a result, each drone is relaunched K times, and the cumulative flight distance across these deliveries must remain within the drone's range, $K\overline{L}_i \leq R$.

We also incorporate the scheduling constraint for routing on a surface to ensure that trucks arrive at retrieval hubs before their respective drones. This prevents drones from waiting at hubs, which would otherwise result in excessive battery consumption and delays. Thus, the time it takes a truck to travel between two consecutive hubs on each ring must be shorter than the corresponding drone flight time, $\frac{\delta_i}{s_t} \leq \frac{\underline{L}_i}{s_d}$.

E.1 Routing on a Circle: Equal Fleet of Trucks on Each Ring

We obtain the optimal solution for the routing on the surface model by considering a fixed fleet of trucks visiting each ring. The circular surface is divided into S concentric rings, with each ring serving an equal number of recipients. Given that recipients are uniformly distributed across the surface, the area of each ring is partitioned equally to ensure balanced delivery assignments.

Following this heuristic, the radius of each ring is derived in the appendix as:

$$D_i = \sqrt{\frac{i}{S}}. \tag{Four.31}$$

The distance between the depot and the first ring is the radius of the first ring, $d_1 = D_1$. For the remaining rings, the distance between ring i is approximated by considering the strip area assigned to each ring as a rectangle. The rectangle's width corresponds to the ring's circumference, and its height represents the distance d_i between consecutive rings. Thus, the distances between rings are determined as:

$$d_i \approx \frac{1}{2SD_i} = \frac{1}{2\sqrt{iS}}. \tag{Four.32}$$

Using the derived expressions for the ring radius D_i and the distance between consecutive rings d_i, we can rewrite the circular routing equations for the surface-based model, where we obtain the minimum and maximum drone flight distances for routing on the surface as follows:

$$\underline{L}_i = \frac{2\pi\sqrt{iS}}{N} + \frac{\sqrt{S}}{2N\sqrt{i}} \quad , \quad \overline{L}_i \approx \frac{2\pi\sqrt{iS}}{N} + \frac{1}{2\sqrt{iS}}. \tag{Four.33}$$

The detailed derivations of these expressions are provided in the appendix.

The range constraint for the surface-based routing model can be rewritten using (Four.33) as:

$$\frac{2K\pi\sqrt{iS}}{N} + \frac{K}{2\sqrt{iS}} \leq R. \tag{Four.34}$$

Similarly, for the scheduling constraint, we apply the updated definitions from (Four.32) and (Four.33):

$$\frac{2\pi\sqrt{iS}}{Ns_t} \leq \frac{2\pi\sqrt{iS}}{Ns_d} + \frac{\sqrt{S}}{2Ns_d\sqrt{i}}. \tag{Four.35}$$

The routing cost for each ring i, denoted as $T_i(S)$, is determined based on both the range and scheduling constraints. The bounds on i, imposed by these constraints in (Four.34) and

(Four.35), define four distinct cases for the total cost structure. The detailed derivation of these cases is provided in the appendix (Routing on a Circular Surface Cost Structure).

From the four cases detailed in the appendix, we focus on *Case1* in the following discussion.

If $S \leq \frac{NR}{2K\pi}$, then we have $S \leq \frac{N^2R^2}{4SK^2\pi^2}$. Since i is the indicator of the ring number, i.e. $i \leq S$, we have $i \leq \frac{N^2R^2}{4SK^2\pi^2}$. Thus, the range constraint presented in (Four.34) is always met, and we can claim that the range constraint is never binding. In this case, the scheduling constraint in (Four.35) determines the structure of the cost function as follows:

$$T_i(S) = \begin{cases} \frac{\sqrt{i}}{s_t\sqrt{S}} + \frac{4K\pi iS+KN}{2Ns_d\sqrt{iS}} & 1 \leq i \leq \frac{s_t}{4\pi(s_d-s_t)} \\ \frac{\sqrt{i}}{s_t\sqrt{S}} + \frac{2\pi K\sqrt{iS}}{s_tN} + \frac{K(1-\frac{2S}{N})}{2s_d\sqrt{iS}} & \frac{s_t}{4\pi(s_d-s_t)} \leq i \leq S \end{cases}. \tag{Four.36}$$

The total cost of routing on a surface is obtained based on equation (Four.30) by summing the routing costs across all rings and adding the fleet amortized ownership cost, as introduced in equation (Four.1). Thus, the total cost is obtained in the appendix as:

$$C_1 = \frac{N}{K}(F_t+F_d) + \begin{cases} \frac{3Ks_dN+2s_dNS+4K\pi s_tS^2}{3Ks_ds_tS} & 1 \leq i \leq \frac{s_t}{4\pi(s_d-s_t)} \\ \frac{3Ks_tN+2s_dNS-6Ks_tS+4K\pi s_dS^2}{3Ks_ts_dS} & \frac{s_t}{4\pi(s_d-s_t)} \leq i \leq S \end{cases}. \tag{Four.37}$$

We now proceed to find the optimal number of rings for the proposed heuristic to minimize the total delivery cost for the two-dimensional distribution over the circular surface, which is derived in the appendix as follow:

$$S^* = \begin{cases} \sqrt{\frac{3}{4\pi}}\sqrt{N} & 1 \leq i \leq \frac{s_t}{4\pi(s_d-s_t)} \\ \sqrt{\frac{3}{4\pi}}\sqrt{\frac{s_t}{s_d}}\sqrt{N} & \frac{s_t}{4\pi(s_d-s_t)} \leq i \leq S \end{cases}. \tag{Four.38}$$

Since the two optimal values are similar, differing only by the factor of speed ratios, the choice between them has minimal impact on the total optimal cost. Moreover, advancements in drone technology suggest that drones will surpass the higher speed threshold. Thus, we consider the second part in the piecewise function of *Case 1* for obtaining the optimal cost. Thus, the optimal total cost for routing on a surface is:

$$C^*(S^*) = \frac{2N}{3Ks_t} + \frac{\sqrt{6\pi N}}{\sqrt{s_d s_t}} - \frac{2}{s_d} + \frac{N}{K}(F_t + F_d). \tag{Four.39}$$

The routing cost structure derived for the surface-based model shows consistency with the circular model in terms of its dependency on truck and drone speeds. In both models, the total cost increases as either the truck or drone speed decreases, reflecting the critical role of speed in determining delivery efficiency. Additionally, the difference between truck and drone speeds impacts the cost, and when the speeds become more comparable, the overall routing cost decreases for both models.

Proposition 6 The asymptotic cost per recipient for a large number of recipients (large N), in routing on a surface, is:

$$\lim_{N\to\infty} \frac{C^*}{N} = \frac{2}{3Ks_t} + \frac{\sqrt{6\pi}}{\sqrt{N}\sqrt{s_d s_t}} + \frac{F_t + F_d}{K}. \tag{Four.40}$$

In the classic TSP literature and its extensions to VRP, when recipients are uniformly distributed over a surface, the cost per recipient scales proportionally to $1/\sqrt{N}$ for large N (Daganzo 2005). Our analysis confirms this relationship.

Section F: Conclusions

Last-mile delivery leg of the supply chain makes up a substantial portion of the shipping cost. Amongst the innovative technologies for improving last-mile delivery, drones provide abundant advantages in road-congested urban areas and rural delivery locations. At the strategic decision-making level, introducing drones to the fleet system requires a high-level analysis of the costs and benefits. Strategic models, however, often miss critical operational constraints such as the limited range of drones, truck capacity, or the presence of more than one truck and drone in the fleet.

This study proposes a strategic-level decision-making model that considers the prominent operational constraints, including i) the drone range limitation, ii) the truck capacity, iii) the presence of multi-truck fleets, iv) assignment of more than one drone to each truck, v) the complexities of multi-launching and re-launching drones, and vi) the synchronization of truck paths and drone trajectories to ensure coordination. The analysis reveals three critical operational scenarios where delivery performance is limited by the truck capacity, the drone range, and the timing coordination of the trucks and drones.

We use stylized routing models to capture the trade-offs in drone-assisted routing and fleet composition strategy. We first consider a circular setting with the one-dimensional distribution of recipients on the boundary of the circle and later extend the model to a two-dimensional distribution where recipients are scattered on the surface of a circle. For routing on a surface, we use heuristics to divide the circular surface into a set of concentric rings and assign each recipient on the circle to their closest ring. This approach allows for extending the proposed circular routing model to routing on a surface. We validate the total delivery cost for routing in the surface model by demonstrating consistency with the classical Traveling Salesman Problem literature, which shows that for uniformly distributed recipients over a surface, the cost per recipient scales proportionally to the square root of the number of recipients.

The insights gained from this research provide direct implications for strategic planning in drone-assisted delivery systems. The proposed models offer a comprehensive understanding of how technological capabilities (e.g., drone speed and range) and operational parameters influence overall system performance. The policy space analysis developed in this research further enables decision-makers to assess system performance under varying conditions and identify opportunities for improvement.

A limitation of this study that can be relaxed is the assumption of fixed and known travel speeds, which may not be reliable when these parameters are random and subject to a large variance. Thus, a stochastic extension of the model can enhance the solution's reliability.

Chapter Five Conclusion

This dissertation investigates the strategic design and optimization of multi-echelon last-mile delivery systems, leveraging emerging delivery technologies, including autonomous vehicles and drones. As e-commerce expands and customer expectations for fast and reliable delivery grow, the last mile has become a critical bottleneck in logistics networks, accounting for nearly 28% of overall delivery costs. By exploring delivery models that integrate traditional trucks with AVs and drones, this thesis presents a comprehensive framework for improving the efficiency of urban and suburban last-mile logistics through these emerging technologies.

The first study introduced and analyzed recipient-dependent AV-enabled last-mile policies, including AV, Hybrid delivery, and Crowdsourcing policies. These models incorporate AVs owned or accessed by recipients, enabling them to contribute to the delivery process. Using stylized models over the specific geometry of ring and circular city settings, upper and lower cost bounds were derived for each policy. We identified dominance regions where each of these policies outperforms the others in terms of delivery cost. We also compared the AV-enabled policies with the status quo truck delivery. We showed that the two-echelon AV-enabled policies are dominant (have lower operational costs), especially when hand-off costs are high or as the number of recipients increases. A case study based on Walmart delivery in Toronto was conducted to validate these analytical findings through a data-driven case, reinforcing the practical applicability of our results.

The second study extended the analysis to the delivery of perishable goods, where timely delivery is critical. We introduced length-bounded (time-sensitive) routing models to capture the constraints faced in delivering perishable products and compared them with conventional capacity-bounded models. Through parametric design, the study demonstrated how AV-based recipient participation can enhance delivery reliability and reduce the risk of spoilage, particularly in dense delivery networks or where hand-off costs are high. The Hybrid and AV policies exhibited expanding dominance regions in time-sensitive contexts, offering a promising alternative to traditional truck delivery for perishable goods. The research also highlighted the trade-offs between delivery capacity, time constraints, and hand-off logistics in the context of AV-enabled recipient participation.

The third study focused on integrating drones with trucks in a multi-echelon setting. We developed a two-stage continuous approximation model that captures fleet sizing and routing decisions under operational constraints: drone range, truck capacity, truck-drone coordination, and the possibility of multi-launch and re-launch operations. The framework distinguishes three operational regions: range-limited, capacity-limited, and synchronization-limited, and delivers closed-form solutions tailored to each case. We extended the model from a one-dimensional ring to a two-dimensional circular surface using a ribbon-based heuristic. The asymptotic properties of delivery cost were validated against classical Traveling Salesman Problem results, confirming the scaling with the square root of the number of recipients for uniformly distributed recipients. These validations strengthen the analytical robustness and practical relevance of the proposed models. The policy space analysis developed provides valuable insights into when and how drone deployment offers strategic advantages and helps quantify the influence of vehicle speeds, payload limits, and coordination strategies.

Together, these studies present a unified approach to modernizing last-mile logistics through emerging delivery technologies. They provide analytical tools and closed-form insights to inform strategic decision-making, while highlighting the potential of parametric design and continuous approximation in complex logistics planning. Across all three papers, the models emphasize scalability, cost-efficiency, and operational feasibility, paving the way for a new generation of delivery systems tailored to the realities of urban and suburban environments.

The findings of this dissertation have important implications for logistics planners, technology developers, and policymakers. Recipient-dependent routing offers cost reductions and operational flexibility, especially as AV ownership rises. Time-sensitive models provide new tools for managing perishable goods, enabling more responsive and resilient supply chains. Drone-assisted delivery models offer a pathway to faster service in rural areas while reducing traffic congestion and emissions in high-density urban areas. Decision-makers can use the policy space characterizations developed in this thesis to evaluate trade-offs and identify optimal configurations under real-world constraints.

Limitations and Future Research

While the analytical models developed in this dissertation offer strong strategic insights, several assumptions can be relaxed in future research. The models developed are based on deterministic parameters (e.g., fixed speed, demand density, and fleet availability), which may not fully capture real-world variability. Future work can introduce stochastic extensions to account for uncertainty in traffic, weather, and demand. For instance, travel speeds and vehicle availability were assumed to be fixed and deterministic; introducing stochastic variability could better reflect real-world conditions. Moreover, the stylized setting assumed known deterministic demand and recipient distributions, which can be relaxed in future studies with consideration of more realistic service areas. Further work could also generalize the urban form beyond stylized circular layouts using empirical street-network data.

The modeling of two-sided markets, particularly in AV-sharing polices and the crowdsourcing element, is another promising direction, especially when platform participation depends on wage offers and pricing strategies. In these settings, the delivery network is affected by the strategic behavior of both supply-side participants (e.g., vehicle owners) and demand-side users (e.g., recipients). Modeling such interactions requires incorporating incentive compatibility, participation thresholds, and pricing mechanisms that can influence service levels and platform sustainability. Future research could explore equilibrium models that capture the dynamic interplay between service pricing, user adoption, and platform profitability, enabling a more realistic and implementable framework for these emerging delivery modes.

Additionally, this work has not explicitly considered the environmental benefits of AVs and drones, such as reduced emissions and fuel consumption, which could further support their adoption. The integrated emission modeling would support broader sustainability evaluation and life-cycle cost analysis, integration with renewable energy systems, and sustainability assessments, which are valuable areas for future exploration.

Bibliography

A Rijpkema W, Rossi R, GAJ van der Vorst J, 2014 *Effective sourcing strategies for perishable product supply chains*. *International Journal of Physical Distribution & Logistics Management* 44(6):494–510.

Agatz N, Bouman P, Schmidt M, 2018 *Optimization approaches for the traveling salesman problem with drone*. *Transportation Science* 52(4):965–981.

Agatz N, Campbell A, Fleischmann M, Savelsbergh M, 2011 *Time slot management in attended home delivery*. *Transportation Science* 45(3):435–449.

Alley S, 2019 *Ups partners with drone startup matternet for medical sample delivery*. https://www.cnbc.com/video/2019/04/03/ups-partners-with-drone-startup-matternet-for-medical-sample-delivery.html. Accessed: 2023-03-16".

Amorim P, Almada-Lobo B, 2014 *The impact of food perishability issues in the vehicle routing problem*. *Computers & Industrial Engineering* 67:223–233.

Ansari S, Başdere M, Li X, Ouyang Y, Smilowitz K, 2018 *Advancements in continuous approximation models for logistics and transportation systems: 1996–2016*. *Transportation Research Part B: Methodological* 107:229–252.

Archetti C, Savelsbergh MW, Speranza MG, 2006 *Worst-case analysis for split delivery vehicle routing problems*. *Transportation science* 40(2):226–234.

Arslan AM, Agatz N, Kroon L, Zuidwijk R, 2019 *Crowdsourced delivery—a dynamic pickup and delivery problem with ad hoc drivers*. *Transportation Science* 53(1):222–235.

Avetisyan A, 2022 *Advantages of parametric modeling: The key points of algorithmic/parametric modeling and its advantages*. URL https://beegraphy.com/blog/advantages-of-parametric-modeling-the-key-points-of-the-algorithmic-parametric-modeling-a accessed: 2025-04-16.

Bagloee SA, Tavana M, Asadi M, Oliver T, 2016 *Autonomous vehicles: challenges, opportunities, and future implications for transportation policies*. *Journal of modern transportation* 24:284–303.

Baldacci R, Mingozzi A, Roberti R, Calvo RW, 2013 *An exact algorithm for the two-echelon capacitated vehicle routing problem*. *Operations Research* 61(2):298–314.

Baloch G, Gzara F, 2020 *Strategic network design for parcel delivery with drones under competition*. *Transportation Science* 54(1):204–228.

Bansal P, Kockelman KM, 2017 *Forecasting americans' long-term adoption of connected and autonomous vehicle technologies*. *Transportation Research Part A: Policy and Practice* 95:49–63.

Baron O, 2010 *Managing perishable inventory*. *Wiley encyclopedia of operations research and management science* .

Baron O, Berman O, Nourinejad M, 2020 *Introducing autonomous vehicles: Adoption patterns and impacts on social welfare*. *Manufacturing & Service Operations Management* .

Bartholdi III JJ, 1995 *A routing system based on spacefilling curves*.

Bartholdi III JJ, Platzman LK, 1988 *Heuristics based on spacefilling curves for combinatorial problems in euclidean space*. *Management Science* 34(3):291–305.

Beardwood J, Halton JH, Hammersley JM, 1959 *The shortest path through many points*. *Mathematical Proceedings of the Cambridge Philosophical Society*, volume 55, 299–327 (Cambridge University Press).

Behrend M, Meisel F, 2018 *The integration of item-sharing and crowdshipping: Can collaborative consumption be pushed by delivering through the crowd?* *Transportation Research Part B: Methodological* 111:227–243.

Bellos I, Ferguson M, Toktay LB, 2017 *The car sharing economy: Interaction of business model choice and product line design*. *Manufacturing & Service Operations Management* 19(2):185–201.

Bertsimas DJ, Simchi-Levi D, 1996 *A new generation of vehicle routing research: robust algorithms, addressing uncertainty*. *Operations research* 44(2):286–304.

Bertsimas DJ, Van Ryzin G, 1991 *A stochastic and dynamic vehicle routing problem in the euclidean plane*. *Operations Research* 39(4):601–615.

Blum C, Roli A, 2003 *Metaheuristics in combinatorial optimization: Overview and conceptual comparison*. *ACM computing surveys (CSUR)* 35(3):268–308.

Bouman P, Agatz N, Schmidt M, 2018 *Dynamic programming approaches for the traveling salesman problem with drone*. *Networks* 72(4):528–542.

Boutilier JJ, Chan TC, 2022 *Drone network design for cardiac arrest response*. *Manufacturing & Service Operations Management* 24(5):2407–2424.

Campbell JF, Sweeney D, Zhang J, 2017 *Strategic design for delivery with trucks and drones*. *Supply Chain Analytics Report SCMA (04 2017)* 47–55.

Carey N, 2016 *Ups launches u.s. drone test flights for urgent medical deliveries*. `https://www.reuters.com/article/united-parcel-drones-delivery-idINL2N1BY1UY`.Accessed: 2022-07-26".

Carlsson JG, Behroozi M, Devulapalli R, Meng X, 2016 *Household-level economies of scale in transportation*. *Operations Research* 64(6):1372–1387.

Carlsson JG, Song S, 2018 *Coordinated logistics with a truck and a drone*. *Management Science* 64(9):4052–4069.

Chen HK, Hsueh CF, Chang MS, 2009 *Production scheduling and vehicle routing with time windows for perishable food products*. *Computers & operations research* 36(7):2311–2319.

Chen Z, He F, Zhang L, Yin Y, 2016 *Optimal deployment of autonomous vehicle lanes with endogenous market penetration*. *Transportation Research Part C: Emerging Technologies* 72:143–156.

Chen Z, Li X, Qu X, 2022 *A continuous model for designing corridor systems with modular autonomous vehicles enabling station-wise docking*. *Transportation science* 56(1):1–30.

Chung SH, Sah B, Lee J, 2020 *Optimization for drone and drone-truck combined operations: A review of the state of the art and future directions*. *Computers & Operations Research* 123:105004.

Cleophas C, Cottrill C, Ehmke JF, Tierney K, 2019 *Collaborative urban transportation: Recent advances in theory and practice*. *European Journal of Operational Research* 273(3):801–816.

D Viniche B, Baron O, Berman O, Nourinejad M, 2024 *Parametric design of time-sensitive routing with recipient-dependent contributions*. *Opher and Berman, Oded and Nourinejad, Mehdi, Parametric Design of Time-Sensitive Routing with Recipient-Dependent Contributions (November 12, 2024)* .

D Viniche B, Baron O, Berman O, Nourinejad M, 2025 *Tactical routing and fleet planning in drone-assisted last-mile delivery*. *Opher and Berman, Oded and Nourinejad, Mehdi, Tactical Routing and Fleet Planning in Drone-Assisted Last-Mile Delivery (January 24, 2025)* .

D Viniche B, Nourinejad M, Baron O, Berman O, 2023a *Recipient-dependent last-mile delivery routing with autonomous vehicle applications*. *Mehdi and Baron, Opher and Berman, Oded, Recipient-*

Dependent Last-Mile Delivery Routing with Autonomous Vehicle Applications (November 05, 2023)
.

D Viniche B, Nourinejad M, Baron O, Berman O, 2023b *Recipient-dependent last-mile delivery routing with autonomous vehicle applications*. *Availble at SSRN* .

Daganzo CF, 2005 *Logistics systems analysis* (Springer Science & Business Media).

D'Andrea R, 2014 *Guest editorial can drones deliver? IEEE Transactions on Automation Science and Engineering* 11(3):647–648.

Dayarian I, Savelsbergh M, 2017 *Crowdshipping and same-day delivery: Employing in-store customers to deliver online orders*. *Production and Operations Management* .

Dayarian I, Savelsbergh M, Clarke JP, 2020 *Same-day delivery with drone resupply*. *Transportation Science* 54(1):229–249.

de Oliveira ÍR, 2017 *Analyzing the performance of distributed conflict resolution among autonomous vehicles*. *Transportation Research Part B: Methodological* 96:92–112.

Discover D, 2022 *Dhl's parcelcopter: Changing shipping forever*. https://www.dhl.com/discover/en-my/business/business-ethics/parcelcopter-drone-technology.Accessed: 2022-07-26".

Dolan, 2022 *The challenges of last mile delivery logistics and the tech solutions cutting costs in the final mile*. https://www.insiderintelligence.com/insights/last-mile-delivery-shipping-explained/. Accessed: 2022-07-20".

Dror M, Trudeau P, 1989 *Savings by split delivery routing*. *Transportation Science* 23(2):141–145.

Dror M, Trudeau P, 1990 *Split delivery routing*. *Naval Research Logistics (NRL)* 37(3):383–402.

Fagnant DJ, Kockelman K, 2015 *Preparing a nation for autonomous vehicles: opportunities, barriers and policy recommendations*. *Transportation Research Part A: Policy and Practice* 77:167–181.

Fagnant DJ, Kockelman KM, 2014 *The travel and environmental implications of shared autonomous vehicles, using agent-based model scenarios*. *Transportation Research Part C: Emerging Technologies* 40:1–13.

FAO, UN, 2023 *The state of food security and nutrition in the world 2023: Urbanization, agrifood systems transformation, and healthy diets across the rural-urban continuum*. URL https://openknowledge.fao.org/server/api/core/bitstreams/

3a8baf8c-960d-4105-9538-e4bd9b1d4503/content/cc7088en.html#/12, accessed: 2024-08-26.

Figliozzi MA, 2020 *Carbon emissions reductions in last mile and grocery deliveries utilizing air and ground autonomous vehicles*. *Transportation Research Part D: Transport and Environment* 85:102443.

Gharehgozli A, Iakovou E, Chang Y, Swaney R, 2017 *Trends in global e-food supply chain and implications for transport: Literature review and research directions*. *Research in transportation business & management* 25:2–14.

Gohram Baloch FG, 2020 *Strategic network design for parcel delivery with drones under competition*. *Transportation Science* 54(1).

Goodman RW, 2005 *Whatever you call it, just don't think of last-mile logistics, last*. *Global Logistics & Supply Chain Strategies* 9(12).

Gustavsson J, Cederberg C, Sonesson U, Van Otterdijk R, Meybeck A, 2011 *Global food losses and food waste*.

Haji M, Kerbache L, Muhammad M, Al-Ansari T, 2020 *Roles of technology in improving perishable food supply chains*. *Logistics* 4(4):33.

Han LD, Chin SM, Franzese O, Hwang H, 2005 *Estimating the impact of pickup-and delivery-related illegal parking activities on traffic*. *Transportation Research Record* 1906(1):49–55.

Harper CD, Hendrickson CT, Mangones S, Samaras C, 2016 *Estimating potential increases in travel with autonomous vehicles for the non-driving, elderly and people with travel-restrictive medical conditions*. *Transportation Research Part C: Emerging Technologies* 72:1–9.

Hartigan JA, Wong MA, 1979 *Algorithm as 136: A k-means clustering algorithm*. *Journal of the Royal Statistical Society. Series C (Applied Statistics)* 28(1):100–108.

He L, 2021 *Could autonomous vehicles put last-mile delivery on the fast track?* *World Economic Forum* .

He L, Liu S, Shen ZJM, 2022 *Smart urban transport and logistics: A business analytics perspective*. *Production and Operations Management* 31(10):3771–3787.

Hochfelder B, 2017 *What retailers can do to make the last mile more efficient*. URL https://www.supplychaindive.com/news/last-mile-spotlight-retail-costs-fulfillment/443094/.

Hsu CI, Hung SF, Li HC, 2007 *Vehicle routing problem with time-windows for perishable food delivery. Journal of food engineering* 80(2):465–475.

Hu M, 2019 *Sharing economy: making supply meet demand* (Springer).

Hwang HS, 1999 *A food distribution model for famine relief. Computers & Industrial Engineering* 37(1-2):335–338.

Jacobs K, Warner S, Rietra M, Mazza L, Buvat J, Khadikar A, Cherian S, Khemka Y, 2019 *The last-mile delivery challenge. Capgemini Research Institute* 1–40.

Jennings D, Figliozzi M, 2019 *Study of sidewalk autonomous delivery robots and their potential impacts on freight efficiency and travel. Transportation Research Record* 2673(6):317–326.

Jeong HY, Song BD, Lee S, 2019 *Truck-drone hybrid delivery routing: Payload-energy dependency and no-fly zones. International Journal of Production Economics* 214:220–233.

Kanellos M, 2014 *Google working on drones too.* `https://www.forbes.com/sites/michaelkanellos/2014/08/29/google-working-on-drones-too/?sh=24085f6479a7.`.Accessed: 2022-07-26".

Kang M, Lee C, 2021 *An exact algorithm for heterogeneous drone-truck routing problem. Transportation Science* 55(5):1088–1112.

Karaesmen IZ, Scheller-Wolf A, Deniz B, 2011 *Managing perishable and aging inventories: review and future research directions. Planning Production and Inventories in the Extended Enterprise: A State of the Art Handbook, Volume 1* 393–436.

Kela,, 2016 *Where is my package? the impact of missed deliveries.* URL `https://medium.com/@Kela/dude-where-is-my-package-the-impact-of-missed-deliveries-7cfb4af37c6`.

Kinderlehrer D, Stampacchia G, 1980 *An introduction to variational inequalities and their applications*, volume 31 (Siam).

Kitjacharoenchai P, Ventresca M, Moshref-Javadi M, Lee S, Tanchoco JM, Brunese PA, 2019 *Multiple traveling salesman problem with drones: Mathematical model and heuristic approach. Computers & Industrial Engineering* 129:14–30.

Koetsier J, 2022 *Health via drone: Zipline now delivering medicine via fixed-wing drones in north carolina.* `https://www.forbes.com/sites/johnkoetsier/2022/06/28/health-via-drone-zipline-now-delivering-medicine-via-fixed-wing-drones-in-north-carolina/?sh=54b11bf35877`. Accessed: 2022-07-26".

Koumari L, 2022 *What is parametric design in architecture?* URL https://parametric-architecture.com/what-is-parametric-design-in-architecture/, accessed: 2025-04-16.

Lagin M, Hrakansson J, Nordström C, Nyberg RG, Öberg C, 2022 *Last-mile logistics of perishable products: a review of effectiveness and efficiency measures used in empirical research*. *International Journal of Retail & Distribution Management* 50(13):116–139.

Langevin A, Mbaraga P, Campbell JF, 1996 *Continuous approximation models in freight distribution: An overview*. *Transportation Research Part B: Methodological* 30(3):163–188.

Laporte G, 1992 *The vehicle routing problem: An overview of exact and approximate algorithms*. *European journal of operational research* 59(3):345–358.

Lemardelé C, Estrada M, Pagès L, Bachofner M, 2021 *Potentialities of drones and ground autonomous delivery devices for last-mile logistics*. *Transportation Research Part E: Logistics and Transportation Review* 149:102325.

Levin MW, Odell M, Samarasena S, Schwartz A, 2019 *A linear program for optimal integration of shared autonomous vehicles with public transit*. *Transportation Research Part C: Emerging Technologies* 109:267–288.

Li B, Liu S, Tang J, Gaudiot JL, Zhang L, Kong Q, 2020a *Autonomous last-mile delivery vehicles in complex traffic environments*. *arXiv preprint arXiv:2001.08096* .

Li Y, Zhang G, Pang Z, Li L, 2020b *Continuum approximation models for joint delivery systems using trucks and drones*. *Enterprise Information Systems* 14(4):406–435.

Liu S, He L, Shen ZJM, 2018 *On-time last mile delivery: Order assignment with travel time predictors*. *Forthcoming in Management Science* .

Liu TX, Yang J, Adamic LA, Chen Y, 2014 *Crowdsourcing with all-pay auctions: A field experiment on taskcn*. *Management Science* 60(8):2020–2037.

Liu W, Sun X, 2022 *Energy-aware and delay-sensitive management of a drone delivery system*. *Manufacturing & Service Operations Management* 24(3):1294–1310.

Macrina G, Pugliese LDP, Guerriero F, Laporte G, 2020 *Crowd-shipping with time windows and transshipment nodes*. *Computers & Operations Research* 113:104806.

Mahmassani HS, 2016 *50th anniversary invited article—autonomous vehicles and connected vehicle systems: flow and operations considerations*. *Transportation Science* 50(4):1140–1162.

Mak HY, 2018 *Peer-to-peer crowdshipping as an omnichannel retail strategy. Available at SSRN 3119687* .

Mathew N, Smith SL, Waslander SL, 2015 *Planning paths for package delivery in heterogeneous multirobot teams*. *IEEE Transactions on Automation Science and Engineering* 12(4):1298–1308.

McEntegart J, 2013 *Amazon to use drones to deliver packages in 30 minutes*. `https://www.tomshardware.com/news/amazon-prime-air-drone-delivery,25252.html`. Accessed: 2022-07-20".

McKinsey, 2019 *Last-mile package delivery in 2030*. `https://www.mckinsey.com/industries/travel-logistics-and-infrastructure/our-insights/last-mile-package-delivery-in-2030`. Accessed: 2022-07-26".

Mersky AC, Samaras C, 2016 *Fuel economy testing of autonomous vehicles*. *Transportation Research Part C: Emerging Technologies* 65:31–48.

Mirzaeian N, Cho SH, Scheller-Wolf A, 2020 *A queueing model and analysis for autonomous vehicles on highways*. *Management Science* .

Morandi N, Leus R, Yaman H, 2024 *The orienteering problem with drones*. *Transportation Science* 58(1):240–256.

Murray CC, Chu AG, 2015 *The flying sidekick traveling salesman problem: Optimization of drone-assisted parcel delivery*. *Transportation Research Part C: Emerging Technologies* 54:86–109.

Murray CC, Raj R, 2020 *The multiple flying sidekicks traveling salesman problem: Parcel delivery with multiple drones*. *Transportation Research Part C: Emerging Technologies* 110:368–398.

Newell GF, Daganzo CF, 1986a *Design of multiple-vehicle delivery tours—i a ring-radial network*. *Transportation Research Part B: Methodological* 20(5):345–363.

Newell GF, Daganzo CF, 1986b *Design of multiple vehicle delivery tours—ii other metrics*. *Transportation Research Part B: Methodological* 20(5):365–376.

Newell GF, Daganzo CF, 1986c *Design of multiple vehicle delivery tours—ii other metrics*. *Transportation Research Part B: Methodological* 20(5):365–376.

Ng M, Dandl F, Mahmassani HS, Bogenberger K, 2024 *Semi-on-demand hybrid transit route design with shared autonomous mobility services*. *arXiv preprint arXiv:2403.15804* .

Nguyen C, Dessouky M, Toriello A, 2014 *Consolidation strategies for the delivery of perishable products*. *Transportation Research Part E: Logistics and Transportation Review* 69:108–121.

Nguyen C, Toriello A, Dessouky M, Moore JE, 2013 *Evaluation of transportation practices in the california cut flower industry*. *Interfaces* 43(2):182–193.

Nourinejad M, Roorda MJ, 2018 *Cruising for parking in the era of autonomous vehicles* .

Osman IH, 1993 *Metastrategy simulated annealing and tabu search algorithms for the vehicle routing problem*. *Annals of operations research* 41(4):421–451.

Osvald A, Stirn LZ, 2008 *A vehicle routing algorithm for the distribution of fresh vegetables and similar perishable food*. *Journal of food engineering* 85(2):285–295.

Otto A, Agatz N, Campbell J, Golden B, Pesch E, 2018 *Optimization approaches for civil applications of unmanned aerial vehicles (uavs) or aerial drones: A survey*. *Networks* 72(4):411–458.

Peng K, Du J, Lu F, Sun Q, Dong Y, Zhou P, Hu M, 2019 *A hybrid genetic algorithm on routing and scheduling for vehicle-assisted multi-drone parcel delivery*. *IEEE Access* 7:49191–49200.

Perboli G, Tadei R, Vigo D, 2011 *The two-echelon capacitated vehicle routing problem: models and math-based heuristics*. *Transportation Science* 45(3):364–380.

Perera S, Dawande M, Janakiraman G, Mookerjee V, 2020 *Retail deliveries by drones: how will logistics networks change? Production and Operations Management* 29(9):2019–2034.

Poikonen S, Campbell JF, 2021 *Future directions in drone routing research*. *Networks* 77(1):116–126.

Poikonen S, Golden B, 2020 *Multi-visit drone routing problem*. *Computers & Operations Research* 113:104802.

Poikonen S, Golden B, Wasil EA, 2019 *A branch-and-bound approach to the traveling salesman problem with a drone*. *INFORMS Journal on Computing* 31(2):335–346.

Portal UG, 2023 *Dubai autonomous transportation strategy*. URL `https://u.ae/en/about-the-uae/strategies-initiatives-and-awards/strategies-plans-and-visions/transport-and-infrastructure/dubai-autonomous-transportation-strategy`.

Psaraftis HN, 1995 *Dynamic vehicle routing: Status and prospects*. *Annals of operations research* 61(1):143–164.

PYMNTS, 2024 *Uber eats and waymo roll out autonomous delivery in phoenix*. URL `https://www.pymnts.com/news/delivery/2024/uber-eats-and-waymo-roll-out-autonomous-delivery-in-phoenix/`, accessed: May 11, 2024.

Qi W, Li L, Liu S, Shen ZJM, 2018 *Shared mobility for last-mile delivery: Design, operational prescriptions, and environmental impact*. *Manufacturing & Service Operations Management* 20(4):737–751.

Ranieri L, Digiesi S, Silvestri B, Roccotelli M, 2018 *A review of last mile logistics innovations in an externalities cost reduction vision*. *Sustainability* 10(3):782.

Redmond C, Yukich J, 1994 *Limit theorems and rates of convergence for euclidean functionals*. *The Annals of Applied Probability* 1057–1073.

Reuters, 2023 *Jaguar land rover opens three european self-driving tech hubs*. URL https://www.reuters.com/business/autos-transportation/jaguar-land-rover-opens-three-european-self-driving-tech-hubs-2023-02-21/.

Roberti R, Ruthmair M, 2021 *Exact methods for the traveling salesman problem with drone*. *Transportation Science* 55(2):315–335.

Rubin BF, 2017 *Amazon prime air drone completes its first us public delivery*. https://www.cnet.com/news/amazon-prime-air-first-drone-delivery-us-public-sunscreen-mars/. Accessed: 2022-07-26".

Sacramento D, Pisinger D, Ropke S, 2019 *An adaptive large neighborhood search metaheuristic for the vehicle routing problem with drones*. *Transportation Research Part C: Emerging Technologies* 102:289–315.

Sagan H, 2012 *Space-filling curves* (Springer Science & Business Media).

Scales L, 1985 *Introduction to non-linear optimization* (Springer-Verlag).

Sharan Architecture, 2024 *Parametric design*. https://en.wikipedia.org/wiki/Parametric_design, URL https://en.wikipedia.org/wiki/Parametric_design, accessed: 2025-04-16.

Stanley Lim, 2023 URL https://hbr.org/2023/11/research-why-so-many-packages-dont-get-delivered#:~:text=Up%20to%2020%25%20of%20e,satisfaction%20and%20damage%20retailers'%20reputations.

Tarantilis CD, Kiranoudis CT, Vassiliadis VS, 2004 *A threshold accepting metaheuristic for the heterogeneous fixed fleet vehicle routing problem*. *European Journal of Operational Research* 152(1):148–158.

Tilley A, 2016 *Ups experiments with drone delivery in partnership with zipline*. https://www.forbes.com/sites/aarontilley/2016/05/09/

ups-experiments-with-drone-delivery-in-partnership-with-zipline/#58f1c1d145a4.Accessed: 2022-07-26".

Tiniç GO, Karasan OE, Kara BY, Campbell JF, Ozel A, 2023 *Exact solution approaches for the minimum total cost traveling salesman problem with multiple drones*. *Transportation Research Part B: Methodological* 168:81–123.

UN, 2024 *End food waste day*. https://www.un.org/en/observances/end-food-waste-day, accessed: 2024-08-26.

Utama DM, Dewi SK, Wahid A, Santoso I, 2020 *The vehicle routing problem for perishable goods: A systematic review*. *Cogent Engineering* 7(1):1816148.

Walmart, 2024 *Sky high ambitions: Walmart to make largest drone delivery expansion of any u.s. retailer*. URL https://www.walmart.com/news/2024/01/09/sky-high-ambitions-walmart-to-make-largest-drone-delivery-expansion-of-any-us-retailer, accessed: 2024-11-29.

Wang X, Poikonen S, Golden B, 2017 *The vehicle routing problem with drones: several worst-case results*. *Optimization Letters* 11(4):679–697.

Wang Z, Sheu JB, 2019 *Vehicle routing problem with drones*. *Transportation research part B: methodological* 122:350–364.

Washington Post, 2018 *Gm launches a peer-to-peer car-sharing service*. URL https://www.washingtonpost.com/technology/.

Wells G, Stevens L, 2016 *Amazon conducts first commercial drone delivery*. https://www.wsj.com/articles/amazon-conducts-first-commercial-drone-delivery-1481725956. Accessed: 2022-07-26".

Winkenbach M, Kleindorfer PR, Spinler S, 2016 *Enabling urban logistics services at la poste through multi-echelon location-routing*. *Transportation Science* 50(2):520–540.

Wu HC, 2007 *The karush–kuhn–tucker optimality conditions in an optimization problem with interval-valued objective function*. *European Journal of operational research* 176(1):46–59.

Xu X, Mahmassani HS, Chen Y, 2019a *Impact of autonomous vehicles on household activity and travel scheduling: An integrated dynamic network modeling approach*. Technical report.

Xu X, Mahmassani HS, Chen Y, 2019b *Privately owned autonomous vehicle optimization model devel-*

opment and integration with activity-based modeling and dynamic traffic assignment framework. *Transportation Research Record* 2673(10):683–695.

Zhao J, Lee JY, 2023 *Effect of connected and autonomous vehicles on supply chain performance*. *Transportation Research Record* 2677(3):402–424.

Appendices

A Appendix of Chapter Two

A.1 Lemma

LEMMA A.1. In the Hybrid policy, the total AV distance is approximated as

$$d_{\mathrm{v}}^{h} \approx 2n(1-r)+\frac{m^{2}\pi^{2}r}{3(1-r)}. \tag{.1}$$

Proof of Lemma A.1: As shown in Figure .1, let $y(\theta)$ be the distance from a hub to a recipient that is located at an angle θ away from a horizontal line that passes the depot. From the geometry of the sector, we have

$$y(\theta)=\sqrt{1+r^{2}-2r\cos\theta}. \tag{.2}$$

We now divide the recipients into two groups, those that fall below and those that fall above the horizontal line. We vary θ between 0 and $m\pi/n$. Between angles θ and $\theta+\delta\theta$ there are $\delta d\theta$ recipients (recall that δ is the density of recipients on the ring) each with an AV travel distance of $y(\theta)$. Thus, the total AV distance in the Hybrid policy is:

$$d_{\mathrm{v}}^{h}=\frac{4n}{m}\int_{0}^{m\pi/n} y(\theta)\rho d\theta, \tag{.3}$$

where n/m is the number of hubs, and the constant 4 captures the outbound/inbound trip and the number of recipients below/above the horizontal line. Each hub serves the recipients on a sector of the circle with angle $2m\pi/n$, which corresponds with the boundaries of (.3).

Using a Taylor expansion of $y(\theta)$ w.r.t. θ with the initial condition of $\theta=0$ (which is a good approximation for a large number of recipients and an error order of two, we get

$$d_v^h = \frac{4n}{m}\int_0^{m\pi/n} \sqrt{1+r^2-2r\cos(\theta)}\rho d\theta$$
$$\approx 2n(1-r) + \frac{m^2\pi^2 r}{3(1-r)} \tag{.4}$$

LEMMA A.2. In the Crowdsourcing policy, the total AV travel distance is approximated as

$$d_v^w \approx 2\pi + \frac{2n(1-r)}{m} + \frac{r\pi^2 m}{n(1-r)}. \tag{.5}$$

Proof of Lemma A.2: The three components in the route length of each AV include the pickup trip from the driver's location (i.e., the AV owner) to the hub equal to $y(m\pi\delta/n)$ per Figure .1, from the hub to the first recipient that is also equal to $y(m\pi\delta/n)$ per Figure .1 and the drop-off trip that travels an arc of the ring to visit all recipients. These sum up to

$$d_v^w \approx 2\pi + \frac{2n}{m} y(\frac{m\pi\delta}{n}), \tag{.6}$$

where the first term, 2π, is the distance on the n/m arcs on a ring, each with length $2\pi m/n$, and the second term is the distance of paths that begin and end at the hub. Inputting $y(m\pi\delta/n)$ from (.2) into (.6) gives (.5).

Figure .1: Distance of the AV mode in the Hybrid policy

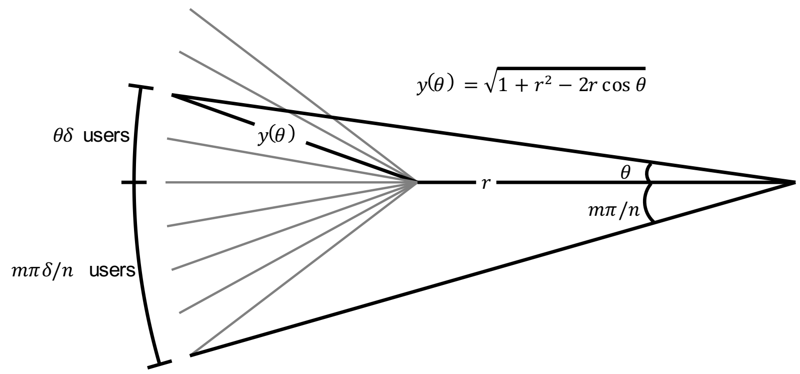

A.2 Theorem 1

Theorem 1 is inspired by the lower bound of Theorem 2 in Carlsson et al. (2016). Their Theorem gives a lower bound on the TSP tour that visits the $\{x_1, x_2, ..., x_n\}$ points in a specific service area for the case where the number of point sets, n, becomes large. We expand their analysis and consider a rectangular service area with the length of $m*a$ and width of $m*b$. We use this Theorem in the lower bounds of the truck, Hybrid, and Crowdsourcing policies for routing on a disk. To prove the lower bound, we first introduce the following Lemma:

LEMMA A.3. Let $\Gamma \subset \mathbb{Z}^2$ denote a rectangular integer lattice in the plane with length $m*a$ and width $m*b$, let $n \geq 2$ be an integer, and let $l > 0$. Let P denote the set of all paths of the form $\{x_1, x_2, \ldots, x_n\}$, with $x_i \in \Gamma$ for each i, and whose length does not exceed l. Then,

$$|P| \leq m^2 ab \binom{l+n-1}{n-1} (\frac{8l}{n-1})^{n-1}. \quad (.7)$$

This lemma is borrowed from Lemma 2 in Carlsson et al. (2016), where in their work they use m^2 choices of the initial point x in the triplet, and we have $m^2 ab$ such choices for the defined rectangular service area.

Theorem 1: For a set of points $\{x_1, x_2, ..., x_n\}$ uniformly distributed on a rectangular service area with the length of ma and width of mb, the expected length of a TSP tour to visit these n points satisfies $E(TSP(x_1, x_2, ...x_n)) \geq \alpha_2 \sqrt{abn}$.

Proof of Theorem 1: We use *Lemma A.3* for the rectangular service area.

For the $\{x_1, x_2, ..., x_n\}$ set, there are $n!$ different possible sequences of points. Thus, there are $n!$ possible paths for visiting these n points.

$$Pr(TSP(x_1, x_2, ...x_n) \leq \alpha_2 \sqrt{abn}) = Pr(\text{length of one of the n! valid paths} \leq \alpha_2 \sqrt{abn}). \quad (.8)$$

As the probability of at least one of these valid paths to be short enough is no more than the sum of the probabilities of each of them (Union Bound), we have:

$$Pr(\text{length of one of the n! valid paths} \leq \alpha_2\sqrt{abn}) \leq n!\,Pr(\text{length}(\rho) \leq \alpha_2\sqrt{abn}). \qquad (.9)$$

where $\rho \in P$ is a path that visits all the points in the set of point $\{x_1, x_2, ..., x_n\}$ in a random sequence.

For the rectangular service area, we consider the example shown in Figures Two.7 and .3. We let L denote a lattice within this service area of the following form:

$$\{\frac{1}{m}, \frac{2}{m}, ..., \frac{am-1}{m}, \frac{am}{m}\}\text{x}\{\frac{1}{m}, \frac{2}{m}, ..., \frac{bm-1}{m}, b\}.$$

Here, ρ is ″simply a path that is sampled uniformly at random from the collection of all possible paths between n points taken from L" (Carlsson et al. 2016), and there are $(m^2ab)^n$ of these sampled paths. We seek to find the portion of these paths with the length of at most $\alpha_2\sqrt{abn}$. Scaling the rectangular lattice of *Lemma A.3* by a factor of $\sqrt{m^2ab}$, the number of paths whose length does not exceed $\alpha_2\sqrt{abn}$ is at most:

$$\begin{aligned} & m^2ab\binom{m\sqrt{ab}\alpha_2\sqrt{abn}+n-1}{n-1}(\frac{8m\sqrt{ab}\alpha_2\sqrt{abn}}{n-1})^{n-1} \\ \leq\ & m^2ab\frac{(m\sqrt{ab}\alpha_2\sqrt{abn}+n-1)^{n-1}}{(n-1)!}(\frac{8m\sqrt{ab}\alpha_2\sqrt{abn}}{n-1})^{n-1}, \end{aligned} \qquad (.10)$$

Thus, the probability that one of these paths has a length less than $\alpha_2\sqrt{abn}$ can be obtained by dividing (.10) by the total number of paths, $(m^2ab)^n$, as follows

$$Pr(\text{length}(\rho) \leq \alpha_2\sqrt{abn}) \leq \frac{m^2ab\frac{(m\sqrt{ab}\alpha_2\sqrt{abn}+n-1)^{n-1}}{(n-1)!}(\frac{8m\sqrt{ab}\alpha_2\sqrt{abn}}{n-1})^{n-1}}{(m^2ab)^n}. \qquad (.11)$$

Therefore:

$$\begin{aligned}
&\lim_{m\to\infty} \sup Pr(\text{length}(\rho) \leq \alpha_2\sqrt{abn}) \\
&\leq \lim_{m\to\infty} \sup \frac{m^2 ab \frac{(m\sqrt{ab}\alpha_2\sqrt{abn}+n-1)^{n-1}}{(n-1)!}(\frac{8m\sqrt{ab}\alpha_2\sqrt{abn}}{n-1})^{n-1}}{(m^2 ab)^n} \\
&= (8ab\alpha_2^2)^{n-1}\frac{n^{n-1}}{(n-1)!(n-1)^{n-1}}.
\end{aligned} \tag{.12}$$

Thus, we conclude that:

$$Pr(TSP(x_1,x_2,...x_n) \leq \alpha_2\sqrt{abn}) \leq n!(8ab\alpha_2^2)^{n-1}\frac{n^{n-1}}{(n-1)!(n-1)^{n-1}} = (8ab\alpha_2^2)^{n-1}\frac{n^n}{(n-1)^{n-1}}, \tag{.13}$$

which goes toward zero for $n\to\infty$ when $8ab\alpha_2^2 < 1$. Using Markov's inequality, $\Pr(X \geq a) \leq \frac{E(X)}{a}$, therefore, $\Pr(X < a) \geq 1 - \frac{E(X)}{a}$.

Thus,

$$\begin{aligned}
&E(TSP(x_1,x_2,...x_n)) \geq (1-(8ab\alpha_2^2)^{n-1}\frac{n^n}{(n-1)^{n-1}})\alpha_2\sqrt{abn} \\
&= \alpha_2\sqrt{abn} - (8ab\alpha_2^2)^{n-1}\frac{n^{n+1/2}}{(n-1)^{n-1}} \sim \alpha_2\sqrt{abn},
\end{aligned} \tag{.14}$$

which proves the lower bound.

A.3 Proofs

Proof of Proposition C.1.1: From (Two.4), the routes are capacity bounding, i.e., $x_t = K$. Therefore, according to (Two.2) and (Two.3), there are $\gamma^t = \lceil n/K \rceil \approx n/K$ routes of length $l_t = 2+(x_t-1)\delta \approx 2+x_t\delta$. Thus, from (Two.1) and $D_t^t = \gamma^t l_t$, the cost of the Truck policy is $z^t \approx 2c_t(\pi + n/K) + c_s n$.

Proof of Proposition C.3.1: Consider the capacity bounding case ($m^{\mathrm{h}} = \lfloor K/m \rfloor \approx K/m$). The first order condition for minimizing the total Hybrid policy cost, z^h, w.r.t. any radius r gives $r_h^* = 1 - \pi m\sqrt{\frac{s_v K}{6(s_v Kn - c_t n - c_t K\pi)}}$. We now check the second order condition z^h, w.r.t. any radius r.

The second derivative is

$$\frac{\partial^2 z^h}{\partial r^2} = \frac{2s_{\mathrm{v}} m^2 \pi^2}{3(1-r)^3} > 0 \qquad \forall r \in [0,1), \tag{.15}$$

Hence, for any given m, the radius r_h^* is a unique global minimum. We check the bounds of $r \in [0,1]$. We have $r_h^* \geq 0$ if $\frac{2mn(n+K\pi)}{2Kn^2 - Km^2\pi^2} \leq \frac{s_{\mathrm{v}}}{c_t}$; and we have $r_h^* \leq 1$ because r_h^* is presented as one minus a positive value per (C.3.1).

We now derive the optimal number of recipients per hub, m_h^*. The first order condition for minimizing the total Hybrid policy cost, z^h, w.r.t. any m gives $m_h^* = \sqrt[3]{\frac{3c_s n(1-r)}{2s_{\mathrm{v}}\pi^2 r}}$. We now check the second order condition of z^h w.r.t. any m. The second derivative is

$$\frac{\partial^2 z^h}{\partial m^2} = \frac{6c_s n(1-r) + 2s_{\mathrm{v}}\pi^2 r m^3}{3m^3(1-r)} > 0 \qquad \forall r \in [0,1). \tag{.16}$$

Hence, m_h^* is unique.

We check the bounds of $m_h^* \in [1,K]$. We have $m_h^* \leq 1$ if $s_{\mathrm{v}} \geq \frac{3c_s n(1-r)}{(2\pi^2 r)}$; and we have $m_h^* \geq K$ if $s_{\mathrm{v}} \leq \frac{3c_s n}{3c_s n + 2K^3\pi^2}$. Thus, we get (C.3.1).

Proof of Proposition C.4.1: We derive the optimal number of recipients per hub in the Crowdsourcing policy, m_w^*. For any given r, the first order necessary condition of optimality w.r.t. m gives $m_w^* = \frac{n}{\pi}\sqrt{\frac{c_s(1-r) + 2s_{\mathrm{v}}(1-r)^2}{r s_{\mathrm{v}}}}$, and the second order condition gives

$$\frac{\partial^2 z^w}{\partial m^2} = \frac{2n(c_s + 2s_{\mathrm{v}}(1-r))}{m^3} > 0 \qquad \forall r \in [0,1]. \tag{.17}$$

Thus, the Crowdsourcing cost, z^w, is also convex w.r.t. m.

We now derive the optimal radius r_w^*, where we have $m^{\mathrm{w}} = \lfloor K/m \rfloor \approx K/m$ based on the truck's capacity. The first order condition for minimizing the total Crowdsourcing cost, z^w, w.r.t. any radius r gives $r_w^* = 1 - m\pi\sqrt{\frac{s_{\mathrm{v}} K}{2n(s_{\mathrm{v}} Kn - c_t mn - c_t K m\pi)}}$. We now check the second order condition z^w, w.r.t. any radius r. The second derivative is

$$\frac{\partial^2 z^w}{\partial r^2} = \frac{2s_v m\pi^2}{2(1-r)^3} > 0, \tag{.18}$$

Hence, r_w^* is unique. We check the bounds of $r \in [0,1]$. The condition $r_w^* > 0$ is satisfied as long as $s_v \geq \frac{2n(n+K\pi)}{4n^2+2Kn\pi-K^2\pi^2}$. Moreover, we have $r_w^* < 1$ because it is presented as one minus a positive value.

Proofs of Truck policy on a disk

Proof of Eq (Two.16)**:** We calculate the number of recipients on ring i having the density of recipients δ and the area surrounding ring i. Recipients assigned to ring i are located in the area A_i between two rings with radius $R_i + \tau/2$ and $R_i - \tau/2$, respectively. Thus:

$$A_i = [\pi(R_i + \frac{\tau}{2})^2) - \pi(R_i - \frac{\tau}{2})^2)] = \pi[(i\tau)^2 - (i\tau - \tau)^2] = \pi\tau^2(2i-1), \tag{.19}$$

Thus, we calculate the number of recipients assigned to ring i as $N_i = \delta A_i$, from which (Two.16) follows:

$$N_i = \delta A_i = (2i-1)\tau^2\pi\delta. \tag{.20}$$

Proof of Proposition D.1.1: Using the number of routes on each ring and the expected length of each truck route for the Truck policy from (Two.18) and (Two.19), respectively, we have:

$$\sum_{i=1}^{C} \gamma_i^t l_{ti} = \sum_{i=1}^{C} (\frac{(2i-1)\tau^2\pi\delta}{K})(2R_i + \frac{2\pi R_i K}{N_i^t} + \frac{K\tau}{2}). \tag{.21}$$

Since $R_i = (i - \frac{1}{2})\tau$, and using (.20),

$$\begin{aligned}\sum_{i=1}^{C} \gamma_i^t l_{ti} &= \sum_{i=1}^{C} (\frac{(2i-1)\tau^2\pi\delta}{K})(\tau(2i-1) + \frac{(2i-1)\tau\pi K}{(2i-1)\tau^2\pi\delta} + \frac{K\tau}{2}) \\ &= \sum_{i=1}^{C} (\frac{(2i-1)\tau^2\pi\delta}{K})(\tau(2i-1) + \frac{K}{\tau\delta} + \frac{K\tau}{2})\end{aligned} \tag{.22}$$

Using the sum of $(2i-1)$ from $i=1$ to $i=C$ which is equal to C^2 and sum of $(2i-1)^2$

from $i = 1$ to $i = C$ which is equal to $(4C^3 - C)/3$ and approximating the number of rings as $C \approx 1/\tau$

$$\sum_{i=1}^{1/\tau} \gamma_i^t l_{ti} \approx \frac{4\delta\pi}{3K} - \frac{\delta\pi\tau^2}{3K} + \frac{\pi}{\tau} + \frac{\delta\pi\tau}{2} \tag{.23}$$

Since τ is small for large δ, the second term is negligible.

$$\sum_{i=1}^{1/\tau} \gamma_i^t l_{ti} \approx \frac{4\delta\pi}{3K} + \frac{\pi}{\tau} + \frac{\delta\pi\tau}{2}, \tag{.24}$$

which we substitute into (Two.17), to get

$$z_u^t(\tau) \approx c_t\left(\frac{4\delta\pi}{3K} + \frac{\pi}{\tau} + \frac{\delta\pi\tau}{2}\right) + c_s^t\delta\pi. \tag{.25}$$

From the first-order condition, $\frac{\partial z_u^t(\tau)}{\partial\tau} = \frac{1}{2}c_t\pi(\delta - \frac{2}{\tau^2}) = 0$, the optimal τ for the Truck policy on a disk is

$$\tau^* = \sqrt{\frac{2}{\delta}}, \tag{.26}$$

Re-writing $z^t(\tau, m)$ from (.25) with this optimal τ^* gives

$$z_u^{t\,*} \approx c_t\pi\left(\frac{4\delta}{3K} + \sqrt{2\delta}\right) + c_s^t\delta\pi. \tag{.27}$$

Proof of Proposition D.1.2: We use (Two.21) as a lower bound on truck route length on ring i

$$l_{ti} = 2R_i + \alpha\sqrt{K\frac{K}{\tau\delta}\tau} = 2R_i + \alpha K\sqrt{\frac{1}{\delta}}. \tag{.28}$$

Using the number of routes on each ring and the expected length of each truck route for the Truck policy from (Two.18) and (Two.21), respectively, we have:

$$\sum_{i=1}^{C} \gamma_i^t l_{ti} = \sum_{i=1}^{C}\left(\frac{(2i-1)\tau^2\pi\delta}{K}\right)\left(2R_i + \alpha K\sqrt{\frac{1}{\delta}}\right). \tag{.29}$$

Since, from (Two.15), we have $R_i = (i - \frac{1}{2})\tau$, we can rewrite (.29) as follows

$$\sum_{i=1}^{C} \gamma_i^t l_{ti} = \sum_{i=1}^{C} (\frac{(2i-1)\tau^2\pi\delta}{K})(\tau(2i-1) + \alpha K\sqrt{\frac{1}{\delta}}) \\ = \sum_{i=1}^{C} (\frac{(2i-1)^2\tau^3\pi\delta}{K} + \alpha(2i-1)\tau^2\pi\sqrt{\delta}). \quad (.30)$$

For the summations, we use

$$\sum_{i=1}^{C}(2i-1) = C^2 \quad , \quad \sum_{i=1}^{C}(2i-1)^2 = (4C^3 - C)/3 \quad (.31)$$

Approximating the number of rings as $C \approx 1/\tau$ in (.30), and using (.31), we have

$$\sum_{i=1}^{1/\tau} \gamma_i^t l_{ti} \approx \frac{4\delta\pi}{3K} - \frac{\delta\pi\tau^2}{3K} + \alpha\pi\sqrt{\delta}. \quad (.32)$$

Since τ is small for large δ, the second term is negligible.

$$\sum_{i=1}^{1/\tau} \gamma_i^t l_{ti} \approx \frac{4\delta\pi}{3K} + \alpha\pi\sqrt{\delta}, \quad (.33)$$

which we substitute into (Two.17) to get (Two.22).

Proofs of Hybrid policy on a disk

Proof of Proposition D.3.1: In the Hybrid policy, there are m^{h} hubs on each truck route on the radius R_i, and hubs are equally spaced from each other. Thus, the length of each truck route on ring i, l_i^{h}, is the sum of (i) inbound and outbound travel distances between the depot and ring, and (ii) truck travel distance on the arc between the hubs:

$$l_i^{\mathrm{h}} \approx 2R_i + m^{\mathrm{h}}\delta_i^h = 2R_i + \frac{2\pi R_i K}{N_i^h}. \quad (.34)$$

Figure .2: Hybrid Policy TSP area

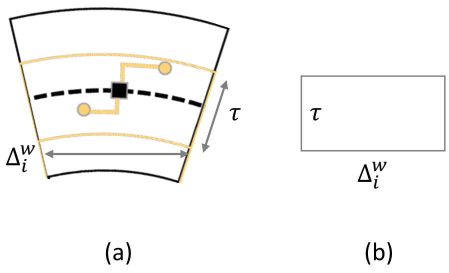

From (.34), (Two.28), (Two.16), and (Two.15) we have

$$\begin{aligned}
\gamma^{\mathrm{h}} l^{\mathrm{h}} &\approx \sum_{i=1}^{C} \frac{n_i^h}{K}(2R_i + \frac{2\pi R_i K}{N_i^h}) = \sum_{i=1}^{C} \frac{2R_i n_i^h}{K} + 2\pi R_i \\
&= \sum_{i=1}^{C} \frac{2(i-1/2)\tau(\pi\delta\tau^2(2i-1))}{K} + \sum_{i=1}^{C} 2\pi(i-1/2)\tau \\
&= \frac{\pi\delta\tau^3}{K} \sum_{i=1}^{C} (2i-1)^2 + 2\pi\tau \sum_{i=1}^{C} (i-1/2) \\
&= \frac{\pi\delta\tau^3}{3K}(4C^3 - C) + \pi\tau C^2
\end{aligned} \tag{.35}$$

where for the summation, we use (.31). Approximating of $C \approx 1/\tau$,

$$\gamma^{\mathrm{h}} l^{\mathrm{h}} \approx \frac{\pi\delta\tau^3}{3K}(\frac{4}{\tau^3} - \frac{1}{\tau}) + \frac{\pi}{\tau} = \frac{4\pi\delta}{3K} - \frac{\pi\delta\tau^2}{3K} + \frac{\pi}{\tau}, \tag{.36}$$

where the last term is negligible due to the small value of powers of τ. Thus,

$$\gamma^{\mathrm{h}} l^{\mathrm{h}} \approx \frac{4\pi\delta}{3K} + \frac{\pi}{\tau}. \tag{.37}$$

The expected average ring and radial distances for AVs in the Hybrid policy are equal to $\frac{\tau}{4}$ and $\frac{\delta_i^h}{4}$, respectively (shown in Figure .2). Thus, the AV travel distance (from the hub to the recipients) in the Hybrid policy can be obtained from the number of recipients multiplied by the sum of these expected ring and radial distances

$$d_{\text{v}}^{h}=\sum_{i=1}^{C}2n_i(\frac{\tau}{4}+\frac{\delta_i^h}{4})=n(\frac{\tau}{2}+\frac{m}{2\delta\tau}). \tag{.38}$$

Recalling that $n=\pi\delta$,

$$d_{\text{v}}^{h}\approx\frac{\delta\pi\tau^2+m\pi}{2\tau}. \tag{.39}$$

The total cost of the Hybrid policy from (Two.27) can now be simplified to

$$z_u^h(\tau,m)\approx c_t(\frac{4\pi\delta}{3K}+\frac{\pi}{\tau})+s_{\text{v}}\frac{\delta\pi\tau^2+m\pi}{2\tau}+c_s^h\frac{n}{m}. \tag{.40}$$

From the first and second-order conditions, it is easily verified that the optimal τ for the Hybrid policy is

$$\tau^*=\sqrt{\frac{2c_t+s_{\text{v}}m}{s_{\text{v}}\delta}}, \tag{.41}$$

which upon substituting into (.40) gives (Two.32).

Proof of Proposition D.3.2: In the lower bound of the Hybrid policy, we approximate the travel distance of each truck using (Two.30). Thus, we use (.34)-(.37) for this part as well. To obtain the lower bound of the Hybrid policy cost, we consider that AVs travel direct routes following Euclidean distance. Thus, the expected travel distance to each customer location is $\sqrt{(\frac{\tau}{4})^2+(\frac{\delta_i^h}{4})^2}$. We now obtain the total AV travel distance in this routing as:

$$d_{\text{v}}^{h}=\sum_{i=1}^{C}2n_i\sqrt{(\frac{\tau}{4})^2+(\frac{\delta_i^h}{4})^2}=\sqrt{\frac{\tau^2}{16}+\frac{m^2}{16\delta^2\tau^2}}\sum_{i=1}^{C}2n_i=2n\sqrt{\frac{\delta^2\tau^4+m^2}{16\delta^2\tau^2}}, \tag{.42}$$

where we used $\sum_{i=1}^{C}n_i=n$. For the total number of recipients, we have $n=\delta\pi$. Thus:

$$d_{\text{v}}^{h}=\frac{\pi}{2\tau}\sqrt{\delta^2\tau^4+m^2}. \tag{.43}$$

Figure .3: Crowdsoucing Policy TSP area

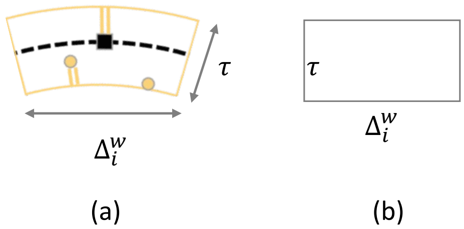

Substituting this into (Two.27) gives the total cost of the Hybrid policy as:

$$z_l^h(\tau,m) \approx c_t(\frac{4\pi\delta}{3K}+\frac{\pi}{\tau})+s_{\mathrm{v}}(\frac{\pi}{2\tau}\sqrt{\delta^2\tau^4+m^2})+c_s^h\frac{\delta\pi}{m}. \tag{.44}$$

Since m is a positive integer we have $\frac{\pi}{2\tau}\sqrt{\delta^2\tau^4} \leq \frac{\pi}{2\tau}\sqrt{\delta^2\tau^4+m^2}$. Thus, we have a lower bound on the Hybrid cost as:

$$z_l^h(\tau,m) \approx c_t(\frac{4\pi\delta}{3K}+\frac{\pi}{\tau})+s_{\mathrm{v}}(\frac{\pi\delta\tau}{2})+c_s^h\frac{\delta\pi}{m}. \tag{.45}$$

From the first and second-order conditions, we can obtain the optimal τ as follows:

$$\tau^* \approx \sqrt{\frac{2c_t}{s_{\mathrm{v}}\delta}}, \tag{.46}$$

which we substitute in (Two.34) and get (Two.35).

Proofs of Crowdsourcing policy on a disk

Proof of Eq (Two.41)**:** In the Crowdsourcing policy, we assume that each AV, responsible for delivering to m recipients, travels the perimeter of the designated area assigned to each hub (depicted in Figure .3). They first travel to their designated hub, i.e., $2\tau/2$, then the entire perimeter, i.e., $2(\tau+\delta_i^w)$ and then the radial local distances to each recipient location, i.e., $m\tau/4$. Thus, the expected travel distance of each Av is:

$$d_{\mathrm{v}\,i}^w \approx 2\frac{\tau}{2}+2(\tau+\delta_i^w)+m\frac{\tau}{4} \tag{.47}$$

an approximation of inbound and outbound travel distances of AV shown with lines between the black square (as the depot) and the perimeter in Figure .3, the second term is the area perimeter, and the last term is perpendicular detours.

Given $\gamma_i^{\mathrm{w}} m^{\mathrm{w}}$ hubs on ring i and noting that $\gamma_i^{\mathrm{w}} \approx \frac{n_i}{mm^{\mathrm{w}}}$, and $\delta_i^{w} = \frac{m}{\delta\tau}$ the total AV distance is

$$
\begin{aligned}
d_{\mathrm{v}}^{w} &= \sum_{i=1}^{C} \gamma_i^{\mathrm{w}} m^{\mathrm{w}} d_{\mathrm{v}\,i}^{w} \approx \sum_{i=1}^{C} \frac{n_i}{mm^{\mathrm{w}}} m^{\mathrm{w}} [\tau + 2(\tau + \delta_i^{w}) + m\frac{\tau}{4}] \\
&= (\frac{\tau(12+m)}{4m} + \frac{2}{\delta\tau}) \sum_{i=1}^{C} n_i. \qquad (.48)
\end{aligned}
$$

Using $\sum_{i=1}^{C} n_i = n = \pi\delta$,

$$
d_{\mathrm{v}}^{w} \approx \frac{\tau\delta\pi(12+m)}{4m} + \frac{2\pi}{\tau} \qquad (.49)
$$

Proof of Proposition D.4.1: The operator's costs for the Crowdsourcing policy is $z^{w} = c_t d_u^{w} + s_{\mathrm{v}} d_v^{w} + c_s^{w} s^{w}$ which can now be simplified using (Two.28), (Two.30), (Two.40), and (Two.41):

$$
z_u^{w}(\tau, m) \approx c_t(\frac{4\pi\delta}{3K} + \frac{\pi}{\tau}) + s_{\mathrm{v}}(\frac{\tau\delta\pi(12+m)}{4m} + \frac{2\pi}{\tau}) + c_s^{w}(n(1+\frac{1}{m})) \qquad (.50)
$$

From the first-order condition,

$$
\frac{\partial z_u^{w}(\tau)}{\partial\tau} = \frac{s_{\mathrm{v}}\pi\delta(12+m)}{4m} - \frac{\pi(c_t + 2s_{\mathrm{v}})}{\tau^2} = 0
$$

Thus, the optimal τ for the Crowdsourcing policy on a disk is

$$
\tau^* = \sqrt{\frac{2m(c_t + 2s_{\mathrm{v}})}{s_{\mathrm{v}}\delta(12+m)}}. \qquad (.51)
$$

Using (.51) in (.50), we have the optimal cost of the crowdsourcing policy as:

$$
z_u^{w}(m)^* \approx c_t\frac{4\delta\pi}{3K} + \frac{\sqrt{m(c_t+2s_{\mathrm{v}})}\sqrt{s_{\mathrm{v}}\delta\pi(12+m)}}{m} + c_s\frac{n(m+1)}{m}. \qquad (.52)
$$

Proof of Proposition D.4.2: We use *Lemma A.3* and *Theorem 1* for each Crowdsourcing AV, which is responsible for visiting m recipients, distributed within an approximately rectangular service area with a length of δ_i^w and width of τ. Thus, the TSP tour length of each crowdsourcing AV is:

$$\alpha_2\sqrt{m\delta_i^w\tau} = \alpha_2\sqrt{m\frac{m}{\delta\tau}\tau} = \alpha_2\sqrt{\frac{m^2}{\delta}}, \tag{.53}$$

and the average travel distance of each AV is:

$$d_{\mathrm{v}\,i}^w = 2\sqrt{(\frac{\tau}{4})^2 + (\frac{\delta_i^w}{4})^2} + \alpha_2\sqrt{\frac{m^2}{\delta}}. \tag{.54}$$

We considered that the number and length of truck routes are the same as the upper bound (also in Proof of Proposition D.4.1). The total AV distance is $d_\mathrm{v}^w = \sum_{i=1}^C \gamma_i^\mathrm{w} m^\mathrm{w} d_{\mathrm{v}\,i}^w$, where $\gamma_i^\mathrm{w} \approx \frac{n_i}{mm^\mathrm{w}}$:

$$d_\mathrm{v}^w = \sum_{i=1}^C \gamma_i^\mathrm{w} m^\mathrm{w} d_{\mathrm{v}\,i}^w \approx \sum_{i=1}^C \frac{n_i}{mm^\mathrm{w}} m^\mathrm{w}(2\sqrt{(\frac{\tau}{4})^2 + (\frac{\delta_i^w}{4})^2} + \alpha_2\sqrt{\frac{m^2}{\delta}}). \tag{.55}$$

Since $(\frac{\delta_i^h}{4})^2 \geq 0$, we have $\sqrt{(\frac{\tau}{4})^2} \leq \sqrt{(\frac{\tau}{4})^2 + (\frac{\delta_i^w}{4})^2}$. Thus, the lower bound on the total AV distance in the Crowdsourcing policy is:

$$d_\mathrm{v}^w \approx \sum_{i=1}^C \frac{n_i}{m}(\frac{\tau}{2} + \alpha_2\sqrt{\frac{m^2}{\delta}}) = (\frac{\tau}{2m} + \alpha_2\sqrt{\frac{1}{\delta}})\sum_{i=1}^C n_i. \tag{.56}$$

Using $\sum_{i=1}^C n_i = n = \pi\delta$, we have:

$$d_\mathrm{v}^w = \frac{\pi\delta\tau}{2m} + \alpha_2\pi\sqrt{\delta}. \tag{.57}$$

Thus, the lower bound on the total cost of the Crowdsourcing policy is:

$$z_l^w(\tau, m) \approx c_t(\frac{\pi}{\tau} + \frac{4\pi\delta}{3K}) + s_\mathrm{v}(\frac{\pi\delta\tau}{2m} + \alpha_2\pi\sqrt{\delta}) + c_s^w(n(1 + \frac{1}{m})). \tag{.58}$$

From the first and second order conditions, this cost is optimized at the following optimal

τ:

$$\tau^* = \sqrt{\frac{2c_t m}{s_\mathrm{v}\delta}}, \tag{.59}$$

which upon substituting into (Two.45) gives (Two.46).

Proof of Asymptotic Properties

Proof of Proposition E.1.1: When $n \to \infty$, the capacity constraint is bounding, i.e. $x_t = k$ and $m^\mathrm{h} = m^\mathrm{w} = k/m$. In the Truck policy, we use (Two.5) to derive the asymptotic cost as

$$C^\mathrm{t}_{\infty,\mathrm{r}} = \lim_{n\to\infty} \frac{2c_t(\pi + \frac{n}{K}) + c_s n}{n} = \frac{2c_t}{K} + c_s. \tag{.60}$$

In the AV policy, we use (Two.6) to derive the asymptotic cost as

$$C^\mathrm{a}_{\infty,\mathrm{r}} = \lim_{n\to\infty} \frac{2s_\mathrm{v} n + c_s}{n} = 2s_\mathrm{v}. \tag{.61}$$

In the Hybrid policy, we derive the asymptotic cost as

$$C^\mathrm{h}_{\infty,\mathrm{r}} = \lim_{n\to\infty} \frac{z^h}{n} = 2s_\mathrm{v} + \frac{c_s}{m} + (\frac{2c_t}{K} - 2s_\mathrm{v})r. \tag{.62}$$

The optimal number of recipients per hub is $m_h^* = k$ because $\frac{\partial C^\mathrm{h}_{\infty,\mathrm{r}}}{\partial m} < 0$. We now look at the first order condition of $C^\mathrm{h}_{\infty,\mathrm{r}}$ w.r.t. radius r. From the derivative $\frac{\partial C^\mathrm{h}_{\infty,\mathrm{r}}}{\partial r} = \frac{2c_t}{K} - 2s_\mathrm{v} > 0$, we have $r_h^* = 0$ when $c_t > s_\mathrm{v}K$. Otherwise, $r_h^* = 1$ when $c_t \leq s_\mathrm{v}K$. Inputting r_h^* in (.62) gives (Two.53).

In the Crowdsourcing policy, we derive the asymptotic cost as

$$C^\mathrm{w}_{\infty,\mathrm{r}} = \lim_{n\to\infty} \frac{z^w}{n} = \frac{c_s K(1+m) + 2s_\mathrm{v}K(1-r) + 2c_t m r}{Km}, \tag{.63}$$

which has the following two derivatives w.r.t. r and m

$$\frac{\partial C^{\mathrm{w}}_{\infty,\mathrm{r}}}{\partial m} = \frac{-2s_{\mathrm{v}}(1-r)-c_s}{m^2} < 0. \tag{.64}$$

$$\frac{\partial C^{\mathrm{w}}_{\infty,\mathrm{r}}}{\partial r} = c_t m - s_{\mathrm{v}} K, \tag{.65}$$

Because (.64) is strictly negative, $m^* = K$. Then, according to (.65) and given $m = K$, $r^* = 0$ if $c_t > s_{\mathrm{v}}$ and $r^* = 1$ if $c_t \leq s_{\mathrm{v}}$. Inputting r^* and m^* in $C^{\mathrm{w}}_{\infty,\mathrm{r}}$ gives (Two.54).

Proof of Proposition E.1.2: We derive asymptotic properties for the routing on a disk when $\delta \to \infty$ for different policies based on (Two.50). For the Truck policy, we use (Two.20) to derive the asymptotic cost:

$$C^{\mathrm{t}}_{\infty,c} = \lim_{\delta\to\infty} \frac{z^t}{\pi\delta} = \lim_{\delta\to\infty} \frac{c_t\pi(\sqrt{2\delta}+\frac{4\delta}{3K}) + c_s^t\delta\pi}{\pi\delta} = \frac{4c_t}{3K} + c_s^t. \tag{.66}$$

For the AV policy, we use the AV cost in (Two.26)

$$C^{\mathrm{a}}_{\infty,c} = \lim_{\delta\to\infty} \frac{z^a}{\pi\delta} = \lim_{\delta\to\infty} \frac{4/3\pi\delta s_{\mathrm{v}} + c_s^a}{\pi\delta} = \frac{4s_{\mathrm{v}}}{3}. \tag{.67}$$

For the Hybrid policy, we use the total cost of the Hybrid policy in (Two.32), where $n = \delta\pi$ to derive the asymptotic cost

$$C^{\mathrm{h}}_{\infty,c} = \lim_{\delta\to\infty} \frac{z^h}{\pi\delta} = \lim_{\delta\to\infty} \frac{\frac{4\pi\delta c_t}{3K} + \pi\sqrt{s_{\mathrm{v}}\delta}\sqrt{2c_t+s_{\mathrm{v}}m} + c_s^h\frac{\delta\pi}{m}}{\pi\delta} = \frac{4c_t}{3K} + \frac{c_s^h}{m}. \tag{.68}$$

The optimal number of recipients per hub is $m_h^* = k$ because $\frac{\partial C^{\mathrm{h}}_{\infty,c}}{\partial m} < 0$. Thus,

$$C^{\mathrm{h}}_{\infty,c} = \frac{4c_t}{3K} + \frac{c_s^h}{K}. \tag{.69}$$

For the Crowdsourcing policy, we use (Two.42) to derive the asymptotic cost

$$C^{\mathrm{w}}_{\infty,c} = \lim_{\delta\to\infty} \frac{z^w}{\pi\delta} = \lim_{\delta\to\infty} \frac{c_t\frac{4\delta\pi}{3K} + \frac{\sqrt{m(c_t+2s_{\mathrm{v}})}\sqrt{s_{\mathrm{v}}\delta\pi(12+m)}}{m} + c_s^w\frac{n(m+1)}{m}}{\pi\delta} = \frac{4c_t}{3K} + \frac{c_s^w(m+1)}{m}. \tag{.70}$$

where the optimal number of recipients per hub is $m_w^* = k$ because $\frac{\partial C^{\mathrm{w}}_{\infty,c}}{\partial m} < 0$, and

$$C^{\mathrm{w}}_{\infty,c} = \frac{4c_t}{3K} + \frac{c_s^w(K+1)}{K}. \tag{.71}$$

B Appendix of Chapter Three

B.1 Proofs

Proof of Proposition E.1.1: From (Three.3), the routes are length bounding, i.e., $l_t = R$, if $K > n(T-2)/(2\pi)$, and otherwise capacity bounding. We focus on the case that routes are length-bounding, then $x_t = (T-2)n/2\pi$ and the number of truck routes are

$$\gamma^t = \lceil \frac{n}{x_t} \rceil \approx \frac{2\pi}{T-2} \tag{.72}$$

each with the length of $l_t = R$. Thus, the cost of the truck policy is

$$z^t \approx \frac{2\pi R c_t}{R-2} + c_s^{\mathrm{t}} n. \tag{.73}$$

When capacity is bounding, $x_t = K$, there are $\gamma^t = \lceil n/K \rceil \approx n/K$ routes of length $l_t = 2 + (x_t - 1)\delta \approx 2 + x_t\delta$. Thus, from (Three.1) and $D_t^t = \gamma^t l_t$, the cost of the truck policy is

$$z^t \approx 2c_t(\pi + n/K) + c_s^{\mathrm{t}} n. \tag{.74}$$

Proof of Proposition E.1.2:

When routes are length-bounding, i.e., ($l^{\mathrm{h}} = T$), given (Three.1) the hybrid policy has a cost of

$$z^h = c_s \frac{n}{m} + 2s_{\mathrm{V}} n(1-r) + s_{\mathrm{V}} \frac{m^2\pi^2 r}{3(1-r)} + c_t \frac{2\pi r T}{T-2r}. \tag{.75}$$

Because the optimal r_h^* is cumbersome to derive, we use the Taylor expansion of z^h, with an error order of three, given by (Three.15):

$$z^h \approx 2s_{\mathrm{V}} n + c_s \frac{n}{m} + (2c_t\pi + \frac{s_{\mathrm{V}} m^2\pi^2}{3} - 2s_{\mathrm{V}} n)r + (\frac{s_{\mathrm{V}} m^2\pi^2}{3} + \frac{4c_t\pi}{T})r^2. \tag{.76}$$

The first order condition for minimizing the total hybrid policy cost, z^h, w.r.t. any radius

r gives $r_{\mathrm{h}}^{*} = \dfrac{(6s_{\mathrm{v}}n - 6c_t\pi - s_{\mathrm{v}}m^2\pi^2)T}{24c_t\pi + 2s_{\mathrm{v}}m^2\pi^2 T}$ in (Three.16) that is within the bounds of $r \in [0,1]$ if $\dfrac{6\pi}{6n - m^2\pi^2} \leq \dfrac{s_{\mathrm{v}}}{c_t} < \dfrac{2\pi(4+T)}{(2n - m^2\pi^2)T}$.

We now check the second order condition of z^h in (Three.15) w.r.t. any radius r,

$$\frac{\partial^2 z^h}{\partial r^2} = \frac{2s_{\mathrm{v}}m^2\pi^2 T + 24c_t\pi}{3T} > 0. \tag{.77}$$

Now, we derive the optimal number of recipients per hub m_h^*. The first order necessary condition of optimality for minimizing the total hybrid policy cost z^h, w.r.t. m gives $m_h^* = \sqrt[3]{\frac{3c_s n(1-r)}{2s_{\mathrm{v}}\pi^2 r}}$. The second order condition of z^h w.r.t. m gives

$$\frac{\partial^2 z^h}{\partial m^2} = \frac{6c_s n(1-r) + 2s_{\mathrm{v}}\pi^2 r m^3}{3m^3(1-r)} > 0 \qquad \forall r \in [0,1). \tag{.78}$$

Hence, r_{h}^* and m_h^* are unique.

The derivation of the capacity-bounding case can be found in Chapter Two.

Proof of Proposition E.1.3:

Consider the length bounding case where ($l^{\mathrm{h}} = T$), given (Three.1) the crowdsourcing policy has a cost of

$$z^w = \frac{c_s(1+m)n}{m} + s_{\mathrm{v}}(2\pi + \frac{2n(1-r)}{m} + \frac{m\pi^2 r}{n(1-r)}) + \frac{2c_t\pi r T}{T-2r}. \tag{.79}$$

Because we cannot find a closed-form r_w^*, we use the Taylor expansion of z^w, with an error order of three:

$$z^w = s_{\mathrm{v}}\left(2\pi + \frac{2n}{m}\right) + c_s\frac{n(m+1)}{m} + (s_{\mathrm{v}}(\frac{\pi^2 m}{n} - \frac{2n}{m}) + 2\pi c_t)r + (\frac{2\pi^2 s_{\mathrm{v}} m}{n} + \frac{8\pi c_t}{T})\frac{r^2}{2}. \tag{.80}$$

The first order condition for minimizing crowdsourcing cost, z^w, w.r.t. any radius r gives (Three.19) that is within the bounds of $r \in [0,1]$. We now check the second order condition z^w, w.r.t. any radius r. The second derivative is

$$\frac{\partial^2 z^w}{\partial r^2} = \frac{2\pi^2 s_{\text{V}} m}{n} + \frac{8\pi c_t}{T} > 0. \tag{.81}$$

Hence, r_w^* is unique.

The derivation of the capacity-bounding case can be found in Chapter Two in the proof of *Proposition 3*.

Proof of Proposition E.3.1:

We now consider the length bounding case. In the truck policy, we derive the asymptotic cost as

$$z_\infty^t = \lim_{n\to\infty} \frac{c_s n(T-2) + 2c_t \pi T}{n(T-2)} = c_s. \tag{.82}$$

In the AV policy, we derive the asymptotic cost as

$$z_\infty^v = \lim_{n\to\infty} \frac{2s_{\text{V}} n + c_s}{n} = 2s_{\text{V}}. \tag{.83}$$

In the hybrid policy, we drive the asymptotic cost as

$$z_\infty^h = \lim_{n\to\infty} \frac{z^h}{n} = \frac{c_s}{m} + 2s_{\text{V}}(1-r), \tag{.84}$$

which gives $r^* = 1$, since $\dfrac{\partial z_\infty^h}{\partial r} = -2s_{\text{V}} < 0$, yielding the final cost in (Three.21).

In the crowdsourcing policy, we drive the asymptotic cost as

$$z_\infty^w = \lim_{n\to\infty} \frac{z^w}{n} = \frac{2s_{\text{V}}}{m}(1-r) + \frac{c_s(1+m)}{m}, \tag{.85}$$

which gives $r^* = 1$, since $\dfrac{\partial z_\infty^w}{\partial r} = \frac{-2s_{\text{V}}}{m} < 0$ yielding the final cost in (Three.21).

Proof of Proposition F.1.1:

The total cost of the truck policy on the circular surface is

$$z^t = c_t \sum_{i=1}^{C} \gamma_i^t l_{t\,i} + c_s^t \rho\pi. \tag{.86}$$

.

Since we are considering the length bounding case, we have

$$z^t = c_t \sum_{i=1}^{C} \gamma_i^t T + c_s^t \rho\pi = c_t T \sum_{i=1}^{C} \gamma_i^t + c_s^t \rho\pi, \tag{.87}$$

where

$$\sum_{i=1}^{C} \gamma_i^t = \sum_{i=1}^{C} \frac{2\pi R_i + \frac{N_i^t \tau}{2}}{T - 2R_i} = \sum_{i=1}^{C} \frac{2\pi(i-\frac{1}{2})\tau + (i-\frac{1}{2})\tau^2\pi\rho\tau}{T - 2(i-\frac{1}{2})\tau} = \sum_{i=1}^{C} \frac{(i-\frac{1}{2})(2\pi\tau + \tau^3\pi\rho)}{T - 2(i-\frac{1}{2})\tau}. \tag{.88}$$

We approximate this by taking the integral over $i = 0$ to C: $\int_{i=0}^{C} \frac{(i-\frac{1}{2})(2\pi\tau+\tau^3\pi\rho)}{T-2(i-\frac{1}{2})\tau}$. Thus:

$$z^t \approx \frac{-c_t T(2+\rho\tau^2)(-2+T\log[1-\frac{2}{T+\tau}])}{4\tau} + c_s^t \rho\pi. \tag{.89}$$

We approximate $T + \tau \approx T$.

$$z^t \approx \frac{-2c_t T(2+\rho\tau^2)(-2+T\log[1-\frac{2}{T}])}{4\tau} + c_s^t \rho\pi. \tag{.90}$$

Take the first order derivative of the cost function with respect to τ:

$$\frac{\partial z^t}{\partial \tau} = \frac{-2c_t(-2+T\log[1-\frac{2}{T}])(-2+\rho\tau^2)}{4\tau^2}. \tag{.91}$$

We put this derivative equal to zero to find the optimal τ. Thus, the optimal τ is:

$$\tau^* = \sqrt{\frac{2}{\rho}}. \tag{.92}$$

By replacing this optimal value in the original cost function, the optimal cost of the truck policy in routing on a circle is:

$$z^{t*} \approx \frac{\sqrt{2}Tc_t(2 - T\log[\frac{T-2}{T}]) + c_s\pi\rho\sqrt{\frac{1}{\rho}}}{\sqrt{\frac{1}{\rho}}} = \sqrt{2\rho}Tc_t(2 - T\log[\frac{T-2}{T}]) + c_s\pi\rho. \qquad (.93)$$

Proof of Proposition F.3.1:

The total cost of the hybrid policy is obtained as follows:

$$z^h(\tau, m) = c_t \sum_{i=1}^{C} \gamma_i^{\mathrm{h}} l_i^{\mathrm{h}} + s_{\mathrm{v}} d_{\mathrm{v}}^h + c_s^h s^h, \qquad (.94)$$

and the number of hand-offs equals the number of hubs, $s^h = \sum_{i=1}^{C} \frac{N_i^h}{m} = \frac{n}{m}$.

Using (Three.32), (Three.34) and (Three.35) we have:

$$z^h(\tau, m) = c_t \sum_{i=1}^{C} \gamma_i^{\mathrm{h}} l_i^{\mathrm{h}} + s_{\mathrm{v}} d_{\mathrm{v}}^h + c_s^h \frac{n}{m} = c_t T \sum_{i=1}^{C} \gamma_i^{\mathrm{h}} + s_{\mathrm{v}} d_{\mathrm{v}}^h + c_s^h \frac{n}{m}. \qquad (.95)$$

where

$$\sum_{i=1}^{C} \gamma_i^{\mathrm{h}} = \sum_{i=1}^{C} \frac{N_i}{(T - 2R_i)\rho\tau} = \sum_{i=1}^{C} \frac{(2i-1)\tau^2\pi\rho}{(T - (2i-1)\tau)\rho\tau} = \sum_{i=1}^{C} \frac{(2i-1)\tau\pi}{T - (2i-1)\tau}$$

We consider the continuous analogue of the given discrete sum and use the approximation of $\sum_{i=1}^{C} \gamma_i^{\mathrm{h}} \approx \int_{i=1}^{C} \gamma_i^{\mathrm{h}}$ which gives the following:

$$\int_{i=1}^{C} \frac{(2i-1)\tau\pi}{T - (2i-1)\tau} = \frac{\pi}{2\tau}(T\log[\frac{T-\tau}{T+\tau-2C\tau}] + 2\tau - 2C\tau).$$

Approximating the number of rings as $C \approx 1/\tau$, we have:

$$\sum_{i=1}^{C} \gamma_i^{\mathrm{h}} \approx \frac{\pi}{2\tau}(T\log[\frac{T-\tau}{T+\tau-2}] + 2\tau - 2).$$

For the AV routing, we use the following heuristic inspired by the upper bound of the hybrid policy in routing on a circle in Chapter Two. Each AV travels from its owner's location to the closest hub, following ring-radial routes (Manhattan distances) on a grid-like city layout. Having the number of recipients and the expected ring and radial distances of each AV route, the total length of AV routing is obtained as follows:

$$d_{\mathrm{v}}^{h} = \sum_{i=1}^{C} 2n_i(\frac{\tau}{4} + \frac{\delta_i^h}{4}) = \sum_{i=1}^{C} 2(2i-1)\tau^2\pi\rho(\frac{\tau}{4} + \frac{m}{4\rho\tau}) = \frac{\tau\pi}{2}(\rho\tau^2 + m)\sum_{i=1}^{C}(2i-1) = \frac{\tau\pi}{2}(\rho\tau^2 + m)C^2 \tag{.96}$$

We approximate the number of rings as $C \approx 1/\tau$. Thus,

$$d_{\mathrm{v}}^{h} \approx \frac{\tau\pi}{2}(\rho\tau^2 + m)\frac{1}{\tau^2} = \frac{\tau^2\rho\pi + m\pi}{2\tau} \tag{.97}$$

Thus, the total cost of the hybrid policy on a circle is:

$$z^h(\tau, m) = c_t T(\frac{\pi}{2\tau} T \log[\frac{T-\tau}{T+\tau-2}] + 2\tau - 2) + s_{\mathrm{v}}(\frac{\tau^2\rho\pi + m\pi}{2\tau}) + c_s^h \frac{n}{m}. \tag{.98}$$

If we approximate $T - \tau \approx T + \tau \approx T$,

$$z^h(\tau, m) = c_t T(\frac{\pi}{2\tau} T \log[\frac{T}{T-2}] + 2\tau - 2) + s_{\mathrm{v}}(\frac{\tau\rho\pi}{2} + \frac{m\pi}{2\tau}) + c_s^h \frac{\rho\pi}{m}. \tag{.99}$$

We take the first-order derivative of the cost function with respect to τ to find its optimal value,

$$\frac{\partial z^h}{\partial \tau} = c_t T(-\frac{\pi T}{2\tau^2} \log[\frac{T}{T-2}] + 2) + s_{\mathrm{v}}\left(\frac{\rho\pi}{2} - \frac{m\pi}{2\tau^2}\right). \tag{.100}$$

Putting this Derivative equal to zero gives the optimal value:

$$\tau^* = \sqrt{\frac{\pi(c_t T^2 \log(\frac{T}{T-2}) + s_{\mathrm{v}} m)}{4c_t T + \pi s_{\mathrm{v}} \rho}} \tag{.101}$$

This is consistent with the hybrid policy on a circle in the capacity-bounding case (D Viniche et al. 2023b). We replace this in the cost function to find the optimal cost of the hybrid policy:

$$z^{h*} = \frac{\pi T c_t m \sqrt{\frac{T^2 c_t \log[\frac{T}{T-2}] + s_{\text{v}} m}{T c_t + s_{\text{v}} \rho}}}{2} + 2T c_t m \sqrt{\frac{T^2 c_t \log[\frac{T}{T-2}] + s_{\text{v}} m}{T c_t + s_{\text{v}} \rho}} \tag{.102}$$
$$-2T c_t m + \pi s_{\text{v}} m \rho \sqrt{\frac{T^2 c_t \log[\frac{T}{T-2}] + s_{\text{v}} m}{T c_t + s_{\text{v}} \rho}} + \frac{c_s^h \rho \pi}{m}.$$

Proof of Proposition F.4.1:

The total cost of the crowdsourcing policy is

$$z^w = c_t d_u^w + s_{\text{v}} d_v^w + c_s^w s^w \tag{.103}$$

where the number of hand-offs is

$$s^w = n + \sum_{i=1}^{C} \frac{N_i}{m} = n(1 + \frac{1}{m}). \tag{.104}$$

AVs are used for crowdsourcing to the m^{w} recipients who visit each hub as one neighbourhood. From each neighborhood, one AV is responsible for visiting the closest hub, picking up the packages, and delivering them to all recipients in that neighborhood, including its owner. We use the following heuristic for AV routing in each neighbourhood where each AV travels the perimeter of its neighborhood and makes small detours from the perimeter to each recipient's location. Again, we consider that AVs travel Manhattan distances and follow ring-radial routes, shown in Figure Three.5c, inspired by the upper bound of the crowdsourcing policy in routing on a circle in Chapter Two. In contrast to truck routing, AVs are assumed to navigate freely through local neighborhoods, enabling more direct and shorter paths. Based on the area around each hub (neighbourhood perimeter), and the expected travel distances from the perimeter to each recipient's location, each AV route is equal to $2\frac{\tau}{2} + 2(\tau + \delta_i^w) + m\frac{\tau}{4}$. Thus, the total AV distance is:

$$d_{\text{v}}^w = \sum_{i=1}^{C} \frac{n_i}{m m^{\text{w}}} m^{\text{w}} [\tau + 2(\tau + \delta_i^w) + m\frac{\tau}{4}] = (\frac{3\tau}{m} + \frac{\tau}{4} + \frac{2}{\rho\tau}) \sum_{i=1}^{C} n_i. \tag{.105}$$

Using $\sum_{i=1}^{C} n_i = n = \pi\rho$, and approximating the number of rings as $C \approx 1/\tau$, we have:

$$d_{\mathrm{v}}^{w} \approx \frac{\tau\rho\pi(12+m)}{4m} + \frac{2\pi}{\tau}. \tag{.106}$$

The truck routing in the crowdsourcing policy is similar to the hybrid policy, so we use (Three.32) and (Three.34),

$$z^{w} = c_t d_u^{w} + s_{\mathrm{v}} d_{\mathrm{v}}^{w} + c_s^{w} s^{w} = c_t T(\frac{\pi}{2\tau} T \log[\frac{T-\tau}{T+\tau-2}] + 2\tau - 2) + s_{\mathrm{v}}(\frac{\tau\rho\pi(12+m)}{4m} + \frac{2\pi}{\tau}) + c_s^{w}\rho\pi(1+\frac{1}{m}). \tag{.107}$$

If we use the approximation of $T-\tau \approx T+\tau \approx T$, we have

$$z^{w} = c_t d_u^{w} + s_{\mathrm{v}} d_{\mathrm{v}}^{w} + c_s^{w} s^{w} = c_t T(\frac{\pi}{2\tau} T \log[\frac{T}{T-2}] + 2\tau - 2) + s_{\mathrm{v}}(\frac{\tau\rho\pi(12+m)}{4m} + \frac{2\pi}{\tau}) + c_s^{w}\rho\pi(1+\frac{1}{m}). \tag{.108}$$

Optimizing for this cost function, we take the derivative of the cost function with respect to τ:

$$\frac{\partial z^{w}}{\partial \tau} = c_t T(-\frac{\pi T}{2\tau^2} \log[\frac{T}{T-2}] + 2) + s_{\mathrm{v}}(\frac{\rho\pi(12+m)}{4m} - \frac{4\pi}{\tau^2}). \tag{.109}$$

Which gives the optimal τ as:

$$\tau^{*} = \sqrt{2}\sqrt{\frac{m\pi\left(4s_{\mathrm{v}} + c_t T^2 \log(\frac{T}{T-2})\right)}{s_{\mathrm{v}}\rho\pi(12+m) + 8c_t T m}}. \tag{.110}$$

We replace this in the cost function to find the optimal cost of the hybrid policy:

$$z^{w*} = \left(2c_t T\tau + \frac{s_{\mathrm{v}}\rho\pi(12+m)\tau}{4m}\right) - \left(\frac{c_t T^2 \pi}{2\tau} \log\left(\frac{T}{T-2}\right) + \frac{2s_{\mathrm{v}}\pi}{\tau}\right) - 2c_t T + c_s^{w}\rho\pi\left(1+\frac{1}{m}\right). \tag{.111}$$

Proof of Proposition F.5.1: We derive asymptotic routing costs for the different policies in routing on a circle when $\delta \to \infty$. For truck policy, using (Three.28), we have

$$z^t_\infty = \lim_{\rho\to\infty} \frac{z^t}{\pi\rho} = c_s. \tag{.112}$$

For AV policy based on, (Three.30), we have:

$$z^v_\infty = \lim_{\rho\to\infty} \frac{z^a}{\pi\rho} = \frac{4}{3} s_\mathrm{V}. \tag{.113}$$

For the hybrid policy, we calculated asymptotic cost using (Three.37),

$$z^h_\infty = \lim_{\rho\to\infty} \frac{z^h}{\pi\rho} = \frac{c^h_s}{m}. \tag{.114}$$

Finally, for the crowdsourcing policy we use (Three.40), and have:

$$z^w_\infty = \lim_{\rho\to\infty} \frac{z^w}{\pi\rho} = \frac{c^w_s(m+1)}{m}. \tag{.115}$$

C Appendix of Chapter Four

C.1 Proofs

Proof of **Proposition 1**:

There are two approaches for proving (Four.15). First is to use the standard KKT conditions (Scales 1985), which yields a system of equations with decision variables and Lagrangian multipliers as the unknowns of the system. However, we take a more straightforward proof approach that relies on the geometrical symmetry of the routes and our stylized model.

From the cost function in (Four.9), we have:

$$T(n_t, n_d) = \frac{l_t}{s_t} + (\frac{\overline{L}}{s_d} - \frac{\delta}{s_t})(m-1),$$

where $\delta \approx \frac{2\pi r x_t}{mN}$ and $\overline{L} = (1-r) + \sqrt{(\delta)^2 + (1-r)^2}$. Since $l_t = r + \delta(m-1)$, we can rewrite the objective function as:

$$T(n_t, n_d) = \frac{r + \delta(m-1)}{s_t} + (\frac{\overline{L}}{s_d} - \frac{\delta}{s_t})(m-1) = \frac{r}{s_t} + (\frac{\overline{L}}{s_d})(m-1). \tag{.116}$$

We use the first-order condition to analyze the optimal share of each truck x_t^*, the optimal number of hubs m^*, and the optimal number of drones in each batch q^*. We take the derivative of the cost function with respect to these decision variables as follows:

We use the first-order condition to find the optimal share of each truck x_t^*; we take the derivative of the cost function with respect to the number of recipients per truck.

$$\frac{\partial T(n_t, n_d)}{\partial x_t} = \frac{(m-1)}{s_d} \frac{\partial \overline{L}}{\partial x_t} = \frac{(m-1)}{s_d} \frac{\left(\frac{2\pi r}{mN}\right)^2 x_t}{\sqrt{\left(\frac{2\pi r x_t}{mN}\right)^2 + (1-r)^2}} \geq 0. \tag{.117}$$

The derivative is always positive, $\frac{\partial T(n_t,n_d)}{\partial x_t} \geq 0$, and in order to minimize the cost function, x_t^* should be as small as possible.

We now take the first-order derivative of the cost function with respect to the number of hubs m:

$$\begin{aligned}
\frac{\partial T(n_t,n_d)}{\partial m} &= \frac{(m-1)}{s_d}\frac{\partial \overline{L}}{\partial m} + \frac{\overline{L}}{s_d}\frac{\partial (m-1)}{\partial m} \\
&= \frac{(m-1)}{s_d}\frac{-\left(\frac{2\pi r x_t}{mN}\right)^2}{m\sqrt{\left(\frac{2\pi r x_t}{mN}\right)^2+(1-r)^2}} + \frac{(1-r)+\sqrt{(\frac{2\pi r x_t}{mN})^2+(1-r)^2}}{s_d} \\
&= \frac{-\frac{m-1}{m}\left(\frac{2\pi r x_t}{mN}\right)^2+(1-r)\sqrt{\left(\frac{2\pi r x_t}{mN}\right)^2+(1-r)^2}+(1-r)^2+\left(\frac{2\pi r x_t}{mN}\right)^2}{s_d\sqrt{\left(\frac{2\pi r x_t}{mN}\right)^2+(1-r)^2}}.
\end{aligned}$$

By combining the first and last terms in the numerator, we have:

$$\frac{\partial T(n_t,n_d)}{\partial m} = \frac{\frac{1}{m}\left(\frac{2\pi r x_t}{mN}\right)^2+(1-r)\sqrt{\left(\frac{2\pi r x_t}{mN}\right)^2+(1-r)^2}+(1-r)^2}{s_d\sqrt{\left(\frac{2\pi r x_t}{mN}\right)^2+(1-r)^2}} \geq 0. \tag{.118}$$

The first-order deviation is always positive, and to minimize the cost function, the optimal number of hubs m^* needs to be the smallest possible value.

While minimizing these two decision variables minimizes the cost, we must check the constraint to ensure their feasible minimum.

$$\begin{aligned}
&(A) \quad (m-1)\overline{L} \leq R, \\
&(B) \quad K \geq x_t, \\
&(C) \quad q(m-1) \geq x_t, \\
&(D) \quad \frac{\delta}{s_t} \leq \frac{L}{s_d}, \\
&(E) \quad n_t \geq \frac{N}{x_t}, \\
&(F) \quad n_d \geq q\frac{N}{x_t}.
\end{aligned}$$

For the optimal share of each truck x_t^*, constraints B and C and D are restricting x_t^* from exceeding a maximum value. Thus, they are not limiting the minimization of x_t^* and are, therefore, non-binding in the optimal solution. From constraints E and F, we have:

$$x_t^* = \max\{\frac{N}{n_t}, q\frac{N}{n_d}\}. \tag{.119}$$

For the optimal number of hubs m^*, we combine constraint C with (.119). Moreover, we need to consider constraint D.

$$m^* = \max\{\frac{N}{n_d}+1, \frac{N}{n_t q}+1, \frac{r}{1-r}\frac{\pi x_t}{N}(\frac{s_d}{s_t}-1)\}. \tag{.120}$$

Considering the approximation of the asymptotic case for a large number of customers, when $n \to \infty$, the third term is small; thus, we have:

$$m^* = \max\{\frac{N}{n_d}, \frac{N}{n_t q}\}+1. \tag{.121}$$

Based on (.119) and (.121), if $q \leq \frac{n_d}{n_t}$ we have $x_t^* = \frac{N}{n_t}$ and $m^* = \frac{N}{n_t q}+1$. On the other hand, if $q \geq \frac{n_d}{n_t}$, $x_t^* = q\frac{N}{n_d}$ and $m^* = \frac{N}{n_d}+1$. Since we want to minimize x_t^* and m^* in order to minimize the total cost, we have $q = \frac{n_d}{n_t}$, $x_t^* = \frac{N}{n_t}$ and $m^* = \frac{N}{n_d}+1$.

To elaborate more on this, we show that if $q \leq \frac{n_d}{n_t}$ or $q \geq \frac{n_d}{n_t}$ one of the two decision variables of x_t^* and m^* are not minimized. If $q < \frac{n_d}{n_t}$, then $m^* = \frac{N}{n_t q}+1$, and since $\frac{N}{n_t q}+1 > \frac{N}{n_d}+1$, in this scenario m^* is not minimized. Also, if $q < \frac{n_d}{n_t}$, then $x_t^* = q\frac{N}{n_d}$, and since $q\frac{N}{n_d} > \frac{N}{n_t}$, in this scenario x_t^* is not minimize. Thus,

$$x_t^* = \frac{N}{n_t}, q^* = \frac{n_d}{n_t}, m^* = \frac{N}{n_d}+1. \tag{.122}$$

Proof of **Proposition 2**:

From the objective function (Four.9) and its revised form in (.116), we have

$$T(n_t, n_d) = \frac{r}{s_t} + (\frac{\overline{L}}{s_d})(m-1),$$

where $\overline{L} = (1-r) + \sqrt{(\delta)^2 + (1-r)^2}$, and $\delta \approx \frac{2\pi r}{m(N/x_t)}$ from (Four.13) and (Four.12), respectively. The partial derivative of the objective function w.r.t. the radius r is:

$$\frac{\partial T(n_t,n_d)}{\partial r} = \frac{1}{s_t} + \frac{(m-1)}{s_d}\left(-1+\frac{\frac{4\pi^2 r x_t^2}{m^2N^2}-(1-r)}{\sqrt{\left(\frac{2\pi r}{m\frac{N}{x_t}}\right)^2+(1-r)^2}}\right). \tag{.123}$$

We use the optimal expressions for m and x_t, provided in (Four.15):

$$\frac{\partial T(n_t,n_d)}{\partial r} = \frac{1}{s_t} + \frac{N}{n_d s_d}\left(-1+\frac{\left(\frac{4\pi^2 r n_d^2}{N^2 n_t^2}-(1-r)\right)}{\sqrt{\left(\frac{2\pi r n_d}{N n_t}\right)^2+(1-r)^2}}\right). \tag{.124}$$

Re-arranging the terms to factor out the speed ratio s_t/s_d, gives $\frac{\partial T}{\partial r} \geq 0$ if $s_t/s_d \leq \tau$ and $\frac{\partial T}{\partial r} < 0$ if $s_t/s_d > \tau$, where the term τ is the critical speed ratio. By putting the first derivative equal to zero, we have:

$$\tau = \frac{n_d\sqrt{4\pi^2 r^2 n_d^2 + (1-r)^2 N^2 n_t^2}}{N\sqrt{4\pi^2 r^2 n_d^2 + (1-r)^2 N^2 n_t^2} - (4\pi^2 r n_d^2 - (1-r) N^2 n_t^2)}, \tag{.125}$$

where r is the optimal radius, which itself depends on the critical speed ratio.

The second-order derivative of the cost with respect to the truck travel radius as follows:

$$\frac{\partial^2 T(n_t,n_d)}{\partial^2 r} = \frac{4Nn_d\pi^2}{\left(N^2 n_t^2 (r-1)^2 + 4n_d\pi^2 r^2\right)\sqrt{1+s_d r\left(r-2+\frac{4\pi^2 r n_d^2}{N^2 n_t^2})\right)}}, \tag{.126}$$

which is always positive by nature. Moreover, the first-order derivative of the cost function with respect to r, both before and after the critical speed ratio, is a monotonic function.

We now proceed to obtain the optimal radius by using constraints (Four.6) and (Four.7), naming them C_1 and C_2, respectively.

$$C1 = (m-1)\overline{L} - R. \tag{.127}$$

Using (Four.13) and the optimal value of m and x_t in (Four.15), we have

$$C_1 = \frac{N}{n_d}\left((1-r)+\sqrt{\delta^2+(1-r)^2}\right) - R, \tag{.128}$$

where $\delta \approx \frac{2\pi r}{m(N/x_t)}$. Thus, taking the first derivative with respect to truck travel distance r

$$\frac{\partial C_1}{\partial r} = \frac{N}{n_d}\left(-1+\frac{\delta\frac{2\pi x_t}{mN}-(1-r)}{\sqrt{\delta^2+(1-r)^2}}\right). \tag{.129}$$

Considering the approximation of the asymptotic case for a large number of customers, i.e., when $n \to \infty$, we have $\frac{\partial C_1}{\partial r} \leq 0$.

We now proceed to the second constraint:

$$C_2 = \frac{\delta}{s_t} - \frac{L}{s_d}. \tag{.130}$$

Using (Four.14), the constraint is:

$$C_2 = \frac{\delta}{s_t} - \frac{2\sqrt{(\delta/2)^2+(1-r)^2}}{s_d}. \tag{.131}$$

Taking the first derivative with respect to r, we have

$$\frac{\partial C_2}{\partial r} = \frac{2\pi n_d}{N n_t s_t} + \frac{2(1-r)}{s_d\sqrt{(\frac{\pi r n_d}{N n_t})^2+(1-r)^2}}, \tag{.132}$$

which is evidently always positive $\frac{\partial C_2}{\partial r} \geq 0$.

We now proceed to derive the optimal truck travel radius. Based on (.124) and (.125), when $\frac{s_t}{s_d} \leq \tau$ we have $\frac{\partial T}{\partial r} \geq 0$ and to minimize the total cost, we need to decrease the r^* as low as possible. On the other hand, based on range constraint in (.128), its derivative with respect to radius in (.129), and the fact that $\frac{\partial C_1}{\partial r} \leq 0$ for r in the range of $[0,1]$, smaller r can violate this constraint. Thus, the optimal radius for this speed range, ${r_1}^*$, can be obtained by solving $C_1 = 0$

for r:

$$C1 = (m-1)\overline{L} - R = 0. \tag{.133}$$

Thus,

$$\frac{N}{n_d}\left(1 - {r_1}^* + \sqrt{\left(\frac{2\pi {r_1}^* n_d}{N n_t}\right)^2 + (1-{r_1}^*)^2}\right) = R, \tag{.134}$$

which gives (for the range 0f $[0,1]$) :

$${r_1}^* = \frac{N n_t^2 R - n_t\sqrt{(N^2 n_t^2 + 4 n_d^2 \pi^2) R^2 - 8 N n_d \pi^2 R}}{4 n_d \pi^2}, \tag{.135}$$

For larger truck speeds when $\frac{s_t}{s_d} \geq \tau$, from (.124) and (.125) we have $\frac{\partial T}{\partial r} \leq 0$ which tends to increase the truck travel radius r. Nevertheless, based on (.131), its derivative with respect to r in (.132), and the fact that $\frac{\partial C_2}{\partial r} \geq 0$, large r would violate the scheduling constraint. Hence, the optimal value of r for this speed range to minimize the cost function but not violate the constraint would be obtained as follows:

$$C_2 = \frac{\delta}{s_t} - \frac{\underline{L}}{s_d} = 0. \tag{.136}$$

Hence,

$$\frac{2\pi {r_2}^* n_d}{N n_t s_t} = \frac{2\sqrt{\left(\frac{\pi {r_2}^* n_d}{N n_t}\right)^2 + (1-{r_2}^*)^2}}{s_d}, \tag{.137}$$

from which we obtain:

$${r_2}^* = \frac{N n_t s_t}{N n_t s_t + n_d \pi \sqrt{s_d^2 - s_t^2}}. \tag{.138}$$

Thus, we derive the optimal radius r^* for the circular routing setting:

$$r^* = \begin{cases} \frac{Nn_t^2R - n_t\sqrt{\left(N^2n_t^2+4n_d^2\pi^2\right)R^2 - 8Nn_d\pi^2R}}{4n_d\pi^2} & s_t/s_d \leq \tau \\ \frac{Nn_ts_t}{Nn_ts_t + n_d\pi\sqrt{s_d^2 - s_t^2}} & s_t/s_d > \tau \end{cases}. \tag{.139}$$

Proof of **Proposition 3**:

Based on (Four.18), for the ring-radial routing, we have:

$$\underline{L} = \overline{L} = L = 2(1-r) + \delta. \tag{.140}$$

The cost function of the ring-radial model, using (Four.9) and (Four.18), is:

$$T(n_t, n_d) = \frac{r}{s_t} + (\frac{L}{s_d})(m-1) = \frac{r}{s_t} + (\frac{2(1-r)+\delta}{s_d})(m-1). \tag{.141}$$

Taking the first derivative of the cost function with respect to r, gives:

$$\frac{\partial T(n_t, n_d)}{\partial r} = \frac{1}{s_t} + (m-1)\left(\frac{2\pi x_t}{mNs_d} - \frac{2}{s_d}\right). \tag{.142}$$

The critical speed ratio can be obtained by re-arranging the terms to factor out the speed ratio when the first derivative equals zero and changes the sign. Using the optimal value of (Four.15), we have:

$$\tau = \frac{Nn_tn_d + n_tn_d^2}{2N^2n_t + 2Nn_tn_d - 2\pi Nn_d}. \tag{.143}$$

Similar to the circular routing, from (.142) we have the case that $\frac{\partial T}{\partial r} \geq 0$ if $\frac{s_t}{s_d} \leq \tau$ and we have $\frac{\partial T}{\partial r} \leq 0$ if $\frac{s_t}{s_d} \geq \tau$.

We now proceed to check the constraints in the ring-radial model. Using (Four.18), we can rewrite the range constrain in (.128) as:

$$C_1 = (m-1)(2(1-r)+\delta) - R. \tag{.144}$$

where $\delta \approx \frac{2\pi r x_t}{mN}$. Taking the first derivative with respect to r, we have:

$$\frac{\partial C_1}{\partial r} = (m-1)\frac{\partial L}{\partial r} = (m-1)(-2+\frac{2\pi x_t}{(m-1)N}). \tag{.145}$$

Considering the asymptotic conditions where N is large, we have $\frac{\partial C_1}{\partial r} \leq 0$.

Since for $\frac{s_t}{s_d} \leq \tau$ we have $\frac{\partial T}{\partial r} \geq 0$ but $\frac{\partial C_1}{\partial r} \leq 0$, the optimal r is this range is bound by range constraint.

$$C1 = (m-1)L - R = 0. \tag{.146}$$

Thus,

$$(m-1)\,(2(1-r_1^*)+\delta) = R, \tag{.147}$$

which gives the optimal r_1^* as:

$$r_1^* = \frac{n_t(2N - n_d R)}{2Nn_t - 2\pi n_d}. \tag{.148}$$

From the scheduling constraint for the ring-radial setting, from (Four.7) and (Four.18), we have:

$$C_2 = \frac{\delta}{s_t} - \frac{L}{s_d} = \frac{\delta}{s_t} - \frac{2(1-r)+\delta}{s_d} = \delta(\frac{1}{s_t} - \frac{1}{s_d}) - \frac{2(1-r)}{s_d}. \tag{.149}$$

We take the first derivative of C_2 for the ring radial setting, with respect to r:

$$\frac{\partial C_2}{\partial r} = \frac{\pi x_t}{mN}(\frac{1}{s_t} - \frac{1}{s_d}) + \frac{2}{s_d}, \tag{.150}$$

which is always positive.

Since for $\frac{s_t}{s_d} \geq \tau$, we have $\frac{\partial T}{\partial r} \leq 0$, but we also have $\frac{\partial C_2}{\partial r} \geq 0$, the optimal radius in this speed region would be bounded by the scheduling constraint.

$$C_2 = \delta(\frac{1}{s_t} - \frac{1}{s_d}) - \frac{2(1-r)}{s_d} = 0. \tag{.151}$$

Thus,

$$\delta(\frac{1}{s_t} - \frac{1}{s_d}) = \frac{2(1-r)}{s_d}, \tag{.152}$$

which gives the optimal radius r_2^* as:

$$r_2^* = \frac{Nn_t s_t}{\pi n_d(s_d - s_t) + Nn_t s_t}. \tag{.153}$$

Finally, we have:

$$r^* = \begin{cases} \frac{n_t(2N - n_d R)}{2Nn_t - 2\pi n_d} & s_t/s_d \le \tau \\ \frac{Nn_t s_t}{\pi n_d(s_d - s_t) + Nn_t s_t} & s_t/s_d > \tau, \end{cases} . \tag{.154}$$

Proof of **Proposition 5**:

We take an approach similar to previous section and use the constraints A-F for the proof of optimal fleet composition in (Four.24)-(Four.25). We first focus on the optimal number of trucks n_t. When the speed ratio is smaller than the first critical threshold $\frac{s_t}{s_d} \le \tau_1$, using constraints A and E gives:

$$(m-1)\overline{L} = R \quad , \quad \frac{\delta}{s_t} = \frac{\underline{L}}{s_d}. \tag{.155}$$

In the fleet composition optimization, we are focusing on the ring-radial setting, thus $\overline{L} = \underline{L}$. Replacing the $\underline{L}$ in E with the $\overline{L}$ from A, we have:

$$\frac{\delta}{s_t} = \frac{R}{(m-1)s_d}. \tag{.156}$$

Using (Four.23), results in following:

$$\frac{2\pi r n_d}{N n_t s_t} = \frac{R n_d}{N s_d}. \tag{.157}$$

Thus,

$$n^*_{t\,1} = \frac{2\pi r s_d}{R s_t}. \tag{.158}$$

For the speed ratio larger than the first threshold $\tau_1 \leq \frac{s_t}{s_d}$, from constraint B, $x_t = K$. Using (Four.23), we have

$$n^*_{t\,2} = \frac{N}{K}. \tag{.159}$$

Moving to the optimal number of drones n_d, when $\frac{s_t}{s_d} \leq \tau_1$ we use the first case in (Four.19) and (Four.24).

$$\begin{aligned}
r^* &= \frac{2Nn^*_t - n^*_d n^*_t R}{2Nn^*_t - 2\pi n^*_d}, \\
n^*_t &= \frac{2\pi r^* s_d}{R s_t}.
\end{aligned}$$

Replacing r^* in n^*_t, we can obtain the optimal number of drones in this speed range:

$$n^*_{d1} = \frac{2N s_d (1 - r^*)}{R(s_d - s_t)}. \tag{.160}$$

When the speed ratio is between the first and second threshold $\frac{s_t}{s_d} \leq \tau_1$, we use the first case of r^* in (Four.19) and the second case of n^*_t in (Four.24) (constraints A and E):

$$\begin{aligned}
r^* &= \frac{2Nn^*_t - n^*_d n^*_t R}{2Nn^*_t - 2\pi n^*_d}, \\
n^*_t &= \frac{N}{K}.
\end{aligned}$$

Thus, the optimal number of drones in this speed range is:

$$n^*_{d2} = \frac{2N^2(1-r)}{NR - 2\pi KR}. \tag{.161}$$

Finally, when the speed ratio is larger than the second threshold, $\tau_2 \leq \frac{s_t}{s_d}$, we use constraints B and F:

$$K = x_t \quad , \quad n_d \geq q\frac{N}{x_t}. \tag{.162}$$

Thus, the optimal number of drones in this speed range is:

$$n^*_{d3} = \frac{N}{K}. \tag{.163}$$

.3.2 Routing on a Circular Surface Cost Structure

In the routing on a circular surface, we divide the circular surface into S concentric rings, each with radius D_i for $i = 1, 2, ..., S$. Given that recipients are uniformly distributed across the surface with a density of ρ, the total number of recipients on the circular surface is $\pi\rho$. The area allocated to each ring i is denoted as A_i, and the number of recipients assigned to ring i is calculated as:

$$N_i = \rho A_i. \tag{.164}$$

The radius of ring i, denote by D_i, is obtained as follows:

$$D_1 = d_0 \ , \quad D_2 = d_0 + d_1 \ , \quad D_i = \sum_{z=0}^{i-1} d_z. \tag{.165}$$

The total distance travelled by each truck is

$$l_i = D_i + \delta_i(m-1), \tag{.166}$$

where m is the number of hubs along a truck's path, and δ_i is the distance between two consecutive hubs on each ring,

$$\delta_i = \frac{2\pi D_i}{(m-1)n_{ti}}. \tag{.167}$$

By applying the Extreme Value Distribution Theorem for uniformly distributed recipients, the minimum and maximum drone flight distances for ring i are:

$$\underline{L}_i = \delta_i + \frac{d_i}{N_i} \quad \& \quad \overline{L}_i = \delta_i + d_i(\frac{N_i - 1}{N_i}), \tag{.168}$$

where N_i is the number of recipients assigned to the ring as given in (.164).

The routing cost per truck on each ring follows the same structure as in equation (Four.9), accounting for both travel distance and waiting time,

$$T_i(D_i, d_i) = \frac{l_i}{s_t} + (\frac{\overline{L}_i}{s_d} - \frac{\delta_i}{s_t})(m-1), \tag{.169}$$

where s_t and s_d represent the truck and drone speeds, respectively.

The range constraint for the routing on a surface model is

$$K\overline{L}_i \leq R, \tag{.170}$$

and the scheduling constrict is

$$\frac{\delta_i}{s_t} \leq \frac{\underline{L}_i}{s_d}. \tag{.171}$$

For routing on a circular surface with equal fleet of trucks on each ring, the number of recipients assigned to each ring is $N_i = n_t K$. Given that the number of recipients is derived from their density and area assigned to each ring, as in (.164), we partition the surface so that all areas are equally A for each ring. Considering that we divide the circular surface into S rings, where the S^{th} (last) ring is the surface region with a radius of one. Thus, the area surrounding each ring and the number of recipients in that area are

$$A = \frac{\pi}{S} \quad \& \quad N_i = \frac{N}{S}, \tag{.172}$$

and the number of trucks on each ring is

$$n_t = \frac{N}{SK}. \tag{.173}$$

To obtain the radius of these S concentric rings, we begin with the first ring, which encloses N_i recipients within the area of A. Hence, we can calculate $D_1 = \sqrt{\frac{1}{S}}$. Subsequently, the area within the second ring is the aggregation of the first ring's area and the area of the strip between the first and second rings, where each of these is equal to A. Therefore, $\pi D_2^2 = 2A = 2\frac{\pi}{S}$ and $D_2 = \sqrt{\frac{2}{S}}$. Using this heuristic, we derive the radius of each ring:

$$D_i = \sqrt{\frac{i}{S}}. \tag{.174}$$

From, (Four.32), the distance between rings i and $i+1$ is:

$$d_i \approx \frac{1}{2SD_i} = \frac{1}{2\sqrt{iS}}. \tag{.175}$$

The travel distance for each truck is given by $l_i = D_i + \frac{2\pi D_i}{n_t}$. Using equations (.173) and (Four.31), we arrive at the following:

$$l_i = \sqrt{\frac{i}{S}} + \frac{2\pi K\sqrt{iS}}{N}. \tag{.176}$$

The inter-hub distance on each ring was previously defined in (.167). Using equations (.173) and (Four.31), we can derive the inter-hub distance:

$$\delta_i = \frac{2\pi\sqrt{iS}}{N}, \tag{.177}$$

Using (Four.32) and (.177), for the minimum drone flight distance in (Four.28), we have:

$$\underline{L}_i = \frac{2\pi\sqrt{iS}}{N} + \frac{\sqrt{S}}{2N\sqrt{i}}. \tag{.178}$$

Moreover, assuming that N_i is significantly larger than 1, i.e., $N_i >> 1$, we have the maximum drone flight distance as $\overline{L}_i = \delta_i + d_i$. Substituting the expressions from (Four.32) and (.177), we obtain the maximum drone flight distance on ring i as follows:

$$\overline{L}_i \approx \frac{2\pi\sqrt{iS}}{N} + \frac{1}{2\sqrt{iS}}, \tag{.179}$$

which has the properties of high values in both the first and last rings corresponding to very small and very large i values, respectively, along with a minimum value of $\overline{L}_{i^*} = \frac{2\sqrt{\pi}}{\sqrt{N}}$ at $i^* = \frac{N}{4\pi S}$.

Based on the range constraint given in (.170), we have $K\overline{L}_i \leq R$. Thus, It is apparent that the drone flight range should at least exceed this minimum threshold for drone delivery to be feasible. Thus, $\frac{2K\sqrt{\pi}}{\sqrt{N}} < R$. The range constraint presented in (.170) can be rewritten by using the new form of maximum drone flight distance derived in (.178):

$$\frac{2K\pi\sqrt{iS}}{N} + \frac{K}{2\sqrt{iS}} \leq R. \tag{.180}$$

The range constraint gives the following bounds for i:

$$-\frac{K^2N}{S(2NR^2 + 2R\sqrt{N^2R^2 - 4NK^2\pi} - 4K^2\pi)} \leq i \leq \frac{N^2R^2 - 2K^2N\pi + NR\sqrt{N^2R^2 - 4NK^2\pi}}{8SK^2\pi^2}. \tag{.181}$$

Considering the asymptotic case when $N \to \infty$, the left-hand side is always true as it has negative values, and i is a positive indicator. On the right-hand side, we can ignore lower degrees of N and simplify the equation as follows:

$$i \leq \frac{N^2R^2}{4SK^2\pi^2}. \tag{.182}$$

If this condition is met, we use the original form of cost presented in (Four.29). Otherwise, the range constraint limits the maximum drone travel distance, and we have $\overline{L}_i = R$.

For the scheduling constraint from (.171) we have $\frac{\delta_i}{s_t} \leq \frac{L_i}{s_d}$. We repeat the process of implementing the new definition provided in (Four.32) and (.177), and thus we have:

$$\frac{2\pi\sqrt{iS}}{Ns_t} \leq \frac{2\pi\sqrt{iS}}{Ns_d} + \frac{\sqrt{S}}{2Ns_d\sqrt{i}}, \tag{.183}$$

which gives:

$$i \leq \frac{s_t}{4\pi(s_d - s_t)}. \tag{.184}$$

If this condition is met, we use the original form of cost presented in (Four.29). Otherwise, the minimum drone travel distance and truck movement (traversing) on the ring are bounded by the scheduling constraint and $\frac{\delta_i}{s_t} = \frac{L_i}{s_d}$.

We obtain the routing cost of each ring i, $T_i(S)$, based on the range and the scheduling constraints. The range constraint and the scheduling constraint presented in (Four.34) and (Four.35), respectively, and their bounds on i, presented in (.182) and (.184), offer four different cases for the total cost structure.

Case 1 If $S \leq \frac{NR}{2K\pi}$, then we have $S \leq \frac{N^2R^2}{4SK^2\pi^2}$. Since i is the indicator of the ring number, i.e. $i \leq S$, we have $i \leq \frac{N^2R^2}{4SK^2\pi^2}$. Thus, the range constraint presented in (Four.34) is always met, and we can claim that the range constraint is never binding. In this case, the scheduling constraint and (.184) would determine the structure of the cost function as follows:

$$T_i(S) = \begin{cases} \frac{\sqrt{i}}{s_t\sqrt{S}} + \frac{4K\pi iS + KN}{2Ns_d\sqrt{iS}} & 1 \leq i \leq \frac{s_t}{4\pi(s_d - s_t)} \\ \frac{\sqrt{i}}{s_t\sqrt{S}} + \frac{2\pi K\sqrt{iS}}{s_tN} + \frac{K(1-\frac{2S}{N})}{2s_d\sqrt{iS}} & \frac{s_t}{4\pi(s_d - s_t)} \leq i \leq S \end{cases}. \tag{.185}$$

Case 2 If $S \leq \frac{s_t}{4\pi(s_d - s_t)}$, based on the fact that $i < S$ (by definition), we conclude that $i < \frac{s_t}{4\pi(s_d - s_t)}$ and inequality in (.184) is always true; Thus, the scheduling constraint is never binding. In this case, the range constraint presented in (Four.34) would determine the structure of the cost of each ring:

$$T_i(S) = \begin{cases} \frac{\sqrt{i}}{s_t\sqrt{S}} + \frac{4K\pi iS+KN}{2Ns_d\sqrt{iS}} & 1 \leq i \leq \frac{N^2R^2}{4SK^2\pi^2} \\ \frac{\sqrt{i}}{s_t\sqrt{S}} + \frac{R}{s_d} & \frac{N^2R^2}{4SK^2\pi^2} \leq i \leq S \end{cases}. \tag{.186}$$

If $S \leq \frac{NR}{2K\pi}$ and $S \leq \frac{s_t}{4\pi(s_d-s_t)}$ are both true, we have the overlap of Case 1 and Case 2 where $T_i(S) = \frac{\sqrt{i}}{s_t\sqrt{S}} + \frac{4K\pi iS+KN}{2Ns_d\sqrt{iS}}$. In this scenario, neither range constraint nor scheduling constraint is binding. If $\frac{N^2R^2}{4SK^2\pi^2} < S$ and $\frac{s_t}{4\pi(s_d-s_t)} < S$, then both range and scheduling constraints can be binding depending on the values of the parameters. Thus, the comparison of the right sides of inequalities (.182) and (.184) would determine the cost structure, and we will have three regions as follows.

Case 3 If $\frac{s_t}{4\pi(s_d-s_t)} \leq \frac{N^2R^2}{4SK^2\pi^2} \leq S$, we have the three regions presented as follows:

$$T_i(S) = \begin{cases} \frac{\sqrt{i}}{s_t\sqrt{S}} + \frac{4K\pi iS+KN}{2Ns_d\sqrt{iS}} & 1 \leq i \leq \frac{s_t}{4\pi(s_d-s_t)} \\ \frac{\sqrt{i}}{s_t\sqrt{S}} + \frac{2\pi K\sqrt{iS}}{s_tN} + \frac{K(1-\frac{2S}{N})}{2s_d\sqrt{iS}} & \frac{s_t}{4\pi(s_d-s_t)} \leq i \leq \frac{N^2R^2}{4SK^2\pi^2} \\ X & \frac{N^2R^2}{4SK^2\pi^2} \leq i \leq S \end{cases}. \tag{.187}$$

Here, in the first region, no constraint is binding; in the second one, the scheduling constraint is binding; and in the third one, both the range and the scheduling constraints are binding.

Case 4 Lastly, in the case that we have both constraints determining the cost structure, if $\frac{N^2R^2}{4SK^2\pi^2} \leq \frac{s_t}{4\pi(s_d-s_t)} \leq S$, We again have three regions with no constraint binding int he first region, and both range and scheduling constraints are binding in the third region. Nevertheless, in this case, the range constraint is binding in the second region.

$$T_i(S) = \begin{cases} \frac{\sqrt{i}}{s_t\sqrt{S}} + \frac{4K\pi iS+KN}{2Ns_d\sqrt{iS}} & 1 \leq i \leq \frac{N^2R^2}{4SK^2\pi^2} \\ \frac{\sqrt{i}}{s_t\sqrt{S}} + \frac{R}{s_d} & \frac{N^2R^2}{4SK^2\pi^2} \leq i \leq \frac{s_t}{4\pi(s_d-s_t)} \\ Y & \frac{s_t}{4\pi(s_d-s_t)} \leq i \leq S \end{cases}. \tag{.188}$$

The total cost of routing on a surface is obtained based on equation (Four.30) by summing the routing costs across all rings and adding the fleet amortized ownership cost, as introduced in equation (Four.1). Considering that the number of trucks and drones is equal in this section, $n_t = n_d$, the total cost is expressed as:

$$C = \Sigma_{i=1}^{S} n_t T_i(S) + \frac{N}{K}(F_t + F_d). \tag{.189}$$

Focusing on *Case1*, we have:

$$C_1 = \frac{N}{K}(F_t + F_d) + \Sigma_{i=1}^{S} n_t \begin{cases} \frac{\sqrt{i}}{s_t\sqrt{S}} + \frac{4K\pi iS+KN}{2Ns_d\sqrt{iS}} & 1 \leq i \leq \frac{s_t}{4\pi(s_d-s_t)} \\ \frac{\sqrt{i}}{s_t\sqrt{S}} + \frac{2\pi K\sqrt{iS}}{s_tN} + \frac{K(1-\frac{2S}{N})}{2s_d\sqrt{iS}} & \frac{s_t}{4\pi(s_d-s_t)} \leq i \leq S \end{cases}. \tag{.190}$$

We approximate this cost by taking the integral of the second term over $i = 0$ to S:

$$C = n_t \int_0^S T_i(S) + \frac{N}{K}(F_t + F_d), \tag{.191}$$

which gives the cost of *Case1* as:

$$C_1 = \frac{N}{K}(F_t + F_d) + n_t \int_{i=0}^{S} \begin{cases} \frac{\sqrt{i}}{s_t\sqrt{S}} + \frac{2K\pi\sqrt{iS}}{s_dN} + \frac{K}{2s_d\sqrt{iS}} & 1 \leq i \leq \frac{s_t}{4\pi(s_d-s_t)} \\ \frac{\sqrt{i}}{s_t\sqrt{S}} + \frac{2\pi K\sqrt{iS}}{s_tN} + \frac{K(1-\frac{2S}{N})}{2s_d\sqrt{iS}} & \frac{s_t}{4\pi(s_d-s_t)} \leq i \leq S \end{cases} \tag{.192}$$

$$= \frac{N}{K}(F_t + F_d) + \begin{cases} \frac{3Ks_dN+2s_dNS+4K\pi s_tS^2}{3Ks_ds_tS} & 1 \leq i \leq \frac{s_t}{4\pi(s_d-s_t)} \\ \frac{3Ks_tN+2s_dNS-6Ks_tS+4K\pi s_dS^2}{3Ks_ts_dS} & \frac{s_t}{4\pi(s_d-s_t)} \leq i \leq S \end{cases}.$$

To solve for the optimal number of rings S, we take the derivative of the cost with respect to the number of rings:

$$\frac{dC_1}{dS} = \begin{cases} -\frac{N}{sdS^2} + \frac{4\pi}{3s_d} & 1 \leq i \leq \frac{s_t}{4\pi(s_d-s_t)} \\ -\frac{N}{sdS^2} + \frac{4\pi}{3s_t} & \frac{s_t}{4\pi(s_d-s_t)} \leq i \leq S \end{cases}. \tag{.193}$$

By setting this derivation equal to zero, we obtain the optimal number of rings as we:

$$S^* = \begin{cases} \sqrt{\frac{3}{4\pi}}\sqrt{N} & 1 \leq i \leq \frac{s_t}{4\pi(s_d - s_t)} \\ \sqrt{\frac{3}{4\pi}}\sqrt{\frac{s_t}{s_d}}\sqrt{N} & \frac{s_t}{4\pi(s_d - s_t)} \leq i \leq S \end{cases}. \tag{.194}$$

As advancing technologies in drone delivery suggest, and based on the improving trend in this industry, we can claim that drones will undoubtedly be more than 7% faster than trucks. Thus, in the piecewise function of *Case 1*, we always have the second part as the optimal number of rings for the proposed heuristics and minimized cost

$$S^* = \sqrt{\frac{3}{4\pi}}\sqrt{\frac{s_t}{s_d}}\sqrt{N} \quad , \quad C^*(S) = \frac{2N}{3Ks_t} + \frac{\sqrt{6\pi N}}{\sqrt{s_d s_t}} - \frac{2}{s_d} + \frac{N}{K}(F_t + F_d). \tag{.195}$$

Using this optimal value to obtain the total optimal cost:

$$C^*(S) = \begin{cases} \frac{2N}{3Ks_t} + \frac{4\sqrt{\pi N}}{\sqrt{3s_d}} + \frac{N}{K}(F_t + F_d) & 1 \leq i \leq \frac{s_t}{4\pi(s_d - s_t)} \\ \frac{2N}{3Ks_t} + \frac{\sqrt{6\pi N}}{\sqrt{s_d s_t}} - \frac{2}{s_d} + \frac{N}{K}(F_t + F_d) & \frac{s_t}{4\pi(s_d - s_t)} \leq i \leq S \end{cases}. \tag{.196}$$

As advancing technologies in drone delivery suggest, and based on the improving trend in this industry, we can claim that drones will undoubtedly be more than 7% faster than trucks. Thus, in the piecewise function of *Case 1*, we always have the second part as the optimal number of rings for the proposed heuristics and minimized cost

$$S^* = \sqrt{\frac{3}{4\pi}}\sqrt{\frac{s_t}{s_d}}\sqrt{N} \quad , \quad C^*(S) = \frac{2N}{3Ks_t} + \frac{\sqrt{6\pi N}}{\sqrt{s_d s_t}} - \frac{2}{s_d} + \frac{N}{K}(F_t + F_d). \tag{.197}$$